

Birla Central Library

PILANI (Jaipur State)

(Engg College Branch)

Class No :- 621.382 .

Book No :- M 414 E.

Accession No :- 33432

Acc. No

ISSUE LABEL

Not later than the latest date stamped below.

--	--	--

In the manufacture of this book, the publishers have observed the recommendations of the War Production Board and any variation from previous printings of the same book is the result of this effort to conserve paper and other critical materials as an aid to war effort.

Electromechanical
Transducers and Wave Filters

BOOKS FROM
BELL TELEPHONE LABORATORIES

THEORY OF VIBRATING SYSTEMS AND SOUND. By IRVING B. CRANDALL, *Late Member of the Technical Staff, Bell Telephone Laboratories.* Second Printing.

CONTEMPORARY PHYSICS. By KARL K. DARROW, *Member of the Technical Staff, Bell Telephone Laboratories.* Second Edition.

SPEECH AND HEARING. By HARVEY FLETCHER, *Acoustical Research Director, Bell Telephone Laboratories.* With an Introduction by H. D. ARNOLD, *Director of Research, Bell Telephone Laboratories.* Second Printing.

PROBABILITY AND ITS ENGINEERING USES. By THORNTON C. FRY, *Member of the Technical Staff, Bell Telephone Laboratories.* Second Printing.

ELEMENTARY DIFFERENTIAL EQUATIONS. By THORNTON C. FRY. Second Edition.

TRANSMISSIONS CIRCUITS FOR TELEPHONIC COMMUNICATION. METHODS OF ANALYSIS AND DESIGN. By K. S. JOHNSON, *Member of the Technical Staff, Bell Telephone Laboratories.* Fifth Printing.

A FUGUE IN CYCLES AND BELS. By JOHN MILLS, *Member of the Technical Staff, Bell Telephone Laboratories.*

TRANSMISSION NETWORKS AND WAVE FILTERS. By T. E. SHEA, *Special Products Engineer, Bell Telephone Laboratories.* Third Printing.

ECONOMIC CONTROL OF QUALITY OF MANUFACTURED PRODUCT. By W. A. SHEWHART, *Member of Technical Staff, Bell Telephone Laboratories.*

THE APPLICATION OF ELECTROMECHANICAL IMPEDANCE ELEMENTS IN TRANSDUCERS AND WAVE FILTERS. By WARREN P. MASON, *Member of the Technical Staff, Bell Telephone Laboratories.*

RHOMBIC ANTENNA DESIGN. By A. E. HARPER, *Bell Telephone Laboratories.*

POISSON'S EXPONENTIAL BINOMIAL LIMIT. By E. C. MOLINA, *Switching Theory Engineer, Bell Telephone Laboratories.*

ELECTROMAGNETIC WAVES. By S. A. SCHELKUNOFF, *Member of the Technical Staff, Bell Telephone Laboratories.*

PUBLISHED BY
D. VAN NOSTRAND COMPANY, INC.

Electromechanical Transducers and Wave Filters

By

WARREN P. MASON, PH.D.

Member of the Technical Staff

BELL TELEPHONE LABORATORIES, INC.

SECOND PRINTING



NEW YORK

D. VAN NOSTRAND COMPANY, INC.

250 FOURTH AVENUE

COPYRIGHT, 1942, BY
D. VAN NOSTRAND COMPANY, INC.

All Rights Reserved

*This book, or any parts thereof, may not
be reproduced in any form without
written permission from the author
and publisher.*

First Published, April 1942
Reprinted November 1943

PRINTED IN THE U. S. A.

PREFACE

DURING the past hundred years there have been many interchanges of concepts and equations between electrical and mechanical theory. This has been made possible through the fundamental analogies that exist between electrical and mechanical systems and which rest finally on the fact that electrical motions and mechanical motions satisfy the same type of differential equations. At first the borrowings were all from mechanical theory. These included the explanation of electrical phenomena and wave propagation by means of mechanical models. The outstanding example from the communication viewpoint was the influence of mechanical theory on the theory of the loading of electrical transmission lines. Here, the solution of the motion of a string loaded with massive beads given 100 years previously by Lagrange, served to guide the theory of electrical loading, and the necessary spacing of coils along a line was shown to be the same as that for massive beads along a string.

With the development of the electrical wave filter and general electrical network theory, the study of combinations of electrical elements progressed farther than similar studies of combinations of mechanical or electro-mechanical elements. As a consequence most recent borrowings have been from electrical network theory.

It is the purpose of this book to set forth the fundamental analogies and interconnections between electrical theory and mechanical theory. Since this book has been written at the Bell Telephone Laboratories it has had the benefit of a stimulating atmosphere for this point of view, for here occurred the invention and development of the electrical wave filter and the further development of later network theory. Here also occurred some of the first applications of network theory to mechanical systems.

Much of the material of this book has had the advantage of a classroom presentation at the invitation of the Department of Electrical Engineering at Stevens Institute during the winter of 1940-41.

The author wishes to acknowledge many helpful suggestions received from his associates, and to thank Messrs. C. D. Hanscom and R. A. Sykes, who have read the manuscript and have offered helpful suggestions. He desires also to thank his wife, Evelyn S. Mason, for very material assistance in the preparation of the manuscript and in the reading of the proof.

WARREN P. MASON.

CONTENTS

CHAPTER	PAGE
I. INTRODUCTION.....	1
II. ELECTRICAL NETWORK THEORY	11
2.1 Transient and Steady State Solutions.....	11
2.2 Equations of Circuit Theory.....	13
2.3 Expression of the Network Equations in Terms of the Image Parameters.....	20
2.4 General Filter Relations and Equivalences.....	28
2.5 Simple Filter Sections.....	36
2.6 Multiple Filter Sections.....	49
2.7 Networks Employing Resistance and Reactance Elements.....	54
2.8 Filter Structures Employing Elements with Distributed Con- stants.....	58
III. APPLICATION OF NETWORK THEORY TO LUMPED ME- CHANCIAL SYSTEMS.....	80
3.1 Electrical and Mechanical Analogies.....	80
3.2 Application of Electromechanical Analogies to the Solution of Lumped Mechanical Systems.....	83
3.3 Mechanical Filters.....	86
3.4 Rotary Mechanical Filters and Constant Speed Devices.....	92
IV. ACOUSTIC EQUATIONS AND NETWORKS.....	101
4.1 General Differential Equation for Acoustic Wave Motion.....	102
4.2 Propagation of Plane Waves in an Acoustic Tube.....	106
4.3 Effect of Viscosity and Heat Conduction on the Transmission of Sound.....	114
4.4 Effect of a Change of Area of the Conducting Tubes—Horn Theory.....	120
4.5 Side Branches and Acoustic Filter Theory.....	126
4.6 Transfer of Sound by Radiation.....	143
4.7 Highly Directional Receiving and Radiating Devices.....	150
V. VIBRATION OF MEMBRANES AND PLATES.....	158
5.1 Variational Equation of Motion for a Thin Stretched Plate.....	158
5.2 Solution for the Displacement of a Stretched Circular Diaphragm.....	163
5.3 Vibrations of Thin Plates—Telephone Receivers.....	167
5.4 Energy Transmitted to Supports—Soundproof Walls.....	174
5.5 Diaphragm with Tension and Stiffness.....	181
VI. ELECTROMECHANICAL CONVERTING SYSTEMS.....	185
6.1 Electromagnetic Types.....	187
6.2 Electrostatic Driving Systems.....	193
6.3 Longitudinal Piezoelectric Driving Systems.....	195
6.4 Bimorph Piezoelectric Crystals.....	209
6.5 Magnetostrictive Driving System.....	215

CHAPTER	PAGE
VII. DESIGN OF ELECTROMECHANICAL SYSTEMS.....	225
7.1 Introduction.....	225
7.2 Moving Coil Loudspeaker.....	226
7.3 Use of a Crystal as a Supersonic Radiator.....	230
7.4 Methods for Measuring Elastic Constants and Internal Dissipation in Vibrating Bars.....	238
VIII. APPLICATION OF ELECTROMECHANICAL IMPEDANCE ELEMENTS IN ELECTRICAL WAVE FILTERS.....	248
8.1 Introduction.....	248
8.2 Equivalent Circuits for Piezoelectric Crystals with Normal and Divided Electrodes.....	249
8.3 Narrow Band Filters Employing Crystals and Condensers.....	258
8.4 Wide Band Pass Crystal Filters Employing Coils as Well as Crystals and Condensers.....	263
8.5 Other Types of Crystal Filters.....	280
8.6 Filters Employing Magnetostrictive Elements.....	285
APPENDIX A. MOTION AND IMPEDANCE OF A BAR VIBRATING IN FLEXURE, TAKING ACCOUNT OF ROTARY INERTIA.....	291
B. GENERAL WAVE PROPAGATION TAKING ACCOUNT OF VISCOSITY EFFECTS.....	298
C. ELASTIC AND PIEZOELECTRIC EQUATIONS FOR CRYSTALS.....	308
INDEX OF SUBJECTS.....	331

LIST OF SYMBOLS EMPLOYED

A, B, C, D, E, F	arbitrary constants
$A + jB$	attenuation and phase constants of an electric or mechanical line
a	radius
B	flux density
BW	band width
c_{11}, c_{ij}	elastic constants
C	capacitance, compliance
C_m	moment of compliance
C_p	specific heat at constant pressure
D	diameter of tube, constant in piezoelectric or magnetostrictive equation
db	decibel
d_{12}, d_{ij}	piezoelectric constants
E	instantaneous potential, E_0 maximum potential
E_x	potential gradient in x direction
F	force
f	frequency
f_{ij}	piezoelectric constants
G	leakance
i	instantaneous current, i_0 maximum value
I	moment of inertia
I_n	Bessel's function of imaginary argument of order n
j	$\sqrt{-1}$
J_n	Bessel's function of the first kind of order n
k	coefficient of electromechanical coupling, ω/v
K	dielectric constant, thermal conductivity
K_{LC}	longitudinally clamped dielectric constant

K_n	Bessel's function of the second kind of order n
KE	kinetic energy
l, l_t, l_w	length, thickness, width
l_1, m_1, n_1	direction cosines
L	inductance
L_{db}	loss in decibels
m	network parameter, constant in flexure equation
M	moment of force, mass
n	integer, relation in flexure equation
N	number of turns, number
p	instantaneous pressure, p_0 static pressure
P	perimeter
P_z	polarization along z axis
PE	potential energy
Q	charge, ratio of reactance to resistance
r	radius, ratio of capacitances, dr element of length along radius
\dot{r}	velocity in the radius direction
R	electrical or mechanical resistance
R_F	reflection factor
R_m	moment of resistance
s	slope, condensation, ds element of length
s_{11}, s_{ij}	elastic compliance constants
S	area, S_h area of holes, dS element of area
t	time
T	tension, temperature, taper constant
T_F	transmission factor
T_f	temperature coefficient of frequency
v	velocity of propagation
v'	velocity of propagation for a short-circuited crystal
V	volume
V_1	volume velocity in first circuit
w, \dot{w}	displacement and velocity normal to the surface

W	total energy
x, \dot{x}	displacement and velocity along x axis, dx element of length in x direction
X	reactance component
X_x, Y_y, Z_z	extensional stresses
X_y, Y_z, Z_x	shearing stresses
x_x, y_y, z_z	extensional strains
x_y, y_z, z_x	shearing strains
$\dot{x}_x, \dot{y}_y, \dot{z}_z, \dot{x}_y, \dot{y}_z, \dot{z}_x$	time rates of strain deformation
y, \dot{y}	displacement and velocity along y axis
Y_0	Young's modulus
Z	impedance, Z_I image impedance, Z_{I_0} image impedance at mean frequency of band, Z_{nn} self-impedance in n th branch, Z_{jk} mutual impedance between the j th and k th branch, Z_0 characteristic impedance of line or tube, Z_s sending end imped- ance, Z_T terminating impedance, Z_{sc} short-circuited impedance, Z_{oc} open-cir- cuited impedance
ϵ	angle
ρ	density, ρ_s surface density
ω	2π times f the frequency, $\Delta\omega$ increment in ω
ω_A	$2\pi f_A$ where f_A is the lower cut-off
ω_B	$2\pi f_B$ where f_B is the upper cut-off
ω_∞	$2\pi f_\infty$ where f_∞ is the frequency of infinite attenuation
$\omega_x, \omega_y, \omega_z$	rotations around the x, y , and z axes.
Δ	impedance determinant, dilation; Δ_{11} mi- nor of determinant
θ	image transfer constant, θ_0 value at zero frequency.
θ	angle of twist, $\dot{\theta}$ angular velocity of twist
δ	type of propagation constant useful in horn theory
$\delta_x, \delta_y, \delta_z$	increments in length along x, y , and z axes

ξ	displacement, $\dot{\xi}$ velocity, $\ddot{\xi}$ acceleration along x axis
η	displacement, $\dot{\eta}$ velocity, $\ddot{\eta}$ acceleration along y axis
ζ	displacement, $\dot{\zeta}$ velocity, $\ddot{\zeta}$ acceleration along z axis
κ	radius of gyration, susceptibility
φ	velocity potential, φ^2 impedance transfor- mation ratio
Φ	total flux
ψ	angle
μ	coefficient of shear viscosity, shearing elas- tic constant
λ	coefficient of dilational viscosity, dilational elastic constant, magnetostrictive con- stant
σ	Poisson's ratio
γ	ratio of specific heats
χ_i	inverse of susceptibility in the i th direction

CHAPTER I

INTRODUCTION

DURING the past few years, apparatus which transfers electrical into acoustical or mechanical energy has received wide application. This has come about through the popular use of radios, phonographs, public address systems, and sound motion pictures. While the fundamental principles of such electro-mechanical or electroacoustic transducers have been known for decades, it is safe to say that the rapid progress and excellent design obtained were due in part to the knowledge borrowed from the related subject of electrical network theory.

In the early days of electricity such quantities as inductance and capacitance were often illustrated by referring to mechanical systems having mass and compliance. With the advent of the use of long transmission lines, loading, and especially electrical wave filters, the investigations of the combination of electrical elements advanced considerably farther than had the study of the combination of mechanical or acoustical elements. Many results and theorems were established in electrical network theory which had their counterparts and uses in mechanical and acoustical theory, but which on account of the slower development of mechanical theory had not been realized or used. With the advent of the loudspeaker, phonograph, etc., the specialized knowledge of electrical wave network theory was applied to the broader field of mechanical wave transmission systems, and resulted in remarkable improvements. Two examples may be cited to show the nature and extent of this improvement. Barton in his "Theory of Sound" cited measurements on the efficiency of acoustic fog horns operated from an electrical source of power and found that the efficiency of conversion from electrical into acoustic energy was less than one per cent. Today large loudspeakers have been developed which

can be used for similar purposes and these have efficiencies of conversion greater than fifty per cent. Another and more striking example is the mechanical phonograph. From the days of its invention by Edison mechanical phonograph reproducers had been constructed from such mechanical units as needles, diaphragms, horns, and their connecting mechanical elements. As late as 1925 the best of such units were capable of reproducing only three octaves. About this time, another mechanical phonograph¹ was constructed from the same sort of elements, but with their dimensions and relationships designed according to relations developed in electrical network theory, and the resulting structure was able to reproduce a frequency band corresponding to five octaves with an increase in efficiency of conversion.

The type of electrical network which has received the greatest application in the design of mechanical and acoustical systems is the electrical wave filter invented by Dr. G. A. Campbell. This may seem surprising at first sight, since the filter is usually regarded as a device for attenuating unwanted frequency bands while passing other frequency bands which it is desired to receive. The filter has two properties which make it of interest in electromechanical transducer systems. These are: first, the filter is able to co-ordinate the action of several resonant elements to produce a device with a uniform transmission over a wide frequency range; and second, the dissipationless filter is a device that delivers to its output all of the energy impressed upon it over the widest possible frequency range consistent with the elements composing it. These properties of the filter have been made use of in purely electrical networks to determine the largest band width a vacuum tube with known characteristics can have and still deliver a specified gain at a specified impedance level. Applied to electromechanical transducer systems, filter theory shows how to combine resonant mechanical or electromechanical elements to produce a uniform conversion of electrical to mechanical energy, or vice versa,

¹ Maxfield and Harrison, Bell System Technical Journal, Vol. V, No. 3, p. 493, 1926.

over a wide frequency range, and it is able to determine the greatest band width that can be obtained without loss of efficiency for any type of conversion element.

It is the purpose of this book to provide an introduction to the use of the results of electrical network theory into the science of acoustical, mechanical and electromechanical systems. In order to provide a background for the application, one chapter is devoted mainly to presenting the results of classical network theory which deals with combinations of lumped inductances, capacitances, and resistances. Starting with Kirchoff's laws, the output current and voltage of a circuit with any number of meshes are given in terms of the input current and voltage and the determinants of the circuit impedances. From these relations, the general network theorems, which include Thevenin's theorem, the reciprocity theorem, and the compensation theorem, are proved. An extended form of the reciprocity theorem is also proved which is useful in electromechanical coupling elements. By employing it the inverse relation, involving the ratio of the electrical effect to the applied mechanical motivation, of an electromechanical element is fully determined when the direct relation, involving the ratio of the mechanical effect to the applied electrical motivation, is known. The image transfer constant and image impedances of a network are defined and evaluated in terms of the impedance determinants. The image parameters allow one to separate the ideal transmission characteristics of a network from the transformation, reflection and interaction characteristics of a network. The image parameters are applicable to any type of network but are particularly advantageous for filters. The ideal filter is defined as a four-terminal network composed of non-dissipative elements which, as judged from its transfer constant alone, transmits continuous bands of real frequencies and attenuates all other frequencies. From this definition and the expression for the image transfer constant in terms of the impedance determinants, the transfer characteristics are derived for ladder, bridge T , and lattice type networks which are the three principal configurations used in electrical networks. Of

these the lattice type is the most general since a balanced lattice network with realizable constants can always be found which is the equivalent of any other configuration, while the inverse is not true. Bartlett's theorem,² which allows one to transfer networks with mirror image symmetry to a lattice, is given and proved and another theorem which is useful in transferring a lattice network into simpler sections is also proved. On account of the greater generality of the lattice network, the filter parameters are defined in terms of the lattice network. Low pass, high pass, band pass and band elimination filters are derived in lattice form and their equivalent ladder forms are obtained from these. A table of filters particularly useful in acoustical and mechanical systems is given. Networks of the equalizer type which employ resistance as well as reactance elements are also discussed.

The lumped constant networks of the classical theory are useful for low and moderately high frequencies, but for the ultra-high frequencies now being used in radio transmission they cannot be applied since it becomes increasingly more difficult to obtain lumped structures. In the limiting case all elements approach straight wires or parallel planes which have the impedance characteristics of electric lines. Consequently it becomes necessary to consider the effect of wave propagation in the elements. For mechanical and acoustical systems, on account of the much lower velocity of propagation, this state of affairs exists for much lower frequencies and it is difficult to obtain any elements which approximate the characteristics of lumped elements. It is interesting to note that one of the first papers³ which considered the effect of wave propagation in the elements of filters had acoustic filters as its subject matter. The formulae derived are also applicable to electrical networks composed of sections of lines. Although the characteristics and parameters of lumped constant filter sections are not applicable

² "Extension of a Property of Artificial Lines," A. C. Bartlett, *Phil. Mag.* **4**, pp. 902-907, Nov. 1927.

³ "A Study of the Regular Combination of Acoustic Elements with Applications to Recurrent Acoustic Filters, Tapered Acoustic Filters, and Horns," W. P. Mason, *B.S.T.J.*, Vol. VI, pp. 258-294, April 1927.

to filters having wave transmitting elements, the definition of filters and their expression in terms of image parameters are still valid. From these relations a complete theory of filters with wave transmitting elements can be developed. The main difference is that in place of a single pass band, a filter with distributed constants will have an infinity of pass bands which are usually harmonically related. A bridge between the lumped constant and distributed constant theory of filters can be made if the frequency is low enough so that all line lengths are less than an eighth of a wavelength. For this case, all lines can be replaced by T or π combinations of coils and condensers and some of the configurations of lumped constant filter theory can be realized. This procedure is particularly useful in obtaining wide band transformers at high frequencies. For higher frequencies for which line lengths cannot be so limited, the more general procedure has to be used.

Applications of electrical network theory to simple mechanical systems are made in later chapters. Although the general similarity between the action of electrical elements, such as inductances and capacitances and mechanical elements such as masses and compliances, has been known for a long time, the utility of mechanical impedance quantities was not realized until the work of Webster,⁴ who applied the mechanical impedance concept to the propagation of sound in horns. The original definition of a mechanical impedance as a ratio of force to velocity for the system results in a mass being equivalent to an inductance, a compliance to a capacitance and a mechanical resistance to an electrical resistance. However, this association is not unique for, as shown by Hanle⁵ and Firestone,⁶ equally consistent results can be obtained by using an inverse system which defines a mechanical impedance as a ratio of velocity to force.

⁴ "Acoustic Impedance and the Theory of Horns and of the Phonograph," A. G. Webster, Nat. Acad. of Science, Vol. 5, 1919, p. 275.

⁵ "Die Darstellung Electromechanischer Gebilde durch rein elektrische Schaltbilder," Hanle, Wiss. Veröff. A. C. Siemens Konzern, Vol. XI, No. 1, 1932.

⁶ "A New Analogy Between Mechanical and Electrical Systems," F. A. Firestone, J. Acoustical Soc. Amer. 4, 249 (1933).

This results in a compliance and an inductance, and a capacitance and a mass respectively being equivalent. In the present book the direct system is followed in all cases except that of electromagnetic and magnetostrictive coupling when a real simplification is realized by using the inverse system. Three specific mechanical problems are considered for one-dimensional systems. The first of these is a vibration reducing support which is shown to be equivalent to a low pass filter. At certain frequencies such a support may transmit more vibration than would be present without the support. This is shown to be due to the transforming action of the misterminated filter section and can be eliminated by introducing a damping which in effect terminates the filter section. The second problem considered is the design of a band pass mechanical filter system such as is used at low frequencies in the telephone system. This filter uses tuned reeds vibrating in flexure and, in order to calculate their equivalent masses and compliances, it is necessary to solve the equation of a bar vibrating in flexure. This is done by an impedance method which gives not only the natural resonances, which are given by the classical formulae, but also the impedance or ratio of force to velocity at the coupled end of the bar. This impedance can be resolved into a mass and a compliance near the first resonance and these values can be used in the design of a mechanical filter which follows the similar procedure set up for electrical filters. The third problem considered is the torsional vibration of a bar. In solving this problem it is useful to introduce a moment impedance which is defined as the ratio of the applied torque or moment of the system to the resulting angular velocity. The solution is applied in evaluating the natural frequencies of a rotating drive shaft with equally spaced cranks and flywheels and in describing the action of a constant speed motor in which the irregularities of the motion are removed by the addition of a low pass filter.

The fourth chapter considers the application of the impedance method to acoustic wave propagation. In general, acoustic wave propagation can take place in three dimensions and for the general case the one-dimensional electrical analogies of elec-

trical network theory are not directly applicable. However, for a specific type of wave such as a plane wave, a spherical wave, or any other type of wave which can be specified by a dimension along the direction of propagation, impedance relations can be defined and considerable progress can be made by considering the electrical analogies. The conditions for plane wave propagation are investigated and it is shown that if all dimensions of the enclosing tube perpendicular to the direction of propagation are less than a wavelength, a plane wave will result in a short distance from the source no matter what the form of the wave at the beginning of the tube. The modification caused by viscosity and heat conduction are considered and an equivalent T network for wave propagation in a tube is worked out. This relation is applied to wave propagation in a horn and in a series of chambers which can be made to have filtering properties. The characteristics and limitations of acoustic filters are considered. Sound may also be transmitted by radiation as well as in a wave guided by a tube. Although it is not possible to represent such a wave transmission by an equivalent circuit, the reaction of the wave on a diaphragm or plane piston can be calculated in the form of a radiation resistance and reactance. The radiation formulae have been applied in calculating the directivity of piston diaphragms and tubular directional microphones.

Two-dimensional mechanically-vibrating systems in the form of stretched diaphragms and thin plates are considered by the impedance method. This gives not only the resonance frequencies of the diaphragm, usually considered in the classical theory of sound, but also the series impedance such a diaphragm or plate exerts between two vibrating media. These results are applied to acoustic filters and telephone receivers. By making greater use of the boundary conditions than has been done heretofore, the energy transmitted by the supporting members is investigated and an equivalent circuit worked out which takes account of transmission through the diaphragm and in the supports. This circuit is applied in investigating the properties of double sound-proof windows and walls.

In the first part of the book, purely electrical circuits are discussed while in the succeeding parts purely mechanical or acoustical structures are discussed. In a large number of structures, however, the energy is converted from electrical form into mechanical or acoustical form or vice versa. In order to accomplish this conversion it is necessary to employ some form of an electromechanical transducer or converting element. The four principal forms used are described and their equations and equivalent circuits are derived. The more usual forms for setting up waves in air are the electromagnetic and the electrostatic types of transducers, which develop mechanical forces by virtue of magnetic attraction or electrostatic repulsion. These have rather low ratios of force to applied current or charge but they can be associated with high mechanical compliances and low masses and hence are more suitable for setting up acoustic waves in air. When it is desired to set up acoustic waves in liquids or solids, piezoelectric crystals or magnetostrictive bars are commonly employed. These have large ratios of force to applied charge or current and are associated with high mechanical impedances so that they are suitable for generating waves in high mechanical impedance structures. In obtaining the equivalent circuits of electromechanical converters, i.e., the combination of electrical and mechanical elements which will represent the action of the device, it is found that much simpler relationships are obtained if the inverse mechanical impedance system is used for electromagnetic and magnetostriction converters, and the direct mechanical impedance system for electrostatic or piezoelectric converters.

The separate results of electrical, mechanical and electromechanical systems are combined in considering the design of composite electromechanical transducers. Wherever considerations of efficiency are of importance the resulting electromechanical circuit reduces to a filter circuit and, by employing the formulae developed for electrical filters, the condition for the widest frequency range and absence from reflections is readily obtained. Specifically an electrodynamic loudspeaker and a supersonic crystal sound generator are considered. It is shown

in the latter case that good efficiency is obtained only if the electrical capacitance of the crystal is neutralized by an inductance and the resulting circuit designed as a filter. A similar use of a crystal in measuring the mechanical properties of a bar is also discussed, and a new method employing two crystals is described. This system makes possible the measurement of the properties of a system with low Q , and is applied to the measurement of the mechanical properties of some plastics.

Although combinations of electrical elements were first studied and applied in wave filters and other structures, it does not follow that they have any inherent advantages over analogous combinations of mechanical or electromechanical elements which can be used as filters. In fact elements which depend on mechanical motion have the great advantage that they have very little energy dissipation associated with their motion and hence the equivalent mechanical elements have a higher ratio of reactance to resistance, or Q , than do their electrical counterparts. The result is that considerably more selective filters can be made from mechanical or electromechanical elements than can be obtained by employing electrical coils and condensers. The type of electromechanical element which has been used most extensively in selective filters is the piezoelectric crystal and particularly the quartz crystal. This element has the advantage of an electromechanical converting system in the piezoelectric effect and a very high mechanical Q . Moreover, a quartz crystal is very stable mechanically and can be cut so that its frequency changes very little over a wide temperature range. For these reasons quartz crystals have been applied extensively when it is desirable to obtain a narrow band filter or a very selective filter. They are used very extensively in the high frequency carrier systems and in the coaxial conductor system which transmits as many as 480 conversations over one pair of conductors. The last chapter considers the application of such elements to filter structures. The production of narrow band filters by the use of crystals alone is discussed. Methods for widening the pass band of such filters by the use of electrical coils are given. Network configurations of such form are used,

that the electrical dissipation of the coils has the effect of an added loss to the attenuation characteristic, this loss being independent of the frequency. The use of crystals in low pass, high pass, and band elimination filters is also discussed. Magnetostrictive bars may also be used in selective filters although the electrical resistance of the driving coils seriously limits their usefulness. The possibilities and limitations of the use of such elements in filters are discussed.

CHAPTER II

ELECTRICAL NETWORK THEORY

2.1. *Transient and Steady State Solutions*

WHEN a sinusoidal voltage is applied to a linear electrical network, the current in the output is a function of time which gradually approaches the sinusoidal form as the time becomes larger. The final sinusoidal form is called the steady state current, while the difference between the actual current and the steady state current at any time is called the transient current.

All network theory, both electrical and mechanical, is based on the steady state solution. This is a proper procedure since the transient conditions are usually of too short a duration to affect the ear or other receiving apparatus and also because the transient solution can always be calculated from the steady state solution by means of the Fourier Integral formulation.¹

Instead of employing a sinusoidal function for time it is usual to employ the function

$$e^{j\omega t} = \cos \omega t + j \sin \omega t \quad (2.1)$$

where

$$j = \sqrt{-1}$$

since by its use a symbolic solution is obtained which is considerably easier to deal with. The actual

time solution can always be obtained by taking the real part of the solution and throwing away the imaginary part. For example suppose that we apply an alternating electromotive force $E = E_0 \cos \omega t$ on the network of Fig. 2.1 which consists of an inductance L , a capacitance C , and a resistance R in series.

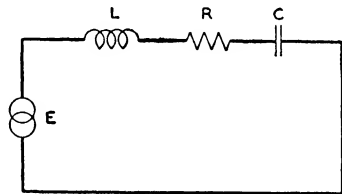


FIG. 2.1—SERIES RESONANT CIRCUIT.

¹ "The Practical Application of the Fourier Integral," G. A. Campbell, B.S.T.J., Oct. 1928, pp. 639-707.

The differential equation for the system is well known to be

$$L \frac{d^2 Q}{dt^2} + R \frac{dQ}{dt} + \frac{Q}{C} = E_0 \cos \omega t \quad (2.2)$$

where L is the inductance, R the resistance, C the capacitance, and Q the quantity of charge flowing in the wire. The current i flowing in the network is the rate of change of the charge Q or

$$i = \frac{dQ}{dt} = j\omega Q \quad (2.3)$$

if we employ the symbolic time variation of (2.1). The complete solution of (2.2) is known to be

$$i = \frac{dQ}{dt} = \frac{E_0 \cos (\omega t - \theta)}{\sqrt{R^2 + \left(\omega L - \frac{1}{\omega C}\right)^2}} + i_1 e^{-\frac{R}{2L}t} \left[\cosh \sqrt{\frac{R^2}{4L^2} - \frac{1}{LC}} t - \frac{\sinh \sqrt{\frac{R^2}{4L^2} - \frac{1}{LC}} t}{\sqrt{1 - \frac{4L}{R^2 C}}} \right] \quad (2.4)$$

where $\tan \theta = \left(\omega L - \frac{1}{\omega C}\right)/R$, i_1 is the initial current at time $t = 0$, and Q_1 the initial charge is zero. When t is very large this reduces to the steady state solution

$$i = E_0 \frac{\left[R \cos \omega t + \left(\omega L - \frac{1}{\omega C}\right) \sin \omega t \right]}{R^2 + \left(\omega L - \frac{1}{\omega C}\right)^2}. \quad (2.5)$$

For the symbolic case we have

$$i_0 e^{j\omega t} \left[j\omega L + R + \frac{1}{j\omega C} \right] = E_0 e^{j\omega t} \text{ or } i_0 e^{j\omega t} = \frac{E_0 e^{j\omega t}}{R + j\left(\omega L - \frac{1}{\omega C}\right)}. \quad (2.6)$$

This gives the same result as (2.5) if we take the real part

$$i_0[\cos \omega t + j \sin \omega t] = \frac{\left\{ E_0 \left[R \cos \omega t + \left(\omega L - \frac{1}{\omega C} \right) \sin \omega t \right] \right\} + j \left\{ R \sin \omega t - \left(\omega L - \frac{1}{\omega C} \right) \cos \omega t \right\}}{R^2 + \left(\omega L - \frac{1}{\omega C} \right)^2} \quad (2.7)$$

The ratio of E to i in equation (2.6) is called the impedance Z so that

$$Z = \frac{E_0 e^{j\omega t}}{i_0 e^{j\omega t}} = \frac{E}{i} = R + j \left(\omega L - \frac{1}{\omega C} \right). \quad (2.8)$$

In obtaining the impedance Z it is not necessary to carry the multiplying factor $e^{j\omega t}$ and this is usually understood. The im-

pedance has a real part R and an imaginary part $\left(\omega L - \frac{1}{\omega C} \right)$.

The real part is termed the resistance while the imaginary part is termed the reactance portion of the impedance. We note

that when $\omega L = \frac{1}{\omega C}$ the reactance part vanishes and we have a condition of resonance.

2.2. Equations of Circuit Theory

The equations for any combination of electrical elements can be derived from Kirchhoff's Laws which can be stated as:

1. The total electromotive force taken around any closed loop or circuit in the network is zero.
2. The sum of the currents entering any branch point in the network is zero.

These two laws allow one to obtain the equations of any configuration of electrical elements. For example, consider the three mesh circuit of Fig. 2.2. From the second law the current in the first branch circuit is $i_1 - i_2$ in order that the three currents in the branch shall add up to zero. Similarly for the second

branch circuit the current is $i_2 - i_3$. Then from the first law we have the three equations:

$$\begin{aligned} E_1 &= i_1[Z_s + Z_{11}] + (i_1 - i_2)[Z_{12}] = i_1[Z_s + Z_{11} \\ &\quad + Z_{12}] - i_2Z_{12} \\ 0 &= -i_1[Z_{12}] + i_2[Z_{12} + Z_{22} + Z_{23}] - i_3Z_{23} \quad (2.9) \\ E_3 &= -i_2Z_{23} + i_3[Z_{23} + Z_{33} + Z_T] \end{aligned}$$

where

$$\begin{aligned} Z_{11} &= \left(j\omega L_{11} + R_{11} - \frac{j}{\omega C_{11}} \right); \\ Z_{12} &= \left(j\omega L_{12} + R_{12} - \frac{j}{\omega C_{12}} \right) \text{ etc.} \end{aligned}$$

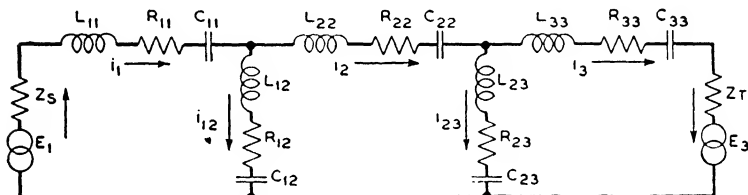


FIG. 2.2—THREE MESH NETWORK.

Let us form the determinant Δ of the impedances inside the network in the form

$$\begin{aligned} \Delta &= \begin{vmatrix} (Z_{11} + Z_{12}), & -Z_{12}, & 0 \\ -Z_{12} & , & (Z_{12} + Z_{22} + Z_{23}), -Z_{23} \\ 0 & , & -Z_{23}, & (Z_{23} + Z_{33}) \end{vmatrix} \\ &= \begin{vmatrix} \alpha_{11} - \alpha_{12} & 0 \\ -\alpha_{12} + \alpha_{22} - \alpha_{23} \\ 0 & -\alpha_{23} + \alpha_{33} \end{vmatrix} \quad (2.10) \end{aligned}$$

If we solve for one of the currents, say i_1 we find that

$$i_1 = \frac{E_1[(\alpha_{22}\alpha_{33} - \alpha_{23}^2) + \alpha_{22}Z_T] + E_3(\alpha_{12}\alpha_{23})}{\left\{ Z_s Z_T \alpha_{22} + Z_s [\alpha_{22}\alpha_{33} - \alpha_{23}^2] + Z_T [\alpha_{11}\alpha_{22} - \alpha_{12}^2] \right\} + [\alpha_{11}(\alpha_{22}\alpha_{33} - \alpha_{23}^2) - \alpha_{12}^2 \alpha_{33}]} \quad (2.11)$$

In terms of the determinant Δ this becomes

$$i_1 = \frac{E_1[\Delta_{11} + \Delta_{1133}Z_T] + E_3\Delta_{13}}{Z_sZ_T\Delta_{1133} + Z_s\Delta_{11} + Z_T\Delta_{33} + \Delta} \quad (2.12)$$

where Δ_{11} ² is the determinate obtained from (2.10) by suppressing the first row and column, Δ_{1133} is the determinate obtained by suppressing the first and third rows and columns, etc. Similarly by symmetry we have

$$i_3 = \frac{E_1\Delta_{13} + E_3[\Delta_{33} + \Delta_{1133}Z_s]}{Z_sZ_T\Delta_{1133} + Z_s\Delta_{11} + Z_T\Delta_{33} + \Delta} \quad (2.13)$$

Although these relations are illustrated for a three mesh circuit, they are applicable to a circuit of any number of meshes as can be shown easily from determinant theory.³

Some interesting relations of general network theory can be derived from these equations. If we let the input and output impedance Z_s and Z_T be equal to zero, i.e., if we deal with the equation of the network alone and write the equations

$$E_3 = E_1A - i_1B; \quad i_3 = i_1C - E_1D, \quad (2.14)$$

we find that

$$A = -\frac{\Delta_{11}}{\Delta_{13}}; \quad B = -\frac{\Delta}{\Delta_{13}}; \quad C = \frac{\Delta_{33}}{\Delta_{13}}; \quad D = \left(\frac{\Delta_{11}\Delta_{33} - \Delta_{13}^2}{\Delta_{13}\Delta}\right). \quad (2.15)$$

From these values we see that

$$AC - BD = -\frac{\Delta_{11}\Delta_{33}}{\Delta_{13}^2} + \left(\frac{\Delta_{11}\Delta_{33} - \Delta_{13}^2}{\Delta_{13}^2}\right) = -1. \quad (2.16)$$

Another useful theorem which can easily be proved from (2.13) is Thevenin's theorem which states

The current in any terminating impedance Z_T connected to any network is the same as if Z_T were connected to a generator whose

² In general $\Delta_{ik} = (-1)^{i+k}$ times the determinate obtained by suppressing the i th row and k th column.

³ The general case is discussed in "Transmission Networks and Wave Filters," T. E. Shea, Ch. II, D. Van Nostrand, or "Communication Networks," E. A. Guillemin, Ch. IV, Vol. I, John Wiley.

voltage is the open circuit voltage of the network and whose internal impedance Z_R is the impedance looking back from the terminals of Z_T , with all generators replaced by impedances equal to the internal impedances of these generators. From equation (2.13) the current i_3 in the terminating impedance Z_T due to the impressed voltage E_1 is

$$i_3 = \frac{E_1 \Delta_{13}}{Z_s Z_T \Delta_{1133} + Z_s \Delta_{11} + Z_T \Delta_{33} + \Delta} \quad (2.17)$$

Now the open circuit voltage E_{30} is equal to $i_3 Z_T$ when $Z_T \rightarrow \infty$, or, from (2.17) will be

$$E_{30} = \frac{E_1 \Delta_{13}}{\Delta_{33} + \Delta_{1133} Z_s} \quad (2.18)$$

The impedance looking into the network with $E_1 = 0$ but terminated in Z_s is

$$Z_R = \frac{E_3}{i_3} = \frac{Z_s \Delta_{11} + \Delta}{\Delta_{33} + \Delta_{1133} Z_s} \quad (2.19)$$

Hence by Thevenin's theorem we should have

$$\begin{aligned} i_3 &= \frac{E_{30}}{Z_R + Z_T} = \frac{\frac{E_1 \Delta_{13}}{\Delta_{33} + \Delta_{1133} Z_s}}{\frac{Z_s \Delta_{11} + \Delta}{\Delta_{33} + \Delta_{1133} Z_s} + Z_T} \\ &= \frac{E_1 \Delta_{13}}{Z_s Z_T \Delta_{1133} + Z_s \Delta_{11} + Z_T \Delta_{33} + \Delta} \end{aligned} \quad (2.20)$$

which is the value given by (2.17). Thevenin's theorem allows us to replace any complicated network by a simple generator with a definite internal impedance.

Another theorem which is immediately obvious from the general network equations (2.12) and (2.13) is the reciprocity theorem which states

In any system composed of linear bilateral elements if any electromotive force E is applied between any two terminals and the current i is measured in any branch, their ratio (called the transfer impedance) will be the same if the positions of E and i are interchanged.

From equation (2.13) the transfer impedance from the first to the third mesh is E_1/i_3 with $E_3 = 0$ or

$$Z_t = \frac{(Z_s Z_T \Delta_{1133} + Z_s \Delta_{11} + Z_T \Delta_{33} + \Delta)}{\Delta_{13}}. \quad (2.21)$$

Similarly from equation (2.12) the transfer impedance from the third to the first branch is

$$Z_t = \frac{E_3}{i_1} = \frac{Z_s Z_T \Delta_{1133} + Z_s \Delta_{11} + Z_T \Delta_{33} + \Delta}{\Delta_{13}} \quad (2.22)$$

which proves the theorem.

Another form of the reciprocity theorem of particular interest for electromagnetically and magnetostrictively coupled electromechanical circuits can be derived as follows. Equation (2.12) can be transposed into the form

$$\begin{aligned} E_1 - i_1 \left(\frac{Z_s Z_T \Delta_{1133} + Z_s \Delta_{11} + Z_T \Delta_{33} + \Delta}{\Delta_{11} + \Delta_{1133} Z_T} \right) \\ = - \frac{E_3 \Delta_{13}}{\Delta_{11} + \Delta_{1133} Z_T}. \end{aligned}$$

Now if the output voltage E_3 is set equal to zero, the short-circuited impedance Z_{sc_1} , looking into the network is

$$Z_{sc_1} = \frac{Z_s Z_T \Delta_{1133} + Z_s \Delta_{11} + Z_T \Delta_{33} + \Delta}{\Delta_{11} + \Delta_{1133} Z_T}.$$

Hence the above equation can be written

$$\frac{E_1 - i_1 Z_{sc_1}}{E_3} = - \frac{\Delta_{13}}{\Delta_{11} + \Delta_{1133} Z_T}. \quad (2.23)$$

If now we eliminate E_1 from equations (2.12) and (2.13) we have the relation

$$\frac{i_3 - E_3 \left(\frac{\Delta_{1133}}{\Delta_{11} + \Delta_{1133} Z_T} \right)}{i_1} = \frac{\Delta_{13}}{\Delta_{11} + \Delta_{1133} Z_T}$$

provided we make use of the well-known relation for a symmetrical determinant

$$\Delta\Delta_{1133} = \Delta_{11}\Delta_{33} - \Delta_{13}^2.$$

Now

$$\frac{\Delta_{11} + \Delta_{1133}Z_T}{\Delta_{1133}} = Z_{0c_2}$$

is the open-circuit impedance measured from the output terminals. Hence

$$\frac{i_3 - E_3/Z_{0c_2}}{i_1} = \frac{\Delta_{13}}{\Delta_{11} + \Delta_{1133}Z_T}. \quad (2.24)$$

Then due to the equality of the absolute values of the right hand sides of (2.23) and (2.24) we have the theorem. "*If in any system composed of linear bilateral elements, a voltage E_1 is placed in the input and the ratio of the input voltage, minus the input current times the short-circuited input impedance, to the output voltage is determined, then due to the reciprocal properties of the network, if the network is energized only by an output voltage E_3 , the negative of this same ratio will exist between the output current i_3 , minus the voltage E_3 divided by the output open-circuited impedance, and the current i_1 existing in the input.*"

If we reverse the input and output currents and voltages it is easy to show that

$$\frac{E_3 - i_3(Z_{sc_2})}{E_1} = -\frac{\Delta_{13}}{\Delta_{33} + \Delta_{1133}Z_s} = -\left(\frac{i_1 - E_1/(Z_{0c_1})}{i_3}\right). \quad (2.25)$$

This form of the reciprocity theorem is of interest in electrostatically and piezoelectrically coupled networks.

A fourth theorem of interest is the compensation theorem which states that

If a network is modified by making a change ΔZ in the impedance of one of its branches, the current increment thereby produced at any point in the network is equal to the current that would be produced at that point by a compensating electromotive force acting in series with the modified branch, whose value is $+i\Delta Z$, where i is the original current which flowed in the modified branch.

To prove the theorem suppose that the impedance of the k th branch is changed from Z_k to $Z_k + \Delta Z_k$. If the current in

Z_k before the change is i_k and a compensating e.m.f. equal to $-i_k\Delta Z_k$ is inserted, the current in all parts of the network will be the same as originally since the compensating e.m.f. cancels the effect of the voltage drop $i_k\Delta Z_k$. Now since the current at any point due to two voltages is the sum of the currents produced by each voltage individually it follows that the compensating voltage $-i_k\Delta Z_k$ has produced an effect equal and opposite to that caused by the increase in impedance ΔZ_k . Hence the increment in current at any point in the network due to ΔZ_k will be equal to the current which would be produced by the negative of the compensation voltage $-\Delta Z_k i_k$.

A special case is that in which the change made is to introduce an open circuit in one branch. The compensation e.m.f. in this case would be infinite and would act through an infinite impedance so the result would be indeterminate. In this case the following method can be used. Let Z_T be the impedance of the network at the terminals of Z_k . The current that flows in Z_k when connected to Z_T may be considered as due to e.m.f. E' in series with Z_k and Z_T or

$$i_k = E' / (Z_k + Z_T)$$

where E' is the voltage which would be measured across the opening of the branch. If we introduce an e.m.f. E equal to $-E'$, the current in the branch reduces to zero and we can open the branch without disturbing the network. Hence the current increment due to the opening of the branch is the current produced by an e.m.f. $E = -E' = -i_k(Z_k + Z_T)$ acting alone in the original network in series with Z_k .

Another special case of interest is that in which a short circuit is placed across two of the wires. This case can be treated as follows. First we measure the potential E_1 across the part to be short-circuited and place a connection between these two wires with a source of e.m.f., E_1 equal to that measured there. This will cause no change in any of the currents since the inserted potential E_1 will be equal to the potential already there, and hence no extra e.m.f. is available to change the currents. Next we insert an e.m.f. $-E_1$ in the cross connection. Since

E_1 and $-E_1$ are equal and opposite, there will be no potential drop across the connection and hence the branch can be short-circuited without changing the current distribution. Hence the currents produced by a short circuit will be equivalent to those produced by placing a source of e.m.f., $-E_1$ across the two wires to be short-circuited.

2.3. *Expression of the Network Equations in Terms of the Image Parameters*

In studying the transmission properties of an electrical network considerable simplification is obtained by introducing the image transfer constant and the image impedances. This allows one to separate the ideal transmission characteristic from the transformation, reflection and interaction characteristics of the network. The image impedances Z_{I_1} and Z_{I_2} are defined as those with which the structure must be terminated so that the impedances seen in both directions from the network at each pair of terminals are the same; while the image transfer constant θ is defined as half the natural logarithm of the ratio of the volt amperes flowing into and out of the network under these conditions. From this definition follows the well-known relation that if two structures are connected in tandem with equal image impedances at their common junction, the image impedances of the composite network will be the same as the image impedances at the free ends of the two networks, while the transfer constant of the composite network will be the sum of the transfer constants of the two structures.

To determine the two image impedances we let $Z_s = Z_{I_1}$, the input image impedance, and $Z_T = Z_{I_2}$, the output image impedance. The impedance looking into the network can be obtained from (2.12) by letting $E_3 = 0$ and taking the ratio

$$Z_{I_1} = \frac{E_1}{i_1} - Z_{I_1} \quad \text{or} \quad Z_{I_1} = \frac{E_1}{2i_1}$$

$$= \frac{Z_{I_1}Z_{I_2}\Delta_{1133} + Z_{I_1}\Delta_{11} + Z_{I_2}\Delta_{33} + \Delta}{2[\Delta_{11} + \Delta_{1133}Z_{I_2}]}$$

Similarly the output image impedance is, from (2.13),

$$\begin{aligned} Z_{I_2} &= \frac{E_3}{i_3} - Z_{I_1} \quad \text{or} \quad Z_{I_2} = \frac{E_3}{2i_1} \\ &= \frac{Z_{I_1}Z_{I_2}\Delta_{1133} + Z_{I_1}\Delta_{11} + Z_{I_2}\Delta_{33} + \Delta}{2[\Delta_{33} + \Delta_{1133}Z_{I_1}]} \end{aligned}$$

Solving these two equations simultaneously we find

$$Z_{I_1} = \sqrt{\frac{\Delta_{33}\Delta}{\Delta_{11}\Delta_{1133}}}; \quad Z_{I_2} = \sqrt{\frac{\Delta_{11}\Delta}{\Delta_{33}\Delta_{1133}}} \quad (2.26)$$

To find the image transfer constant we have from (2.17)

$$i_3 = \frac{E_1\Delta_{13}}{Z_{I_1}Z_{I_2}\Delta_{1133} + Z_{I_1}\Delta_{11} + Z_{I_2}\Delta_{33} + \Delta},$$

if we let $Z_s = Z_{I_1}$; $Z_T = Z_{I_2}$. The voltage in the output impedance Z_{I_2} is $E_3 = i_3Z_{I_2}$, hence

$$E_3i_3 = i_3^2Z_{I_2} = \frac{E_1^2Z_{I_2}\Delta_{13}^2}{(Z_{I_1}Z_{I_2}\Delta_{1133} + Z_{I_1}\Delta_{11} + Z_{I_2}\Delta_{33} + \Delta)^2} \quad (2.27)$$

The volt amperes into the network will be $E_1/2 \times E_1/2 Z_{I_1}$ since half the applied voltage E_1 appears across the terminals of the network. Introducing these values, and the values of (2.25) we find

$$\begin{aligned} e^{-2\theta} &= \frac{E_3i_3}{\frac{E_1}{2}i_1} = \frac{4Z_{I_1}Z_{I_2}\Delta_{13}^2}{(Z_{I_1}Z_{I_2}\Delta_{1133} + Z_{I_1}\Delta_{11} + Z_{I_2}\Delta_{33} + \Delta)^2} \\ &= \frac{\frac{\Delta_{13}^2}{\Delta\Delta_{1133}}}{\left[1 + \sqrt{\frac{\Delta_{33}\Delta_{11}}{\Delta\Delta_{1133}}}\right]^2} \quad (2.28) \end{aligned}$$

Making use of the well-known relation for a symmetrical determinant

$$\Delta\Delta_{1133} = \Delta_{11}\Delta_{33} - \Delta_{13}^2 \quad (2.29)$$

this can be written in the form

$$e^{-2\theta} = \frac{\sqrt{\frac{\Delta_{11}\Delta_{33}}{\Delta\Delta_{1133}}} - 1}{\sqrt{\frac{\Delta_{11}\Delta_{33}}{\Delta\Delta_{1133}}} + 1}. \quad (2.30)$$

In terms of the hyperbolic tangents and cosines the transfer constant can be written more simply as

$$\tanh \theta = \frac{1 - e^{-2\theta}}{1 + e^{-2\theta}} = \sqrt{\frac{\Delta\Delta_{1133}}{\Delta_{11}\Delta_{33}}}; \quad (2.31)$$

$$\cosh \theta = \frac{1}{\sqrt{1 - \tanh^2 \theta}} = \frac{1}{\sqrt{1 - \frac{\Delta\Delta_{1133}}{\Delta_{11}\Delta_{33}}}} = \frac{\sqrt{\Delta_{11}\Delta_{33}}}{\Delta_{13}}.$$

In terms of the A , B , C , and D constants of equation (2.14) we have

$$Z_{I_1} = \sqrt{\frac{BC}{AD}}; \quad Z_{I_2} = \sqrt{\frac{AB}{CD}}; \quad \tanh \theta = \sqrt{\frac{BD}{AC}};$$

$$\cosh \theta = \sqrt{\frac{AC}{AC - BD}} = \sqrt{-AC}. \quad (2.32)$$

Introducing these values into (2.14), we have a relation between the image parameters and the voltage and currents

$$E_3 = \sqrt{\frac{Z_{I_2}}{Z_{I_1}}} \left[-E_1 \cosh \theta + i_1 Z_{I_1} \sinh \theta \right];$$

$$i_3 = \sqrt{\frac{Z_{I_1}}{Z_{I_2}}} \left[i_1 \cosh \theta - \frac{E_1}{Z_{I_1}} \sinh \theta \right]. \quad (2.33)$$

Returning now to the case where the terminating impedances Z_s and Z_T are general impedances rather than the image impedances, and substituting the values of the determinants

evaluated previously in equation (2.17) for the current in the output of the network, we can write

$$i_3 = \frac{E_1 \sqrt{Z_{I_1} Z_{I_2}}}{(Z_s Z_T + Z_{I_1} Z_{I_2}) \sinh \theta + (Z_s Z_{I_2} + Z_T Z_{I_1}) \cosh \theta}.$$

Introducing the expression for $\sinh \theta$ and $\cosh \theta$

$$\sinh \theta = \frac{e^\theta - e^{-\theta}}{2}; \quad \cosh \theta = \frac{e^\theta + e^{-\theta}}{2}$$

and rearranging the equations we have

$$i_3 = \frac{E_1}{2Z_s} \sqrt{\frac{Z_{I_1}}{Z_{I_2}}} \left[\frac{2Z_s}{Z_{I_1} + Z_s} \right] \left[\frac{2Z_{I_2}}{Z_{I_2} + Z_T} \right] e^{-\theta} \\ \times \frac{1}{\left[1 - e^{-2\theta} \left(\frac{Z_{I_1} - Z_s}{Z_{I_1} + Z_s} \right) \left(\frac{Z_{I_2} - Z_T}{Z_{I_2} + Z_T} \right) \right]}. \quad (2.34)$$

The current in the termination if there were no network there will be $i_3' = E_1/(Z_s + Z_T)$. Hence the effect of inserting the structure between the terminal impedances Z_s and Z_T will be to change the current in the output by the factor

$$F = \frac{Z_s + Z_T}{2Z_s} \sqrt{\frac{Z_{I_1}}{Z_{I_2}}} \left(\frac{2Z_s}{Z_{I_1} + Z_s} \right) \left(\frac{2Z_{I_2}}{Z_{I_2} + Z_T} \right) e^{-\theta} \\ \times \frac{1}{\left[1 - e^{-2\theta} \left(\frac{Z_{I_1} - Z_s}{Z_{I_1} + Z_s} \right) \left(\frac{Z_{I_2} - Z_T}{Z_{I_2} + Z_T} \right) \right]}. \quad (2.35)$$

The interpretation of the equation can be obtained by considering several limiting cases. We consider first the case of a symmetrical network, i.e., $Z_{I_1} = Z_{I_2}$, with Z_s and Z_T equal to the image impedance. Then the factor F reduces to $e^{-\theta}$. Hence, we can say that $e^{-\theta}$ is the transfer factor of a symmetrical network terminated in its image impedances. We next

consider the case where the network is terminated in its image impedances but these are different. Then F becomes

$$F = \frac{Z_{I_1} + Z_{I_2}}{2\sqrt{Z_{I_1}Z_{I_2}}} e^{-\theta}. \quad (2.36)$$

As shown in Fig. 2.3 this can be interpreted as the factor resulting from a perfect transformer of impedance ratio Z_{I_2}/Z_{I_1} ,

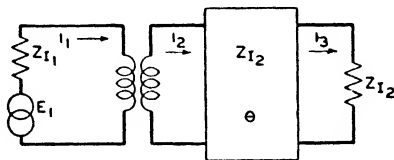


FIG. 2.3—TRANSFORMER AND SYMMETRICAL NETWORK.

together with a symmetrical network whose transfer constant is θ and whose impedance is Z_{I_2} . For

$$i_1 = \frac{E}{2Z_{I_1}}; \quad i_2 = i_1 \sqrt{\frac{Z_{I_1}}{Z_{I_2}}} = \frac{E}{2\sqrt{Z_{I_1}Z_{I_2}}}; \quad i_3 = i_2 e^{-\theta} = \frac{E e^{-\theta}}{2\sqrt{Z_{I_1}Z_{I_2}}}.$$

The current in the absence of the network is $E_1/(Z_{I_1} + Z_{I_2})$, hence the transfer factor is as given by equation (2.36). This shows that a dissymmetrical network acts as a combination of a perfect transformer whose impedance ratio is the ratio of the image impedances and a symmetrical network having the transfer constant θ .

Next suppose that $Z_T = Z_{I_2}$, but that Z_s is different from Z_{I_1} , the input image impedance. Then the factor becomes

$$F = \left(\frac{Z_s + Z_{I_2}}{2Z_s} \right) \left(\frac{2Z_s}{Z_{I_1} + Z_s} \right) \sqrt{\frac{Z_{I_1}}{Z_{I_2}}} e^{-\theta}. \quad (2.37)$$

This can still be interpreted by the circuit of Fig. 2.3 if we replace Z_{I_1} by Z_s , for then

$$i_3 = \frac{E}{Z_s + Z_{I_1}} \times \sqrt{\frac{Z_{I_1}}{Z_{I_2}}} e^{-\theta} = \frac{E}{2Z_s} \left(\frac{2Z_s}{Z_s + Z_{I_1}} \right) \sqrt{\frac{Z_{I_1}}{Z_{I_2}}} e^{-\theta}. \quad (2.38)$$

However, the factor $\frac{2Z_s}{Z_{I_1} + Z_s}$ has a special significance for Heaviside⁴ has shown that at any junction point between two media having different impedances, say Z_s and Z_{I_1} , there is a reflection of current from the second toward the first which is equal to the current which would flow if the impedance of the second medium were equal to that of the first times the reflection factor

$$R_F = \frac{Z_s - Z_{I_1}}{Z_s + Z_{I_1}} \quad (2.39)$$

while the current in the second medium will be the unmodified current times the transmission factor

$$T_F = \frac{2Z_s}{Z_s + Z_{I_1}}. \quad (2.40)$$

Hence on the input side of the junction, the current will be the sum of the unmodified current plus the reflected current or

$$\frac{E}{2Z_s} \left[1 + \frac{Z_s - Z_{I_1}}{Z_s + Z_{I_1}} \right] = \frac{E}{Z_s + Z_{I_1}}. \quad (2.41)$$

Similarly on the output side of the junction the current is the unmodified current times the transmission factor T_F or

$$\frac{E}{2Z_s} \left(\frac{2Z_s}{Z_s + Z_{I_1}} \right) = \frac{E}{Z_s + Z_{I_1}}. \quad (2.42)$$

Returning to equation (2.38) the current i_3 in the output can be interpreted as the unmodified current $(E/2Z_s)$ times the transmission factor $\left(\frac{2Z_s}{Z_s + Z_{I_1}} \right)$ in going from one impedance medium to another, times the current transformation factor of the network $\sqrt{Z_{I_1}/Z_{I_2}}$, times the transfer factor $e^{-\theta}$ of a symmetrical network. If $Z_s = Z_{I_1}$ but $Z_T \neq Z_{I_2}$, the expression becomes

$$i_3 = \frac{E_1}{2Z_{I_1}} \sqrt{\frac{Z_{I_1}}{Z_{I_2}}} \left(\frac{2Z_{I_2}}{Z_{I_2} + Z_T} \right) e^{-\theta}. \quad (2.43)$$

⁴ "Electromagnetic Theory," Heaviside, Vol. II, p. 79.

This can be interpreted in the same way since the third factor will then be the transmission factor in going from the output image impedance of the network to the terminating impedance Z_T .

When neither the input nor output impedances are equal to their image impedances another factor called the interaction factor enters. If we expand this in powers of $e^{-2\theta}$, the interpretation is simple for

$$\frac{1}{1 - e^{-2\theta} \left[\frac{Z_{I_1} - Z_s}{Z_{I_1} + Z_s} \right] \left[\frac{Z_{I_2} - Z_T}{Z_{I_2} + Z_T} \right]} = 1 + e^{-2\theta} \left[\frac{Z_{I_1} - Z_s}{Z_{I_1} + Z_s} \right] \left[\frac{Z_{I_2} - Z_T}{Z_{I_2} + Z_T} \right] \\ + e^{-4\theta} \left[\frac{Z_{I_1} - Z_s}{Z_{I_1} + Z_s} \right]^2 \left[\frac{Z_{I_2} - Z_T}{Z_{I_2} + Z_T} \right]^2 + \dots \quad (2.44)$$

The second term in this series represents the current which has been reflected from the output junction of the network, transmitted through the network, reflected from the input junction and then transmitted to the termination. Similarly the second and higher powers represent outputs for which this process has occurred two or more times. If both the terminating and input impedances differ appreciably from their image impedances in the unattenuated pass band of a filter, this may cause a considerable distortion, but if the impedances are well matched, this effect is small. A perfect match on either side will cause the factor to disappear since although a reflection from one junction may occur, the reflected wave will not be transmitted back to the termination unless the other junction is also unmatched.

It is convenient to express the insertion ratios of powers and currents in logarithmic units since then the effect of successive changes can be regarded as additive. For expressing the magnitude of a ratio there are two commonly used logarithmic units. One is the decibel which may be called the common logarithmic unit, while the other is the neper which may be called the natural logarithmic unit. Two powers are said to differ by one bel or 10 decibels when one is 10 times the other. If we have a

ratio of two powers P_1 and P_2 the number of decibels by which they differ is

$$N_{db} = 10 \log_{10} \frac{P_1}{P_2}. \quad (2.45)$$

The same unit, the decibel, can also be used to indicate current or voltage ratio provided the respective voltages or currents are associated with identical impedances. Then since the powers are proportional to the squares of the voltages or currents, the number of decibels to give the same result as (2.45) will be

$$N_{db} = 20 \log_{10} \left| \frac{V_1}{V_2} \right| \quad \text{or} \quad N_{db} = 20 \log_{10} \left| \frac{I_1}{I_2} \right|. \quad (2.46)$$

The natural logarithmic unit, the neper, which is often preferable in computations involving transfer constants, etc., is given by

$$N_{nep} = \log_e \left| \frac{V_1}{V_2} \right| = \log_e \left| \frac{I_1}{I_2} \right|. \quad (2.47)$$

The relation between the two is given by

$$\frac{N_{db}}{N_{nep}} = 20 \log_{10} e = 8.686. \quad (2.48)$$

Returning to equation (2.35), it is seen that the ratio F can be expressed as the sum of a number of separate terms.

$$\begin{aligned} 20 \log_{10} |F| &= 20 \log_{10} \left| \frac{Z_s + Z_T}{2Z_s} \sqrt{\frac{Z_{I_1}}{Z_{I_2}}} \right| + 20 \log_{10} \left| \frac{2Z_s}{Z_{I_1} + Z_s} \right| \\ &+ 20 \log_{10} \left| \frac{2Z_{I_2}}{Z_{I_2} + Z_T} \right| + 20 \log_{10} \left| e^{-\theta} \right| \\ &+ 20 \log_{10} \left| \frac{1}{1 - e^{-2\theta} \left(\frac{Z_{I_1} - Z_s}{Z_{I_1} + Z_s} \right) \left(\frac{Z_{I_2} - Z_T}{Z_{I_2} + Z_T} \right)} \right|. \quad (2.49) \end{aligned}$$

The lines indicate that the absolute values of these ratios only are of significance from the point of view of obtaining the number of *db*. The first term gives the ideal transformer loss—which may be a gain—in going from the impedance Z_s to the impedance Z_T . The next two factors are transmission factors expressing the loss in going from Z_s to Z_{I_1} and from Z_{I_1} to Z_T . If the transfer constant θ is divided into a real and imaginary part

$$\theta = A + jB \quad (2.50)$$

the absolute value of the fourth factor is $20 \log_{10} e^{-A}$ which is known as the attenuation loss. The fifth factor is called the interaction loss.

2.4. *General Filter Relations and Equivalences*

The previous analysis in terms of image parameters is applicable to all kinds of networks including transmission lines, phase and attenuation equalizers, attenuators, and filters. In the present section consideration will be limited to filters. In general a filter is a network in which currents lying within specified continuous frequency ranges are transmitted freely while currents of all other frequencies are suppressed. On account of the unavoidable losses put in by terminal mismatches of impedance, loss due to resistive elements, etc., this does not provide an exact basis for analysis. In order to eliminate these effects we assume non-dissipative elements in the filter and perfect terminations, i.e., terminations equal to the image impedances. For this case the only factor left is the transfer constant and hence we define a filter to be a four terminal network composed of non-dissipative elements which as judged from its transfer constant alone transmits continuous bands of real frequencies and attenuates all other real frequencies. No actual filter reaches this ideal but deviations caused by dissipative elements, etc., are easily evaluated and appear as small corrections to the filter losses.

Filters may be obtained in a variety of network configurations of which the T and π network of Fig. 2.4A, the bridge T of Fig. 2.4B and the balanced lattice of Fig. 2.4C are the most

used. If we work out the mesh equations of the T network of Fig. 2.4A we find

$$\begin{aligned} E_2 &= -E_1 \left(\frac{Z_1 + 2Z_2}{2Z_2} \right) + i_1 \frac{Z_1(Z_1 + 4Z_2)}{4Z_2}; \\ i_2 &= i_1 \left(\frac{Z_1 + 2Z_2}{2Z_2} \right) - \frac{E_1}{Z_2}. \end{aligned} \quad (2.51)$$

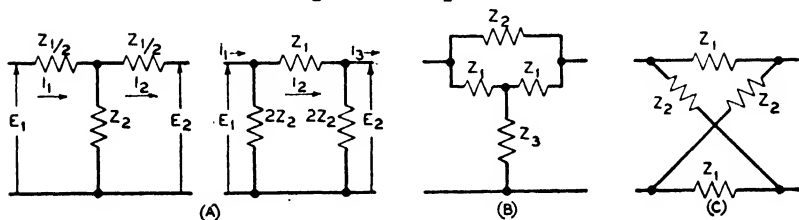


FIG. 2.4— T , π , BRIDGE T , AND LATTICE NETWORKS.

Comparing these with equations (2.32) and (2.33) we have

$$\begin{aligned} \cosh \theta &= \left(\frac{Z_1 + 2Z_2}{2Z_2} \right); \quad \tanh \theta = \frac{\sqrt{Z_1(Z_1 + 4Z_2)}}{(Z_1 + 2Z_2)}; \\ Z_{I_1} &= Z_{I_2} = \sqrt{\frac{Z_1(Z_1 + 4Z_2)}{4}}. \end{aligned}$$

For the π network we have the relations

$$\begin{aligned} \cosh \theta &= \left(\frac{Z_1 + 2Z_2}{2Z_2} \right); \quad \tanh \theta = \frac{\sqrt{Z_1(Z_1 + 4Z_2)}}{Z_1 + 2Z_2}; \\ Z_{I_1} &= Z_{I_2} = \sqrt{\frac{4Z_1Z_2^2}{Z_1 + 4Z_2}}. \end{aligned} \quad (2.52)$$

We see therefore that the π network has the same transfer constant as the T but a different image impedance.

The π network can be regarded as the sum of the characteristics of two L networks of the type shown in Fig. 2.5 placed back to back for if we work out the mesh equations of Fig. 2.5 we have

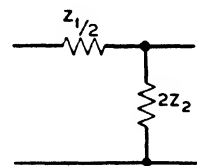


FIG. 2.5— L NETWORK.

$$E_2 = -E_1 + \frac{i_1 Z_1}{2}; \quad i_2 = i_1 \left(\frac{Z_1 + 4Z_2}{4Z_2} \right) - \frac{E_1}{2Z_2}. \quad (2.53)$$

Hence we have from (2.33)

$$\begin{aligned}\cosh \theta &= \sqrt{\frac{Z_1 + 4Z_2}{4Z_2}}; \quad Z_{I_1} = \sqrt{\frac{Z_1(Z_1 + 4Z_2)}{4}}; \\ Z_{I_2} &= \sqrt{\frac{4Z_1Z_2^2}{Z_1 + 4Z_2}}.\end{aligned}\tag{2.54}$$

Now since $\cosh \frac{\theta}{2} = \sqrt{\frac{\cosh \theta + 1}{2}}$ we find that the image transfer constant of the L network is half the image transfer constant of the T or π network while the image impedances on the series or shunt ends are respectively equal to the image impedances of the T or π networks. Hence a T network can be constructed by connecting the two shunt arms of two L networks together, at which point they will have the same image impedances, and adding their image transfer constants. Similarly the π network can be obtained by adding together two L networks at their series arms.

In a similar manner the expressions for the image parameters for the bridge T and the lattice networks are

Bridge T

$$\begin{aligned}\cosh \theta &= \frac{Z_1(Z_1 + Z_3) + Z_2(2Z_1 + Z_3)}{Z_1(Z_1 + Z_2) + Z_2(Z_1 + Z_3)}; \\ Z_{I_1} &= Z_{I_2} = \sqrt{\frac{Z_1Z_3(Z_1 + 2Z_3)}{(2Z_1 + Z_3)}}\end{aligned}\tag{2.55}$$

Lattice

$$\begin{aligned}\cosh \theta &= \left(\frac{Z_1 + Z_2}{Z_2 - Z_1}\right); \quad \tanh \frac{\theta}{2} = \frac{\cosh \theta - 1}{\sinh \theta} = \sqrt{\frac{Z_1}{Z_2}}; \\ Z_{I_1} &= Z_{I_2} = \sqrt{Z_1Z_2}.\end{aligned}\tag{2.56}$$

We next consider the conditions for unattenuated transmission from input to output which results in all the input power being delivered to the output provided there are no impedance

mismatches. As mentioned before θ in general is composed of an attenuation constant A and a phase constant B given by

$$\theta = A + jB.$$

Then

$$\begin{aligned} \cosh \theta &= \cosh (A + jB) \\ &= \cosh A \cos B + j \sinh A \sin B. \end{aligned} \quad (2.57)$$

Now if the impedances of the networks of Fig. 2.4 are all reactive the ratios of the impedances are all real and consequently $\cosh \theta$ must be real. This can only be satisfied if $A = 0$ or $B = 0, \pi, 2\pi$ or some higher multiples of π radians. If the attenuation A is zero, $\cosh A = 1$ and consequently

$$A = 0 \quad \text{when} \quad -1 < \cosh \theta < +1. \quad (2.58)$$

On the other hand if $B = 0, \pi, 2\pi$, etc., $\cos B = \pm 1$ and $|\cosh \theta| > 1$. Hence if the absolute value of $\cosh \theta$ is greater than unity the attenuation is finite and free transmission does not occur. When $\cosh \theta$ is between -1 and $+1$ the attenuation is zero and all the power supplied to the network is transmitted to the termination. For the T or π network of Fig. 2.4A the condition for full transmission is

$$-1 < \cosh \theta = \frac{Z_1 + 2Z_2}{2Z_2} < +1 \quad \text{or} \quad -1 < \frac{Z_1}{4Z_2} < 0. \quad (2.59)$$

$$\text{Inverting we also have} \quad 0 < \frac{Z_1/2 + 2Z_2}{Z_1/2} < -\infty.$$

For the bridge T and lattice networks of Fig. 2.4B and C the conditions are

$$\begin{aligned} -2 < \frac{Z_1 Z_3}{Z_1^2 + 2Z_1 Z_2 + Z_2 Z_3} < 0 \quad \text{or inverting} \\ 0 < \frac{(Z_1 + 2Z_2)}{\left(\frac{Z_1 Z_3}{Z_1 + 2Z_3}\right)} < -\infty \end{aligned} \quad (2.60)$$

for the bridge T and for the lattice

$$-1 < \frac{Z_1}{Z_2 - Z_1} < 0 \quad \text{or inverting} \quad 0 < \frac{Z_2}{Z_1} < -\infty. \quad (2.61)$$

We note that the conditions for the lattice are much the simplest and that the other networks can be reduced to the lattice with lattice impedances which are combinations of the T and bridge T impedances. In fact it can be shown that any symmetrical network (i.e., with equal image impedances) can be reduced to a lattice network, having realizable impedances in each of the lattice arms. For networks which have mirror image symmetry, the equivalent lattice arms are easily found by using Bartlett's bisection theorem⁵ which states that *for networks having mirror image symmetry, the series arms of the equivalent lattice network are found by cutting the section in two along the line of symmetry, short circuiting all the cut wires and using the resulting two terminal networks as the series arms, while the lattice arms are obtained by using the two terminal networks formed by open circuiting all the cut wires.* This theorem is easily proved by using the compensation theorem discussed above.

A network with mirror image symmetry can be divided into two equal parts with a number of connecting wires as shown in

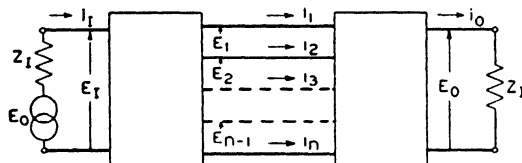


FIG. 2.6—NETWORK POSSESSING MIRROR IMAGE SYMMETRY.

Fig. 2.6. We assume that the network is terminated on each end by impedances Z_I the image impedance and acted upon by the voltage E_0 in series with the input image impedance Z_I . From equation (2.33) we can write the relation between the input and output currents and voltages.

$$\begin{aligned}
 i_O &= i_I \cosh \theta - \frac{E_I}{Z_I} \sinh \theta = i_I \cosh \theta - \frac{(E_0 - i_I Z_I)}{Z_I} \sinh \theta \\
 E_O &= -E_I \cosh \theta + i_I Z_I \sinh \theta \\
 &= -(E_0 - i_I Z_I) \cosh \theta + i_I Z_I \sinh \theta.
 \end{aligned}
 \tag{2.62}$$

⁵ "Extension of a Property of Artificial Lines," A. C. Bartlett, Phil. Mag. 4, pp. 902-907, Nov. 1927.

To obtain the impedance of the network with all the wires open circuited, we introduce a series of compensating voltages e_1 to e_n in the wires with currents i_1 to i_n flowing in them, of such a value that they cause equal and opposite currents to flow in these wires. Since no currents flow in these wires they can be cut without affecting the current distribution and hence the set of compensation voltages will cause a current $-i_o$ to flow in the termination. Due to the symmetry of the network the compensation voltages will also cause a current $-i_o$ to flow in the input of the network resulting in a current i_A equal to

$$\begin{aligned} i_A &= i_I - i_o = i_I - \left(i_I \cosh \theta - \left(\frac{E_0 - i_I Z_I}{Z_I} \right) \sinh \theta \right) \\ &= i_I (1 - \cosh \theta + \sinh \theta) - \frac{E_0 \sinh \theta}{Z_I}. \end{aligned} \quad (2.63)$$

The impedance Z_{oc} looking into the network with open circuit wires is

$$\frac{E_0}{i_A} = Z_I + Z_{oc} = \frac{E_0}{i_I (1 - \cosh \theta + \sinh \theta) - \frac{E_0 \sinh \theta}{Z_I}}. \quad (2.64)$$

Since $E_0/i_I = 2Z_I$ as can be seen from Fig. 2.6, we find that

$$Z_{oc} = Z_I \left(\frac{1 + \cosh \theta - \sinh \theta}{1 - \cosh \theta + \sinh \theta} \right) = Z_I \coth \frac{\theta}{2}. \quad (2.65)$$

To obtain the short-circuited impedance of the network we introduce a series of compensating voltages $-E_1$ to $-E_{n-1}$ between the wires, which are equal and opposite to the voltages already existing there. There is then no potential difference between any of the wires so they can be short circuited without affecting the current distribution. Therefore these voltages will introduce an equal and opposite current i_o in the termination and due to the symmetry of the network these voltages will introduce a positive i_o in the input of the network. Hence the current i_B is

$$i_B = i_I + i_o = i_I (1 + \cosh \theta + \sinh \theta) - \frac{E_0 \sinh \theta}{Z_I} \quad (2.66)$$

and the short-circuited impedance of the network is

$$Z_{sc} = \frac{E_0}{i_B} - Z_I = Z_I \left[\frac{1 - \cosh \theta + \sinh \theta}{1 + \cosh \theta - \sinh \theta} \right] = Z_I \tanh \frac{\theta}{2}. \quad (2.67)$$

Now from equation (2.56) for a lattice network

$$\begin{aligned} Z_1 &= Z_I \sqrt{\frac{\cosh \theta - 1}{\cosh \theta + 1}} = Z_I \tanh \frac{\theta}{2}; \\ Z_2 &= Z_I \sqrt{\frac{\cosh \theta + 1}{\cosh \theta - 1}} = Z_I \coth \frac{\theta}{2}. \end{aligned} \quad (2.68)$$

Hence the short-circuited half of the network will have the impedance of the series arm Z_1 of the equivalent lattice, while the open-circuited half of the network will have the impedance of the lattice arm Z_2 , which proves the theorem.

As an example of the use of Bartlett's bisection theorem the equivalent lattice networks of a T network and a bridge T

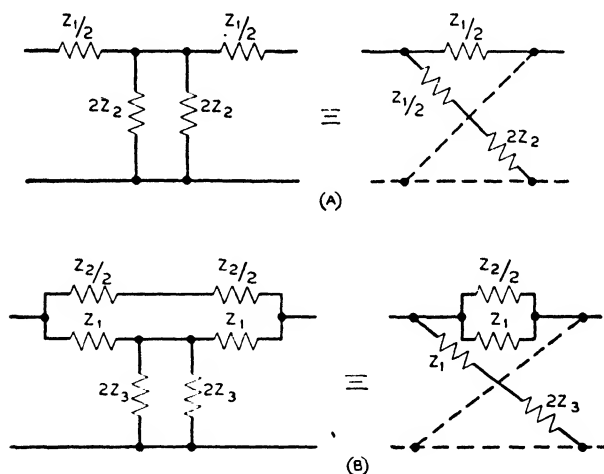


FIG. 2.7—METHOD FOR REDUCING T AND BRIDGE T NETWORKS TO LATTICE NETWORKS.

network are given in Fig. 2.7. Both the T and the bridge T can be divided into two networks with connecting wires, one of which is the mirror image of the other. The series arm of the T , $Z_{1/2}$ is obtained by short circuiting the cut wires while the

lattice arm is this network with the cut wires open circuited. Similarly for the bridge T the series arm is Z_1 shunted by $Z_2/2$, while the lattice arm is Z_1 in series with $2Z_3$. In the lattice representation the dotted lines indicate that the dotted series arm is the same as the series arm shown while the dotted lattice arm is the same as the lattice arm shown.

Another class of networks which can be reduced to a balanced lattice with realizable constants is one in which the network is balanced and contains a number of straight through connections and symmetrical crossed connections as shown in

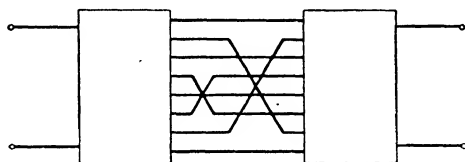


FIG. 2.8—SYMMETRICAL NETWORK WITH STRAIGHT AND INVERTED CONNECTIONS.

Fig. 2.8. For this case the equivalent series arm will be the impedance of the input to the network with all the straight through connections short circuited and all the crossed connections open circuited, while the equivalent lattice arm will be the impedance of the input to the network with all the straight through connections open circuited and all the crossed wires short circuited. The method of proof follows that given above. If we put short circuiting compensating voltages between all the straight through wires and open circuiting compensating voltages in all of the crossed wires we will produce a current i_o in the output equal and opposite to that already there. Due to the symmetry this same current will be produced in the input in such a direction as to add to i_I and hence the input impedance with all the straight through wires shorted and all the crossed

wires opened will be $Z_I \tanh \frac{\theta}{2} = Z_1$.

Similarly if we open the straight through wires by means of series compensating voltages and short the crossed wires by means of shunt compensating voltages the current $-i_o$ will be

produced in both input and output circuits resulting in the input impedance

$$Z_I \coth \frac{\theta}{2} = Z_2 \quad (2.69)$$

which proves the theorem.

As an example of the use of this theorem the network relations shown in Fig. 2.9A and B are easily proved. The first

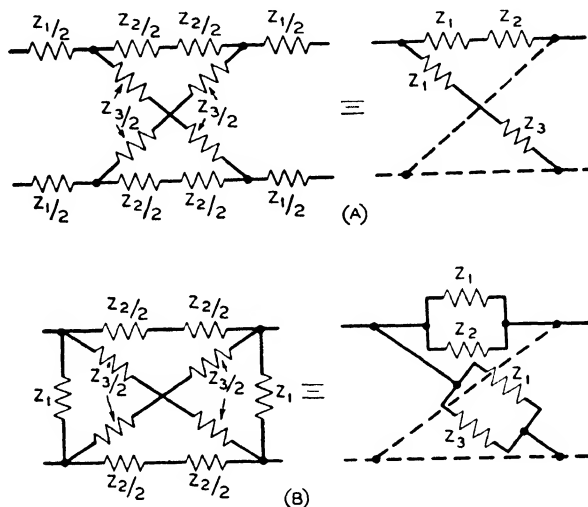


FIG. 2.9—Two Lattice Network Equivalences.

relation follows since for the series arm of the equivalent lattice we short circuit the straight through wires and open circuit the crossed wires for the series arm and vice versa for the lattice arm. The relation in Fig. 2.9B is also obvious. These relations are useful in reducing a lattice network to a T , π or bridge T network.

2.5. Simple Filter Sections

Since all the types of filter sections can be reduced to a lattice network, it has become customary to describe the characteristics of the lattice sections and to derive the ladder or bridge T sections by employing the transformations given above. The simplest type of band-pass section is the one shown in

Fig. 2.10A. In this filter we have a series resonant circuit in both the series and lattice arms, the series arm resonating at f_A and the lattice arm in f_B . In determining the constants it is assumed that $f_A < f_B$. The impedances of the two arms are

$$Z_1 = \frac{-j}{\omega C_1} \left[1 - \frac{\omega^2}{\omega_A^2} \right]; \quad Z_2 = \frac{-j}{\omega C_2} \left[1 - \frac{\omega^2}{\omega_B^2} \right] \quad (2.70)$$

$$\text{where } f_A = \frac{1}{2\pi \sqrt{L_1 C_1}}; \quad f_B = \frac{1}{2\pi \sqrt{L_2 C_2}}.$$

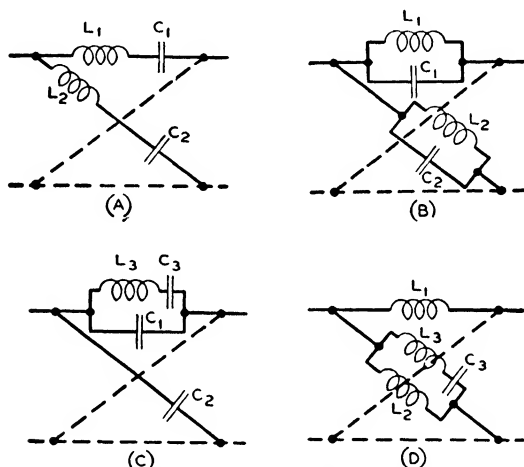


FIG. 2.10—FOUR TYPES OF SIMPLE BAND-PASS LATTICE FILTERS.

In specifying the transfer constant θ it is simpler to use the expression for $\tanh \frac{\theta}{2}$ of equation (2.56) since it involves only a ratio of the two impedances. Then we have

$$Z_I = \sqrt{Z_1 Z_2} = \sqrt{\frac{-1}{\omega^2 C_1 C_2} \left[1 - \frac{\omega^2}{\omega_A^2} \right] \left[1 - \frac{\omega^2}{\omega_B^2} \right]};$$

$$\tanh \frac{\theta}{2} = \sqrt{\frac{Z_1}{Z_2}} = \sqrt{\frac{C_2}{C_1} \left(\frac{1 - \frac{\omega^2}{\omega_A^2}}{1 - \frac{\omega^2}{\omega_B^2}} \right)}. \quad (2.71)$$

Examining the first equation we see that when $\omega < \omega_A$ or $\omega > \omega_B$, the expression for Z_I is imaginary indicating a reactance, while when $\omega_A < \omega < \omega_B$, the term is real showing that for frequencies between f_A and f_B the image impedance is a resistance, which indicates a transmission of power. The expression for the transfer constant can be written in the form

$$\tanh \frac{\theta}{2} = \sqrt{\frac{C_2 \left(1 - \frac{\omega^2}{\omega_A^2}\right)}{C_1 \left(1 - \frac{\omega^2}{\omega_B^2}\right)}} = m \sqrt{\frac{1 - \frac{\omega^2}{\omega_A^2}}{1 - \frac{\omega^2}{\omega_B^2}}} \text{ where } m = \sqrt{\frac{C_2}{C_1}}. \quad (2.72)$$

The characteristic obtained depends on the value of m . The filter has one frequency f_∞ for which the transfer constant has an infinite attenuation and this frequency is determined by the value of m . When $\theta \rightarrow \infty$, $\tanh \theta/2 \rightarrow 1$ and hence

$$m = \sqrt{\frac{1 - \frac{\omega_\infty^2}{\omega_B^2}}{1 - \frac{\omega_\infty^2}{\omega_A^2}}} = \tanh \frac{\theta_0}{2} \quad (2.73)$$

where θ_0 is the attenuation when $\omega = 0$. From (2.73) we see that when $0 < m < \frac{f_A}{f_B}$ the attenuation peak is on the upper side as indicated in Fig. 2.11 which shows some typical attenuation characteristics calculated from (2.72) when $f_B = 1.10 f_A$.

When θ is real, an attenuation exists while when θ is imaginary, which occurs when $f_A < f < f_B$, the attenuation is zero and only a phase shift occurs. The curves of Fig. 2.11 show the attenuation expressed in nepers (neper = 8.686 db) and the phase shift expressed in radians. When $1 \gtrless m \gtrless \infty$, the peak occurs below the band as shown in Fig. 2.11 for several values of m . When $\frac{f_A}{f_B} \gtrless m \gtrless 1$, there is no peak on either side but a finite attenuation at all frequencies. This is illustrated by the

dash line in Fig. 2.11 which shows the characteristic for $m = \sqrt{f_A/f_B}$.

All of the constants of the filter can be determined when Z_{I_0} , the characteristic impedance at the mean frequency $\sqrt{f_A f_B}$,

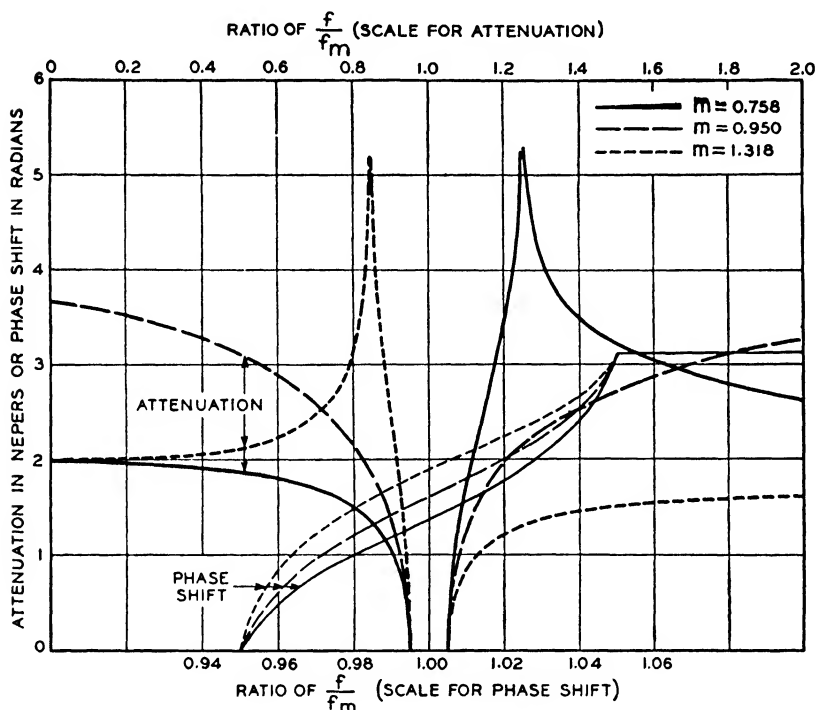


FIG. 2.11—TYPICAL BAND-PASS ATTENUATION AND PHASE CHARACTERISTICS.

the two cut-off frequencies f_A and f_B , and the value of m are given. From (2.70) and (2.71)

$$\begin{aligned}
 Z_{I_0} &= \frac{1}{2\pi} \sqrt{\frac{-1}{f_A f_B C_1 C_2} \left(1 - \frac{f_A f_B}{f_A^2}\right) \left(1 - \frac{f_A f_B}{f_B^2}\right)} \\
 &= \frac{1}{2\pi \sqrt{C_1 C_2}} \left(\frac{f_B - f_A}{f_A f_B} \right) \quad (2.74)
 \end{aligned}$$

$$f_A = \frac{1}{2\pi \sqrt{L_1 C_1}}; \quad f_B = \frac{1}{2\pi \sqrt{L_2 C_2}}; \quad m = \sqrt{\frac{C_2}{C_1}}.$$

Solving for the elements of the filter we find

$$\begin{aligned} L_1 &= \frac{Z_{I_0} f_B m}{2\pi f_A (f_B - f_A)}; \quad L_2 = \frac{Z_{I_0} f_A}{2\pi f_B m (f_B - f_A)}; \\ C_1 &= \frac{(f_B - f_A)}{2\pi Z_{I_0} f_A f_B m}; \quad C_2 = \frac{m(f_B - f_A)}{2\pi Z_{I_0} f_A f_B}. \end{aligned} \quad (2.75)$$

The three other networks of Fig. 2.10 will give the same transfer constant as the one discussed but different image impedances. For these networks we have respectively

$$\begin{aligned} \tanh \frac{\theta}{2} &= m \sqrt{\frac{(1 - \omega^2/\omega_A^2)}{(1 - \omega^2/\omega_B^2)}}; \\ Z_I &= \sqrt{\frac{-\omega^2 L_1 L_2}{(1 - \omega^2/\omega_A^2)(1 - \omega^2/\omega_B^2)}}; \quad m = \sqrt{\frac{L_1}{L_2}} \\ \tanh \frac{\theta}{2} &= m \sqrt{\frac{(1 - \omega^2/\omega_A^2)}{(1 - \omega^2/\omega_B^2)}}; \\ Z_I &= \sqrt{\frac{-1}{\omega^2 C_1 C_2} \frac{(1 - \omega^2/\omega_A^2)}{(1 - \omega^2/\omega_B^2)}}; \quad m = \sqrt{\frac{C_2}{C_1}} \\ \tanh \frac{\theta}{2} &= m \sqrt{\frac{(1 - \omega^2/\omega_A^2)}{(1 - \omega^2/\omega_B^2)}}; \\ Z_I &= \sqrt{-\omega^2 L_1 L_2 \frac{(1 - \omega^2/\omega_B^2)}{(1 - \omega^2/\omega_A^2)}}; \quad m = \sqrt{\frac{L_1}{L_2}}. \end{aligned} \quad (2.76)$$

The design constants of the network of Fig. 2.10B are given in equation (2.77). The other two are left as exercises for the reader.

$$\begin{aligned} L_1 &= \frac{Z_{I_0} m (f_B - f_A)}{2\pi f_A f_B}; \quad L_2 = \frac{Z_{I_0} (f_B - f_A)}{2\pi m f_A f_B}; \\ C_1 &= \frac{f_A}{2\pi f_B (f_B - f_A) m Z_{I_0}}; \quad C_2 = \frac{m f_B}{2\pi f_A (f_B - f_A) Z_{I_0}}. \end{aligned} \quad (2.77)$$

All of the networks of Fig. 2.10 can be reduced to T or π form for certain ranges of the parameter m by employing the

network relations of Fig. 2.9. For example if $m < 1$, then for Fig. 2.10A, $L_2 > L_1$; $C_1 > C_2$.

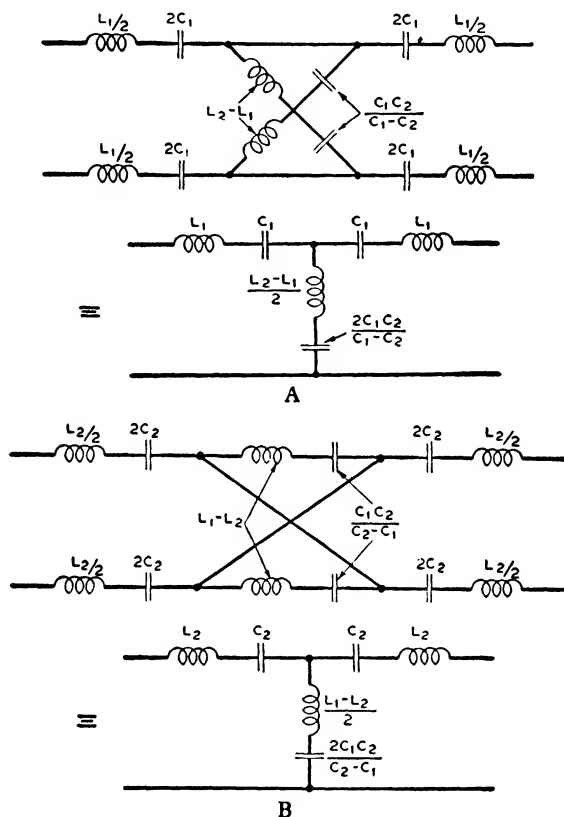


FIG. 2.12—REDUCTION OF LATTICE-TYPE BAND FILTERS TO *T* NETWORK FORM.

Then L_2 and C_2 can be represented by the series combinations

$$L_2 = L_1 + (L_2 - L_1); \quad C_2 = C_1 \frac{\frac{C_1 C_2}{C_1 - C_2}}{C_1 + \frac{C_1 C_2}{C_1 - C_2}} \quad (2.78)$$

where C_2 is C_1 in series with the capacitance $C_1 C_2 / (C_1 - C_2)$. Then L_1 and C_1 can be placed in series with the arms of the lattice leaving the network shown in Fig. 2.12A. From the

values given in (2.75) the shunt elements are found to be

$$\frac{L_2 - L_1}{2} = \frac{Z_{I_0}(f_A^2 - f_B^2 m^2)}{4\pi f_A f_B m(f_B - f_A)}; \quad \frac{2C_1 C_2}{C_1 - C_2} = \frac{(f_B - f_A)m}{\pi f_A f_B Z_{I_0}(1 - m^2)}. \quad (2.79)$$

This combination is realizable for all values of m from

$$0 \leq m \leq \frac{f_A}{f_B}.$$

In case $m = f_A/f_B$, the inductance vanishes giving a capacitance

$$C = \frac{1}{\pi Z_{I_0}(f_A + f_B)}. \quad (2.80)$$

In case $m > 1$, $L_1 > L_2$ and $C_2 > C_1$. For this case we take out L_2 and C_2 leaving the network shown in Fig. 2.12B. The shunt elements have the value

$$\frac{L_1 - L_2}{2} = \frac{Z_{I_0}(f_B^2 m^2 - f_A^2)}{4\pi f_A f_B m(f_B - f_A)}; \quad \frac{2C_1 C_2}{C_2 - C_1} = \frac{(f_B - f_A)m}{\pi f_A f_B Z_{I_0}(m^2 - 1)}. \quad (2.81)$$

These elements are realizable for all values of $m > 1$. In case $m = 1$, the shunt capacitance becomes infinite leaving only a coil having the value

$$\frac{Z_{I_0}(f_A + f_B)}{4\pi f_A f_B}. \quad (2.82)$$

Hence one can realize in ladder form the characteristics of the lattice filter except for the values of m between

$$\frac{f_A}{f_B} < m < 1.$$

In a similar manner one can realize in ladder form the characteristics of the lattice filters of Figs. 2.10B, C and D, but this is left as an exercise for the reader.

We next consider the simplest types of low-pass, high-pass, and all-pass filters which can be obtained in lattice form. These can readily be obtained from the band-pass filter of Fig. 2.10

by letting $f_A \rightarrow 0$, $f_B \rightarrow \infty$, or $f_A \rightarrow 0$ and $f_B \rightarrow \infty$. Considering first the low-pass filter, we have

$$\begin{aligned} \tanh \frac{\theta}{2} &= f_A \xrightarrow{\lim} 0 \left(m \sqrt{\frac{1 - \omega^2/\omega_A^2}{1 - \omega^2/\omega_B^2}} \right) \\ &= f_A \xrightarrow{\lim} 0 \left(\sqrt{\frac{1 - \omega_\infty^2/\omega_B^2}{1 - \omega_\infty^2/\omega_A^2}} \sqrt{\frac{1 - \omega^2/\omega_A^2}{1 - \omega^2/\omega_B^2}} \right) \\ &= \sqrt{1 - \omega_B^2/\omega_\infty^2} \sqrt{\frac{-\omega^2/\omega_B^2}{1 - \omega^2/\omega_B^2}}. \end{aligned} \quad (2.83)$$

For a low-pass filter, the multiplying constant m is defined as

$$m_{\text{low-pass}} = \sqrt{1 - \omega_B^2/\omega_\infty^2}. \quad (2.84)$$

The four structures of Fig. 2.10, reduce to the two structures of Fig. 2.13, when $f_A \rightarrow 0$, which have respectively the image impedances

$$Z_I = \sqrt{\frac{L_1}{C_2} \left(1 - \frac{\omega^2}{\omega_B^2} \right)}; \quad Z_I = \sqrt{\frac{L_2}{C_1} \left(\frac{1}{1 - \omega^2/\omega_B^2} \right)}. \quad (2.85)$$

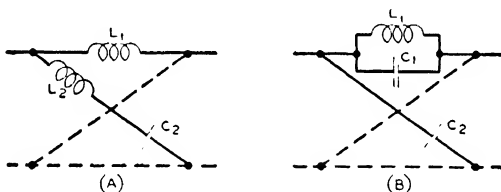


FIG. 2.13—LATTICE-TYPE LOW-PASS FILTERS.

Introducing the value of m into the design equations (2.75) and letting $f_A \rightarrow 0$, we find the resulting constants

$$L_1 = \frac{Z_{I_0} m}{2\pi f_B}; \quad L_2 = \frac{Z_{I_0}}{2\pi m f_B}; \quad C_1 = \infty; \quad C_2 = \frac{m}{2\pi Z_{I_0} f_B} \quad (2.86)$$

where m is defined as in (2.84). For the type of Fig. 2.13B, introducing the value of m into the design equations (2.77) and letting $f_A \rightarrow 0$, we have

$$L_1 = \frac{Z_{I_0} m}{2\pi f_B}; \quad L_2 = \infty; \quad C_1 = \frac{1}{2\pi m Z_{I_0} f_B}; \quad C_2 = \frac{m}{2\pi Z_{I_0} f_B}. \quad (2.87)$$

Since for all possible values of the peak frequency f_∞ , $m \geq 1$, these filters can be realized in ladder form as shown on Fig. 2.14.

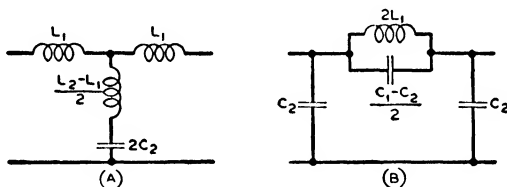


FIG. 2.14—LADDER TYPE LOW-PASS FILTERS.

The high-pass filter can be obtained from the band-pass by letting $f_B \rightarrow \infty$. For this case

$$\begin{aligned} \tanh \frac{\theta}{2} &= \lim_{f_B \rightarrow \infty} \left[\sqrt{\frac{1 - \omega_\infty^2/\omega_B^2}{1 - \omega_\infty^2/\omega_A^2}} \sqrt{\frac{1 - \omega^2/\omega_A^2}{1 - \omega^2/\omega_B^2}} \right] \\ &= \frac{1}{\sqrt{1 - \omega_\infty^2/\omega_A^2}} \sqrt{1 - \omega^2/\omega_A^2}. \end{aligned} \quad (2.88)$$

For the high-pass case the parameter m is defined by

$$m = \frac{1}{\sqrt{1 - \omega_\infty^2/\omega_A^2}} \text{ and lies between } 1 \leq m < \infty. \quad (2.89)$$

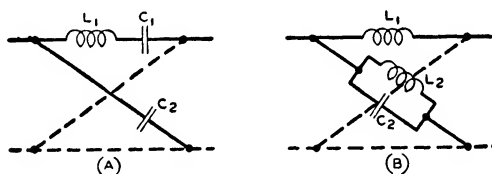


FIG. 2.15—LATTICE-TYPE HIGH-PASS FILTERS.

The four structures of Fig. 2.10 reduce to the two of Fig. 2.15 when $f_B \rightarrow \infty$, and these have respectively the image impedances

$$Z_I = \sqrt{\frac{-(1 - \omega^2/\omega_A^2)}{\omega^2 C_1 C_2}}; \quad Z_I = \sqrt{\frac{-\omega^2 L_1 L_2}{1 - \omega^2/\omega_A^2}}. \quad (2.90)$$

The design equations for the two types are respectively

$$L_1 = \frac{Z_{I_0} m}{2\pi f_A}; L_2 = 0; C_1 = \frac{1}{2\pi m Z_{I_0} f_A}; C_2 = \frac{m}{2\pi Z_{I_0} f_A} \quad (A) \quad (2.91)$$

$$L_1 = \frac{Z_{I_0} m}{2\pi f_A}; L_2 = \frac{Z_{I_0}}{2\pi m f_A}; C_1 = 0; C_2 = \frac{m}{2\pi f_A Z_{I_0}} \quad (B)$$

These can be realized in the ladder networks shown in Fig. 2.16A and B for all values of m .

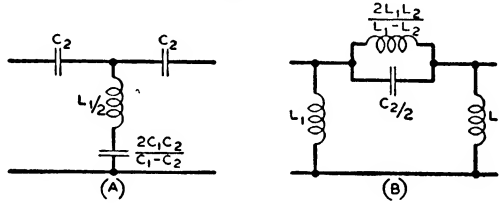


FIG. 2.16—LADDER-TYPE HIGH-PASS FILTERS.

For the all-pass filter $f_A \rightarrow 0; f_B \rightarrow \infty$. This gives

$$\begin{aligned} \tanh \frac{\theta}{2} &= \lim_{f_A \rightarrow 0} \left[\sqrt{\frac{1 - \omega_\infty^2 / \omega_B^2}{1 - \omega_\infty^2 / \omega_A^2}} \sqrt{\frac{1 - \omega^2 / \omega_A^2}{1 - \omega^2 / \omega_B^2}} \right] \\ &= \frac{1}{\sqrt{-\omega_\infty^2}} \sqrt{-\omega^2}. \quad (2.92) \end{aligned}$$

Since there is no peak in the pass band ω_∞ must be imaginary or this becomes

$$\tanh \frac{\theta}{2} = m \sqrt{-\omega^2} \quad \text{where} \quad m = \frac{1}{\sqrt{-\omega_\infty^2}} = \frac{1}{\omega_\alpha} = \frac{1}{2\pi f_\alpha} \quad (2.93)$$

where f_α is a real frequency. The only network which will realize this condition is shown in Fig. 2.17. From either equation (2.75) or (2.77) we find

$$L_1 = \frac{Z_{I_0}}{2\pi f_\alpha}; C_2 = \frac{1}{2\pi f_\alpha Z_{I_0}};$$

$$Z_{I_0} = \sqrt{\frac{L_1}{C_2}}.$$

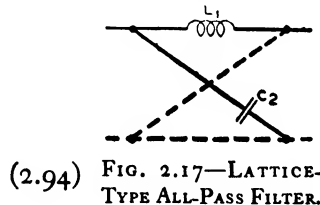


FIG. 2.17—LATTICE-TYPE ALL-PASS FILTER.

This network can be realized only in lattice form. All these types of networks are the simplest type possible and are designated as the elementary sections. Each section has 180° phase shift from one band edge to the other, and has a possibility of one attenuation peak.

In the discussion of simple filter sections we have so far limited the discussion to those sections which utilize all of their elements in increasing the image attenuation and none of them in improving the image impedance. As a result the image impedances are of the "constant K " type which for a band-pass filter are given by equation (2.76), for a low-pass by equation (2.85) and for a high-pass by equation (2.90). In general these "constant K " type image impedances are impedances which are not very constant across the entire pass band of the filter. As a result rather large reflection losses are encountered near the edges of the pass band which in general tend to limit the selectivity of the filter. For this reason impedance elements are often devoted solely to the purpose of improving the image impedance characteristic.

The lattice type filter is especially advantageous for this purpose since the image attenuation and the image impedance can be separately controlled. This follows from the fact that the transfer constant θ and image impedance Z_I are given by the equation

$$\theta = 2 \tanh^{-1} \sqrt{\frac{Z_1}{Z_2}}; \quad Z_I = \sqrt{Z_1 Z_2} \quad (2.56)$$

where Z_1 and Z_2 are the impedances of the series and lattice arms respectively. Then since the transfer constant is determined by the ratio and the image impedance by the product of these two impedances, these two quantities can be separately controlled.

An example of a band-pass filter section which has an attenuation equivalent to a simple filter section but a different characteristic impedance is shown in Fig. 2.18. This filter has two resonance circuits in parallel for each arm. The reactance of the series arm is shown by the full line while the reactance of

the lattice arm is shown by the dotted line. The reactances of both arms coincide at f_1 and at f_4 . Since the reactances of the

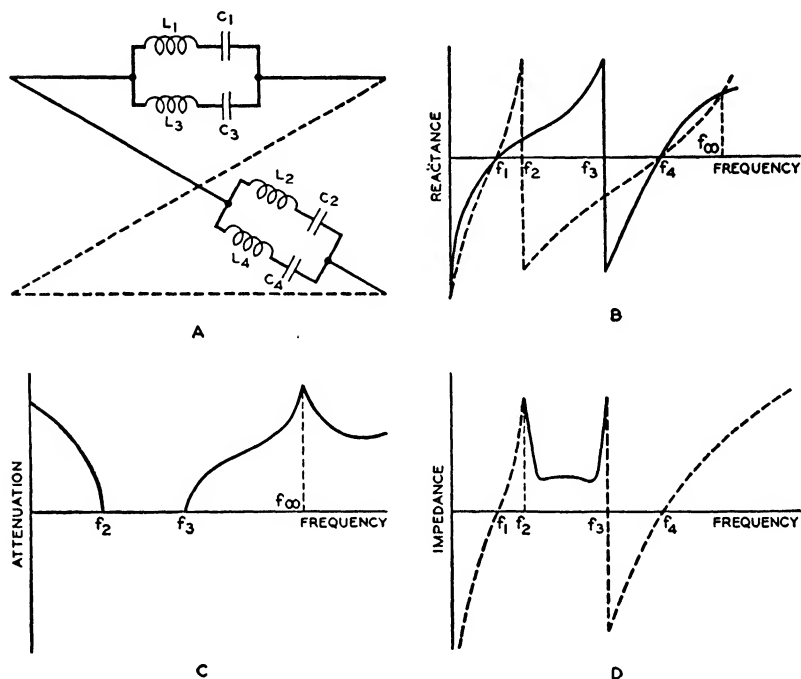


FIG. 2.18—SIMPLE BAND-PASS FILTER WITH IMPEDANCE CORRECTION.

arms are opposite from f_2 to f_3 and of the same sign everywhere else there will be a pass band from f_2 to f_3 and an attenuation band at all other frequencies. The impedances of the two arms can be written

$$\begin{aligned}
 Z_1 &= \frac{-j}{\omega(C_1 + C_3)} \left[\frac{\left(1 - \frac{\omega^2}{\omega_1^2}\right) \left(1 - \frac{\omega^2}{\omega_4^2}\right)}{1 - \frac{\omega^2}{\omega_3^2}} \right]; \\
 Z_2 &= \frac{-j}{\omega(C_2 + C_4)} \left[\frac{\left(1 - \frac{\omega^2}{\omega_1^2}\right) \left(1 - \frac{\omega^2}{\omega_4^2}\right)}{1 - \frac{\omega^2}{\omega_2^2}} \right].
 \end{aligned} \tag{2.95}$$

Hence the transfer constant θ is given by the equation

$$\tanh \frac{\theta}{2} = \sqrt{\frac{Z_1}{Z_2}} = \sqrt{\left(\frac{C_2 + C_4}{C_1 + C_3}\right) \frac{(1 - \omega^2/\omega_2^2)}{(1 - \omega^2/\omega_3^2)}} = m \sqrt{\frac{1 - \omega^2/\omega_A^2}{1 - \omega^2/\omega_B^2}} \quad (2.96)$$

since ω_2 is the lower cutoff ω_A , and ω_3 the upper cutoff ω_B . This is the same form as the second equation of (2.76) and hence by adjusting the ratio $(C_2 + C_4)/(C_1 + C_3)$, the point of infinite attenuation can be made to come at any desired point. The image attenuation is equal to that for one simple section.

The image impedance, however, will be different from the constant K type given previously, for the image impedance will be

$$Z_I = \sqrt{Z_1 Z_2} \\ = \sqrt{\frac{-1(1 - \omega^2/\omega_1^2)^2(1 - \omega^2/\omega_4^2)^2}{\omega^2(C_1 + C_3)(C_2 + C_4)(1 - \omega^2/\omega_2^2)(1 - \omega^2/\omega_3^2)}}. \quad (2.97)$$

The resulting image impedance characteristic is shown in Fig. 2.18D. By bringing the critical frequencies f_1 and f_4 close to the cutoff frequencies f_2 and f_3 respectively, the image impedance over the pass band can be made nearly a constant resistance over a region which comprises the whole pass band nearly to the cutoff frequencies. Hence such a filter will give small reflection losses near the cutoff and can be used in very selective filters. If only one side of the filter has to be very selective, it is necessary to use only one extra critical frequency for which the reactances of the two arms coincide.

While this method of impedance correcting a filter is most easily applied to a lattice filter it can also be applied with limitations to ladder filters.⁶ A simple example is the low-pass filter of Fig. 2.14B. For a π section, the image impedance at mid shunt is of the "constant K " type but if we use the T form of the same filter, the image impedance has one disposable critical

⁶ See "Extensions to the Theory and Design of Electrical Wave Filters," O. J. Zobel, B.S.T.J., April 1931, pp. 284-342.

frequency as shown in Fig. 2.19. This figure shows the T network, the equivalent lattice, the reactance characteristics of the two arms, the attenuation characteristic and the image

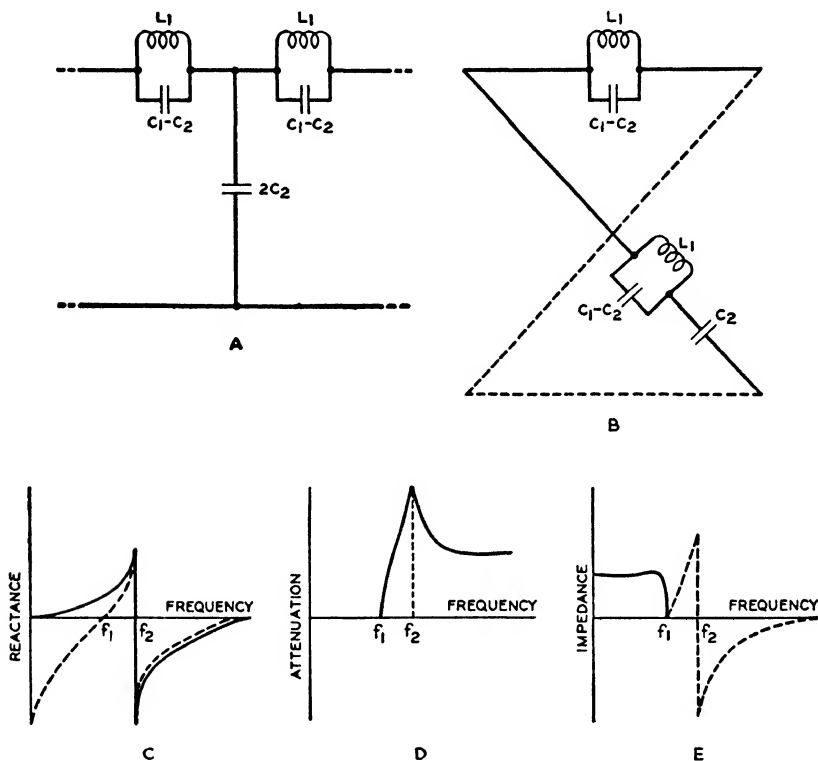


FIG. 2.19—IMPEDANCE CORRECTION APPLIED TO A T NETWORK.

impedance. Since both arms have a common anti-resonant frequency f_2 , the image impedance can be made constant over most of the pass band by bringing f_2 close to f_1 . We note, however, that the frequency of infinite attenuation comes at f_2 and hence the image impedance and attenuation characteristics are not independent in a ladder filter as they are in a lattice filter.

2.6. Multiple Filter Sections

We next consider more complicated filter sections which have image attenuations in one section which are larger than

can be obtained in the simple sections discussed above. Only the attenuation characteristics are discussed since the discussion of image impedances given above is applicable to any type of section. In this section it is shown that the attenuation characteristics of multiple sections will be

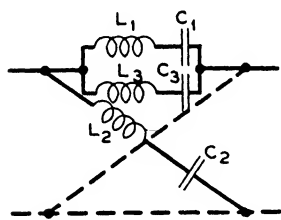


FIG. 2.20—LATTICE-TYPE BAND-PASS FILTER WITH TWO EQUIVALENT SECTIONS.

be the sum of the attenuation characteristics of two or more simple sections.

We consider first filter sections having 360° image phase shift from one cutoff frequency to the other, and a possibility of two attenuation peaks. Such filters can be realized in a variety of ways in a lattice section, but one of the simplest is shown in Fig. 2.20.

The characteristics of this filter can be derived from the impedances of the two arms

$$Z_1 = \frac{-j}{\omega(C_1 + C_3)} \left[\frac{(1 - \omega^2/\omega_A^2)(1 - \omega^2/\omega_B^2)}{1 - \omega^2/\omega_2^2} \right]; \quad (2.98)$$

$$Z_2 = \frac{-j}{\omega C_2} \left[1 - \frac{\omega^2}{\omega_2^2} \right]$$

where $\omega_2^2 = [\omega_A^2 \omega_B^2 (C_1 + C_3) / (\omega_B^2 C_3 + \omega_A^2 C_1)]$.

The resonant frequencies of the $L_1 C_1$ and $L_3 C_3$ arms, respectively, are f_A and f_B , while f_2 is the anti-resonant frequency of the $L_1 C_1$ arm with the $L_3 C_3$ arm. In order to make a single pass band the resonance of the lattice arm has to agree with f_2 . From these impedances we have

$$Z_I = \sqrt{Z_1 Z_2} = \sqrt{\frac{-1}{\omega^2 (C_1 + C_3) C_2} (1 - \omega^2/\omega_A^2)(1 - \omega^2/\omega_B^2)}$$

$$\tanh \frac{\theta}{2} = \sqrt{\frac{Z_1}{Z_2}} = B \sqrt{\left[\frac{(1 - \omega^2/\omega_A^2)(1 - \omega^2/\omega_B^2)}{(1 - \omega^2/\omega_2^2)^2} \right]}$$

where $B = \sqrt{\frac{C_2}{C_1 + C_3}}. \quad (2.99)$

We wish to show now that this type of section has a transfer constant equal to the sum of two of the simpler sections shown in Fig. 2.10. To show this we write

$$\tanh \frac{\theta_1 + \theta_2}{2} = \frac{\tanh \frac{\theta_1}{2} + \tanh \frac{\theta_2}{2}}{1 + \tanh \frac{\theta_1}{2} \tanh \frac{\theta_2}{2}}. \quad (2.100)$$

Substituting the value of $\tanh \theta/2$ given by equation (2.74) in (2.100), and letting the two cutoffs f_A and f_B coincide for the two sections we have

$$\tanh \frac{\theta_1 + \theta_2}{2} = \frac{m_1 + m_2}{1 + m_1 m_2} \sqrt{\frac{(1 - \omega^2/\omega_A^2)(1 - \omega^2/\omega_B^2)}{(1 - \omega^2/\omega_2^2)^2}} \quad (2.101)$$

$$\text{where } \omega_2^2 = \frac{\omega_A^2 \omega_B^2 (1 + m_1 m_2)}{\omega_A^2 + \omega_B^2 m_1 m_2}.$$

Comparing (2.101) with (2.99) we find that

$$\theta = \theta_1 + \theta_2; \quad B = \frac{m_1 + m_2}{1 + m_1 m_2} = \tanh \left[\frac{\theta_{01} + \theta_{02}}{2} \right]. \quad (2.102)$$

We see then that a section with three resonant frequencies can be made to have the same transfer constant as the sum of two simple sections. It is, however, more general since in equations (2.101) and (2.102) real values of ω_2^2 and B can be obtained by taking

$$m_1 = m_r + jm_i; \quad m_2 = m_r - jm_i \quad (2.103)$$

that is the parameter m_1 can be made complex if the second parameter is made its conjugate. Such complex sections can be made to have attenuation peaks which are finite even in the absence of dissipation.

All the data are given for determining the element values of the filter for

$$Z_{I_0} = \frac{f_B - f_A}{2\pi f_A f_B (C_1 + C_3) C_2}; \quad \sqrt{\frac{C_2}{C_1 + C_3}} = \frac{m_1 + m_2}{1 + m_1 m_2};$$

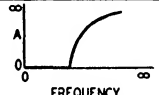
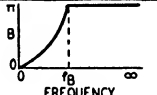
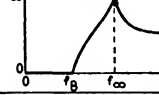
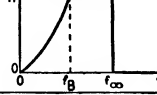
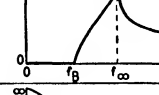
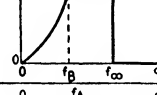

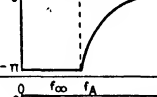
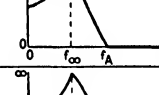
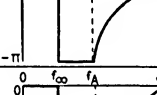
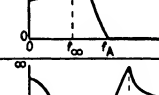

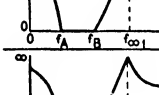
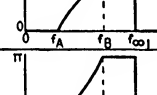
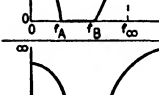
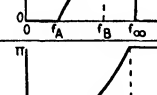
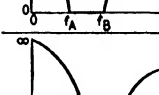

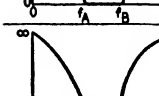
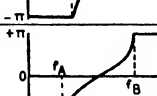
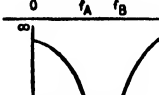

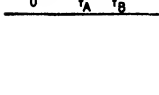
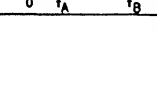
$$\omega_A = \frac{1}{\sqrt{L_1 C_1}} \quad (2.104)$$

$$\omega_B = \frac{1}{\sqrt{L_3 C_3}}; \quad \omega_2 = \frac{1}{\sqrt{L_2 C_2}}; \quad \omega_2 = \omega_A \omega_B \sqrt{\frac{C_1 + C_3}{\omega_A^2 C_1 + \omega_B^2 C_3}}.$$

TABLE I
STANDARD TYPES OF ELECTRICAL WAVE FILTERS

	STRUCTURE	MID SERIES IMAGE IMPEDANCE	MID SHUNT IMAGE IMPEDANCE
1			
2			
3			
4			
5			
6			
7			
8			
9			
10			
11			
12			

TABLE I
STANDARD TYPES OF ELECTRICAL WAVE FILTERS

ATTENUATION	PHASE	ELEMENT VALUES
		$L_1 = \frac{Z_0}{\pi f_B} ; C_2 = \frac{1}{\pi f_B Z_0}$
		$L_1 = \frac{m Z_0}{\pi f_B} ; m = \sqrt{1 - \frac{f_B^2}{f_{\infty}^2}}$ $L_2 = \frac{(1-m^2) Z_0}{4 \pi f_B} ; C_2 = \frac{m}{\pi f_B Z_0}$
		$L_1 = \frac{m Z_0}{\pi f_B} ; C_1 = \frac{1-m^2}{4 \pi f_B Z_0}$ $C_2 = \frac{m}{\pi f_B Z_0} ; m = \sqrt{1 - \frac{f_B^2}{f_{\infty}^2}}$
		$L_2 = \frac{Z_0}{4 \pi f_A} ; C_1 = \frac{1}{4 \pi f_A Z_0}$
		$C_1 = \frac{m}{4 \pi f_A Z_0} ; m = \frac{1}{\sqrt{1 - \frac{f_A^2}{f_{\infty}^2}}}$ $L_2 = \frac{m Z_0}{4 \pi f_A} ; C_2 = \left(\frac{m}{m^2 - 1} \right) \frac{1}{\pi f_A Z_0}$
		$L_1 = \left(\frac{m}{m^2 - 1} \right) \frac{Z_0}{\pi f_A} ; C_1 = \frac{m}{4 \pi f_A Z_0}$ $L_2 = \frac{m Z_0}{4 \pi f_A} ; m = \frac{1}{\sqrt{1 - \frac{f_{\infty}^2}{f_A^2}}}$
		$L_1 = \frac{m Z_0 (f_B - f_A)}{\pi f_A f_B} ; C_1 = \frac{f_A}{4 \pi f_B (f_B - f_A) m Z_0}$ $L_2 = \frac{Z_0 (f_A^2 - m^2 f_B^2)}{4 \pi f_A f_B m (f_B - f_A)} ; C_2 = \frac{(f_B - f_A) m}{\pi f_A f_B Z_0 (1 - m^2)}$
		$L_1 = \frac{Z_0 m (f_A - m^2 f_B) (f_B - f_A)}{\pi f_A^2 f_B (1 - m^2)} ; C_1 = \frac{f_A^2 - m^2 f_B^2}{4 \pi Z_0 m f_B (m^2 f_B + f_A) (f_B - f_A)}$ $L_2 = \frac{Z_0 (m^2 f_B + f_A) (f_B - f_A)}{4 \pi f_A^2 f_B m} ; C_2 = \frac{m f_B}{\pi Z_0 (m^2 f_B + f_A) (f_B - f_A)}$
		$L_1 = \frac{Z_0}{\pi (f_B - f_A)} ; C_1 = \frac{f_B - f_A}{4 \pi f_A^2 Z_0}$ $C_2 = \frac{1}{\pi Z_0 (f_A + f_B)}$
		$L_1 = \frac{f_A Z_0}{\pi f_B (f_B - f_A)} ; C_1 = \frac{f_B - f_A}{4 \pi f_A f_B Z_0}$ $L_2 = \frac{(f_A + f_B) Z_0}{4 \pi f_A f_B} ; C_2 = \frac{1}{\pi (f_B - f_A) Z_0}$
		$L_1 = \frac{Z_0}{\pi (f_B - f_A)} ; C_1 = \frac{f_B - f_A}{4 \pi f_A f_B Z_0}$ $L_2 = \frac{(f_B - f_A) Z_0}{4 \pi f_A f_B} ; C_2 = \frac{1}{\pi (f_B - f_A) Z_0}$
		$L_1 = \frac{Z_0}{\pi f_B} ; L_2 = \frac{Z_0 (f_B^2 - f_A^2)}{4 \pi f_A^2 f_B}$ $C_2 = \frac{f_B}{\pi Z_0 (f_B^2 - f_A^2)}$

This gives six equations for solving for the element values which are

$$C_1 = \frac{(f_B - f_A)}{2\pi f_A f_B Z_{I_0}(m_1 + m_2)}; \quad C_2 = \frac{(f_B - f_A)(m_1 + m_2)}{2\pi f_A f_B Z_{I_0}(1 + m_1 m_2)};$$

$$C_3 = \frac{(f_B - f_A)m_1 m_2}{2\pi f_A f_B Z_{I_0}(m_1 + m_2)} \quad (2.105)$$

$$L_1 = \frac{f_B Z_{I_0}(m_1 + m_2)}{2\pi f_A (f_B - f_A)}; \quad L_2 = \frac{(f_A^2 + m_1 m_2 f_B^2) Z_{I_0}}{2\pi f_A f_B (f_B - f_A)(m_1 + m_2)}$$

$$L_3 = \frac{Z_{I_0}(m_1 + m_2) f_A}{2\pi f_B (f_B - f_A) m_1 m_2}.$$

In a similar manner to that discussed for the simplest section, low-pass, high-pass and all-pass filters can be derived from the band-pass filter for limiting conditions of the band. Equivalent ladder networks may also be derived but due to the more complicated calculations they are not attempted here. A list of the principal filter sections together with their design constants are shown on Table I, pages 52, 53.

More complicated filter sections still can be obtained by adding more series resonant circuits in each arm of the network of Fig. 2.20. Adding a series resonant circuit to the lattice arm of Fig. 2.20 will add another simple filter section and give 540° phase shift in the band and the possibility of three m values for the filter. No more general characteristics can be obtained, however, than can be obtained by adding one of the sections of Fig. 2.10A to the section of Fig. 2.20. Very often in meeting complicated phase and attenuation characteristics it is desirable to design the structure as a complicated multi-resonant lattice filter circuit. All of the common elements can be taken out in series or shunt by employing the relations of Fig. 2.9 and there may remain a residue which cannot be realized in ladder form but has to be left in a balanced lattice form.

2.7. Networks Employing Resistance and Reactance Elements

We have so far discussed filters composed of ideal resistanceless elements and have derived the characteristics of such filter

sections. Although the determination of the effect of dissipation in a filter circuit is a long and tedious process, certain approximate relationships can be derived which materially aid in predicting the effect of dissipation.

In a filter composed of coils and condensers, most of the dissipation occurs in the coils, provided mica, air, or other high-grade dielectrics are used. In a coil the ratio, Q , of reactance to resistance rarely exceeds a value of 300 whereas for mica or air condensers, that value may be as high as 3,000 to 10,000. Hence the resistances associated with the condensers can usually be neglected compared to the coil resistances.

Now if all the resistances associated with the filter can be placed on the ends of the filter either in series or shunt, the distorting effects of these resistances can be eliminated by adjusting the terminal resistances so that the total resistance of the termination plus the coil resistance will be equal to the terminating resistance for the ideal filter. For this case the effect of the terminal resistances will be to add a constant loss to the characteristics of an ideal filter, this loss being independent of the frequency. When such a process can be carried out, the filter is said to be resistance compensated. While this process cannot be applied to many electrical filters it can be applied to a number of the crystal and magnetostrictive filters discussed in Chapter VIII.

One electrical filter for which this process can be carried out is the lattice filter of Fig. 2.10A. The resistances associated with the coils L_1 and L_2 can be taken outside and put in series with the termination by virtue of the equivalence of Fig. 2.9A provided the two resistances are equal. If they are not equal they can be made equal by adding a small ohmic resistance to the smallest one. To determine how much loss these resistances will cause we assume that the m for the filter is greater than 1 so that L_1 will be larger than L_2 . Then Z_{I_0} the terminating impedance of the ideal filter will be

$$Z_{I_0} = \frac{2\pi f_A(f_B - f_A)L_1}{mf_B}. \quad (2.106)$$

If the coil has a ratio of reactance to resistance equal to Q , the resistance in series with the termination due to the coils will be

$$R_C = \frac{2\pi \sqrt{f_A f_B} L_1}{Q}. \quad (2.107)$$

Hence the actual termination for the resistance-compensated filter will be

$$R_T = Z_{I_0} - R_C = \frac{2\pi f_A (f_B - f_A) L_1}{m f_B} \left[1 - \frac{f_B}{f_A} \frac{m \sqrt{f_A f_B}}{(f_B - f_A) Q} \right]. \quad (2.108)$$

The loss caused by the resistance R_C , will be

$$L_{db} = 20 \log_{10} \left| \frac{R_T}{R_T + R_C} \right| = 20 \log_{10} \left[1 - \left(\frac{f_B}{f_A} \right) \frac{m \sqrt{f_A f_B}}{(f_B - f_A) Q} \right]. \quad (2.109)$$

For example for a 5 per cent band width or

$$BW = \frac{f_B - f_A}{\sqrt{f_A f_B}} = 0.05 \quad (2.110)$$

and a value of $m = 1$ the loss for a coil having a Q of 200 is 1.0 *db*. It is obvious from (2.109) that there is a limit to the band-width for which resistance compensation can be carried out given approximately by

$$BW \doteq \frac{m}{Q}. \quad (2.111)$$

Another case for which an approximate formula has been worked out is where all the coils are assumed to have the same resistance to inductance ratio R/L and all the condensers have the same leakance to capacitance ratio G/C . For such a filter it has been shown⁷ that to a first approximation the attenuation and phase in the pass band of the filter are given by

$$A \doteq \left(\frac{R}{2L} + \frac{G}{2C} \right) \frac{\partial B_0}{\partial \omega}; \quad B \doteq B_0 \quad (2.112)$$

where B_0 is the image phase shift of the ideal filter expressed in radians, and A the attenuation of the filter in nepers. Since

⁷ See "Communication Networks," E. A. Guillemin, Vol. II, pp. 445-447, John Wiley.

the attenuation depends on the rate of change of the phase shift with frequency, we see from Fig. 2.11 that a loss distortion will occur near the edges of the band where the slope of the phase curve is greater than it is near the center of the band.

Another type of electrical network employing resistance and reactance elements is the constant resistance attenuation equalizer.⁸ Several forms are shown in Fig. 2.21. These networks

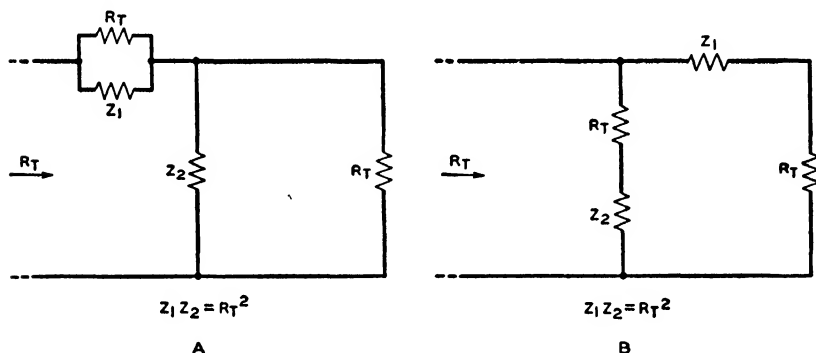


FIG. 2.21—CONSTANT RESISTANCE EQUALIZERS.

have the property that if they are terminated in the proper resistance R_T the impedance looking into them will be R_T at all frequencies. To show this let us consider the L network of Fig. 2.21A. If we work from a sending end resistance R_S and terminate the network in the impedance R_T the currents in the input and output of the network are

$$i_I = \frac{E}{R_S + R_T}; \quad i_0 = \frac{E}{(R_S + R_T) \left(1 + \frac{Z_1}{R_T} \right)}. \quad (2.113)$$

Similar equations hold for the network of Fig. 2.21B. Since the network is terminated in its iterative impedance, the transfer constant θ is given by

$$e^{-\theta} = \frac{i_0}{i_I} = \frac{1}{1 + \frac{Z_1}{R_T}}. \quad (2.114)$$

⁸ See "Transmission Circuits for Telephone Communication," K. S. Johnson, Ch. 18, D. Van Nostrand.

The attenuation constant being the real part of the transfer constant is given by

$$e^{-A} = \left| \frac{1}{1 + \frac{Z_1}{R_T}} \right| = \frac{1}{\sqrt{\left(1 + \frac{R_1}{R_T}\right)^2 + \left(\frac{X_1}{R_T}\right)^2}} \quad (2.115)$$

where R_1 is the resistance component of Z_1 and X_1 the reactance component.

In order to fulfill the condition that $Z_1 Z_2 = R_T^2$, if Z_1 consists of series impedance elements, Z_2 must consist of the inverse type of impedance elements in shunt, having such a value that the products of corresponding impedance elements are equal to R_T^2 . If a given frequency attenuation characteristic is to be obtained, this is usually done by empirically determining element values for Z_1 which will give the closest fit to the desired characteristic.

2.8. *Filter Structures Employing Elements with Distributed Constants*

As higher and higher frequencies are used it becomes more difficult to obtain lumped elements such as coils and condensers. The effect of the interconnecting wires becomes larger and has to be taken into account. In the limiting cases at very high frequencies all of the elements approach straight wires which have the impedance characteristics of electric lines. As a result, at the ultra high frequencies filter structures and transformers are constructed out of sections of lines.

For mechanical vibrations, on account of the much lower velocity of propagation this state of affairs exists for much lower frequencies. In fact, in acoustic networks, where the velocity of propagation is lowest of all, it is difficult to obtain any elements which approach the characteristics of lumped electrical elements such as coils and condensers. Any useful and workable theory of acoustic systems inherently has to deal with elements in which wave motion takes place, and which therefore are analogous to combinations of electric lines. It is the purpose

of the present section to consider the characteristics of filters and transformers constructed from sections of transmission lines.

The equations of a transmission line can be obtained with sufficient accuracy for the purpose by considering that the line is composed of distributed series inductance L , resistance R , shunt capacitance C , and leakance G . In actual practice such lines may be constructed of parallel wires as shown in Fig. 2.22,

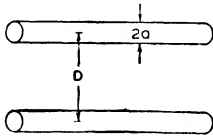


FIG. 2.22—BALANCED TRANSMISSION LINE

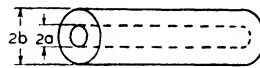


FIG. 2.23—COAXIAL TRANSMISSION LINE.

or coaxial cylindrical conductors as shown in Fig. 2.23. The latter construction has the advantage that it is shielded and will not permit radiation into the surrounding medium nor pick up radiation from it. Consequently coaxial conductors are usually used in high frequency filter and transformer construction.

It is shown in standard works on electromagnetic theory ⁹ that the series resistance, inductance, and capacitance per centimeter length for a copper coaxial conductor are given by the equations

$$R = 41.6 \times 10^{-9} \sqrt{f} \left(\frac{1}{a} + \frac{1}{b} \right) \text{ ohms per centimeter}$$

$$L = 2 \log_e \frac{b}{a} \times 10^{-9} \text{ henries per cm.} \quad (2.116)$$

$$C = \frac{1.11 \times 10^{-12}}{2 \log_e \frac{b}{a}} \text{ farads per cm.}$$

where f is the frequency, b is the inside radius of the outer conductor, and a the outside radius of the inner conductor. The distributed leakance G is usually low and can be neglected when a dry atmosphere is inside the conductor. For a balanced

⁹ "Alternating Currents," A. Russel, Vol. I, Cambridge Press.

transmission line the values of the distributed constants for copper conductors are

$$R = \frac{83.2 \times 10^{-9} \sqrt{f}}{a} \text{ ohms per cm.}$$

$$L = 4 \log_e \frac{D}{a} \times 10^{-9} \text{ henries per cm.} \quad (2.117)$$

$$C = \frac{1.111 \times 10^{-12}}{4 \log_e \frac{D}{a}} \text{ farads per cm.}$$

where a is the radius of each wire, and D the spacing between wires.

The differential equations for a line with distributed constants are

$$\frac{dE}{dx} = -i(j\omega L + R); \quad \frac{di}{dx} = -E(G + j\omega C) \quad (2.118)$$

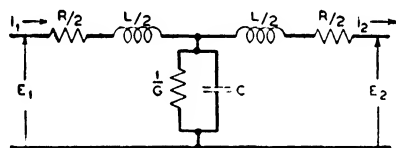


FIG. 2.24—EQUIVALENT LUMPED CIRCUIT FOR A TRANSMISSION LINE.

as can readily be seen from Fig. 2.24 which shows a small section of line of length dx . Equations (2.118) are satisfied by an equation of the form

$$i = Ae^{\theta x} + Be^{-\theta x}. \quad (2.119)$$

Substituting this equation in (2.118) and differentiating we find that it is a solution provided

$$\theta = \sqrt{(R + j\omega L)(G + j\omega C)}. \quad (2.120)$$

A simple and convenient form for writing the resulting equations is to express the voltage and current at some distance x along the line in terms of the initial voltage and current at the

beginning of the line. When $x = 0$, $i_0 = (A + B)$. Differentiating (2.119) we have

$$E = \frac{-A\theta e^{\theta x} + B\theta e^{-\theta x}}{G + j\omega C} = \sqrt{\frac{R + j\omega L}{G + j\omega C}} [-Ae^{\theta x} + Be^{-\theta x}]. \quad (2.121)$$

Hence $E_0 = (-A + B)\sqrt{\frac{R + j\omega L}{G + j\omega C}}$. Introducing the values of

i_0 and E_0 into equations (2.119) and (2.121) we have the two equations for a line

$$i = i_0 \cosh \theta x - \frac{E_0}{\sqrt{\frac{R + j\omega L}{G + j\omega C}}} \sinh \theta x \quad (2.122)$$

$$E = E_0 \cosh \theta x - i_0 \sqrt{\frac{R + j\omega L}{G + j\omega C}} \sinh \theta x$$

since $\cosh \theta x = \frac{e^{\theta x} + e^{-\theta x}}{2}$; $\sinh \theta x = \frac{e^{\theta x} - e^{-\theta x}}{2}$.

Comparing (2.122) with equations (2.33) and noting that E is of opposite sign from E_3 of equation (2.32), we see that $\theta = \sqrt{(R + j\omega L)(G + j\omega C)}$ is the transfer constant for a unit length of the line while

$$Z_0 = \sqrt{\frac{R + j\omega L}{G + j\omega C}} \quad (2.123)$$

is the image impedance of the line.

For all cases of interest $R \ll \omega L$ and $G \ll \omega C$. Hence the following approximation formulae give sufficiently accurate results.

$$\begin{aligned} \theta &= (A + jB) = \sqrt{(R + j\omega L)(G + j\omega C)} \\ &\doteq \frac{1}{2} \left(R \sqrt{\frac{C}{L}} + G \sqrt{\frac{L}{C}} \right) + j\omega \sqrt{LC} \end{aligned} \quad (2.124)$$

$$Z_0 = R + jX = \sqrt{\frac{R + j\omega L}{G + j\omega C}} \doteq \sqrt{\frac{L}{C}} \left[1 - \frac{j}{2} \left(\frac{R}{\omega L} - \frac{G}{\omega C} \right) \right].$$

When the lengths of the lines used to construct filters are small, i.e., less than an eighth of a wavelength, useful results can be obtained by replacing the transmission lines by their equivalent T or π networks. These can be derived by comparing equations (2.51) and (2.52) for T and π networks with equations (2.122) for a line. Solving for the elements of the T and π networks we find, respectively, noting that E_2 is of the opposite sign from E ,

T Network

$$\frac{Z_1}{2} = Z_0 \tanh\left(\frac{\theta x}{2}\right); \quad Z_2 = \frac{Z_0}{\sinh \theta x}$$

π Network

$$Z_1 = Z_0 \sinh \theta x; \quad 2Z_2 = Z_0 \coth \frac{\theta x}{2}. \quad (2.125)$$

When the dissipation is neglected for these lines as is usually done when theoretical filter characteristics are to be obtained, these network elements become

T Network

$$\frac{Z_1}{2} = jZ_0 \tan \frac{Bx}{2}; \quad Z_2 = \frac{-jZ_0}{\sin Bx}$$

π Network

$$Z_1 = jZ_0 \sin Bx; \quad 2Z_2 = -jZ_0 \cot \frac{Bx}{2} \quad (2.126)$$

where B is $\omega \sqrt{LC}$. For short lengths the T network representation is equivalent to two series coils and a shunt condenser having the values

$$L_1 = \frac{\sqrt{L/C} \tan \omega \sqrt{LC} \left(\frac{x}{2}\right)}{\omega} \doteq \frac{Lx}{2}; \quad C_1 = \frac{\sin \omega \sqrt{LC} x}{\omega \sqrt{\frac{L}{C}}} \doteq Cx. \quad (2.127)$$

That is, for short lines, the series inductances are each half the distributed inductance of the section of line while the shunt

capacitance is the total distributed capacitance of the line. This approximation holds within 5 per cent as long as the line length is less than an eighth wavelength. For the π network representation, with the line less than an eighth wavelength, the network consists of two end capacitances and a series inductance having the values

$$C_1 = \frac{\tan \omega \sqrt{LC} (x/2)}{\omega \sqrt{\frac{L}{C}}} \doteq \frac{Cx}{2} ; \quad L_1 = \frac{\sqrt{\frac{L}{C}} \sin \omega \sqrt{LC} x}{\omega} \doteq Lx. \quad (2.128)$$

For this case the two end capacitances are each half the distributed capacitance of the line and the series inductance is the total distributed inductance of the line.

Short sections of lines have been used at single frequencies or narrow frequency ranges as the equivalent of tuned circuits and transformers. For example the input impedance of a short-circuited quarter wave line will have the impedance of an anti-resonant circuit for frequencies near the antiresonant frequency, while a half wave line will act as a series resonant circuit. For the quarter wave line this relation can be shown from (2.122), for the impedance of the line short circuited on the end ($E = 0$) is

$$Z = \frac{E_0}{i_0} = \sqrt{\frac{R + j\omega L}{G + j\omega C}} \tanh \theta l \quad (2.129)$$

where l is the length of the line. Now since $\theta l = (A + jB)l$ where A is the attenuation of the line per unit length and B the phase shift, we have

$$\tanh \theta l = \tanh (A + jB)l = \frac{\tanh Al + j \tan Bl}{1 + j \tanh Al \tan Bl}. \quad (2.130)$$

Near the quarter wavelength frequency, which occurs when

$$Bl = \frac{\pi}{2},$$

$$Bl = \frac{\omega l}{v} = \frac{\omega_A l}{v} \left(1 + \frac{\Delta \omega}{\omega_A} \right) = \frac{\pi}{2} \left(1 + \frac{\Delta \omega}{\omega_A} \right) \quad (2.131)$$

and equation (2.130) can be expanded into the form

$$\tanh \theta l = \frac{\left[1 + \left(\frac{\pi \Delta\omega}{2 \omega_A}\right)^2\right] \tanh Al - j \frac{\pi \Delta\omega}{2 \omega_A} \times \frac{1}{\cosh^2 Al}}{\left(\frac{\pi \Delta\omega}{2 \omega_A}\right)^2 + \tanh^2 Al}. \quad (2.132)$$

This follows since

$$\begin{aligned} \tan Bl = \tan \frac{\pi}{2} \left(1 + \frac{\Delta\omega}{\omega_A}\right) &= \frac{\tan \frac{\pi}{2} + \tan \left(\frac{\pi \Delta\omega}{2 \omega_A}\right)}{1 - \tan \frac{\pi}{2} \tan \left(\frac{\pi \Delta\omega}{2 \omega_A}\right)} \\ &= - \frac{1}{\tan \left(\frac{\pi \Delta\omega}{2 \omega_A}\right)} \doteq - \frac{2}{\pi} \frac{\omega_A}{\Delta\omega} \end{aligned} \quad (2.133)$$

where $\Delta\omega$ is the difference in frequency between the actual frequency f and the antiresonant frequency f_A , multiplied by 2π .

From equations (2.124) the image impedance Z_0 and the attenuation become

$$\begin{aligned} Z_0 &= \sqrt{\frac{R + j\omega L}{G + j\omega C}} \doteq \sqrt{\frac{L}{C}} \left[1 - \frac{j}{2\omega} \left(\frac{R}{L} - \frac{G}{C}\right)\right]; \\ \tanh Al \doteq Al &= \frac{1}{2} \left(R \sqrt{\frac{C}{L}} + G \sqrt{\frac{L}{C}}\right) l. \end{aligned} \quad (2.134)$$

Introducing these expressions into (2.129) we find for the impedance of the line near its quarter wave frequency, to significant powers of $\Delta\omega/\omega_A$

$$Z_L = \frac{\frac{2L}{C} \left[\left(R + \frac{GL}{C}\right) l - j \left(\pi \sqrt{\frac{L}{C}} \frac{\Delta\omega}{\omega_A}\right) \right]}{\left(R + \frac{GL}{C}\right)^2 l^2 + \left(\pi \sqrt{\frac{L}{C}} \frac{\Delta\omega}{\omega_A}\right)^2}. \quad (2.135)$$

If we compare this to the impedance of a coil with series resistance in parallel with a condenser with shunt leakance, we have

$$Z_C = \frac{(R_1 + j\omega L_1) \left(\frac{1}{G_1 + j\omega C_1} \right)}{R_1 + j\omega L_1 + \left(\frac{1}{G_1 + j\omega C_1} \right)}$$

$$= \frac{R_1 + G_1(R_1^2 + \omega^2 L_1^2) - j\omega \left[R_1^2 C_1 - \left(1 - \frac{\omega^2}{\omega_A^2} \right) L_1 \right]}{\left[R_1 G_1 + 1 - \frac{\omega^2}{\omega_A^2} \right]^2 + \omega^2 [L_1 G_1 + R_1 C_1]^2} \quad (2.136)$$

where $\omega_A^2 = \frac{1}{L_1 C_1} = (2\pi f_A)^2$, f_A being the antiresonant frequency of the combination. Near this frequency,

$$\frac{\omega}{\omega_A} = \frac{\omega_A + \Delta\omega}{\omega_A} = \left(1 + \frac{\Delta\omega}{\omega_A} \right). \quad (2.137)$$

Hence the impedance of the coil becomes

$$Z_C = \frac{R_1 + G_1 \left(R_1^2 + \frac{L_1}{C_1} \right) - j \left[R_1^2 \sqrt{\frac{C_1}{L_1}} + \frac{2\Delta\omega}{\omega_A} \sqrt{\frac{L_1}{C_1}} \right]}{\left(R_1 G_1 + \frac{2\Delta\omega}{\omega_A} \right)^2 + \left[\sqrt{\frac{L_1}{C_1}} G_1 + R_1 \sqrt{\frac{C_1}{L_1}} \right]^2}. \quad (2.138)$$

Comparing (2.135) with (2.138), we see that a line near its quarter wavelength point can be represented by a coil L_1 in series with a resistance R_1 paralleled by a condenser C_1 and leakage G_1 having the values

$$L_1 = \frac{8}{\pi^2} (Ll); \quad C_1 = \frac{1}{2} (Cl); \quad R_1 = \frac{8}{\pi^2} (Rl); \quad G_1 = \frac{Gl}{2}. \quad (2.139)$$

Hence the effective Q of the coil L_1 is the same as the Q of the distributed series element while the effective Q or ratio of reactance to resistance of the condenser C_1 the same as the Q of the distributed shunt element.

In a similar way a short-circuited half wavelength line represents a series-tuned circuit having the equivalent lumped values

$$L_1 = \left(\frac{Ll}{2}\right); \quad C_1 = \frac{2}{\pi^2} (Cl); \quad R_1 = \left(\frac{Rl}{2}\right); \quad G_1 = \frac{2}{\pi^2} (Gl). \quad (2.140)$$

In this case also the ratio of reactance to resistance for the equivalent lumped elements is the same as for the distributed elements.

Another use to which lines have been put is as single frequency transformers. One of the simplest of such transformers is the quarter wavelength transformer of image impedance Z_0 , which when terminated in an impedance Z_T will give an input impedance Z_S equal to

$$Z_S = \frac{Z_0^2}{Z_T}. \quad (2.141)$$

This can be shown from equations (2.122) when the dissipation is neglected. For this case the equations become

$$\left. \begin{aligned} i &= i_0 \cos Bl - \frac{jE_0}{Z_0} \sin Bl \\ E &= E_0 \cos Bl - ji_0 Z_0 \sin Bl. \end{aligned} \right\} \quad (2.142)$$

If we terminate the line in Z_T or set $E/i = Z_T$, the ratio of E_0/i_0 becomes

$$Z_S = \frac{E_0}{i_0} = Z_0 \left[\frac{Z_T \cos Bl + jZ_0 \sin Bl}{Z_0 \cos Bl + jZ_T \sin Bl} \right]. \quad (2.143)$$

For a quarter wavelength line, $\cos Bl = 0$; $\sin Bl = 1$, so that

$$Z_S = \frac{Z_0^2}{Z_T} \quad (2.144)$$

and the device acts as a single frequency transformer. At the half wavelength frequency, $\cos Bl = -1$; $\sin Bl = 0$ and the impedance looking into the device is

$$Z_S = Z_T. \quad (2.145)$$

This length has been used to some extent when it is desired to measure the impedance of a system with a device located some distance from the desired impedance.

Lines can also be used in transmission systems which cover wide frequency ranges, in particular in filters and transformers.¹⁰ Using the filter networks of Table I as a basis, the design equations for a number of the simpler ones are easily worked out. In general in such filters transmission lines and condensers only are employed since the Q of electrical coils in this frequency range is inferior to what can be obtained with the

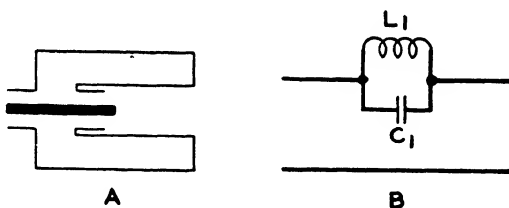


FIG. 2.25—SERIES ELEMENT FORMED FROM FLARED OUTER CONDUCTOR.

other type elements. Shunt elements can be obtained by shunting the main transmission line by a line or a combination of lines and condensers. Series elements such as condensers can be obtained by connecting plates to the two broken ends of the inside conductor of a coaxial transmission line and separating them by a definite distance. Series coils can be obtained by using the distributed inductance of the main transmission line. Salinger¹¹ has recently pointed out that series elements may also be obtained by flaring out the outside conductor, as shown in Fig. 2.25. This requires that all the current flow through the flare before returning to the main conducting line and hence the impedance of the flaring sections will be in series with the line impedance. As an example of a coaxial filter let us consider the band-pass filter shown in Fig. 2.26A which consists of a

¹⁰ A number of such filters and transformers are discussed in a former paper "Filters and Transformers Using Coaxial and Balanced Transmission Lines," W. P. Mason and R. A. Sykes, B.S.T.J., July 1937.

¹¹ "A Coaxial Filter for Vestigial Sideband Transmission in Television," Proc. I.R.E., Nov. 1940, p. 533.

series condenser $2C_1$ on either end of a length of transmission line having an image impedance Z_0 and a transfer constant θ_x . If we use the T network representation of the line, the equivalent circuit is that shown in Fig. 2.26B which is the same as the band-pass filter circuit No. 9 of Table I, pages 52, 53. From these formulae the required constants of the line can be obtained. In case lines longer than an eighth of a wavelength are used, more accurate results can be obtained by using the exact formulae of equation (2.127). Many other filter structures can be constructed using condensers and short sections of lines. A

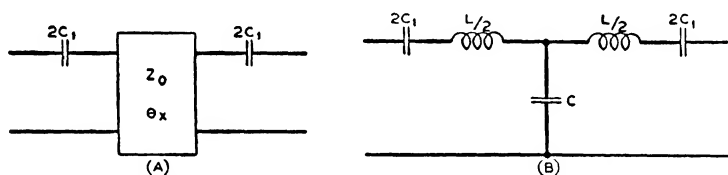


FIG. 2.26—BAND-PASS FILTER EMPLOYING A LINE SECTION WITH SERIES CONDENSERS.

partial list of these is shown on Table II, page 69, together with the design formulae and the characteristics obtainable.

Another use to which short sections of lines and condensers have been put, is in obtaining wide-band transformers. Such transformers have been used in transforming from the high impedance of vacuum tubes such as diodes to the impedance of transmission lines, over a wide frequency range. Such transformers usually have to absorb the capacitance associated with the tubes, and this is usually the limiting factor in the impedance and transformation that can be obtained. One of the simplest and most commonly used transformers of this type is the one shown in Fig. 2.27A. This transformer consists of a series section of line of high impedance joined on another series line of low impedance, with a very short section of short-circuited line of low impedance, connected to them at their junction. On the high impedance end of the transformer, the shunt capacitance of the tube C_A has to be absorbed and a larger capacitance C_B is placed across the low impedance end. The equivalent circuit of the transformer is shown in Fig. 2.27B. The capacitance C_1 consists of the tube capacitance and half

TABLE II
FILTERS CONSTRUCTED FROM SHORT SECTIONS OF LINES AND CONDENSERS

STRUCTURE	EQUIVALENT LUMPED CIRCUIT	ATTENUATION CHARACTERISTIC	ELEMENT VALUES
			$L_0 = \frac{Z_0}{\pi(f_B - f_A)}; C_1 = \frac{f_B - f_A}{4\pi f_A^2 Z_0}; C_0 = \frac{1}{\pi Z_0(f_A + f_B)}$ $Z_0 = \sqrt{\frac{L_0}{C_0}} = Z_0 \sqrt{\frac{f_B + f_A}{f_B - f_A}} \quad 1 = \frac{3 \times 10^{10}}{\pi \sqrt{f_B^2 - f_A^2}} \text{ (CM)}$
			$L_0 = \frac{Z_0}{\pi f_B}; (C_1 + C_0) = \frac{1}{\pi f_B Z_0}$ $Z_0 = \sqrt{\frac{L_0}{C_0}} = \frac{Z_0}{\sqrt{1 - C_1 \pi f_B Z_0}}$ $1 = \frac{3 \times 10^{10}}{\pi f_B} \sqrt{1 - C_1 \pi f_B^2 Z_0} \text{ (CM)}$
			$L_{01} = \frac{Z_{01}}{\pi(f_A + f_B)}; L_{02} = \frac{(f_B - f_A) Z_{01}}{4\pi f_A f_B}$ $\frac{(C_1 + C_{01} + C_{02})}{2} = \frac{1}{2\pi(f_B - f_A) Z_{01}}$ $Z_{01} Z_{02}, L_{01}, \text{ AND } L_{02} \text{ NOT UNIQUELY DETERMINED}$
			$C_1 = \frac{(f_A + f_B)}{4\pi f_A f_B Z_{01}}; (C_2 + C_0) = \frac{f_A}{\pi f_B (f_B - f_A) Z_{01}}$ $L_0 = \frac{(f_B - f_A) Z_{01}}{4\pi f_A f_B}; Z_{01} = \frac{f_A}{f_B} \sqrt{\frac{f_B Z_{01} (f_B - f_A) C_2}{1 - \pi C_2 Z_{01} (f_B - f_A) f_A}}$ $1 = \frac{3 \times 10^{10}}{2\pi f_B} \sqrt{1 - \pi C_2 Z_{01} (f_B - f_A) f_A}$

the distributed capacitance of the first line. The inductance L_1 is the total distributed inductance of the first line, L_2 that of the shunt line, and L_3 that of the second series line. The capacitance C_2 consists of half the distributed capacitances of the three lines added together, while C_3 is the sum of the capacitance C_B and half the distributed capacitance of the second series line. In practice L_2 is a very small inductance and the combination $L_2 C_2$ resonates at a considerably higher frequency

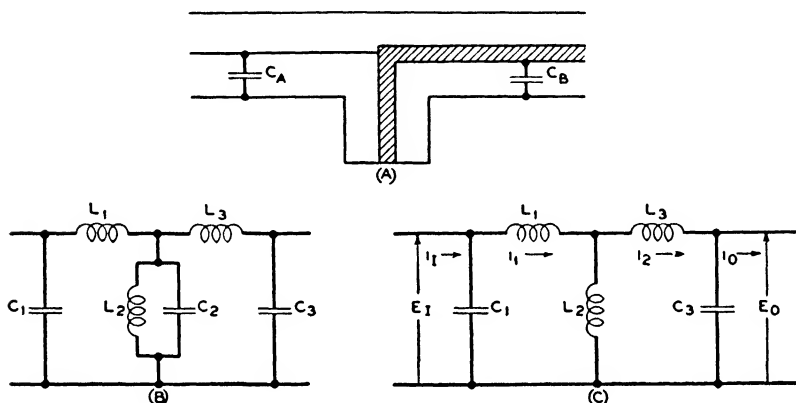


FIG. 2.27—TRANSFORMING BAND-PASS FILTER EMPLOYING LINES AND CONDENSERS.

than the pass band. For this case we can neglect C_2 or compensate for it by making L_2 slightly larger. Hence the network to analyze is Fig. 2.27C. If we write out the network equations for this combination, with the voltages and currents as shown, we find:

$$E_0 = \left(\frac{L_2 + L_3}{L_2} \right) \left[-E_1 \left(1 - \frac{\omega^2 (L_1 L_2 + L_1 L_3 + L_2 L_3) C_1}{L_2 + L_3} \right) - j \frac{i_1 \omega (L_1 L_2 + L_1 L_3 + L_2 L_3)}{L_2 + L_3} \right]$$

$$i_0 = \frac{L_1 + L_2}{L_2} \left[i_1 \left(1 - \omega^2 \frac{(L_1 L_2 + L_1 L_3 + L_2 L_3) C_3}{L_1 + L_2} \right) - j \frac{E_1}{\omega (L_1 + L_2)} \left[1 - \omega^2 ((L_2 + L_3) C_3 + (L_1 + L_2) C_1) + \omega^4 (L_1 L_2 + L_1 L_3 + L_2 L_3) C_1 C_3 \right] \right]. \quad (2.146)$$

Comparing these with the general line parameter equation (2.33) we see that to make the transformation ratio constant over the transformer pass band we must have

$$\frac{C_1}{L_2 + L_3} = \frac{C_3}{L_1 + L_2} \quad \text{or} \quad (L_1 + L_2)C_1 = (L_2 + L_3)C_3. \quad (2.147)$$

Introducing this relation in (2.146) and comparing with (2.33) we have

$$Z_{I_1} = \sqrt{\frac{-\omega^2(L_1L_2 + L_1L_3 + L_2L_3)(L_1 + L_2)}{\left\{ L_2^2(L_2 + L_3)(1 - 2\omega^2(L_2 + L_3)C_3) + \omega^4(L_1L_2 + L_1L_3 + L_2L_3)C_1C_3 \right\}}};$$

$$\frac{Z_{I_1}}{Z_{I_2}} = \frac{L_1 + L_2}{L_2 + L_3} = \varphi^2 \quad (2.148)$$

$$\cosh \theta = \frac{\sqrt{(L_1 + L_2)(L_2 + L_3)}}{L_2} \left(1 - \omega^2 \frac{(L_1L_2 + L_1L_3 + L_2L_3)C_1}{L_2 + L_3} \right).$$

Solving for the element values in terms of the two cutoff frequencies f_A and f_B , and the impedance Z_{I_0} and Z_{I_2} at the mean frequency of the filter, one finds the design formulae

$$L_1 = Z_{I_1} \frac{(f_B - f_A)[f_A^2(1 + \varphi) + f_B^2(1 - \varphi)]}{4\pi f_A^2 f_B^2};$$

$$L_2 = \frac{\sqrt{Z_{I_1}Z_{I_2}}(f_B - f_A)^2(f_A + f_B)}{4\pi f_A^2 f_B^2}$$

$$L_3 = \frac{\sqrt{Z_{I_1}Z_{I_2}}(f_B - f_A)[f_A^2(1 + \varphi) + f_B^2(\varphi - 1)]}{4\pi f_A^2 f_{B_2}} \quad (2.149)$$

$$C_1 = \frac{1}{2\pi(f_B - f_A)Z_{I_1}} \quad C_2 = \frac{1}{2\pi(f_B - f_A)Z_{I_2}}.$$

As an example of the use of such a filter Fig. 2.28 shows the line values for a transformer used to connect a diode with a 1500-ohm resistive impedance shunted by $1 \mu\mu f$, to a 70-ohm transmission line over a 10 per cent frequency band from 522 megacycles to 578 megacycles.

For higher frequencies the approximations used above are not adequate. For these cases we turn to the equations for a

line (2.122) and consider combinations of two equal series lines shunted by an impedance Z_s , which in this case is represented

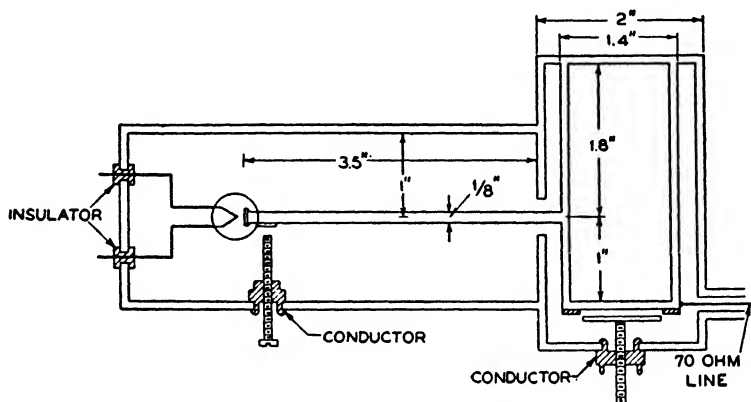


FIG. 2.28—CONSTRUCTION OF TRANSFORMING BAND-PASS FILTER.

by a short-circuited section of line. Then the equations for this combination are, if we neglect dissipation as usual,

$$\begin{aligned}
 i_{12} &= i_1 \cos \frac{\omega l_1}{2v} - j \frac{E_1 \sin \frac{\omega l_1}{2v}}{Z_{01}}; \\
 i_2 &= i_{21} \cos \frac{\omega l_1}{2v} - j \frac{E_{12}}{Z_{01}} \sin \frac{\omega l_1}{2v}; \\
 E_{12} &= E_1 \cos \frac{\omega l_1}{2v} - j i_1 Z_{01} \sin \frac{\omega l_1}{2v}; \\
 E_2 &= E_{12} \cos \frac{\omega l_1}{2v} - j i_2 Z_{01} \sin \frac{\omega l_1}{2v}; \\
 i_{12} - i_{21} &= \frac{E_{12}}{Z_s}
 \end{aligned} \tag{2.150}$$

where $Z_{01} = \sqrt{\frac{L}{C}}$ = image impedance of the two equal lines.

$v = \frac{1}{\sqrt{LC}}$ = the velocity of propagation, L and C the distributed inductance and capacitance per cm. length of the line, and

Z_s the shunt impedance introduced in this case by the shunt short-circuited line. Eliminating all terms except the first and last we have

$$\begin{aligned}
 i_2 &= i_1 \left[\cos \frac{\omega l_1}{v} + j \frac{Z_{01}}{2Z_s} \sin \frac{\omega l_1}{v} \right] \\
 &\quad - j \frac{E_1}{Z_{01}} \left[\sin \frac{\omega l_1}{v} - j \frac{Z_{01}}{Z_s} \cos^2 \frac{\omega l_1}{2v} \right] \\
 E_2 &= E_1 \left[\cos \frac{\omega l_1}{v} + j \frac{Z_{01}}{2Z_s} \sin \frac{\omega l_1}{v} \right] \\
 &\quad - j i_1 Z_{01} \left[\sin \frac{\omega l_1}{v} + j \frac{Z_{01}}{Z_s} \sin^2 \frac{\omega l_1}{2v} \right].
 \end{aligned} \tag{2.151}$$

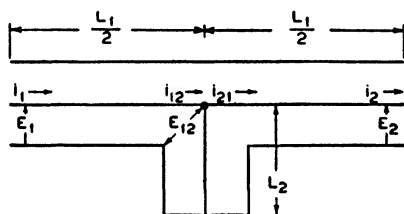


FIG. 2.29—BAND FILTER CONSTRUCTED FROM TRANSMISSION LINES.

Comparing with equation (2.33) and noting that E_2 of (2.151) is of opposite sign to E_3 in (2.33) we have

$$\begin{aligned}
 \cosh \theta &= \left(\cos \frac{\omega l_1}{v} + j \frac{Z_{01}}{2Z_s} \sin \frac{\omega l_1}{v} \right); \\
 Z_1 &= Z_{01} \sqrt{\frac{\sin \frac{\omega l_1}{v} + j \frac{Z_{01}}{Z_s} \sin^2 \frac{\omega l_1}{2v}}{\sin \frac{\omega l_1}{v} - j \frac{Z_{01}}{Z_s} \cos^2 \frac{\omega l_1}{2v}}}.
 \end{aligned} \tag{2.152}$$

The type of filter obtained depends on the shunt impedance Z_s . For the short-circuited line of Fig. 2.29 the impedance Z_s is

$$Z_s = jZ_{02} \tan \frac{\omega l_2}{v}. \tag{2.153}$$

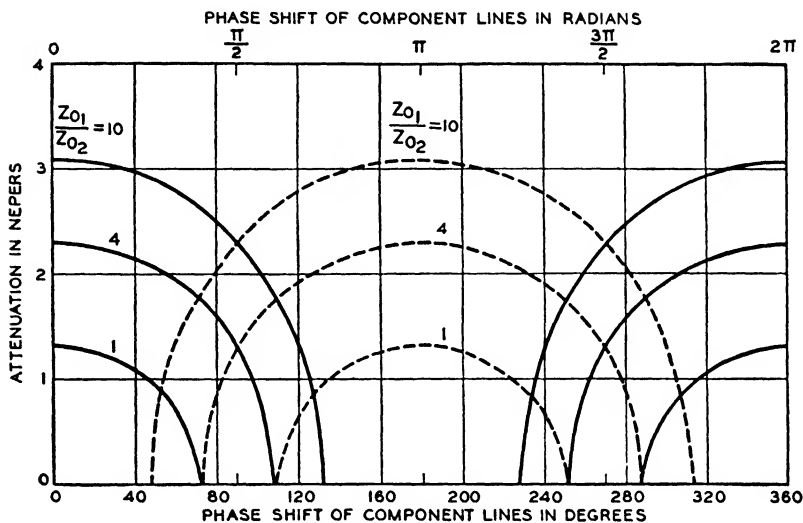


FIG. 2.30—ATTENUATION CHARACTERISTIC OF TRANSMISSION LINE BAND-PASS FILTER.

Introducing this into (2.152) we have

$$\cosh \theta = \cos \frac{\omega l_1}{v} + \frac{Z_{01}}{2Z_{02}} \frac{\sin \frac{\omega l_1}{v}}{\tan \frac{\omega l_2}{v}}; \quad (2.154)$$

$$Z_I = Z_{01} \sqrt{\frac{1 + \frac{Z_{01}}{2Z_{02}} \frac{\tan \frac{\omega l_1}{2v}}{\tan \frac{\omega l_2}{v}}}{1 - \frac{Z_{01}}{2Z_{02}} \frac{\cot \frac{\omega l_2}{2v}}{\tan \frac{\omega l_2}{v}}}}.$$

Figure 2.30 shows a calculation of the real part of the transfer constant θ when $l_2 = \frac{l_1}{2}$ for several values of the ratio Z_{01}/Z_{02} . The resulting filter is a band-pass filter with bands occurring when the length l_1 is an odd half wavelength. To get a narrow

band it is necessary to make the characteristic impedance Z_{0_2} small compared to Z_{0_1} the line impedance. If in place of a short-circuited shunt line we introduce an open-circuited line in shunt, the resulting characteristic is shown by the dotted lines of Fig. 2.30. For this case a low- and band-pass filter results with the mid frequency of the pass band coming when the length l_1 is an integral (including zero) number of wavelengths.

Another method of obtaining filters by combinations of lines is to connect line sections of different characteristic impedances

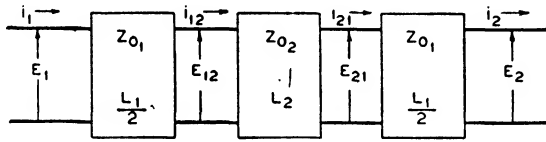


FIG. 2.31—BAND-PASS FILTER FORMED FROM TRANSMISSION LINES IN TANDEM.

together. This corresponds in the mechanical case to a stratified medium, with the different layers having different impedances and velocities of propagation. This type of filter can be analyzed by considering the combinations of lines shown in Fig. 2.31. The equations for the separate lines are

$$\begin{aligned}
 E_{12} &= E_1 \cos \frac{\omega l_1}{2v} - j i_1 Z_{0_1} \sin \frac{\omega l_1}{2v}; \\
 E_{21} &= E_{12} \cos \frac{\omega l_2}{v} - j i_{12} Z_{0_2} \sin \frac{\omega l_2}{v}; \\
 i_{12} &= i_1 \cos \frac{\omega l_1}{2v} - j \frac{E_1}{Z_{0_1}} \sin \frac{\omega l_1}{2v}; \\
 i_{21} &= i_{12} \cos \frac{\omega l_2}{v} - j \frac{E_{12}}{Z_{0_2}} \sin \frac{\omega l_2}{v}; \\
 E_2 &= E_{21} \cos \frac{\omega l_1}{2v} - j i_{21} Z_{0_1} \sin \frac{\omega l_1}{2v}; \\
 i_2 &= i_{21} \cos \frac{\omega l_1}{2v} - j \frac{E_{21}}{Z_{0_1}} \sin \frac{\omega l_1}{2v}.
 \end{aligned} \tag{2.155}$$

Combining these equations we have the network equations

$$\begin{aligned}
 E_2 &= E_1 \left[\cos \frac{\omega l_1}{v} \cos \frac{\omega l_2}{v} - \left(\frac{Z_{01} + \frac{Z_{02}}{Z_{01}}}{2} \right) \sin \frac{\omega l_1}{v} \sin \frac{\omega l_2}{v} \right] \\
 &\quad - j i_1 Z_{01} \left[\sin \frac{\omega l_1}{v} \cos \frac{\omega l_2}{v} + \left(\frac{Z_{02}}{Z_{01}} \cos^2 \frac{\omega l_1}{2v} - \frac{Z_{01}}{Z_{02}} \sin^2 \frac{\omega l_1}{2v} \right) \sin \frac{\omega l_2}{v} \right] \\
 i_2 &= i_1 \left[\cos \frac{\omega l_1}{v} \cos \frac{\omega l_2}{v} - \left(\frac{Z_{01} + \frac{Z_{02}}{Z_{01}}}{2} \right) \sin \frac{\omega l_1}{v} \sin \frac{\omega l_2}{v} \right] \quad (2.156) \\
 &\quad - j \frac{E_1}{Z_{01}} \left[\sin \frac{\omega l_1}{v} \cos \frac{\omega l_2}{v} + \sin \frac{\omega l_2}{v} \left(\frac{Z_{01}}{Z_{02}} \cos^2 \frac{\omega l_1}{2v} - \frac{Z_{02}}{Z_{01}} \sin^2 \frac{\omega l_1}{2v} \right) \right].
 \end{aligned}$$

For the simplest and most useful case where $l_1 = l_2 = l$, the transfer constant and characteristic impedance become

$$\begin{aligned}
 \cosh \theta &= \cos^2 \frac{\omega l}{v} - \left(\frac{Z_{01} + \frac{Z_{02}}{Z_{01}}}{2} \right) \sin^2 \frac{\omega l}{v}; \\
 Z_I &= Z_{01} \sqrt{\frac{Z_{02} \cos^2 \frac{\omega l}{2v} - Z_{01} \sin^2 \frac{\omega l}{2v}}{Z_{01} \cos^2 \frac{\omega l}{2v} - Z_{02} \sin^2 \frac{\omega l}{2v}}}. \quad (2.157)
 \end{aligned}$$

A plot of the attenuation characteristic for several values of the factor $\frac{1}{2} \left[\frac{Z_{01}}{Z_{02}} + \frac{Z_{02}}{Z_{01}} \right]$ is shown in Fig. 2.32. As a filter this combination is a low- and band-pass filter. The centers of the pass bands come when

$$\frac{\omega l}{v} = 0, \pi, 2\pi, 3\pi, \text{ etc.}$$

At zero frequency and the mid frequency of the second and alternate pass bands the image impedance is $Z_{I_0} = \sqrt{Z_{01} Z_{02}}$. For the first low-pass band and every alternate band above that, the image impedance at the center of the band is $Z_{I_1} = Z_{01} \sqrt{Z_{01}/Z_{02}}$.

The stratified medium type of filter has been used as a transforming network in reducing the reflection of light from glass and other transparent objects. The propagation of plane

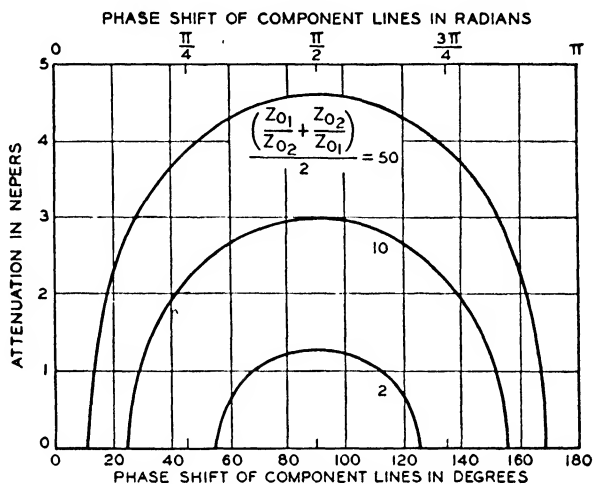


FIG. 2.32—ATTENUATION CHARACTERISTIC OF TANDEM LINE BAND-PASS FILTER.

waves of light are governed by equations similar to those for an electric wave. The velocity of propagation and the image impedance for the medium are given by

$$v = \frac{1}{\sqrt{\mu K}}; \quad Z_0 = \sqrt{\frac{\mu}{K}} = \mu v \quad (2.158)$$

where μ is the permeability and K the dielectric constant of the medium. Since all the materials used in light propagation have the same permeability as air, the ratio between the impedance of air and the impedance of the medium is

$$\frac{Z_{0A}}{Z_{0m}} = \frac{\mu v_A}{\mu v_m} = \frac{v_A}{v_m} = n \quad (2.159)$$

where n is called the index of refraction. The index of refraction of most glasses is around 1.6. Hence by equation (2.39) there will be a reflection of energy when the wave goes from air to glass. The reflection factor of (2.39) is a current reflection

factor and has to be squared to get the power or intensity reflection factor. For an index of refraction of 1.6 the power reflected will be

$$R_p = \left[\frac{Z_{0A} - Z_{0m}}{Z_{0A} + Z_{0m}} \right]^2 = \left[\frac{\frac{Z_{0A}}{Z_{0m}} - 1}{\frac{Z_{0A}}{Z_{0m}} + 1} \right]^2 = \left(\frac{n - 1}{n + 1} \right)^2 = 0.0533 \quad (2.160)$$

for $n = 1.6$. Hence over 5 per cent of the light intensity is reflected from glass.

The simplest means for reducing this reflection is to use¹² a quarter wave plate of a material whose index of refraction is equal to the square root of that for the glass. This use of a quarter wave plate is entirely similar to the use of a quarter wavelength transmission line for impedance transformation as discussed in equation (2.143). Furthermore, we see from equation (2.143) that such a plate will reduce the reflection over a considerable frequency range, for the power reflection factor will be

$$\begin{aligned} R_p &= \left[\frac{(Z_A Z_p - Z_p Z_m) \cos Bl + j[Z_A Z_m - Z_p^2] \sin Bl}{(Z_A Z_p + Z_p Z_m) \cos Bl + j[Z_A Z_m + Z_p^2] \sin Bl} \right]^2 \\ &= \left[\frac{n_p(1 - n_m) \cos Bl + j[n_m - n_p^2] \sin Bl}{n_p(1 + n_m) \cos Bl + j[n_m + n_p^2] \sin Bl} \right]^2 \quad (2.161) \end{aligned}$$

where Z_A is the impedance of air, Z_p the impedance of the quarter wave plate, and Z_m the impedance of the medium. If the index of refraction n_p of the plate is equal to the square root of n_m , the index of the medium, the absolute value of this equation reduces to

$$\begin{aligned} (R_p) &= \left| \left[\frac{\sqrt{n_m}(1 - n_m) \cos Bl}{\sqrt{n_m}(1 + n_m) \cos Bl + j2n_m \sin Bl} \right]^2 \right| \\ &= \frac{1}{1 + \frac{4n_m}{(1 - n_m)^2 \cos^2 Bl}} \quad (2.162) \end{aligned}$$

¹² This method of reducing reflections has been discussed by C. H. Cartwright and A. F. Turner, Phys. Rev., March 15, 1939, Abstract 22, page 595.

Hence the reflection varies from zero up to the value obtained without the intermediate layer. Over the visible light region, which occupies a two to one frequency range, if the quarter wave frequency is set at the middle of this region, and the index of refraction is 1.6, the reflected light will vary from 0 to 1.4 per cent.

Another application of the stratified filter in optics is the reflection of one part of the frequency range and transmission of another part.¹³ For this purpose films of alternately low and high index of refraction and equal optical thicknesses are required. This application is entirely similar to the stratified filter described previously. As can be seen from Figure 2.32, the highest attenuation and consequently the greatest reflection will occur when each layer is a quarter wavelength thick, while transmission will occur at higher or lower frequencies than this.

¹³ See "Multilayer Films of High Reflecting Power." C. H. Cartwright and A. F. Turner, *Phys. Rev.*, June 1, 1939, page 1128.

CHAPTER III

APPLICATION OF NETWORK THEORY TO LUMPED MECHANICAL SYSTEMS

3.1. *Electrical and Mechanical Analogies*

IN the early days of electricity, as mentioned in the introduction, electrical quantities such as inductances and capacitances were often illustrated by referring to systems having masses and compliances. In fact the word electromotive force obtains its name from its similarity of effect to a mechanical force while a current of electricity being the product of the number of

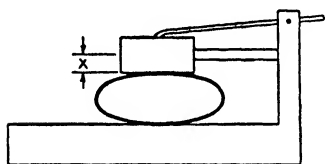


FIG. 3.1—SPRING, MASS AND MECHANICAL RESISTANCE SYSTEM.

charges by the velocity of propagation is similar to a current of air in which the value is determined by the product of the number of particles by the average velocity.

The formal basis for such an analogy is that analogous systems satisfy the same type of differential equations. An inductance, capacitance, and resistance in series satisfies the differential equation

$$L \frac{d^2Q}{dt^2} + R \frac{dQ}{dt} + \frac{Q}{C} = E \quad (3.1)$$

where Q is the charge flowing in the wire, E the applied electromotive force, L , R and C the inductance, resistance and capacitance of the circuit. A mechanical system satisfying the same type of differential equation is the one shown in Fig. 3.1. Here we have a spring shown as an elliptical spring, mounted on an immovable base, with a mass on top of it. The mass rubs against a fixed support, generating friction, when the mass is acted on by a force which works between the mass and the

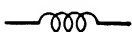

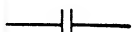
fixed support. The differential equation for this type of system is

$$M \frac{d^2 x}{dt^2} + R \frac{dx}{dt} + \frac{x}{C} = F = M \frac{dv}{dt} + Rv + \int \frac{v dt}{C} \quad (3.2)$$

where x is the displacement of the center of the mass from its equilibrium position, F the applied force, v the velocity, and M , R , and C respectively, the mass, mechanical resistance and the compliance (inverse of stiffness) of the system. We see then that between the two systems there exist the following analogies shown in Table III:

TABLE III

DIRECT RELATION BETWEEN MECHANICAL AND ELECTRICAL QUANTITIES

Mechanical Quantity	Electrical Quantity	Mechanical Energy Stored or Dissipated	Electrical Energy Stored or Dissipated	Symbol Employed for Both Systems
Force = F	Electromotive Force = E			
Displacement = x	Charge = Q			
Velocity = v	Current = i			
Mass = M	Inductance = L	$\frac{1}{2} Mv^2$	$\frac{1}{2} Li^2$	
Mechanical Resistance = R	Electrical Resistance = R	Rv^2	Ri^2	
Compliance = C	Capacitance = C	$\frac{1}{2} \frac{x^2}{C} = \frac{1}{2} CF^2$	$\frac{1}{2} \frac{Q^2}{C} = \frac{1}{2} CE^2$	

The energies associated with the electrical and mechanical elements are shown on the third and fourth columns.

The importance of analogies of this sort is not the obtaining of the equivalent electrical quantities but the reduction of the difficult differential equations of the type shown in (3.2) to the symbolic solutions employed in electrical network theory and also the ability to apply the results of electrical network theory to mechanical systems when such an application is advan-

tageous. To do this one can think in terms of the mechanical quantities only, but it is advantageous to use the same symbols as in electrical network theory in order to easily identify the relation of interest in electrical network theory.

The system of analogies given above was the first one employed and is the one most commonly used today. It is, however, not unique, for as shown by Hahnle¹ and Firestone,² it is possible to reverse the association given above. In this second system a force is taken as the analogue of a current, while a velocity is taken as the analogue of an electromotive force. An electrical circuit equivalent to the mechanical system of Fig. 3.1 will be the one shown in Fig. 3.2, consisting of an inductance, resistance and capacitance in parallel. Then the differential equation for this system is

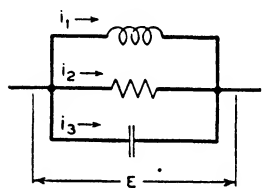


FIG. 3.2—ELECTRICAL SYSTEM EQUIVALENT TO THE MECHANICAL SYSTEM OF FIG. 3.1.

$$i = i_1 + i_2 + i_3 = \frac{1}{L} \int E dt + \frac{E}{R} + C \frac{dE}{dt}. \quad (3.3)$$

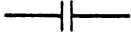

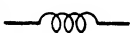
Comparing this with the second form of equation (3.2) the analogies shown in Table IV result. Both systems can be used with all mechanical systems equally well. It will be noted that the electrically equivalent networks given by the two systems are inverse networks, i.e., the product of the two impedances is a real constant. For apparatus employing electromechanical coupling elements, the first system gives simpler results for electrostatic or piezoelectric coupling elements, while the second system gives simpler results for electromagnetic, or magnetostrictive elements. In the present book, the first system is used in all cases except when electromagnetic coupling elements are employed when a real simplification is obtained by employing the second system.

¹ "Die Darstellung Electromechanischer Gebilde durch rein elektrische Schaltbilder," Wiss. Veröff. a.c. Siemens Konzern, Vol. XI, No. 1, 1932.

² "A New Analogy Between Mechanical and Electrical Systems," F. A. Firestone, J. Acoustical Soc. Am. 4, 249-267 (1933).

TABLE IV

INVERSE RELATION BETWEEN MECHANICAL AND ELECTRICAL QUANTITIES

Mechanical Quantity	Electrical Quantity	Mechanical Energy Stored or Dissipated	Electrical Energy Stored or Dissipated	Symbol Employed for Both Systems
Force = F Impulse = $\int F dt$	Current = i Charge = Q			
Velocity = v	Electromotive Force = E			
Displacement = x	$\int E dt$			
Mass = M	Capacitance = C	$\frac{1}{2} mv^2$	$\frac{1}{2} CE^2$	
Mechanical Resistance = R	Leakance = G	Rv^2	GE^2	
Compliance = C	Inductance = L	$\frac{1}{2} CF^2$	$\frac{1}{2} Li^2$	

3.2. Application of Electromechanical Analogies to the Solution of Lumped Mechanical Systems

One of the simplest mechanical constructions, and one which has been studied extensively, is a system for reducing the vibration transmitted by an unbalanced rotating machine to its supports. When an unbalanced machine rotates, it generates a force tending to pull the machine alternately toward and away from the support, and may cause unpleasant and dangerous vibrations in the support. If the support is very stiff, the equivalent circuit for such an arrangement is shown in Fig. 3.3, where F is the unbalanced force generated by the rotating machinery, M the mass of the machine, C the compliance of the

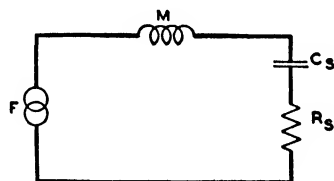


FIG. 3.3—EQUIVALENT CIRCUIT OF ROTATING MACHINE AND SUPPORT.

support and R any mechanical resistance associated with the displacement of the support or loss of energy to other surrounding objects by propagation of mechanical energy. If the frequency of the unbalanced force is anywhere near the frequency

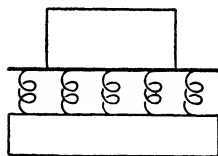


FIG. 3.4—SPRING MOUNTING FOR ROTATING MACHINE.

of resonance of the mass of the machine with the compliance of the support, quite large vibrations may be set up which may cause vibrations in surrounding objects or may even fracture the supports.

The commonest method for reducing this vibration is to mount the machine on a flexible support as shown schematically in Fig. 3.4. The effect of this mounting is to add a coupling compliance C between the mass and the impedance of the support as shown by Fig. 3.5. The position of any element of the network is easily verified by putting forces between the point of interest and an immovable ground. For example, if we put a constant force between the top of the spring carriage and an immovable ground, the spring carriage will be displaced as will also the support. The complete force will come across both elements and hence they must be in parallel as shown in Fig. 3.5.

The mass M and compliance C form a half section of a low-pass filter of the kind shown in Table I, filter 1. This filter cuts off when the frequency is greater

than $f_B = \frac{1}{2\pi \sqrt{MC}}$. If the fre-

quency of the applied unbalance is greater than this cut off frequency, a beneficial result will be obtained, for then the filter section will introduce attenuation and a smaller vibration will be transmitted to the surround-

ing objects. If, however, the frequency is in the pass band of the filter, no benefit will occur and in fact the addition of the spring may cause more vibration to be transmitted to the supports than would be transmitted if the spring were not there.

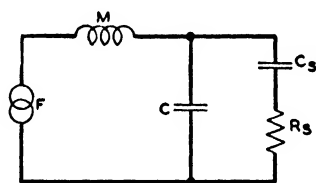


FIG. 3.5—EQUIVALENT CIRCUIT FOR MACHINE AND SPRING SUPPORT.

This follows from the fact that the characteristic impedances for the two ends of the filter are different as shown on Table I, pages 52, 53, with the inductance end having a low impedance near the cutoff while the capacitance end has a high impedance. The filter then may act like an ideal transformer and get more energy into the high impedance supports from the low impedance generator than could be gotten if the compliance had not been put in.

One method for eliminating the effect of this transformation ratio is to introduce mechanical resistance in the form of dash

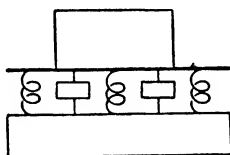


FIG. 3.6—ROTATING MACHINE WITH SPRING MOUNTING AND DAMPERS.

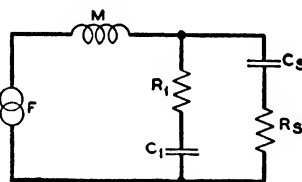


FIG. 3.7—EQUIVALENT CIRCUIT FOR MACHINE, SPRING MOUNTING, AND DAMPERS.

pots or oil dampers as shown in Fig. 3.6. This will put a mechanical resistance R in series with the compliance since as shown by Fig. 3.6 the velocity of motion of the damper depends on the difference in the velocities of the two ends of the spring. The effect of this resistance can best be analyzed by replacing the series combination R_1, C_1 of Fig. 3.7 by a parallel combination R_2, C_2 which can always be done at any frequency. The value of the shunt combination is given by

$$R_1 - \frac{j}{\omega C_1} = \frac{R_2 \left(\frac{-j}{\omega C_2} \right)}{R_2 - \frac{j}{\omega C_2}} = \frac{\frac{R_2}{\omega^2 C_2^2} - j \frac{R_2}{\omega C_2}}{R_2^2 + \frac{1}{\omega^2 C_2^2}}. \quad (3.4)$$

Hence

$$C_2 = \frac{C_1}{1 + \omega^2 R_1^2 C_1^2}; \quad R_2 = \frac{\frac{1}{\omega^2 C_1^2} + R_1^2}{R_1}. \quad (3.5)$$

For example if $R_1 = \frac{1}{2\omega_B C_1}$,

$$C_2 = \frac{C_1}{\left(1 + \frac{\omega^2}{4\omega_B^2}\right)}; \quad R_2 = \frac{1}{2\omega_B C_1} \left[\frac{1}{2} + \frac{4\omega_B^2}{\omega^2} \right] \quad (3.6)$$

and the terminating impedance is low enough so that the transformer gain disappears while the loss of attenuation at high frequencies, due to the added resistance, is small.

3.3. Mechanical Filters

In the telephone system combinations of mechanical springs and masses are used to some extent in place of electrical wave

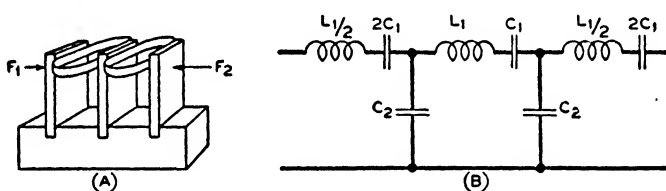


FIG. 3.8—MECHANICAL FILTER CONSTRUCTED FROM FLEXURE BARS.

filters. They are particularly advantageous for very low frequencies where the sizes of the electrical elements required becomes very large or where it is desired to obtain the required attenuation in a small frequency range. This can be done with mechanical filters on account of the small amount of mechanical resistance associated with the motion of the elements.

One of the commonest types employed is the band-pass filter shown in Fig. 3.8A. The filter consists of reeds clamped in a heavy base and connected together at their tops by thin coupling springs. The equivalent circuit of this combination is that shown in Fig. 3.8B. The reeds represent the series-resonant circuits while the coupling compliances are represented by the capacitance C_2 . From Fig. 3.8B it is obvious that the center reed has to be twice as stiff and have twice the equivalent mass that the end two reeds have.

The equivalent mass and stiffness of a bar clamped on one end and vibrated on the other can be calculated from the equations for a flexurally vibrating bar given by Lamb.³ If y is the lateral displacement of the beam shown in Fig. 3.9 which has its length along the x axis, we have from beam theory

$$\text{Slope} = s = - \frac{\partial y}{\partial x}$$

$$\text{Moment} = M = - Y_0 I \frac{\partial s}{\partial x} = Y_0 I \frac{\partial^2 y}{\partial x^2} \quad (3.7)$$

$$\text{Lateral force} = F = \frac{\partial M}{\partial x} = Y_0 I \frac{\partial^3 y}{\partial x^3}$$

where Y_0 is the value of Young's modulus along the length of the bar and I is the moment of inertia of the section which is equal to the area of the section times the square of the radius of gyration κ . For a rectangular section in which the y or thickness dimension is l , the moment of inertia is the area of the section S times $l^2/12$, while for a circular section the moment of inertia is the area times $r^2/4$ where r is the radius of the section.

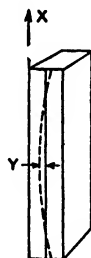


FIG. 3.9—BAR BENT IN FLEXURE.

The lateral force is the force exerted on the section externally in the direction of y . For a small section dx the resultant force exerted on the section will be

$$F_1 - F_2 = F_1 - \left(F_1 + \frac{\partial F}{\partial x} dx \right) = - \frac{\partial F}{\partial x} dx \quad (3.8)$$

where F_1 is the force exerted on the section at $x = x$ by the adjacent part of the bar and F_2 that exerted at $x = x + dx$. To obtain the equation of motion this force must be equated to the mass times the acceleration of the section or

$$- \frac{\partial F}{\partial x} dx = S \rho \frac{\partial^2 y}{\partial t^2} dx. \quad (3.9)$$

³ "Dynamical Theory of Sound," Lamb, E. Arnold, London.

Introducing the value of F from (3.7), we have

$$Y_0 \kappa^2 \frac{\partial^4 y}{\partial x^4} + \rho \frac{\partial^2 y}{\partial t^2} = 0 \quad (3.10)$$

as the equation of motion.⁴

For simple harmonic motion, we assume the symbolic time variation given by (2.1) and obtain

$$\frac{\partial^4 y}{\partial x^4} = \frac{\omega^2 \rho}{Y_0 \kappa^2} y = n^4 y. \quad (3.11)$$

A solution of this equation is

$$y = A \cosh nx + B \sinh nx + C \cos nx + D \sin nx \quad (3.12)$$

as can readily be verified by differentiation.

The bar of the filter of Fig. 3.8 is clamped at its base where $x = 0$. This means that the displacement $y = 0$ when $x = 0$, also that the slope $-\frac{\partial y}{\partial x}$ is zero at $x = 0$ since the bar cannot start to bend in its clamped part if it is rigidly clamped. The first condition $y = 0$ when $x = 0$ is satisfied if

$$A + C = 0 \quad \text{or} \quad C = -A. \quad (3.13)$$

The slope of the bar is then

$$-s = \frac{\partial y}{\partial x} = n [A \sinh nx + B \cosh nx - C \sin nx + D \cos nx]. \quad (3.14)$$

This will be zero when $x = 0$ if

$$B + D = 0 \quad \text{or} \quad D = -B. \quad (3.15)$$

Hence the solution incorporating these conditions is

$$y = A(\cosh nx - \cos nx) + B(\sinh nx - \sin nx). \quad (3.16)$$

We next consider the condition at the vibrating end. It is acted upon by a lateral force produced by the difference of force

⁴ This equation neglects the effect of rotary inertia. The modification caused by this term is discussed in Appendix A.

of the driving element and the coupling spring. However, neither of these elements introduce any moment tending to bend the bar at its tip so one condition is that

$$M = Y_0 I \frac{\partial^2 y}{\partial x^2} = 0 \text{ when } x = l \text{ the length of the bar.} \quad (3.17)$$

Introducing the value of (3.16) into this equation, differentiating and setting $M = 0$ when $x = l$ we have

$$B = -A \left(\frac{\cosh nl + \cos nl}{\sinh nl + \sin nl} \right). \quad (3.18)$$

Introducing this value into (3.16), we have

$$y = A \left[\cosh nx - \cos nx - \left(\frac{\cosh nl + \cos nl}{\sinh nl + \sin nl} \right) (\sinh nx - \sin nx) \right]. \quad (3.19)$$

We are now in a position to determine the impedance of the vibrating reed as measured by the ratio of force to velocity for the end of the rod. Introducing (3.19) into the expression for F given by (3.7), we have

$$F = Y_0 I \frac{\partial^3 y}{\partial x^3} = AY_0 I n^3 \left[\sinh nx - \sin nx - \left(\frac{\cosh nl + \cos nl}{\sinh nl + \sin nl} \right) (\cosh nx + \cos nx) \right]. \quad (3.20)$$

Similarly for the velocity \dot{y} we have

$$\dot{y} = j\omega y = j\omega A \left[\cosh nx - \cos nx - \left(\frac{\cosh nl + \cos nl}{\sinh nl + \sin nl} \right) (\sinh nx - \sin nx) \right]. \quad (3.21)$$

Taking the ratio at the point $x = l$, we have

$$Z = \frac{F}{\dot{y}} = - \frac{jY_0 I n^3}{\omega} \left[\frac{1 + \cosh nl \cos nl}{\sin nl \cosh nl - \sinh nl \cos nl} \right]. \quad (3.22)$$

Several limiting conditions are of interest. When $\omega \rightarrow 0$ we have, expanding the functions in power series,

$$Z = \frac{-j}{\omega} \frac{3Y_0 I}{l^3} = -\frac{j}{\omega} \frac{Y_0 l^3 l_w}{4l^3} \quad (3.23)$$

so that at low frequencies the reed acts as a compliance having the value $C = l^3/3 Y_0 I$. As the frequency is increased the impedance approaches a resonant frequency given by

$$\cosh nl \cos nl = -1. \quad (3.24)$$

The first value of nl which satisfies this equation is

$$nl = 1.875104 = m_1. \quad (3.25)$$

Introducing the value of n from (3.11), the frequency of resonance becomes

$$f = \frac{\kappa m_1^2 \sqrt{Y_0/\rho}}{2\pi l^2} = \frac{l_1 m_1^2 \sqrt{Y_0/\rho}}{2\pi \sqrt{I_2} l^2} \quad (3.26)$$

for a bar of rectangular cross section. This is the well-known formula for the natural resonance of a bar clamped on one end and free on the other.

To obtain the impedance near the resonant frequency we can let

$$\begin{aligned} nl &= \sqrt{\frac{\omega}{\kappa}} \sqrt{\rho/Y_0} l = \sqrt{\frac{\omega_R + \Delta\omega}{\kappa}} \sqrt{\rho/Y_0} l \\ &= m \sqrt{1 + \frac{\Delta\omega}{\omega_R}} \doteq m \left(1 + \frac{1}{2} \frac{\Delta\omega}{\omega_R} \right). \end{aligned} \quad (3.27)$$

Expanding the terms of (3.22) by the multiple angle formulae

$$\begin{aligned} \cos(\alpha + \beta) &= \cos \alpha \cos \beta - \sin \alpha \sin \beta \\ \sin(\alpha + \beta) &= \sin \alpha \cos \beta + \cos \alpha \sin \beta \\ \cosh(\alpha + \beta) &= \cosh \alpha \cosh \beta + \sinh \alpha \sinh \beta \\ \sinh(\alpha + \beta) &= \sinh \alpha \cosh \beta + \cosh \alpha \sinh \beta \end{aligned} \quad (3.28)$$

and assuming $\Delta\omega$ is a small quantity so that

$$\cos \frac{m\Delta\omega}{2\omega_R} = \cosh \frac{m\Delta\omega}{2\omega_R} = 1; \quad \sin \frac{m\Delta\omega}{2\omega_R} = \sinh \frac{m\Delta\omega}{2\omega_R} = \frac{m\Delta\omega}{2\omega_R} \quad (3.29)$$

we have

$$Z = \frac{-jY_0In^3}{\omega} \left[\frac{\left\{ \begin{aligned} &1 + \cosh m \cos m + \\ &\frac{m\Delta\omega}{2\omega_R} (\sinh m \cos m - \cosh m \sin m) \end{aligned} \right\}}{\left\{ \begin{aligned} &\sin m \cosh m - \sinh m \cos m \\ &+ \frac{m\Delta\omega}{\omega_R} (\sinh m \sin m) \end{aligned} \right\}} \right] \quad (3.30)$$

Near the resonant frequency which occurs when $1 + \cosh m \cos m = 0$ we have to first powers of $\Delta\omega$

$$Z = + \frac{jY_0In^3m\Delta\omega}{2\omega_R^2} = \frac{jY_0In^4l\Delta\omega}{2\omega_R^2} \quad (3.31)$$

Above the resonance frequency this will be a positive reactance while below it is a negative reactance. Hence, near the resonance frequency the impedance of a clamped reed can be represented by a series compliance C and mass M having the impedance

$$Z = \frac{-j}{\omega C} + j\omega M = \frac{-j}{\omega C} [1 - \omega^2 MC] = \frac{-j}{\omega C} \left[1 - \frac{\omega^2}{\omega_R^2} \right] \quad (3.32)$$

where the resonant frequency f_R is given by

$$(2\pi f_R)^2 = \omega_R^2 = \frac{1}{MC} \quad (3.33)$$

When ω is near ω_R

$$\omega = (\omega_R + \Delta\omega). \quad (3.34)$$

Introducing this in (3.32) we have

$$Z = \frac{-j}{\omega C} \left[1 - \left(\frac{\omega_R^2 + 2\omega_R\Delta\omega + \Delta\omega^2}{\omega_R^2} \right) \right] = \frac{+j}{\omega C} \left(\frac{2\Delta\omega}{\omega_R} \right) \quad (3.35)$$

Comparing this with equation (3.31) we find that the equivalent compliance and mass of the clamped vibrating reed as measured at its free end, are given by

$$C = \frac{4}{Y_0In^4l} = \frac{4l^3}{Y_0Im^4}; \quad M = \frac{1}{\omega_R^2 C} = \frac{Y_0In^4l}{4\omega_R^2} = \frac{\rho l S}{4} \quad (3.36)$$

Hence the motional mass is one-fourth the total mass of the bar and the compliance C near the resonant frequency is

$$\left(\frac{12}{m^4}\right) = 0.971 C_0 \quad (3.37)$$

or the compliance is 0.971 times the compliance measured by static means.

On account of the complicated form of the coupling compliance, this compliance is not easily calculated but can be measured statically or by determining the band width of the filter section. All of the design formulae for the elements are given in Table I, filter 9. The image impedances are usually determined by the impedances of the driving elements used to drive and pick up the output of the filter section.

Other forms of mechanical filters are also used and their elements can be determined in a similar manner to the example given here. To be successful the mode of motion used has to be well isolated from other possible modes of motion, for otherwise spurious and unwanted pass bands are likely to result. For this reason flexure modes are particularly good, for they usually occur at considerably lower frequencies than the frequencies for which other modes can be excited.

3.4. *Rotary Mechanical Filters and Constant Speed Devices*

Longitudinally and flexurally vibrating systems such as discussed in the last two sections cannot be used effectively in low-pass filters or any systems which transfer power by a constant velocity of motion. For this purpose torsionally vibrating systems which have a rotary motion as the zero frequency motion are commonly employed. It is the purpose of this section to discuss torsionally vibrating systems and their application to filters and constant speed motors.

In a rotary system having an angular velocity $\dot{\theta} = \frac{d\theta}{dt}$, the kinetic energy stored is equal to $\frac{1}{2}I\dot{\theta}^2$ where θ is measured in radians. For a solid circular disk having a radius R and length

l , this can be shown as follows. Any element of volume of a cylindrical shell of thickness dr , subtending the angle $d\theta$, will have the total mass

$$dM = \rho l r dr d\theta \quad (3.38)$$

where r is the distance of the element from the center. If the angular velocity of the element is $\dot{\theta}$, the linear velocity v will be $r\dot{\theta}$. Hence the kinetic energy of the element will be

$$KE = \frac{1}{2} dM v^2 = \frac{1}{2} \rho l r^3 \dot{\theta}^2 dr d\theta. \quad (3.39)$$

Integrating this with respect to r and θ to obtain the complete kinetic energy we have

$$KE = \frac{1}{2} \rho l \dot{\theta}^2 \int_0^R r^3 dr \int_0^{2\pi} d\theta = \frac{\pi}{4} \rho l R^4 \dot{\theta}^2. \quad (3.40)$$

Since the mass of the element is

$$M = \pi R^2 \rho l \quad (3.41)$$

and the radius of gyration κ is given by

$$\kappa^2 = \frac{R^2}{2} \quad (3.42)$$

equation (3.40) can be written

$$KE = \frac{1}{2} M \kappa^2 \dot{\theta}^2 = \frac{1}{2} I \dot{\theta}^2. \quad (3.43)$$

When a rod of circular section is twisted by equal and opposite couples applied to the two ends, the twisting is assumed to take place in such a manner that each transverse section remains in its own plane. The couple required to twist the section through a given angle depends on the rigidity modulus μ and the moment of compliance of the system. The total potential energy of twisting for a rod of unit length may be calculated as follows. Let us consider a thin tube of radius r and thickness dr , and let θ denote the angular displacement of any section distant x from the origin. The rate of twist at x is equal to $d\theta/dx$, and the shear of the material composing the section will be $r d\theta/dx$. The opposing force per unit area is $\mu r d\theta/dx$,

where μ is the modulus of shear. Since now the area of the section is $2\pi r dr$, the total moment about the axis will be

$$2\pi\mu r^3 dr \frac{d\theta}{dx}. \quad (3.44)$$

The total moment for a solid rod of radius R and length unity will be

$$M = 2\pi\mu \int_0^R r^3 dr \int_0^1 \frac{d\theta}{dx} dx = \frac{2\pi\mu R^4}{4} \theta = \mu S \kappa^2 \theta, \quad (3.45)$$

where S is the cross-sectional area of the rod. The total energy stored in the rod by twisting through an angle θ_0 will be

$$\int_0^{\theta_0} M d\theta = \mu S \kappa^2 \int_0^{\theta_0} \theta d\theta = \frac{1}{2} \mu S \kappa^2 \theta_0^2 = \frac{1}{2} \frac{\theta_0^2}{C_M} \quad (3.46)$$

where C_M is the moment of compliance per unit length.

Similarly if we have a frictional or viscous drag on the surface of the rod we would have a moment of resistance R_M which was the ratio of angular velocity $\dot{\theta}$ to the applied moment M .

If we take the moment or torque M as the analogue of the voltage E , and $\dot{\theta}$ the angular velocity as the analogue of the current, we can construct a table of analogies for a torsional system similar to Table III, page 81, for a longitudinal system. This correspondence is given in Table V, page 95.

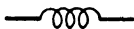

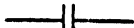
As a first example let us consider the propagation of a torsional wave down a circular rod of radius R . If we consider a small section of length dx , and neglect the resistance associated with the motion, the equations of motion are the following

$$\begin{aligned} \frac{\partial}{\partial t} (I \dot{\theta}) dx &= M_1 + M_2 = - \frac{\partial M}{\partial x} dx; \\ M(C dx) &= (\theta_1 - \theta_2) = - \frac{\partial \theta}{\partial x} dx. \end{aligned} \quad (3.47)$$

The first equation states that the time rate of increase of angular momentum is equal to the sum of the moments applied to the section at the two ends. Since these are of opposite sign

$$M_2 = - \left(M_1 + \frac{\partial M_1}{\partial x} dx \right). \quad (3.48)$$

TABLE V
TORSIONAL SYSTEM

Mechanical Quantity	Electrical Quantity	Mechanical Energy Stored or Dissipated	Electrical Energy Stored or Dissipated	Symbol Used
Moment or Torque = M	Electromotive force = E			
Angle of twist = θ	Charge = Q			
Angular velocity = $\dot{\theta}$	Current = i			
Moment of Inertia = I	Inductance = L	$\frac{1}{2} I \dot{\theta}^2$	$\frac{1}{2} L i^2$	
Moment of Resistance, = R_M	Electrical Resistance = R	$R_M \dot{\theta}^2$	$R i^2$	
Moment of Compliance = C_M	Capacitance = C	$\frac{1}{2} \frac{\theta^2}{C_M} = \frac{1}{2} C_M M^2$	$\frac{1}{2} \frac{Q^2}{C} = \frac{1}{2} C E^2$	

The second equation states that the difference in the twist angle on the two ends of the sections is equal to the average moment times the moment of compliance per unit length C times the length dx . These equations are entirely similar to equations (2.118) for an electric line. Hence by analogy we can write the solution in the form

$$\theta = \theta_0 \cos \omega \sqrt{IC} x - \frac{M_0}{\sqrt{I}} \sin \omega \sqrt{IC} x \quad (3.49)$$

$$M = M_0 \cos \omega \sqrt{IC} x - \theta_0 \sqrt{I} \sin \omega \sqrt{IC} x$$

where θ_0 and M_0 are the angular velocity and torque applied at the beginning of the rod while θ and M are the angular velocity and torque at any point x along the rod. From these equa-

tions, by analogy with the electrical case, we find that the velocity and image impedance of the rod for torsional waves are

$$v = \frac{1}{\sqrt{IC}} = \frac{1}{\sqrt{\rho S \kappa^2 \times \frac{1}{\mu S \kappa^2}}} = \sqrt{\frac{\mu}{\rho}} \quad (3.50)$$

$$Z_0 = \sqrt{\frac{I}{C}} = \sqrt{\rho S \kappa^2 \times \mu S \kappa^2} = S \kappa^2 \sqrt{\rho \mu} = \frac{\pi R^4}{2} \sqrt{\rho \mu}.$$

If the rod is used as a shaft transmitting a constant angular velocity of zero frequency, equations (3.49) reduce to

$$\theta = \theta_0; \quad M = M_0. \quad (3.51)$$

In addition since $\theta = j\omega\theta$, the first equation of (3.49) yields the equation

$$\theta = \theta_0 - \frac{M_0}{\sqrt{\frac{I}{C}}} \sqrt{IC} x \quad \text{or} \quad \theta - \theta_0 = \frac{M_0 x}{\frac{\pi}{2} R^4 \mu} \quad (3.52)$$

and the angle through which the shaft will be twisted is proportional to the torque and the length and inversely proportional to the shearing constant μ and the fourth power of the radius.

Connecting rods are subject to the difficulty that an irregularity of the motion of the driving system or the load may set up dangerous alternating stresses in the rod which may crack the rod. This will be recognized as the problem of resonances in a line not terminated in its image impedance. If the driving rod has any flywheels or cranks this condition is made worse due to the fact that the natural resonant frequencies become lower, in which frequency range the irregularities are likely to be larger. If the cranks or flywheels are spaced uniformly along the driving rod, as they will be in a multi-cylinder engine,⁵ it will readily be recognized that the system forms a low-pass filter of the distributed type discussed in section (2.8). The equivalent circuit, as shown in Fig. 3.10B, would consist of

⁵ Such a case is discussed by means of equations of finite differences, by M. A. Biot, *Journal of Applied Physics*, Vol. II, No. 8, p. 530, August 1940.

sections of line representing sections of the driving rod, separated by series inductances representing the moment of inertia of the cranks or flywheels. The inductances will be in series since their angular velocity depends on the difference in the torques applied by the two sections of driving rod attached to the flywheels or cranks.

The methods of working out the propagation characteristics of such a system are entirely similar to the methods of section

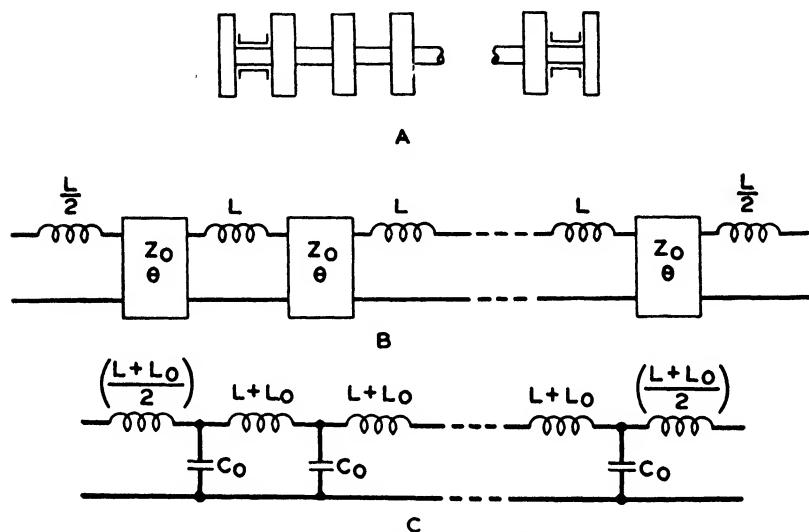


FIG. 3.10—ROTARY DRIVE SYSTEM WITH CRANKS OR FLYWHEELS.

(2.8). If the length of the driving shaft between cranks is small, the equivalent circuit can be obtained by replacing the line section, representing the driving rod section by its T network equivalent as shown in Fig. 3.10C. Here L_0 and C_0 will be, respectively, the total moment of inertia and the total moment of compliance of one section of the driving rod, given by

$$L_0 = \frac{\pi R^4 \rho l}{2}; \quad C_0 = \frac{2l}{\pi R^4 \mu} \quad (3.53)$$

while L will be the moment of inertia of the flywheel or crank,

The circuit of Fig. 3.10C will obviously be the circuit of a low-pass filter having a value of $m = 1$. One question of

interest is what will be the critical frequencies for which large amplitudes may be obtained for small irregularities. The resonant frequencies depend on the type of termination used which will usually be a high impedance compared to the image impedance of the rod or filter. This follows from the fact that the large moments of inertia of the driving and driven systems will introduce a high impedance over the band of the filter. From equation (2.34) when the attenuation through the transmission section is low and hence $A \rightarrow 0$, the angular velocity in the termination becomes

$$\theta = \frac{2M_0 \sqrt{Z_{I_1} Z_{I_2}}}{e^{jB}[Z_{I_1} + Z_s][Z_{I_2} + Z_T] - e^{-jB}[Z_{I_1} - Z_s][Z_{I_2} - Z_T]} \quad (3.54)$$

where B is the total image phase shift in the transmission circuit. In case both Z_T and Z_s are much larger than Z_{I_1} and Z_{I_2} , the value of θ becomes

$$\theta = \frac{M_0 \sqrt{Z_{I_1} Z_{I_2}}}{Z_s Z_T} \frac{1}{\sin B} \quad (3.55)$$

and the natural resonant frequencies will occur when

$$\sin B = 0 \quad \text{or} \quad B = \pi, 2\pi, \dots, 2n\pi. \quad (3.56)$$

It will be noted that these same natural frequencies occur if Z_s and Z_T are much smaller than Z_{I_1} and Z_{I_2} . All of the natural frequencies occur in the band of the filter and can be evaluated by solving the equation

$$2\pi, 4\pi, \dots, 2n\pi = nB = 2n \tan^{-1} \sqrt{\frac{\omega^2/\omega_B^2}{1 - \omega^2/\omega_B^2}} \quad (3.57)$$

where ω_B is the cut-off frequency of the low-pass filter shown on Fig. 3.10C and n is the number of sections. This follows from equation (2.83), which gives the propagation characteristic of a low-pass filter, from which the phase shift B can be determined. For any other sort of a termination the natural frequencies can be calculated from (3.54).

A somewhat similar type of mechanical filter, with a damping resistance, has been used in producing constant speed

motors for use in phonograph record recording.⁶ For this system a synchronous electric motor drives a rotating turntable through a reduction gear. Speed changes at audible frequencies introduce extraneous sounds into the records and speed changes at frequencies below the audible range produce changes in pitch. There are in general two points of origin for these variations, the turntable and the gears. Variations in load on the turntable produce changes in frequency while from the gear three sorts of variation arise, those due to inaccuracies in spacing of the teeth, to errors in the shape of the teeth and to the successive shift in driving load from tooth to tooth.

In order to make the frequency of the gear irregularities higher, four gears were cut at one time and turned at 90 degree

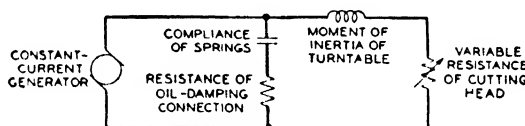


FIG. 3.11—EQUIVALENT CIRCUIT OF CONSTANT SPEED MOTOR.

intervals. This had the effect of making the gear frequency four times as high and the amplitude one-fourth as great. These gears were all driven independently by the driving motor and were coupled to the turntable through large mechanical compliances. The compliance of the springs and the moment of inertia of the turntable make up a half section of a low-pass filter which will reduce any irregularities above the cut-off frequency. Since, however, there are no resistances associated with the motion, any irregularities whose frequencies lie within the pass band may be greatly increased due to the transforming action of the filter, as discussed in connection with the vibration damping system of section (3.2). To get around this difficulty the motor also drives the turntable through an oil-damping connection consisting of an outside case, two rotatable paddle wheels, and a viscous oil.

The equivalent circuit of the combination beyond the gearing is that shown in Fig. 3.11. The compliance of the springs

⁶ Bell Laboratories Record, L. A. Elmer, 7, p. 446, 1929.

and the resistance of the oil-damping connection are in the shunt branch since they are not brought into play unless there is a difference in velocity between the driving motor and the turntable. Furthermore, they are in a series connection as can be seen by the fact that if either of them has a very high impedance, the load will be driven principally through the higher impedance unit. As in section (3.2) it is best to make their impedance about equal at the upper cut-off frequency.

The variable resistance shown in series with the moment of inertia of the turntable is due to the motion of the stylus on the wax, and this resistance depends on the depth of the stylus. With this system the effects of gear irregularities and a variable load on the rate of rotation, have been made very small.

CHAPTER IV

ACOUSTIC EQUATIONS AND NETWORKS

THE mechanical transmission systems considered in the last chapter were all of the one-dimensional type, and hence had their counterparts in lumped and distributed electrical systems. In acoustics, on the other hand, we are dealing in general with propagation in three dimensions. Hence not every acoustical case will have an electrical counterpart of the type discussed in Chapter II. When, however, we deal with definite types of waves such as plane waves or spherical waves, we are changing the three-dimensional character of the motion into a motion which can be specified by specifying the dimension along the direction of propagation only. The propagation characteristics for these wave types are very similar to those for electrical waves, and considerable simplification and progress have been made by considering the electrical analogies. It is the purpose of the present chapter to derive the equations of acoustics and to consider problems involving the propagation of particular wave types in acoustic systems.

In the mechanical systems considered in Chapter III, the mechanical impedance was defined as the ratio of force to velocity. These were the natural units to use since the force was usually the force between two adjacent points and no consideration of area was involved. In acoustics, however, the force is the force between two adjacent areas and it is more usual and logical to consider the force per unit area or the pressure. Similarly if there is a difference of area occurring, it is the total area times velocity that is continuous and this has been called the volume velocity. The acoustic impedance then is defined as the ratio of pressure to volume velocity.

4.1. General Differential Equation for Acoustic Wave Motion

The equations of motion for acoustic waves are based on three separate physical laws, Newton's laws of motion, the thermodynamic relation between pressure and volume in a gas, and the equations of continuity. The equations derived from the three separate relations can be combined into one unified equation by using the concept of a velocity potential due originally to Lagrange.

To apply Newton's laws of motion we consider a small element of volume dx, dy, dz . The net force in the x direction is due to the difference in pressure on the two sides of the element or

$$F = (p_1 - p_2)dy dz = \left[p_1 - \left(p_1 + \frac{\partial p}{\partial x} \right) dx \right] dy dz$$

$$= - \frac{\partial p}{\partial x} dx dy dz. \quad (4.1)$$

The mass of material in the element of volume is $\rho dx dy dz$ where ρ is the density of the material. This force will cause an acceleration of the material of the element given by the equation

$$\rho \ddot{\xi} dx dy dz = - \frac{\partial p}{\partial x} dx dy dz \quad (4.2)$$

where ξ is the displacement of the element of volume considered moving with the material. Similarly for the y and z direction we have the three equations

$$\rho \ddot{\xi} = - \frac{\partial p}{\partial x}; \quad \rho \ddot{\eta} = - \frac{\partial p}{\partial y}; \quad \rho \ddot{\zeta} = - \frac{\partial p}{\partial z}. \quad (4.3)$$

The pressure p in these equations is the excess pressure of the medium, i.e., the increase or decrease of the pressure from the average pressure of the medium. In deriving the equations of motion the assumption is made that this increment of pressure is small compared to the average or static pressure. It is desirable to relate the ratio of this increment of pressure p to the static pressure p_0 , to some of the physical properties of the

medium. These properties of interest are the dilation Δ and the condensation s defined by

$$\Delta = \frac{dV}{V_0}; \text{ i.e., } V = V_0(1 + \Delta) \quad (4.4)$$

and

$$s = \frac{d\rho}{\rho_0}; \text{ i.e., } \rho = \rho_0(1 + s). \quad (4.5)$$

That is, the dilation is the increase in volume occupied by a given amount of material in an expanded or compressed state divided by the volume V_0 it would occupy if it were under static pressure p_0 . Similarly, the condensation s is the increase in density of material in a given volume divided by the density existing when the pressure is p_0 . From (4.4) and (4.5) since the product $\rho V = \rho_0 V_0$ we have

$$(1 + \Delta)(1 + s) = 1 \quad \text{or} \quad s = -\Delta \quad (4.6)$$

if we neglect the small product term $s\Delta$.

For a perfectly elastic fluid we have

$$-\frac{dv}{V} \frac{1}{dp} = C; \quad C = \frac{1}{\kappa} \quad (4.7)$$

in which C is the compressibility which is the inverse of the bulk modulus κ .

For a perfect gas in which the changes of pressure are adiabatic or so rapid that the heat generated does not have time to flow from the hot compressed parts to the cool rarified parts we have the gas law

$$pV^\gamma = p_0V_0^\gamma \quad (4.8)$$

where γ is the ratio of the specific heats of the medium. $\gamma = 1.408$ for air. If the volume and pressure of the mass of gas under consideration changes by the amounts dV and dp we have from (4.8)

$$(p_0 + dp)(V_0 + dV)^\gamma = p_0V_0^\gamma. \quad (4.9)$$

Expanding these terms by the binomial theorem and neglecting powers of dp and dV higher than the first we have

$$p_0 \left(1 + \frac{dp}{p_0}\right) V_0^\gamma \left[1 + \gamma \frac{dV}{V_0}\right] = p_0V_0^\gamma. \quad (4.10)$$

Hence

$$\frac{dp}{p_0} = -\gamma \frac{dV}{V_0} = -\gamma \Delta = \gamma s \text{ and } p = p_0(1 + \gamma s). \quad (4.11)$$

Introducing this value into (4.7) we find that the bulk modulus κ (sometimes called the modulus of cubic elasticity) is

$$\kappa = \frac{1}{C} = p_0 \gamma. \quad (4.12)$$

To obtain the complete equations we need one other relationship, the equation of continuity which can be derived

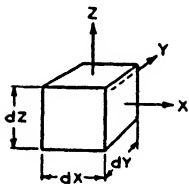


FIG. 4.1—ELEMENTARY CUBE.

by considering the small cubical volume of Fig. 4.1. The principle of continuity states that "The difference between the amounts of fluid which flow in and out of a small closed surface during a small interval of time dt must be equal to the increase in the amount of the fluid, during the same interval, that the surface contains." The increase of material in

the volume due to motion in the x direction is

$$\begin{aligned} dt[(\rho \xi)_1 - (\rho \xi)_2] dy dz &= dt \left[(\rho \xi)_1 - \left((\rho \xi)_1 + \frac{\partial(\rho \xi)}{\partial x} dx \right) \right] dy dz \\ &= - \frac{\partial(\rho \xi)}{\partial x} dx dy dz dt \quad (4.13) \end{aligned}$$

where the subscripts refer to the first and second x faces. We have similar equations for the y and z directions. The total increase of fluid contained in the elementary volume dx, dy, dz in time dt is

$$\frac{\partial \rho}{\partial t} dx dy dz dt. \quad (4.14)$$

Hence, equating the expression to satisfy the principle of continuity we have

$$\frac{\partial \rho}{\partial t} + \frac{\partial}{\partial x} (\rho \xi) + \frac{\partial}{\partial y} (\rho \eta) + \frac{\partial}{\partial z} (\rho \zeta) = 0. \quad (4.15)$$

Replacing ρ by $\rho_0(1 + s)$ and neglecting $s\xi$ compared to ξ , this equation becomes

$$\frac{\partial s}{\partial t} + \frac{\partial \xi}{\partial x} + \frac{\partial \eta}{\partial y} + \frac{\partial \zeta}{\partial z} = 0 \quad (4.16)$$

which can be combined with (4.3) and (4.11) to give the necessary relationships.

In place of dealing with three separate equations it is more economical to deal with one equation if a function can be found from which all the other quantities can be obtained by differentiation. Such a quantity is the velocity potential φ which we can define as such a function that

$$\xi = -\frac{\partial \varphi}{\partial x}; \quad \eta = -\frac{\partial \varphi}{\partial y}; \quad \zeta = -\frac{\partial \varphi}{\partial z}. \quad (4.17)$$

From (4.3) and (4.11), neglecting second order quantities, we have

$$\ddot{\xi} = -\frac{p_0 \gamma}{\rho_0} \frac{\partial s}{\partial x} = -v^2 \frac{\partial s}{\partial x}; \quad \ddot{\eta} = -v^2 \frac{\partial s}{\partial y}; \quad \ddot{\zeta} = -v^2 \frac{\partial s}{\partial z} \quad (4.18)$$

where v is the velocity of propagation of a wave in the gas. To obtain φ then we can integrate (4.17), obtaining

$$\begin{aligned} -\frac{\partial \varphi}{\partial x} = \xi = -v^2 \frac{\partial}{\partial x} \int_0^t s \, dt + \xi_0; \quad -\frac{\partial \varphi}{\partial y} = \eta = -v^2 \frac{\partial}{\partial y} \int_0^t s \, dt + \eta_0; \\ -\frac{\partial \varphi}{\partial z} = \zeta = -v^2 \frac{\partial}{\partial z} \int_0^t s \, dt + \zeta_0 \end{aligned} \quad (4.19)$$

where the constants ξ_0, η_0, ζ_0 are the original component velocities where $t = 0$. If we take for these constants $\xi_0 = -\frac{\partial \varphi_0}{\partial x}$, etc., we have

$$\varphi = v^2 \int_0^t s \, dt + \varphi_0 \quad (4.20)$$

which is the velocity potential function sought for. Equation (4.20) yields at once the relationship

$$\frac{\partial \varphi}{\partial t} = \dot{\varphi} = v^2 s = \left(\frac{p_0 \gamma}{\rho_0} \right) s = \left(\frac{p_0 \gamma}{\rho_0} \right) \left(\frac{p}{\gamma p_0} \right) = \frac{p}{\rho_0} \quad (4.21)$$

by equation (4.11).

Introducing this relation into the equation of continuity (4.16), we have

$$\frac{\partial^2 \varphi}{\partial t^2} - v^2 \left(\frac{\partial^2 \varphi}{\partial x^2} + \frac{\partial^2 \varphi}{\partial y^2} + \frac{\partial^2 \varphi}{\partial z^2} \right) = 0 \quad (4.22)$$

which is the general wave equation for propagation in three dimensions satisfied by the velocity potential φ . In this equation v is the velocity of propagation of the sound wave.

4.2. Propagation of Plane Waves in an Acoustic Tube

A good many of the commercial acoustic applications depend on the propagation of sound waves in tubes. For this use it is commonly assumed that plane waves exist, i.e., the particle

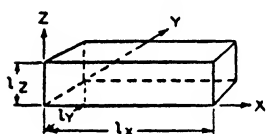


FIG. 4.2—CROSS-SECTION OF RECTANGULAR TUBE.

velocity is all along the direction of propagation, and zero in the other two directions. This assumption is legitimate for frequencies which are not too high but breaks down at higher frequencies. Since some of the failures of acoustic devices to operate properly can be traced to this assumption it appears worth while to investigate the conditions under which it is valid. This can be done by solving the wave equation (4.22) for a rectangular pipe with its length along the x axis, its width along the y axis and its thickness or smallest dimension along the z axis as shown in Fig. 4.2. We are ordinarily only interested in simple harmonic motion and employ the symbolic solution as explained in Chapter II, which is obtained by writing φ as $\varphi e^{j\omega t}$. Then equation (4.22) becomes

$$\frac{\partial^2 \varphi}{\partial x^2} + \frac{\partial^2 \varphi}{\partial y^2} + \frac{\partial^2 \varphi}{\partial z^2} + \frac{\omega^2}{v^2} \varphi = 0. \quad (4.23)$$

A wave equation of this type can usually be solved by assuming that the solution is a product of three separate functions, each of which is a function of one of the dimensions. For this case

$$\varphi = X(x)Y(y)Z(z). \quad (4.24)$$

Introducing this value into (4.23) and dividing by φ we have

$$\frac{\frac{\partial^2 X}{\partial x^2}}{X} + \frac{\frac{\partial^2 Y}{\partial y^2}}{Y} + \frac{\frac{\partial^2 Z}{\partial z^2}}{Z} + \frac{\omega^2}{v^2} = 0. \quad (4.25)$$

This can be written in the form

$$\frac{\frac{\partial^2 Z}{\partial z^2}}{Z} = -\frac{\frac{\partial^2 X}{\partial x^2}}{X} - \frac{\frac{\partial^2 Y}{\partial y^2}}{Y} - \frac{\omega^2}{v^2} = -a_1^2. \quad (4.26)$$

That is, we have on the left-hand side a function of z only, while on the right-hand side we have a function of x and a function of y together with a constant ω^2/v^2 . The only way this equation can be valid for all values of x and y is to put the right-hand side equal to a constant $-a_1^2$. This leaves the equation

$$\frac{\frac{\partial^2 Y}{\partial y^2}}{Y} = -\frac{\frac{\partial^2 X}{\partial x^2}}{X} - \frac{\omega^2}{v^2} + a_1^2 = -a_2^2. \quad (4.27)$$

Finally the equation for the function X becomes

$$\frac{\frac{\partial^2 X}{\partial x^2}}{X} = -\frac{\omega^2}{v^2} + a_1^2 + a_2^2. \quad (4.28)$$

The equations (4.26), (4.27) and (4.28) are solved by writing

$$Z = E \cos a_1 z + F \sin a_1 z$$

$$Y = C \cos a_2 y + D \sin a_2 y \quad (4.29)$$

$$X = \left[A \cos \sqrt{\frac{\omega^2}{v^2} - a_1^2 - a_2^2} x + B \sin \sqrt{\frac{\omega^2}{v^2} - a_1^2 - a_2^2} x \right]$$

and since the value of φ is a product of these three functions, the solution will be this product.

Some of the constants can be determined by the condition that at the wall of the tubing, the particle velocity normal to the tubing must equal zero since the air wave cannot penetrate the metal. According to Fig. 4.2 this occurs when $z = 0$;

$z = l_z$; $y = 0$, $y = l_y$. Then since the particle velocity in the two directions is, by (4.17), the negative derivative of φ by z , we find

$$\dot{\xi} = -\frac{\partial \varphi}{\partial z} = [E a_1 \sin a_1 z - F a_1 \cos a_1 z] Y(y) X(x). \quad (4.30)$$

Since $\dot{\xi} = 0$ when $z = 0$

$$F = 0. \quad (4.31)$$

To satisfy the condition that $\dot{\xi} = 0$ when $z = l_z$ we can let

$$a_1 = \frac{m\pi}{l_z}; \quad m = 0, 1, 2, 3, \text{ etc.},$$

since then the sin term will vanish when $z = l_z$. A complete solution of the function Z will then be

$$Z = \left(\sum_{m=0}^{m=\infty} E_m \cos \frac{m\pi z}{l_z} \right). \quad (4.32)$$

Similarly the function Y can be determined as

$$Y = \left(\sum_{n=0}^{n=\infty} C_n \cos \frac{n\pi y}{l_y} \right); \quad n = 0, 1, 2, 3, \text{ etc.} \quad (4.33)$$

Finally, the complete solution for φ , the velocity potential, is given by

$$\begin{aligned} \varphi = \sum_{m=0}^{\infty} \sum_{n=0}^{\infty} \left[\left[A_{m,n} \cos \sqrt{\frac{\omega^2}{v^2} - \frac{m^2 \pi^2}{l_z^2} - \frac{n^2 \pi^2}{l_y^2}} x + B_{m,n} \right. \right. \\ \left. \left. \sin \sqrt{\frac{\omega^2}{v^2} - \frac{m^2 \pi^2}{l_z^2} - \frac{n^2 \pi^2}{l_y^2}} x \right] \left(\cos \frac{m\pi z}{l_z} \right) \left(\cos \frac{n\pi y}{l_y} \right) \right] \end{aligned} \quad (4.34)$$

since the values of E_m and C_n are included in the constants $A_{m,n}$ $B_{m,n}$.

This solution represents a double infinity of different types of waves transmitted down the tube. If $m = n = 0$, the wave transmitted is

$$\varphi = A_{0,0} \cos \frac{\omega x}{v} + B_{0,0} \sin \frac{\omega x}{v} \quad (4.35)$$

while the particle velocity $\xi = -\frac{\partial\varphi}{\partial x}$ is given by

$$\xi = -\frac{\partial\varphi}{\partial x} = A_{0,0} \frac{\omega}{v} \sin \frac{\omega x}{v} - B_{0,0} \frac{\omega}{v} \cos \frac{\omega}{v} x. \quad (4.36)$$

This particle velocity is not a function of y , or z , and hence the solution is that for a plane wave. Since the propagation constant for such a wave is $\frac{j\omega x}{v}$, the wave is not attenuated and is propagated freely down the tube.

Let us consider next one of the other waves, say $m = 0$, $n = 1$. Then

$$\begin{aligned} \varphi &= \left(A_{0,1} \cos \sqrt{\frac{\omega^2}{v^2} - \frac{\pi^2}{l_y^2}} x + B_{0,1} \sin \sqrt{\frac{\omega^2}{v^2} - \frac{\pi^2}{l_y^2}} x \right) \cos \frac{\pi y}{l_y} \\ \xi &= -\frac{\partial\varphi}{\partial x} = \sqrt{\frac{\omega^2}{v^2} - \frac{\pi^2}{l_y^2}} \left[A_{0,1} \sin \sqrt{\frac{\omega^2}{v^2} - \frac{\pi^2}{l_y^2}} x \right. \\ &\quad \left. - B_{0,1} \cos \sqrt{\frac{\omega^2}{v^2} - \frac{\pi^2}{l_y^2}} x \right] \cos \frac{\pi y}{l_y}. \end{aligned} \quad (4.37)$$

We see that for this case the particle velocity is a function of y , in fact it has a positive value at $y = 0$, 0 at

$y = \frac{l_y}{2}$ and a negative value when $y = l_y$. Such

a wave might be set up by a diaphragm which vibrated as shown in Fig. 4.3. We note however that as long as

$$\frac{\omega}{v} < \frac{\pi}{l_y} \quad (4.38)$$

the value of the angle of the sine or cosine term is imaginary. This corresponds to a propagation constant equal to

$$\theta = \sqrt{\frac{\pi^2}{l_y^2} - \frac{\omega^2}{v^2}} x \quad (4.39)$$

and hence the wave will be attenuated by $\sqrt{\pi^2/l_y^2 - \omega^2/v^2}$ nepers per centimeter as long as $f < v/2l_y$, or in other words as

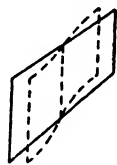


FIG. 4.3—SHAPE OF DIAPHRAGM TO SET UP FIRST OVERTONE MODE.

long as $l_y < \lambda/2$ or less than half a wavelength. The setting up of this type of wave requires a diaphragm that vibrates dissymmetrically, which rarely happens. The first symmetrical wave occurs when $n = 2$ and this will be attenuated if the distance l_y or l_z is less than a wavelength.

For the general case the values of $A_{m,n}$ and $B_{m,n}$ can be determined by the diaphragm displacement and the pressure existing over the mouth of the tube when $x = 0$. For this case

$$\begin{aligned}\varphi &= \sum_{m=0}^{\infty} \sum_{n=0}^{\infty} \left(A_{m,n} \cos \frac{m\pi z}{l_z} \cos \frac{n\pi y}{l_y} \right) \\ \xi &= -\frac{\partial \varphi}{\partial x} = \sum_{m=0}^{\infty} \sum_{n=0}^{\infty} \left(-B_{m,n} \cos \frac{m\pi z}{l_z} \cos \frac{n\pi y}{l_y} \right) \quad (4.40) \\ &\quad \left(\sqrt{\frac{\omega^2}{v^2} - \frac{n^2 \pi^2}{l_y^2} - \frac{m^2 \pi^2}{l_z^2}} \right).\end{aligned}$$

Hence if φ and ξ are specified as functions of y and z the constants $A_{m,n}$ and $B_{m,n}$ can be determined by employing a double Fourier series analysis. However, if both l_y and l_z are less than a wavelength then after a short distance down the tube the higher modes of motion will disappear due to the high attenuation and only a plane wave will be left. Hence under these conditions it is legitimate to assume only plane wave motion in analyzing the performance of sound in tubes.

If the tube is circular and there is no dissymmetry of the motion for different angles, the limiting condition is readily found to be

$$D = \frac{3.832}{\pi} \lambda \quad (4.41)$$

where D is the diameter of the tube and λ the wavelength.

Since the plane wave motion is the one which will ultimately exist in most tubes it is worth while to investigate it farther. Equations (4.35) and (4.36) give the velocity potential φ and particle velocity ξ in terms of the constants $A_{0,0}$ and $B_{0,0}$. As in the case of the electric line it is advantageous to express the

pressure and particle velocity at any distance along the tube in terms of the pressure and particle velocity at the beginning of the tube. From equations (4.21) and (4.35) the pressure at any point is given by

$$\check{p} = j\omega\rho\varphi = j\omega\rho \left[A_{0,0} \cos \frac{\omega x}{v} + B_{0,0} \sin \frac{\omega x}{v} \right]. \quad (4.42)$$

When $x = 0$

$$A_{0,0} = \frac{p_1}{j\omega\rho}. \quad (4.43)$$

Similarly from (4.36)

$$B_{0,0} = -\frac{\xi_1 v}{\omega}. \quad (4.44)$$

As pointed out in the introduction it is advantageous to use the volume velocity

$$\check{V}_1 = \xi_1 S \quad (4.45)$$

where S is the cross-sectional area of the tube, in place of the linear velocity. Hence

$$B_{0,0} = -\frac{\xi_1 S v}{S\omega} = -\frac{V_1 v}{S\omega}. \quad (4.46)$$

Introducing the values of these constants in (4.36) and (4.42) the equations of a plane wave in a tube become

$$\begin{aligned} p &= p_1 \cos \frac{\omega x}{v} - j \frac{\rho v}{S} V_1 \sin \frac{\omega x}{v} \\ V &= V_1 \cos \frac{\omega x}{v} - j \frac{p_1 S}{\rho v} \sin \frac{\omega x}{v}. \end{aligned} \quad (4.47)$$

Since in an acoustic system pressure is the analogue of voltage, and volume velocity of current, we see on comparing (4.47) with equation (2.142) for a dissipationless line that

$$\frac{\rho v}{S} = Z_0 \quad (4.48)$$

is the acoustic image impedance of the tube. The quantity ρv has been called the specific radiation resistance of the tube.

The energies associated with an acoustic wave are partly kinetic and partly potential. The kinetic energy is by definition

$$KE = \frac{1}{2}\rho \iiint (\xi^2 + \eta^2 + \zeta^2) dV \quad (4.49)$$

that is, it will be the sum of one half the mass times the square of the velocity summed over all the particles. The potential energy of the element of volume dV is the work that will be done during the expansion of the corresponding quantity of gas from its actual to its normal volume. At any stage of the expansion when the condensation is s' the effective pressure will be

$$p_0 + p = p_0 + v^2 \rho s' \quad (4.50)$$

by equation (4.21). To obtain the work, this pressure has to be multiplied by the corresponding increment of volume and integrated over the expansion range. The whole work gained during the expansion from dV to $dV(1+s)$ is therefore

$$\rho v^2 dV \int_0^s s' ds' = \frac{1}{2} \rho v^2 s^2 dV. \quad (4.51)$$

Integrating over the whole volume the total potential energy will be

$$PE = \frac{1}{2} \rho v^2 \iiint s^2 dV = \frac{1}{2 \rho v^2} \iiint p^2 dV. \quad (4.52)$$

In a plane progressive wave the ratio of p/V is the same at any point. Inserting this condition in (4.47) we have for a plane progressive wave

$$\frac{p}{V} = \frac{p_1}{V_1} = \frac{\rho v}{S}; \quad p = p_1 e^{\frac{-j\omega x}{v}}; \quad V = V_1 e^{\frac{-j\omega x}{v}}. \quad (4.53)$$

To obtain the energy in the wave we have to reinsert the time variation $e^{+j\omega t}$ which has been understood and take the real part. This results in

$$p = p_m \cos \omega \left(t - \frac{x}{v} \right); \quad V = V_m \cos \omega \left(t - \frac{x}{v} \right)$$

$$\text{or } \xi = \xi_m \cos \omega \left(t - \frac{x}{v} \right). \quad (4.54)$$

Squaring and inserting in (4.49) and (4.52) we have

$$\begin{aligned}
 KE &= \frac{1}{2} \rho \xi_m^2 \iiint \cos^2 \omega \left(t - \frac{x}{v} \right) dV \\
 &= \frac{1}{4} \rho \xi_m^2 S \int_0^l \left[1 - \cos 2\omega \left(t - \frac{x}{v} \right) \right] dx \\
 PE &= \frac{p_m^2}{2\rho v^2} \iiint \cos^2 \omega \left(t - \frac{x}{v} \right) dV \\
 &= \frac{1}{4} \frac{p_m^2 S}{\rho v^2} \int_0^l \left[1 - \cos 2\omega \left(t - \frac{x}{v} \right) \right] dx.
 \end{aligned} \tag{4.55}$$

In these equations p_m and ξ_m are the maximum values of pressure and velocity at the beginning of the tube and S the cross-sectional area. Integrating over a number of complete cycles the cyclic terms are small compared to the constant term and hence the average energies per cubic centimeter are

$$KE = \frac{1}{4} \rho \xi_m^2; \quad PE = \frac{1}{4} \frac{p_m^2}{\rho v^2}. \tag{4.56}$$

Since from (4.53) $p_m/\xi_m = \rho v$

$$KE = PE = \frac{1}{4} \rho \xi_m^2 = \frac{1}{4} \frac{p_m^2}{\rho v^2} \tag{4.57}$$

and the potential and kinetic energies of a plane progressive wave are equal. The total energy for the wave is

$$\frac{1}{2} \rho \xi_m^2 = \frac{1}{2} \frac{p_m^2}{\rho v^2} = W. \tag{4.58}$$

Another quantity of interest is the rate at which energy is transmitted across a unit area of a plane parallel to the wave front. Since in a second's time the total energy transmitted across the surface will occupy a region v centimeters long, this rate can be obtained by multiplying (4.58) by v , giving

$$\text{power per square cm} = \frac{1}{2} \rho v \xi_m^2 = \frac{1}{2} \frac{p_m^2}{\rho v}. \tag{4.59}$$

This quantity has been called the intensity of sound radiation.

4.3. *Effect of Viscosity and Heat Conduction on the Transmission of Sound*

The derivation of the equation of motion of sound given in section (4.1) neglects the effects of viscosity due to the walls of the tube which will cause a considerable change in the motion of sound in an enclosed tube. The coefficient of viscosity is defined as equal to the tangential force exerted on a unit area of either of two horizontal planes placed a unit distance apart in the viscous substance, one of the planes being fixed and the other moving with a unit velocity. Since the fluid touching each of the planes remains fixed to the plane, the tangential force on a unit area is equal to

$$F = \mu \frac{(v_2 - v_1)}{y} = \mu \frac{dv}{dy} \text{ in the limit} \quad (4.60)$$

where $v_2 - v_1$ is the relative velocity of one plane with respect to the other and y their separation. In a tube, since the walls are stationary, $v_1 = 0$.

We shall investigate first the effect of viscosity in modifying the flow of air through a narrow slit of thickness l , assuming rectilinear flow of all the air particles. At the edges of the slit the velocity of air will be zero since the first layer is assumed to cling to the surface of the plane. Let us consider an element of volume of the gas of thickness dx along the length of the slit, and dimension dy in a direction across the slit. The other dimension is taken as unity. Then the viscous force acting along the surface when $y = y_0$ for the length dx will be

$$F_{x_1} = \mu \left(\frac{\partial v}{\partial y} \right)_{y=y_0} dx. \quad (4.61)$$

The force at $y = y_0 + dy$ will be in the opposite direction and equal to

$$F_{x_2} = \mu \left(\frac{\partial v}{\partial y} \right)_{y=y_0+dy} dx. \quad (4.62)$$

Hence the total viscous force on the layer will be

$$(F_{x_1} - F_{x_2}) = \mu \left[\left(\frac{\partial v}{\partial y} \right)_{y=y_0} - \left(\frac{\partial v}{\partial y} \right)_{y=y_0+dy} \right] dx = - \mu \frac{\partial^2 v}{\partial y^2} dx dy. \quad (4.63)$$

In moving the element there will be an inertia force equal to

$$\rho \, dx \, dy \, \frac{\partial v}{\partial t}. \quad (4.64)$$

The sum of these must be equated to the difference in forces acting on the element or

$$\left[\rho \frac{\partial v}{\partial t} - \mu \frac{\partial^2 v}{\partial y^2} \right] dx \, dy = (p_1 - p_2) dy = - \frac{\partial p}{\partial x} dx \, dy \quad (4.65)$$

where p_1 is the gas pressure on the first x face and p_2 that on the second. For simple harmonic motion this becomes

$$\left[k^2 v - \frac{\partial^2 v}{\partial y^2} \right] = \frac{(p_1 - p_2)}{\mu \, dx} \quad (4.66)$$

where

$$k = \sqrt{+\frac{j\omega\rho}{\mu}} = \sqrt{\frac{\omega\rho}{2\mu}} (1 + j).$$

Assuming that the applied pressure does not vary with y over the surface of the slot perpendicular to the displacement, a solution of (4.66) is

$$v = A_1 e^{ky} + A_2 e^{-ky} + \frac{p_1 - p_2}{k^2 \mu \, dx}. \quad (4.67)$$

If we determine the constants A_1 and A_2 so that v vanishes when $y = 0$ and $y = l_t$, the thickness of the slot, we have

$$v = \frac{(p_1 - p_2)}{k^2 \mu \, dx} \left[1 - \left(\frac{\sinh ky + \sinh k(l_t - y)}{\sinh kl_t} \right) \right]. \quad (4.68)$$

The total volume of air per second through one centimeter width of the slit of thickness l_t and length dx is

$$V = \int_0^{l_t} v \, dy = \frac{(p_1 - p_2) l_t}{k^2 \mu \, dx} \left[1 - \frac{\tanh \frac{kl_t}{2}}{k \frac{l_t}{2}} \right]. \quad (4.69)$$

When the slit is very narrow or the frequency very low, we have, expanding the hyperbolic tangent in its series form

$$\begin{aligned} V &= \frac{(p_1 - p_2)l_t}{k^2\mu dx} \left[1 - \left(1 - \frac{k^2 l_t^2}{12} + \frac{k^4 l_t^4}{120} \right) \right] \\ &= \frac{(p_1 - p_2)l_t^3}{12\mu dx} \left[1 - \frac{k^2 l_t^2}{10} \right]. \quad (4.70) \end{aligned}$$

This equation shows that a small slit of length dx , unity width, and thickness l_t acts as a series acoustic impedance equal to

$$\begin{aligned} Z &= \frac{(p_1 - p_2)}{V} = \frac{12\mu dx}{l_t^3 \left(1 - \frac{k^2 l_t^2}{10} \right)} \\ &= \frac{12\mu dx}{l_t^3} \left(1 + \frac{j\omega\rho}{\mu} \frac{l_t^2}{10} \right) = \left(\frac{12\mu}{l_t^3} + \frac{j6}{5} \frac{\omega\rho}{l_t} \right) dx. \quad (4.71) \end{aligned}$$

That is, the impedance represents a series resistance plus a mass reactance equal to $6/5$ times that of the free air in the same sized space. By making the thickness l_t very small, the resistance term can be made larger than the reactance term over wide frequency ranges. The resistance of a single slit is much too large but the resistance can be reduced by putting a number of slits in parallel. One way of doing this is to wind a spiral form in which the slit distance between spirals is accurately controlled.

The equivalent impedance of a small circular hole has been shown to be ¹

$$Z = \frac{dx}{\pi R^2} \left(\frac{8\mu}{R^2} + \frac{4}{3} j\omega\rho \right). \quad (4.72)$$

A simple way to get a large number of holes in a sheet is to use a piece of silk cloth. The ratio of reactance to resistance can be controlled by the mesh of the cloth and such materials have been used in microphones and telephone receivers for many years. The absolute value of the resistance of such a cloth can be measured by measuring the rate of air flow under a steady pressure difference between the two sides of the cloth.

¹ See "Vibrating Systems and Sound," I. B. Crandall, Appendix A.

For higher frequencies and larger slit thickness the effect of the air drag on the sides of the tube can still be obtained from equation (4.69). For high frequencies and large widths the value of $k \frac{l_t}{2}$ becomes large and

$$\tanh \frac{k}{2} l_t = \frac{\tanh \sqrt{\frac{\omega \rho}{2\mu}} \frac{l_t}{2} + j \tan \sqrt{\frac{\omega \rho}{2\mu}} \frac{l_t}{2}}{1 + j \tanh \sqrt{\frac{\omega \rho}{2\mu}} \frac{l_t}{2} \tan \sqrt{\frac{\omega \rho}{2\mu}} \frac{l_t}{2}} \rightarrow 1. \quad (4.73)$$

Hence, equation (4.69) can be put into the form

$$\begin{aligned} \rho l_t \left[j\omega \frac{\partial \xi}{\partial t} \left(1 + \sqrt{\frac{\mu}{2\omega\rho}} \frac{(2l)}{(l_t)} \right) + \sqrt{\frac{\omega\mu}{2\rho}} \frac{(2l)}{(l_t)} \frac{\partial \xi}{\partial t} \right] dx \\ = (p_1 - p_2) l_t = -\frac{\partial p}{\partial x} l_t dx \quad (4.74) \end{aligned}$$

where l is the length of the slit, and V the volume velocity is the particle velocity $\frac{\partial \xi}{\partial t}$ times the cross-sectional area l_t . The ratio $2l/l_t$ is the ratio of the perimeter of the surface touching the air to this area. Also from (4.11) and (4.16) we have for a plane wave where the pressure difference is maintained by the compression of the air

$$\frac{\partial p}{\partial x} = -p_0 \gamma \frac{\partial^2 \xi}{\partial x^2} \quad (4.75)$$

for a wave in the x direction. Hence the equation of wave motion taking account of viscosity becomes

$$\frac{\partial^2 \xi}{\partial t^2} \left(1 + \frac{P}{S} \sqrt{\frac{\mu}{2\omega\rho}} \right) + \frac{P}{S} \sqrt{\frac{\omega\mu}{2\rho}} \frac{\partial \xi}{\partial t} = \frac{p_0 \gamma}{\rho} \frac{\partial^2 \xi}{\partial x^2} = v^2 \frac{\partial^2 \xi}{\partial x^2}. \quad (4.76)$$

In addition, for a wide tube, there is a loss of energy due to heat conduction, which occurs owing to the fact that the compressed heated portion loses some energy by heat conduction to the cooler rarified parts before the compression can be propagated onward. The consideration of this problem is a matter for the

kinetic theory of gases. The latest results² indicate that this increases the effective coefficient of viscosity by about 114 per cent.

The solution of equation (4.76) equivalent to that of a line given in Chapter II becomes

$$\begin{aligned} V &= V_1 \cosh \theta x - \frac{p_1 S}{Z_0} \sinh \theta x \\ p &= p_1 \cosh \theta x - \frac{V_1 Z_0}{S} \sinh \theta x \end{aligned} \quad (4.77)$$

where V is the volume velocity at any distance along the tube, V_1 the volume velocity at the beginning, p the pressure at any distance, p_1 the pressure at the beginning and

$$\begin{aligned} \theta &= \sqrt{-\frac{\omega^2}{v^2} \left[\left(1 + \frac{P}{S} \sqrt{\frac{\mu}{2\omega\rho}} \right) - j \frac{P}{S} \sqrt{\frac{\mu}{2\omega\rho}} \right]} \\ &\doteq \frac{1}{2} \frac{P}{vS} \sqrt{\frac{\mu\omega}{2\rho}} + j \frac{\omega}{v} \left(1 + \frac{1}{2} \frac{P}{S} \sqrt{\frac{\mu}{2\omega\rho}} \right) \end{aligned} \quad (4.78)$$

$$Z_0 = \frac{p_0 \gamma \theta}{j\omega} \doteq \sqrt{p_0 \gamma \rho} \left[\left(1 + \frac{1}{2} \frac{P}{S} \sqrt{\frac{\mu}{2\omega\rho}} \right) - j \frac{1}{2} \frac{P}{S} \sqrt{\frac{\mu}{2\omega\rho}} \right]. \quad (4.79)$$

The real part of equation (4.78) is the attenuation constant, while the imaginary part is the phase constant per *cm*. In terms of a circular pipe, the attenuation is equal to

$$A = \frac{1}{r} \sqrt{\frac{\pi f \mu'}{p_0 \gamma}} = \frac{2.94 \times 10^{-5} \sqrt{f}}{r} \text{ nepers per cm} \quad (4.80)$$

where μ' is the increased value of viscosity. The constants used in calculating this value are

$$\begin{aligned} \mu &= 1.84 \times 10^{-4} \text{ g/cm sec} \\ \mu' &= 3.94 \times 10^{-4} \text{ g/cm sec} \\ p_0 &= 1.014 \times 10^6 \text{ dynes/cm}^2 \\ \gamma &= 1.408 \end{aligned}$$

² "Attenuation of Sound in Tubes," R. D. Fay, J. Acoustical Soc. Am., Vol. 12, No. 1, July 1940.

For example, for a tube one inch in inside diameter the attenuation per foot is about 0.2 *db* at 1000 cycles. From (4.80) we see that the attenuation is proportional to the square root of the frequency and inversely proportional to the diameter.

In the following sections it is a matter of some interest to obtain *T* and π network representations of an acoustic tube. These can be obtained from the *T* and π network representations of a line given by equation (2.125). For lines less than an eighth of a wavelength these are given closely by

T Network

$$\frac{Z_1}{2} = Z_0 \tanh \frac{\theta x}{2} \doteq \frac{Z_0 \theta x}{2}; \quad Z_2 = \frac{Z_0}{\sinh \theta x} \doteq \frac{Z_0}{\theta x} \quad (4.81)$$

π Network

$$Z_1 = Z_0 \sinh \theta x \doteq Z_0 \theta x; \quad 2Z_2 = Z_0 \coth \frac{\theta x}{2} \doteq \frac{2Z_0}{\theta x}.$$

Inserting the values of θ and Z_0 from (4.78) and (4.79) we have

T Network

$$\frac{Z_1}{2} = \left[\frac{P}{S} \sqrt{\frac{\mu \omega \rho}{2}} + j \omega \rho \left(1 + \frac{P}{S} \sqrt{\frac{\mu}{2 \omega \rho}} \right) \right] \frac{l}{2S}; \quad Z_2 = \frac{-j \rho v^2}{\omega S l} \quad (4.82)$$

π Network

$$Z_1 = \left[\frac{P}{S} \sqrt{\frac{\mu \omega \rho}{2}} + j \omega \rho \left(1 + \frac{P}{S} \sqrt{\frac{\mu}{2 \omega \rho}} \right) \right] \frac{l}{S}; \quad 2Z_2 = \frac{-j 2 \rho v^2}{\omega S l}.$$

Hence in the series arm we have a resistance proportional to the square root of the frequency, and an acoustic mass usually called an inertance nearly equal to the density ρ times the ratio of the length l divided by the area. The shunt arm is dissipationless and consists of a compliance equal to ρv^2 divided by the volume of the tube. For tubes longer than an eighth of a wavelength these approximations do not hold well and the more general equations (4.81) have to be used.

At considerably higher frequencies than those used in voice transmission other effects come in to alter the attenuation and phase characteristics.³ One of the most important of these is the interchange of energy between the longitudinal pressure wave and the rotational energy of the molecules of the gas which causes high attenuation in the frequency range between 20 and 100 kilocycles. At voice frequencies this source of loss is proportional to the frequency and amounts to usually less than 5 per cent of the viscous and heat conduction losses.

4.4. *Effect of a Change of Area of the Conducting Tubes—Horn Theory*

On account of the high acoustic impedance of metal tubes compared to the impedance of air, most of the sound energy in an air wave inside the tube is confined there and cannot get out to the atmosphere surrounding the tube. The tube then acts as a transmission line for transmitting acoustic energy from one point to another. Acoustic energy is usually generated in a small region such as a diaphragm chamber and often has to be delivered to a large space such as a room. In getting from the small space to the large space a change in area of the tube is advantageous. Such changes usually occur when a diaphragm air chamber is connected to a horn, and in the horn itself where a change of area occurs continuously from the throat to the mouth.

If the change of area between two uniform tubes is small the effect of the change of area is taken account of by writing

$$\xi_1 S_1 = \xi_2 S_2 \quad \text{or} \quad V_1 = V_2 \quad \text{and} \quad p_2 = p_1. \quad (4.83)$$

That is, the volume velocity, V , which is the average particle velocity ξ times the area S , out of one tube is equal to the

³ Viscosity also contributes to the attenuation of a plane wave propagated in a free atmosphere as shown in Appendix B. At voice frequencies this effect is usually much smaller than the viscosity attenuation contributed by the walls of the tube. Since, however, it increases as the square of the frequency, at supersonic frequencies this source of attenuation may be larger than the effect of the tube walls.

volume velocity entering the other tube, and the pressures for the adjacent tubes are equal. When the change of area is large, as in a diaphragm chamber with a small horn opening, this approximation is not adequate, for it neglects the fact that a compression of the air can take place as well as a flow from the chamber. For this case

$$p_2 = p_1; \quad V_2 = V_1 - jp_1\omega C \quad (4.84)$$

where C the compliance of the air chamber can be shown to be

$$C = V/\rho v^2 \quad (4.85)$$

where V is the volume of the chamber.

When the change in area is quite small, however, the compliance can be neglected and equations (4.83) are a good approximation. Let us consider two uniform tubes of cross section S_1 and S_2 joined together at their midpoint as shown on Fig. 4.4. If $l/2$ is the length of each tube the equation of a plane wave in the first section can be written

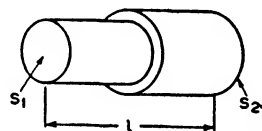


FIG. 4.4—TWO CONCENTRIC PIPES OF DIFFERENT AREA.

$$p_{12} = p_1 \cos \frac{\omega l}{2v} - jV_1 \frac{\rho v}{S_1} \sin \frac{\omega l}{2v};$$

$$V_{12} = V_1 \cos \frac{\omega l}{2v} - \frac{jp_1}{(\rho v/S_1)} \sin \frac{\omega l}{2v} \quad (4.86)$$

where p_1 and p_{12} are the pressures at the beginning of the tube and at a distance $l/2$ along the tube, while V_1 and V_{12} are the volume velocities at the beginning and at $x = l/2$. These equations follow from (4.47). Inserting these values and replacing the particle velocity by the volume velocity divided by the area we have equations (4.86).

For the second section of area S_2 we have

$$p_2 = p_{21} \cos \frac{\omega l}{2v} - jV_{21} \frac{\rho v}{S_2} \sin \frac{\omega l}{2v};$$

$$V_2 = V_{21} \cos \frac{\omega l}{2v} - \frac{jp_{21}}{\rho v/S_2} \sin \frac{\omega l}{2v} \quad (4.87)$$

where p_{21} and V_{21} are the pressure and volume velocity at the beginning of the tube and p_2 and V_2 the same quantities for the end of the tube. By equation (4.83) we have

$$p_{12} = p_{21}; \quad V_{12} = V_{21}.$$

Hence combining equations (4.86) and (4.87) we have two relations between the input and output pressures and volume velocities which are

$$\begin{aligned} p_2 &= p_1 \left[\left(\frac{S_1 + S_2}{2S_2} \right) \cos \frac{\omega l}{v} + \frac{S_2 - S_1}{2S_2} \right] \\ &\quad - jV_1 \frac{\rho v}{S_1} \left(\frac{S_1 + S_2}{2S_2} \right) \sin \frac{\omega l}{v} \\ V_2 &= V_1 \left[\frac{S_1 + S_2}{2S_1} \cos \frac{\omega l}{v} - \left(\frac{S_2 - S_1}{2S_1} \right) \right] \\ &\quad - j \frac{p_1 S_1}{\rho v} \left[\frac{S_1 + S_2}{2S_1} \right] \sin \frac{\omega l}{v}. \end{aligned} \quad (4.88)$$

We are interested in a series of such combinations in which the ratio of the end areas of each one is the same. Hence we set $S_2 = S_1 e^{2Tl}$; $S_3 = S_2 e^{2Tl}$, etc., where T is a constant determining the rate of taper. Introducing this value into (4.88) we have

$$\begin{aligned} p_2 &= e^{-Tl} \left[p_1 \left(\cosh Tl \cos \frac{\omega l}{v} + \sinh Tl \right) \right. \\ &\quad \left. - jV_1 \frac{\rho v}{S_1} \left(\cosh Tl \sin \frac{\omega l}{v} \right) \right] \\ V_2 &= e^{Tl} \left[V_1 \left(\cosh Tl \cos \frac{\omega l}{v} - \sinh Tl \right) \right. \\ &\quad \left. - j \frac{p_1 S_1}{\rho v} \left(\cosh Tl \sin \frac{\omega l}{v} \right) \right]. \end{aligned} \quad (4.89)$$

It is convenient to introduce another parameter δ defined by

$$\cosh \delta = \cosh Tl \cos \frac{\omega l}{v}. \quad (4.90)$$

In terms of this parameter equation (4.89) can be written

$$\begin{aligned}
 p_2 &= e^{-Tl} \left[p_1 \left[\cosh \delta + \frac{\sinh \delta}{\sqrt{1 - \coth^2 Tl \sin^2 \frac{\omega l}{v}}} \right] \right. \\
 &\quad \left. - \frac{V_1 \rho v}{S_1} \frac{\sinh \delta}{\sqrt{1 - \frac{\tanh^2 Tl}{\sin^2 \frac{\omega l}{v}}}} \right] \\
 V_2 &= e^{Tl} \left[V_1 \left[\cosh \delta - \frac{\sinh \delta}{\sqrt{1 - \coth^2 Tl \sin^2 \frac{\omega l}{v}}} \right] \right. \\
 &\quad \left. - \frac{p_1 S_1}{\rho v} \frac{\sinh \delta}{\sqrt{1 - \frac{\tanh^2 Tl}{\sin^2 \frac{\omega l}{v}}}} \right].
 \end{aligned} \tag{4.91}$$

If we write similar equations for other sections and combine them it is readily shown that

$$\begin{aligned}
 p_n &= e^{-nTl} \left[p_1 \left(\cosh n\delta + \frac{\sinh n\delta}{\sqrt{1 - \coth^2 Tl \sin^2 \frac{\omega l}{v}}} \right) \right. \\
 &\quad \left. - \frac{V_1 \rho v}{S_1} \frac{\sinh n\delta}{\sqrt{1 - \frac{\tanh^2 Tl}{\sin^2 \frac{\omega l}{v}}}} \right] \\
 V_n &= e^{nTl} \left[V_1 \left(\cosh n\delta - \frac{\sinh n\delta}{\sqrt{1 - \coth^2 Tl \sin^2 \frac{\omega l}{v}}} \right) \right. \\
 &\quad \left. - \frac{p_1 S_1}{\rho v} \left(\frac{\sinh n\delta}{\sqrt{1 - \frac{\tanh^2 Tl}{\sin^2 \frac{\omega l}{v}}}} \right) \right].
 \end{aligned} \tag{4.92}$$

We see then that this exponential structure in effect is a step down transformer for stepping down the pressure and stepping up the volume velocity. The step down ratio e^{-nTl} is equal to the square root of the small area divided by the large area while the impedance ratio, defining the impedance as the ratio of pressure to volume velocity is the ratio of the small area to the large area.

If we terminate the horn in a sending impedance Z_s/S_1 and a terminating impedance Z_T/S_n , i.e., in terms of their impedances per square cm, and express the result in a series of factors as was done in equation (2.35) the expression becomes

$$p_n = p_0 \frac{[Z_{0_1} + Z_{0_2}]Z_T}{(Z_s + Z_{0_1})(Z_{0_2} + Z_T)} \times e^{-nTl} e^{-n\delta} \quad (4.93)$$

$$\left[1 - e^{-2n\delta} \frac{(Z_{0_1} - Z_s)(Z_{0_2} - Z_T)}{(Z_{0_1} + Z_s)(Z_{0_2} + Z_T)} \right]$$

where $Z_{0_1} = \rho v \left[\frac{\sqrt{\sin^2 \frac{\omega l}{v} - \tanh^2 Tl} - j \tanh Tl}{\sin \frac{\omega l}{v}} \right];$

$$Z_{0_2} = \rho v \left[\frac{\sqrt{\sin^2 \frac{\omega l}{v} - \tanh^2 Tl} + j \tanh Tl}{\sin \frac{\omega l}{v}} \right].$$

Z_{0_1} and Z_{0_2} are the impedances per square centimeter looking toward and away from the source if the structure continues indefinitely. They are not equal to the image impedances of the structure but serve an equally useful purpose. Equation (4.93) shows that the structure acts as a transformer stepping the impedance down from the small end to the large end. As long as δ is imaginary the structure introduces no attenuation.

From the defining equation (4.90) it is obvious that the structure will have no attenuation when

$$\frac{1}{\cosh Tl} > \cos \frac{\omega l}{v} > -\frac{1}{\cosh Tl}. \quad (4.94)$$

At zero frequency where $\cos \frac{\omega l}{v} = 1$, the structure attenuates as it does at all the half wavelength points and their multiples. Hence by putting a taper to the structure it will act as a transformer in the regions around the odd quarter wavelengths.

To obtain the equations for a horn we can let the distance between successive area changes be vanishingly small. Then the parameters become

$$\begin{aligned} \cosh \delta &= \cosh Tl \cos \frac{\omega l}{v} \\ &= \left(1 + \frac{T^2 l^2}{2!} + \frac{T^4 l^4}{4!}\right) \left(1 - \frac{\omega^2 l^2}{v^2 2!} + \frac{\omega^4 l^4}{v^4 4!} + \dots\right) \\ &= 1 + \frac{l^2 \left(T^2 - \frac{\omega^2}{v^2}\right)}{2!} + \frac{l^4 \left(T^4 - \frac{6\omega^2}{v^2} T^2 + \frac{\omega^4}{v^4}\right)}{4!} + \dots \end{aligned} \quad (4.95)$$

For small values of l this reduces to

$$\cosh \delta = \cosh \sqrt{\left(T^2 - \frac{\omega^2}{v^2}\right)} l$$

$$Z_{01} = \rho v \left(\sqrt{1 - \frac{T^2 v^2}{\omega^2}} - j \frac{T v}{\omega} \right); \quad Z_{02} = \rho v \left(\sqrt{1 - T^2 \frac{v^2}{\omega^2}} + j \frac{T v}{\omega} \right). \quad (4.96)$$

When $\omega/v \gg T$ the impedances reduce to ρv the characteristic impedance of air. Near the cutoff frequency

$$\frac{\omega}{v} = T \quad \text{or} \quad f = \frac{T v}{2\pi}, \quad (4.97)$$

the impedance differs considerably from this and large interaction peaks occur, causing the horn to introduce unevenness of response.

4.5. *Side Branches and Acoustic Filter Theory*

In acoustic structures part of the energy transmitted by a tube is often diverted into another tube or side branch. Often only a single side branch exists and it has an important effect on the transmission of sound in the main tube. The most prominent example of this is in acoustic filters which will be discussed in this section.

Acoustic filters are devices for transmitting a given series of waves whose frequencies lie in a preassigned frequency range called the pass band and attenuating frequencies which lie outside of this range. The largest field of application of such filters is in mufflers used on automobiles, exhaust engines, air ducts and other applications in which an undesirable noise is propagated along a pipe or closed space. Since a steady or slowly varying stream of gas has to be passed, while the more rapid vibrations constituting the undesired noise have to be suppressed, a low-pass acoustic filter is required. Mufflers existed long before the theory of acoustic filters was worked out but the mufflers were designed as a series of baffles. Most recently designed mufflers have a straight conducting path with side branches in conformance with acoustic filter theory and are proportioned to attenuate most of the frequencies above 100 cycles. As a result they are considerably more effective than early mufflers and introduce considerably less back pressure on the automobile engine.

The idea of using acoustic tubes to produce interference between sound waves and a suppression of certain frequencies originates with Herschel (1833) and was applied by Quincke to stop tones of definite pitch from reaching the ear. Following the development of electrical wave filters, G. W. Stewart⁴ showed that combinations of tubes and resonators could be devised which would give transmission characteristics at low frequencies similar to electrical filters. This would correspond to using the T network equivalents of lines discussed in section

⁴ Phys. Rev. 20, 528 (1922); 23, 520 (1924); 25, 90 (1925). See also "Acoustics," Stewart and Lindsay, Ch. VII, D. Van Nostrand.

(2.8) and using their low frequency element values. A theory of acoustic filters taking account of the wave motion was given by the writer in 1927⁵ and it is this theory which is discussed and extended in this chapter. Since then Lindsay⁶ and his collaborators have discussed a number of cases and have extended the theory to solid metallic structures with various types of side branches and obstructions.

The present section discusses the methods for obtaining the image impedances and transfer constants of various types of acoustic filters. This is a proper procedure since if these parameters are known, the insertion loss of the filter can be obtained by using the insertion loss factor of equation (2.35) or (2.49). Thus, if one wishes to know the effect of inserting a filter in the middle of a long pipe, he has only to set Z_S and Z_T of equation (2.35) equal to $\frac{Z_0}{S}$ of equation (4.79) and the attenuation, reflection, and interaction factors are given by (2.35) when the image impedances and image transfer constant of the filter are known. When the filter is terminated in a short section of pipe open to the air the filter may act as a transformer at certain frequencies in the pass band and produce more vibration of that frequency than would be present without the filter.

When low frequencies are of interest or very small structures are used, i.e., when the dimensions are less than an eighth wavelength, some progress can be obtained by using the T or π network representations of a line discussed in section (4.3). For example, let us consider the structure shown in Table VI, filter 1, pages 128, 129. This is a low-pass filter having a main conducting tube of length l_1 and cross-sectional area S_1 , shunted by a side branch of cross-sectional area S_2 and length l_2 . Between the main tube and the side branch is a partition of thickness l_t with

⁵ "A Study of the Regular Combination of Acoustic Elements, with Applications to Recurrent Acoustic Filters, Tapered Acoustic Filters, and Horns," B.S.T.J., Vol. VI, pp. 258-294, April, 1927.

⁶ An excellent review and résumé of the literature on gaseous and solid acoustic filters is given by Lindsay, "The Filtration of Sound I," J. App. Phys. 9, 612 (1938); "The Filtration of Sound II"; J. App. Phys. 10, 680, (1939).

TABLE VI

TABLE OF ACOUSTIC FILTERS

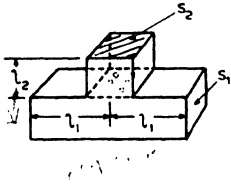
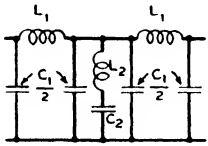
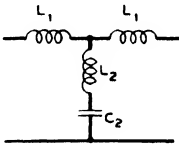
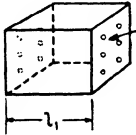
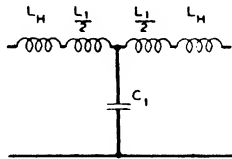
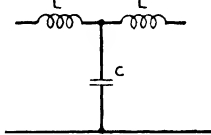
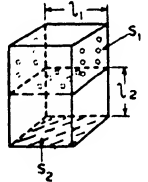
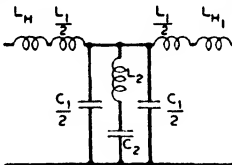
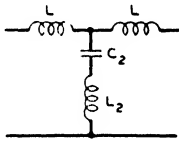
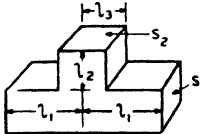
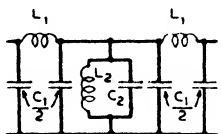
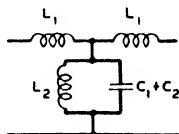
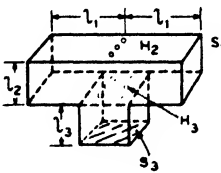
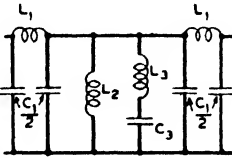
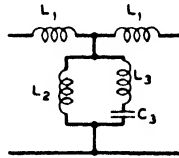
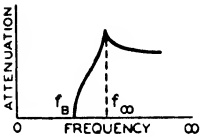
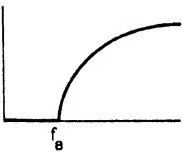
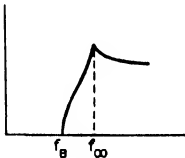
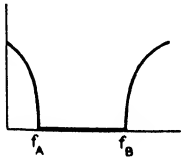
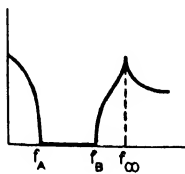
NO	FILTER	EQUIVALENT CIRCUIT	APPROXIMATE EQUIVALENCE
1			
2			
3			
4			
5			

TABLE VI
TABLE OF ACOUSTIC FILTERS

ATTENUATION CHARACTERISTIC	DESIGN CONSTANTS
	$\frac{l_1}{s_1} = \frac{m z_0}{2 \pi f_B \rho}; \quad v_2 = s_2 l_2 = \frac{m \rho v^2}{\pi f_B z_0}$ $\left[\frac{l_t + 2r}{N s_H} + \frac{l_2}{2 s_2} \right] = \frac{(1-m^2) z_0}{4 m \pi f_B \rho}; \quad m = \sqrt{1 - \frac{f_B^2}{f_\infty^2}}$
	$\left(\frac{l_t + 2r}{s_H N} + \frac{l_1}{2 s_1} \right) = \frac{z_0}{2 \pi \rho f_B}$ $l_1 s_1 = \frac{\rho v^2}{\pi f_B z_0}$
	$\left[\left(\frac{l_t + 2r}{N s_H} \right)_1 + \frac{l_1}{2 s_1} \right] = \frac{m z_0}{2 \pi \rho f_B}; \quad m = \sqrt{1 - \frac{f_B^2}{f_\infty^2}}$ $\left[\left(\frac{l_t + 2r}{N s_H} \right)_2 + \frac{l_2}{2 s_2} \right] = \frac{(1-m^2) z_0}{4 m \pi f_B \rho}; \quad s_2 l_2 = \frac{m \rho v^2}{\pi f_B z_0}$
	$\frac{l_1}{s_1} = \frac{z_0}{2 \pi \rho f_B}; \quad \left(l_2 + l_2' + \frac{l_3}{2} \right) \sqrt{\frac{1}{2} + \frac{l_1 s_1}{(l_2 + l_2' + \frac{l_3}{2}) s_2}} = \frac{v}{2 \pi f_A}$ $s_2 \sqrt{\frac{1}{2} + \frac{l_1 s_1}{(l_2 + l_2' + \frac{l_3}{2}) s_2}} = \frac{2 f_A f_B \rho v}{z_0 (f_B^2 - f_A^2)}$
	$\frac{l_1}{s_1} = \frac{z_0 m}{2 \pi f_A \rho}; \quad \left(\frac{l_t + 2r}{s_H N} \right)_2 = \frac{z_0 (1-m^2)}{4 \pi f_A m \rho}; \quad m = \sqrt{1 - \frac{f_\infty^2}{f_B^2}}$ $\left(\frac{l_t + 2r}{s_H N} \right)_3 + \frac{l_3}{s_3} = \frac{z_0 (1-m^2) (f_A^2 - m^2 f_B^2)}{4 \pi f_A m (f_B^2 - f_A^2) \rho}; \quad l_3 s_3 = \frac{(f_B^2 - f_A^2) m \rho v^2}{\pi f_A f_B^2 z_0 (1-m^2)}$

a number N of holes of radii r . The equivalent circuit of this combination is as shown on column 2. This is obtained by replacing the first halves and last halves of the main conducting tubes by their π network equivalents and the shunt chamber by its T network equivalent. In addition there is a series inertance due to the holes in the tube wall as shown by equation (4.72). The effective length will be longer than l_t , the thickness of tube wall, for as shown in section (4.6), equation (4.130), an added inertance occurs from radiation equal to

$$L = \frac{\rho r}{S_H} \quad (4.98)$$

where r is the radius and S_H the area of the hole. This radiation inertance occurs for both sides of the hole so that the total inertance L_3 is

$$L_3 = \frac{\rho(l_t + 2r)}{S_H N} \quad (4.99)$$

where N is the number of holes.

When the circuit of filter 1 is analyzed by the methods of Chapter II, the filter is a low- and band-pass filter. The upper-pass band is considerably above the low-pass band and for most purposes can be neglected. This amounts to neglecting the compliances C_1 which have high impedances at the lower frequencies. If we neglect the compliances C_1 the filter is a low-pass filter of the type shown in Table I, number 2, pages 52, 53. From these equations the dimensions in terms of the frequencies are

$$\begin{aligned} \frac{l_1}{S_1} &= \frac{mZ_{I_0}}{2\pi f_B \rho}; \quad V_2 = S_2 l_2 = \frac{m\rho v^2}{\pi f_B Z_{I_0}}; \\ \left(\frac{l_t + 2r}{NS_H} + \frac{l_2}{2S_2} \right) &= \frac{(1 - m^2)Z_{I_0}}{4m\pi f_B \rho}. \end{aligned} \quad (4.100)$$

These do not determine the dimensions completely but only the ratios so that considerable latitude in choice of dimensions is possible.

Table VI on pages 128, 129 shows a number of other filters which can be analyzed in a similar manner and can give good

results for small dimensions. However, for the large dimensions common in air ducts and internal combustion engine exhausts, the dimensions are considerably larger than can be treated by this method. For the larger filters the characteristics can be analyzed by employing the equations for the propagation of a plane wave in a tube.

Suppose that we have a straight conducting tube and a side branch as shown in Fig. 4.5. By assuming pistons acting at the common boundaries of the side branch and main branch open-

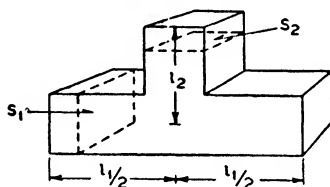


FIG. 4.5—MAIN CONDUCTING TUBE WITH SIDE BRANCH.

ings, and using methods similar to those used in section (4.2) it is possible to solve for the impedance relations existing in the side branch. The first approximation holding at very low frequencies indicates that

$$V_{12} = V_{21} + V_S; \quad p_{12} = p_{21} = p_S \quad (4.101)$$

where V_{12} is the volume velocity into the chamber from the main branch opening, V_{21} the volume velocity out of the main branch, and V_S is the volume velocity into the side branch. The average pressures across the three openings are equal. As the frequency increases the main effect is to add an end correction to the tubes entering the chamber. For example, we should measure the length of the main conducting tube from the center of the side branches, and the length of the side branches from the centers of the main conducting tubes.

The theory of acoustic filters is obtained from a consideration of the reaction of side branches on the transmission of sound in the main branch. The general effect of such a side branch of impedance Z_S/S_2 —where Z_S is the specific impedance of the side branch and S_2 its area—can be obtained by writing the equations of the main branch and the side branch which are

$$\begin{aligned}
p_{12} &= p_1 \cos \frac{\omega l_1}{2v} - j \frac{V_1 \rho v}{S_1} \sin \frac{\omega l_1}{2v}; \\
p_2 &= p_{21} \cos \frac{\omega l_1}{2v} - j V_{21} \frac{\rho v}{S_1} \sin \frac{\omega l_1}{2v}; \\
V_{12} &= V_1 \cos \frac{\omega l_1}{2v} - j \frac{p_1 S_1}{\rho v} \sin \frac{\omega l_1}{2v}; \\
V_2 &= V_{21} \cos \frac{\omega l_1}{2v} - j p_{21} \frac{S_1}{\rho v} \sin \frac{\omega l_1}{2v}; \\
V_S &= \frac{p_S S_2}{Z_S}; \quad p_{12} = p_{21} = p_S.
\end{aligned} \tag{4.102}$$

Combining these equations with the aid of (4.101) we have

$$\begin{aligned}
p_2 &= p_1 \left[\cos \frac{\omega l_1}{v} + j \frac{\rho v S_2}{2Z_S S_1} \sin \frac{\omega l_1}{v} \right] \\
&\quad - j \frac{V_1 \rho v}{S_1} \left(\sin \frac{\omega l_1}{v} + j \frac{\rho v S_2}{Z_S S_1} \sin^2 \frac{\omega l_1}{2v} \right) \\
V_2 &= V_1 \left[\cos \frac{\omega l_1}{v} + j \frac{\rho v S_2}{2Z_S S_1} \sin \frac{\omega l_1}{v} \right] \\
&\quad - j \frac{p_1 S_1}{\rho v} \left(\sin \frac{\omega l_1}{v} - j \frac{\rho v S_2}{Z_S S_1} \cos^2 \frac{\omega l_1}{2v} \right).
\end{aligned} \tag{4.103}$$

Comparing this with equation (2.32) for a filter section, this can be written

$$p_2 = p_1 \cosh \theta - V_1 \frac{Z_0}{S_1} \sinh \theta;$$

$$V_2 = V_1 \cosh \theta - j \frac{p_1 S_1}{Z_0} \sinh \theta$$

$$\text{where} \quad \cosh \theta = \left(\cos \frac{\omega l_1}{v} + j \frac{\rho v S_2}{2Z_S S_1} \sin \frac{\omega l_1}{v} \right); \tag{4.104}$$

$$Z_0 = \rho v \sqrt{\frac{\sin \frac{\omega l_1}{v} + j \frac{\rho v S_2}{Z_S S_1} \sin^2 \frac{\omega l_1}{2v}}{\sin \frac{\omega l_1}{v} - j \frac{\rho v S_2}{Z_S S_1} \cos^2 \frac{\omega l_1}{2v}}}.$$

The type of filter obtained with this structure depends on the side branch impedance Z_s . As long as Z_s is of such a value as to make the expression for $\cosh \theta$ greater in magnitude than one, an attenuation band occurs, while if $\cosh \theta$ is less than one a pass band occurs. The cutoff frequencies occur when $\cosh \theta = \pm 1$. From equations (4.104) the cutoff frequencies occur when

$$Z_s = j \frac{\rho v S_2}{2S_1} \cot \frac{\omega l_1}{2v} \quad \text{or} \quad Z_s = -j \frac{\rho v S_2}{2S_1} \tan \frac{\omega l_1}{2v}. \quad (4.105)$$

A low-pass type of filter is obtained by using a side branch closed on the end. For that case the volume velocity on the end is zero and the impedance at the input of the tube is

$$\frac{Z_s}{S_2} = \frac{p}{V} = -j \frac{\rho v}{S_2} \cot \frac{\omega l_2}{v} \quad (4.106)$$

as can be seen from equations (4.102) by setting $V_{12} = 0$ and solving for the ratio p_1/V_1 . Introducing this value of Z_s in equation (4.104) we have

$$\cosh \theta = \left(\cos \frac{\omega l_1}{v} - \frac{S_2 \sin \frac{\omega l_1}{v}}{2S_1 \cot \frac{\omega l_2}{v}} \right); \quad (4.107)$$

$$Z_0 = \rho v \sqrt{\frac{1 - \frac{S_2}{2S_1} \left(\tan \frac{\omega l_1}{2v} \right) \left(\cot \frac{\omega l_2}{v} \right)}{1 + \frac{S_2}{2S_1} \left(\cot \frac{\omega l_1}{2v} \right) \left(\cot \frac{\omega l_2}{v} \right)}}. \quad (4.108)$$

The most effective filter from the point of view of large attenuation will occur if $\cot \frac{\omega l_2}{v}$ is small when $\sin \frac{\omega l_1}{v}$ is large. This is best satisfied by letting $l_2 = l_1$ since the sine will be unity when

the cotangent vanishes. Fig. 4.6 shows a plot of the attenuation characteristic of such a filter as a function of the ratio S_2/S_1 . The larger this ratio is the higher the attenuation and the larger part of the frequency range is covered. A filter of this sort will have an attenuation band which centers around the odd quarter wavelength points of the side branch and pass bands which center around the half wavelength frequencies of the side branch. The specific characteristic impedance for this case is given by

$$Z_0 = \rho v \sqrt{\frac{1 - \frac{S_2}{2S_1} \left(\tan \frac{\omega l_1}{2v} \right)}{1 + \frac{S_2}{2S_1} \left(\cot \frac{\omega l_1}{v} \right)}}. \quad (4.109)$$

At zero frequency and at the mid-band frequencies of the even order higher pass bands, the nominal specific characteristic impedance becomes

$$Z_{0_0} = \frac{\rho v}{\sqrt{1 + \frac{S_2}{S_1}}} \quad (4.110)$$

while at the odd order bands it is

$$Z_{0_0} = \rho v \sqrt{1 + \frac{S_2}{S_1}}.$$

Hence, if it is desired to obtain uniform transmission for the lowest pass band, the terminating impedance on the ends of the filter should be considerably below the impedance of the main conducting tube for plane wave transmission.

The largest attenuation is obtained when the ratio of the side branch area to the main branch area is large. In the limit the largest ratio will be obtained when all sides of the main conducting tube are surrounded by side branches or in other

words a cylindrical side branch, as shown in Fig. 4.7, is used. Furthermore a larger side branch volume will be obtained by

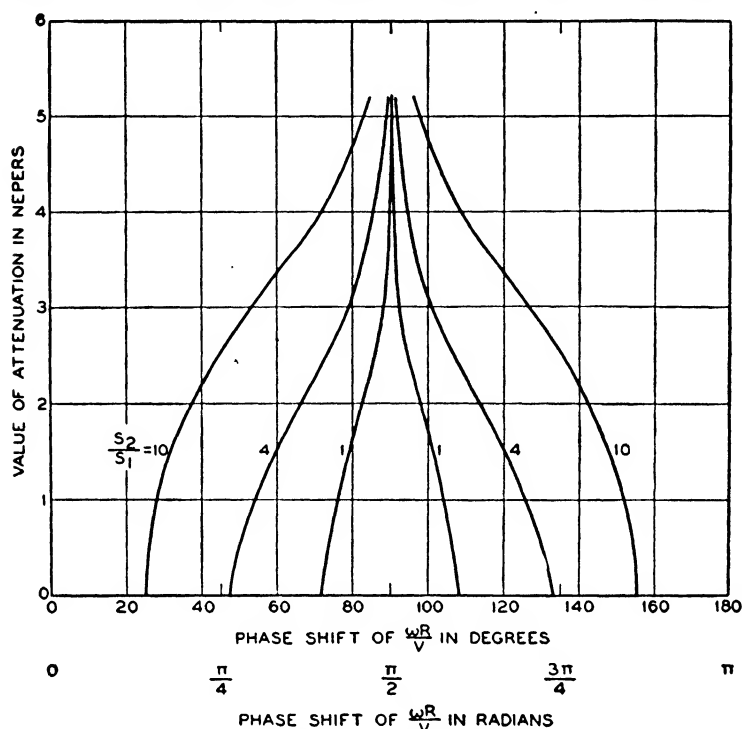


FIG. 4.6—ATTENUATION CHARACTERISTIC OF ACOUSTIC LOW- AND BAND-PASS FILTER.

letting the cylindrical side branch cover the complete length of the main conducting tube. The impedance of such a side branch can be calculated by assuming that a radial piston acts in the opening. The wave equation for cylindrical coordinates and simple harmonic motion takes the form:

$$\frac{\partial^2 \varphi}{\partial r^2} + \frac{1}{r} \frac{\partial \varphi}{\partial r} + \frac{\partial^2 \varphi}{\partial x^2} + \frac{\omega^2}{v^2} \varphi = 0. \quad (4.111)$$

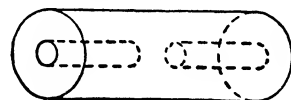


FIG. 4.7—LOW-PASS ACOUSTIC FILTER CONSTRUCTED FROM COAXIAL PIPES.

A solution of this takes the form of a product of a function of the radius times a function of the length dimension x or

$$\varphi = R(r)X(x). \quad (4.112)$$

Separating these functions as before, we have the two equations.

$$\frac{\partial^2 X(x)}{\partial x^2} = -a_1^2 X(x) \quad (4.113)$$

$$\frac{\partial^2 R(r)}{\partial r^2} + \frac{1}{r} \frac{\partial R(r)}{\partial r} + \left(\frac{\omega^2}{v^2} - a_1^2 \right) R(r) = 0. \quad (4.114)$$

A solution of (4.113) which at the same time assures that the particle velocity $\dot{\xi} = -\frac{\partial \varphi}{\partial x}$ vanishes at the two ends of the chamber, $x = 0$ and $x = l_x$, is

$$X(x) = \cos \frac{n\pi x}{l_x} \quad n = 0, 1, 2, \text{ etc.} \quad (4.115)$$

The solution of equation (4.114) is well known to be a Bessel's function of zero order

$$R(r) = AJ_0(kr) + BK_0(kr) \quad (4.116)$$

where $k = \sqrt{\frac{\omega^2}{v^2} - \frac{n^2 \pi^2}{l_x^2}}$, and J_0 is the Bessel's function of the first kind and K_0 the Bessel's function of the second kind. Hence the complete solution of (4.111) for this case is

$$\varphi = \sum_{n=0}^{\infty} [A_n J_0(kr) + B_n K_0(kr)] \cos \frac{n\pi x}{l_x}; \quad n = 0, 1, 2, 3, \text{ etc.} \quad (4.117)$$

To determine the constants A_n and B_n we have the condition that at $r = r_2$, the outer radius, the particle velocity $\dot{r} = -\frac{\partial \varphi}{\partial r} = 0$ while at $r = r_1$, the inner radius, the particle velocity is zero except over the center part where it is constant and equal to \dot{r}_1 , the value of the radial piston velocity. Introducing the first condition we have

$$\dot{r}_2 = -\left(\frac{\partial \varphi}{\partial r} \right)_{r=r_2} = \sum_{n=0}^{\infty} \left[A_n k J_1(kr) + B_n k K_1(kr) \right] \cos \frac{n\pi x}{l_x} \Big|_{r=r_2} = 0. \quad (4.118)$$

Hence

$$B_n = -A_n \frac{J_1(kr_2)}{K_1(kr_2)}. \quad (4.119)$$

Introducing this result the particle velocity at $r = r_1$ becomes

$$\dot{r}_1 = - \frac{\partial \varphi}{\partial r} = \sum_{n=0}^{\infty} \left[A_n k \left(J_1(kr_1) - \frac{J_1(kr_2)}{K_1(kr_2)} K_1(kr_1) \right) \right] \cos \frac{n\pi x}{l_x}. \quad (4.120)$$

The actual evaluation of the series depends on what proportion of the total length the entrance to the side branch covers. For this approximation to be valid this length has to be less than a half wavelength. If the opening is symmetrical with respect to the two ends, it is readily seen that the constants A_n disappear for all odd values of n . For an opening symmetrically situated and having the width l_w the constants may be determined as follows.

A_0 is determined by multiplying both sides of (4.120) by dx and integrating from $x = 0$ to $x = l_x$ along the sides of the cylinder $r = r_1$. There results

$$A_0 = \frac{1}{\frac{\omega l_x}{v} X_0} \int_0^{l_x} \dot{r}_1 dx = \frac{\dot{r}_1 l_w}{\frac{\omega}{v} X_0 l_x} \quad (4.121)$$

where X_0 is the expression

$$X_0 = \left[J_1 \left(\frac{\omega}{v} r_1 \right) - \frac{J_1 \left(\frac{\omega}{v} r_2 \right)}{K_1 \left(\frac{\omega}{v} r_2 \right)} K_1 \left(\frac{\omega}{v} r_1 \right) \right]. \quad (4.122)$$

Similarly the constants A_1, A_2 , etc., are determined by multiplying both sides of (4.120) by $\cos \frac{\pi x}{l_x}, \cos \frac{2\pi x}{l_x}$, etc., and integrating. We have

$$A_n = \frac{4\dot{r}_1 (-1)^{\frac{n}{2}} \sin \frac{n\pi l_w}{2l_x}}{n\pi} \left[\frac{1}{\sqrt{\frac{\omega^2}{v^2} - \frac{n^2 \pi^2}{l_x^2}} X_n} \right] \text{ if } n \text{ is even} \quad (4.123)$$

= 0 if n is odd

where

$$X_n = \left[J_1 \left(\sqrt{\frac{\omega^2}{v^2} - \frac{n^2 \pi^2}{l_x^2}} r_1 \right) - \frac{J_1 \left(\sqrt{\frac{\omega^2}{v^2} - \frac{n^2 \pi^2}{l_x^2}} r_2 \right)}{K_1 \left(\sqrt{\frac{\omega^2}{v^2} - \frac{n^2 \pi^2}{l_x^2}} r_2 \right)} K_1 \left(\sqrt{\frac{\omega^2}{v^2} - \frac{n^2 \pi^2}{l_x^2}} r_1 \right) \right].$$

To obtain the impedance of the side branch we need to divide the average pressure over the side branch by the volume velocity $2\pi r_1 l_w \dot{r}_1$. Since the pressure p is equal to $j\rho\omega\varphi$ for simple harmonic motion, the average pressure divided by the volume velocity will be

$$Z_S = \frac{j\rho v}{2\pi r_1 l_x} \left[Y_0 + \frac{l_x^2}{l_w^2} \sum_{n=2}^{\infty} \frac{16 Y_n \sin^2 \frac{n\pi l_w}{2l_x}}{n^2 \pi^2 \sqrt{1 - \left(\frac{n v}{2f l_x} \right)^2}} \right] \quad (4.124)$$

where

$$Y_n = \frac{\left\{ J_0 \left(\sqrt{\frac{\omega^2}{v^2} - \frac{n^2 \pi^2}{l_x^2}} r_1 \right) K_1 \left(\sqrt{\frac{\omega^2}{v^2} - \frac{n^2 \pi^2}{l_x^2}} r_2 \right) - J_1 \left(\sqrt{\frac{\omega^2}{v^2} - \frac{n^2 \pi^2}{l_x^2}} r_2 \right) K_0 \left(\sqrt{\frac{\omega^2}{v^2} - \frac{n^2 \pi^2}{l_x^2}} r_1 \right) \right\}}{\left\{ J_1 \left(\sqrt{\frac{\omega^2}{v^2} - \frac{n^2 \pi^2}{l_x^2}} r_1 \right) K_1 \left(\sqrt{\frac{\omega^2}{v^2} - \frac{n^2 \pi^2}{l_x^2}} r_2 \right) - J_1 \left(\sqrt{\frac{\omega^2}{v^2} - \frac{n^2 \pi^2}{l_x^2}} r_2 \right) K_1 \left(\sqrt{\frac{\omega^2}{v^2} - \frac{n^2 \pi^2}{l_x^2}} r_1 \right) \right\}}.$$

Having found the side branch impedance Z_S , we can insert it in equation (4.104) to determine the transfer constant.

A specific filter having the dimensions shown in Fig. 4.8 has been calculated up to 1200 cycles. The result is a narrow

pass band present whenever the length of the filter is $\frac{1}{2}$ wavelength or a multiple of this. The frequency of maximum attenuation depends largely on the difference in length between the inner and outer diameter. The attenuation reaches a maximum when this distance is approximately an odd quarter wavelength.

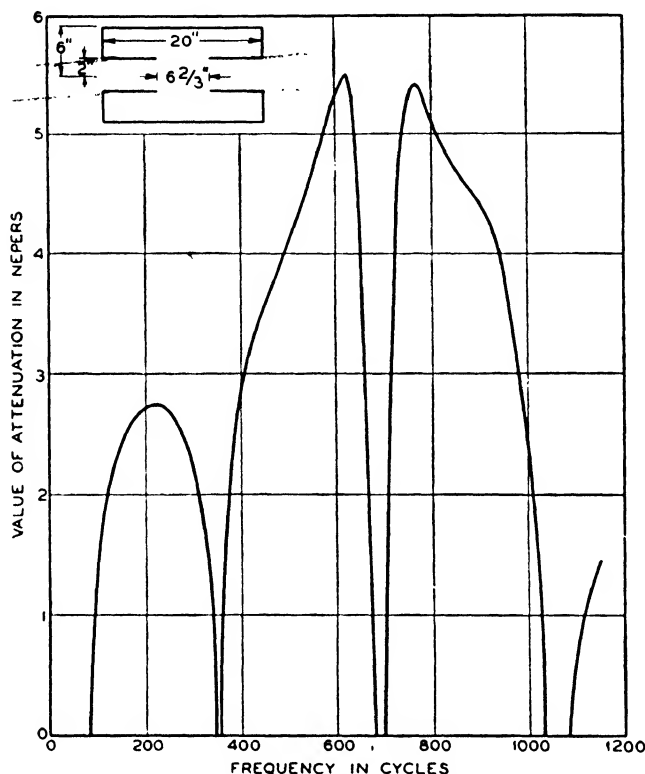


FIG. 4.8—ATTENUATION CHARACTERISTIC OF LOW-PASS ACOUSTIC FILTER.

Experimental measurements show that these extra pass bands really exist. Figure 4.9, solid line, shows measured attenuation curves of a two section filter both sections having the dimensions shown by the Type A section. This curve was obtained in a measuring system described in a former paper.⁷ This system consisted of two loud speakers, one for driving and

⁷ "Propagation Characteristics of Sound Tubes and Acoustic Filters," W. P. Mason, Phys. Rev., Vol. 31, No. 2, p. 283, 1928.

one for receiving, coupled together through the acoustic resistances similar to the tubular directional microphone described in section (4.7). The energy was fed into one of these loud speakers through several of the long tubes of the input resistance and

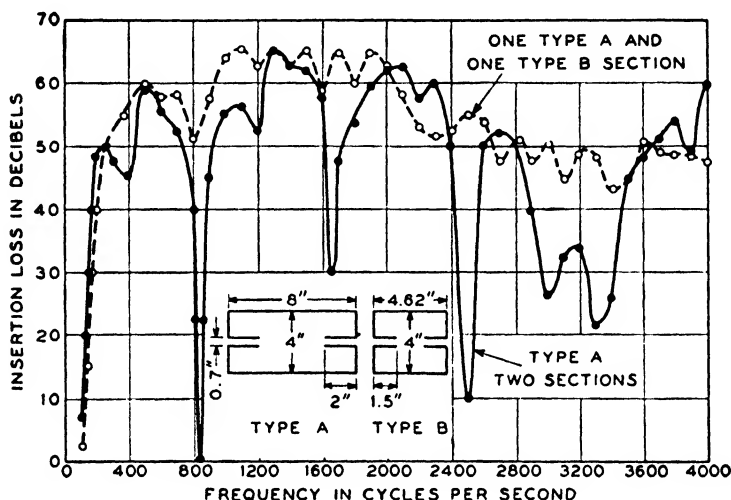


FIG. 4.9—MEASURED ATTENUATION OF A LOW-PASS ACOUSTIC FILTER.

the output energy was measured by taking off a small portion through some of the long tubes of the output resistance and energizing the other loud speaker. The complete system is shown in Fig. 4.10. The insertion loss was measured by taking

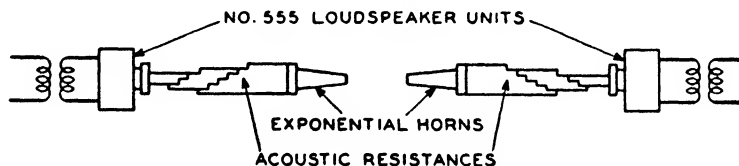


FIG. 4.10—MEASURING SYSTEM FOR ACOUSTIC FILTERS.

the difference in loss between that measured with the filter in and that measured with the filter out. Since the impedance looking both ways from the junction is a resistance, this represents the insertion factor as defined in Chapter II, expressed in

terms of the terminating resistances. In order to vary these resistances small sections of exponential horns were used on the ends of the resistances. These act as transformers to step the value of the acoustic resistance to higher values. By adjusting the length and hence the size of the end opening it was possible to vary the resistance over a wide range.

The full line of Fig. 4.9 shows that the additional pass bands occur at the half wavelength frequencies. In order to get rid of these objectionable bands it is necessary to insert another section of a low-pass filter which has different secondary bands. This can be done by making the length a different value. The dotted line of Fig. 4.9 shows the effect of using one section of Type A and one section of Type B. The extra pass bands are removed and a true low-pass filter is obtained which has a high attenuation from 150 cycles to 4000 cycles.

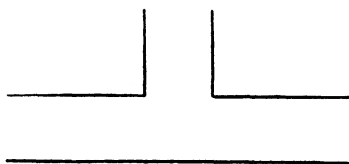


FIG. 4.11—HIGH-PASS ACOUSTIC FILTER WITH OPEN SIDE BRANCH.

Besides low-pass filters of the type discussed above, band-pass filters can also be constructed. They have not received the practical applications that the low-pass type have but they may be used to some extent in separating out various speech bands or for similar application. Their characteristics can be obtained from equations (4.104) by inserting a different type of side branch impedance Z_s . Probably the simplest type of side branch impedance is obtained by using a tube open to the atmosphere, as shown in Fig. 4.11. The impedance at the end of an open tube is nearly equivalent to a short circuit. A slightly better approximation is to use the approximation employed with organ pipes, namely, to consider the tube extended by a length amounting to 0.57 times the radius of the tube, and to consider the extended tube terminated in a zero impedance. For this corrected length the impedance of the side branch will be

$$\frac{Z_s}{S_2} = \frac{p}{V} = +j \frac{\rho v}{S_2} \tan \frac{\omega l_2}{v}. \quad (4.125)$$

For this case the transfer constant and image impedance becomes

$$\cosh \theta = \left(\cos \frac{\omega l_1}{v} + \frac{S_2}{2S_1} \frac{\sin \frac{\omega l_1}{v}}{\tan \frac{\omega l_2}{v}} \right)$$

$$Z_0 = \rho v \sqrt{\frac{\sin \frac{\omega l_1}{v} + \frac{S_2}{S_1} \frac{\sin^2 \frac{\omega l_1}{2v}}{\tan \frac{\omega l_2}{v}}}{\sin \frac{\omega l_1}{v} - \frac{S_2}{S_1} \frac{\cos^2 \frac{\omega l_1}{2v}}{\tan \frac{\omega l_2}{v}}}} \quad (4.126)$$

The best ratio of l_1 to l_2 depends on what frequency range requires the largest attenuation. If it is desirable to have a large attenuation for low frequencies, the length l_2 should be considerably smaller than l_1 ; on the other hand, if a large attenuation is desired above the first pass band the best ratio is obtained when $l_2 = 2l_1$, for then the minimum value of $\tan \frac{\omega l_2}{v}$

comes at the maximum value of $\sin \frac{\omega l_1}{v}$. The solid lines of Fig.

2.30 show a plot of the attenuation given by equation (4.126) when $l_2 = l_1$ for several ratios of $S_2/S_1 = Z_{01}/Z_{02}$.

The theory of acoustic filters is based on the assumption of plane wave motion in the main conducting tube. This is a legitimate assumption as long as the largest cross-sectional dimension of any conducting tube is less than a wavelength for a symmetrically constructed arrangement. If the dimensions are greater than a wavelength, the higher modes of vibration discussed in section (4.2) can be set up, and these are not influenced by a side branch as are the plane waves. For a given frequency range to be attenuated, this sets a limit to the size of the main conducting tubes. If large-sized tubes are to be

quieted up to a high frequency this can still be done by section-alizing the construction. This in effect puts a number of conducting tubes in parallel as far as the passage of air through them is concerned and hence the air-carrying capacity can be made as large as desired. At the same time the attenuation can be made large up to high frequencies. In this manner acoustic filters can be made effective up to high frequencies for very large air-carrying ducts.

4.6. *Transfer of Sound by Radiation*

When sound is to be transferred from one point to another it may be guided as in a tube or it may be unguided as in direct radiation from a radiating source. The characteristics of a guided source have already been discussed in the previous sections and it is the purpose of this section to discuss the characteristics of unguided radiation.

Most of the properties of radiated waves can be determined by a consideration of a simple point source or combination of such sources. A point source is a small spherical surface which pulsates radially with a velocity \dot{r} which is the same for all angular directions. To determine the properties of a point source we have to transform the general velocity potential equation into spherical coordinates. For simple harmonic motion and for symmetry for all angular directions, this takes the simple form

$$\frac{\partial^2 \varphi}{\partial r^2} + \frac{2}{r} \frac{\partial \varphi}{\partial r} + \frac{\omega^2}{v^2} \varphi = 0. \quad (4.127)$$

This equation is satisfied by

$$\varphi = A e^{-\frac{j\omega r}{v}} + B e^{\frac{j\omega r}{v}}. \quad (4.128)$$

The first term represents a wave going out from the radiator toward large values of r whereas the second term represents a wave coming from large values of r toward the source. For a point source only the first kind of wave will exist and hence we

can set $B = 0$. The particle velocity in the radial direction will then be

$$\dot{r} = -\frac{\partial \varphi}{\partial r} = A \left(\frac{j\omega}{vr} e^{-\frac{j\omega r}{v}} + \frac{e^{-\frac{j\omega r}{v}}}{r^2} \right). \quad (4.129)$$

For large values of the radius r the second term can be neglected with respect to the first, and hence ultimately the particle velocity will be inversely proportional to the radius. Since the pressure p of the wave is $j\omega\rho\varphi$, the particle velocity for large distances will be in phase with the pressure. Near the radiator, however, there is a quadrature component which varies inversely as the square of the radius. The specific impedance that the air impresses on the radiator at its radius r_0 will be

$$\frac{p}{\dot{r}} = \frac{A \left(\frac{j\omega\rho e^{-\frac{j\omega r_0}{v}}}{r_0} \right)}{A \left(\frac{j\omega}{r_0 v} e^{-\frac{j\omega r_0}{v}} + \frac{e^{-\frac{j\omega r_0}{v}}}{r_0^2} \right)} = \frac{\rho v \left(\frac{\omega^2 r_0^2}{v^2} + \frac{j\omega r_0}{v} \right)}{1 + \frac{\omega^2 r_0^2}{v^2}}. \quad (4.130)$$

The real part represents the radiation resistance while the imaginary part represents the radiation reactance. When the frequency is very low or the radiator very small the reactance term predominates. The effect is to add a mass per unit area equal to

$$\frac{\rho r_0}{1 + \frac{\omega^2 r_0^2}{v^2}} \doteq \rho r_0. \quad (4.131)$$

For the whole sphere the added mass is this times the area or $M = 4\pi\rho r_0^3$ which is three times the mass of the medium displaced. If the medium is one with a high density such as water this may add considerable mass to the radiating diaphragm and cause a lowering of the natural frequency of the radiating system. The resistance coefficient is quite small until $\frac{\omega r_0}{v}$ approaches unity. This illustrates the difficulty of driving a medium with a small size radiator.

The ideal point source is one in which the radius r_0 becomes vanishingly small. For this case the inverse square term predominates and

$$A = r_0^2 \dot{r}_0. \quad (4.132)$$

The velocity potential at any point r is equal to

$$\varphi = \frac{r_0^2 \dot{r}_0 e^{-\frac{j\omega r}{v}}}{r} = \frac{dS \dot{r}_0}{4\pi r} e^{-\frac{j\omega r}{v}} \quad (4.133)$$

where dS is the area of the radiating point source.

If we have a larger radiating area, such as a piston, the radiation can be calculated by assuming a number of point sources distributed over the surface of the radiator. This would strictly give a radiator which would radiate equally on both sides. Along the plane of the radiator beyond the radiating surface the particle velocity across this plane will be zero on account of the symmetry of the radiation. Hence we could insert an infinite baffle along this plane without disturbing the radiation, since there is no particle velocity across this plane in any case. The radiator formed by a distribution of point sources over a plane surface is then equivalent to two radiating pistons, each radiating into a semi-infinite medium. In general, we are interested in only the radiation from one side of a piston into a semi-infinite medium. For this case the divergence of the radiation of each elementary source is limited by the baffle to a hemisphere and hence the potential at any point distant r from the elementary source is

$$\varphi = \frac{dS \dot{r}_0 e^{-\frac{j\omega r}{v}}}{2\pi r}. \quad (4.134)$$

The potentials from the separate sources are additive and hence the total velocity potential is

$$\varphi = \frac{1}{2\pi} \int \int_S \frac{\xi e^{-\frac{j\omega r}{v}}}{r} dS = -\frac{1}{2\pi} \int \int_S \frac{\frac{\partial \varphi}{\partial n} e^{-\frac{j\omega r}{v}}}{r} dS \quad (4.135)$$

where ξ is the particle velocity normal to the radiating surface and hence $\xi = -\frac{\partial \varphi}{\partial n}$ taken normal to the surface. This equa-

tion can be used to calculate the radiation in a semi-infinite medium for any radiating surface whose particle velocity is known over the surface.

As an example of the use of such a formula we shall consider the radiation from a circular piston of uniform displacement working in an infinite baffle. Suppose that we consider a point at distance R from the center of the radiator and at an angle

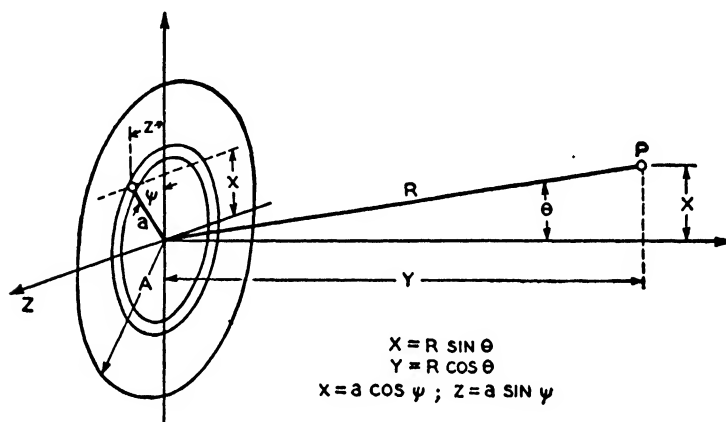


FIG. 4.12—COORDINATES FOR CALCULATING RADIATION FROM PISTON RADIATOR.

of θ from the normal to the radiator surface as shown in Fig. 4.12. We consider first the contribution of a ring of thickness da , and distance a from the center, to the velocity potential φ . From Fig. 4.12 we see that the distance r from any point on the ring to P is given by

$$r = \sqrt{(R \sin \theta - a \cos \psi)^2 + R^2 \cos^2 \theta + a^2 \sin^2 \psi}$$

$$= \sqrt{R^2 + a^2 - 2Ra \sin \theta \cos \psi} \quad (4.136)$$

Hence the integral (4.135) becomes

$$\varphi = \frac{1}{2\pi} \int_0^A a \xi da \int_0^{2\pi} e^{\frac{-j\omega}{v} \sqrt{R^2 + a^2} \sqrt{1 - \frac{2Ra}{R^2 + a^2} \sin \theta \cos \psi}} \frac{d\psi}{\sqrt{R^2 + a^2} \sqrt{1 - \frac{2Ra}{R^2 + a^2} \sin \theta \cos \psi}} d\psi.$$

(4.137)

The value of φ is principally of interest when $R \gg a$ since all radiators are small compared to the distance they are required to radiate. Hence equation (4.137) can be written

$$\varphi = \frac{1}{2\pi} \int_0^A \frac{a \xi e^{-\frac{j\omega}{v} R}}{R} da \int_0^{2\pi} e^{\frac{j\omega}{v} a \sin \theta \cos \psi} d\psi. \quad (4.138)$$

The second integral with respect to ψ is a well-known Bessel's function integral which is

$$J_0\left(\frac{\omega}{v} a \sin \theta\right) = \frac{1}{2\pi} \int_0^{2\pi} e^{\frac{j\omega}{v} a \sin \theta \cos \psi} d\psi. \quad (4.139)$$

Hence equation (4.138) becomes

$$\varphi = \frac{e^{-\frac{j\omega}{v} R}}{R} \int_0^A \xi a J_0\left(\frac{\omega}{v} a \sin \theta\right) da. \quad (4.140)$$

For the radiating piston ξ is constant over the surface and can be removed from the integral. The resulting equation is the well-known Bessel's function integral

$$\varphi = \frac{e^{-\frac{j\omega R}{v}} \xi A}{R} \frac{J_1\left(\frac{\omega}{v} A \sin \theta\right)}{\frac{\omega}{v} \sin \theta} = \frac{e^{-\frac{j\omega R}{v}}}{\pi R} \left(\frac{\pi A^2 \xi J_1\left(\frac{\omega}{v} A \sin \theta\right)}{\frac{\omega}{v} A \sin \theta} \right). \quad (4.141)$$

The series expansion of the Bessel's function of the first order is

$$J_1(x) = \frac{x}{2} \left(1 - \frac{x^2}{2 \cdot 2^2} + \frac{x^4}{2 \cdot 4 \cdot 2^2 \cdot 6} - \frac{x^6}{2 \cdot 4 \cdot 6 \cdot 2^2 \cdot 6 \cdot 8} \right). \quad (4.142)$$

Hence, near the axis when $\sin \theta \rightarrow 0$, the velocity potential is equal to

$$\varphi_n = \frac{e^{-\frac{j\omega R}{v}}}{2\pi R} (S\xi) \quad (4.143)$$

where S is the area of the radiator. Hence, along the axis of the radiator the effect is the same as for a point source having a radiating strength of $S\xi$.

Off the axis, however, the radiation is considerably less strong. At a given distance R from the piston the ratio of the velocity potential and hence also the pressure and particle velocity as a function of the angle from the axis becomes

$$\left(\frac{\varphi}{\varphi_n}\right) = \frac{2J_1\left(\frac{\omega}{v} A \sin \theta\right)}{\frac{\omega}{v} A \sin \theta}. \quad (4.144)$$

A plot of this equation is shown in Fig. 4.13. It is obvious that if $\frac{\omega}{v} A$ is less than π or the diameter of the radiator is less than a wavelength, the device is not very directive but approaches more nearly the character of a point source. As the radiator

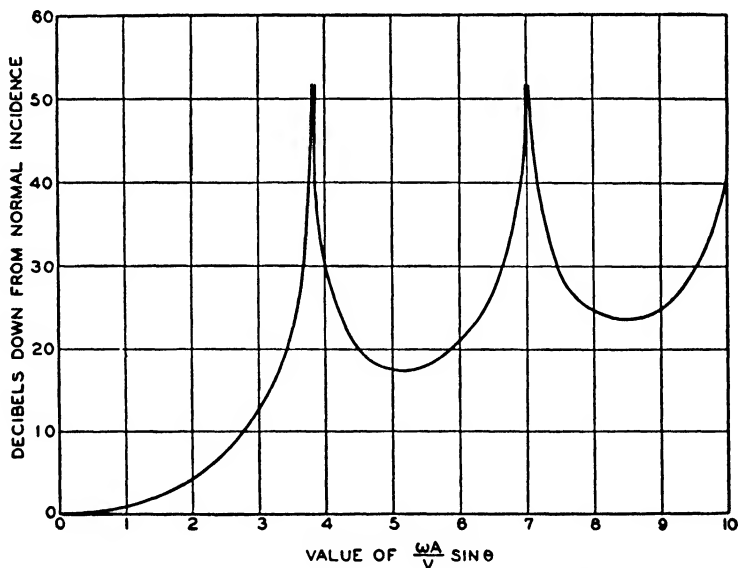


FIG. 4.13—DIRECTIVITY PATTERN FOR PISTON RADIATOR.

becomes larger it becomes more directive and is able to concentrate the radiation in a narrower angle. The first secondary lobe is down about 17 *db* with respect to the main radiating lobe. This example illustrates the directivity in radiation or

reception that flat plates working in baffles will have. In general, removing the baffle will lower the directivity of the device.

Another question of some interest in connection with a radiating piston is the reaction of the air on the piston. This can be expressed in the form of an impedance Z which is the

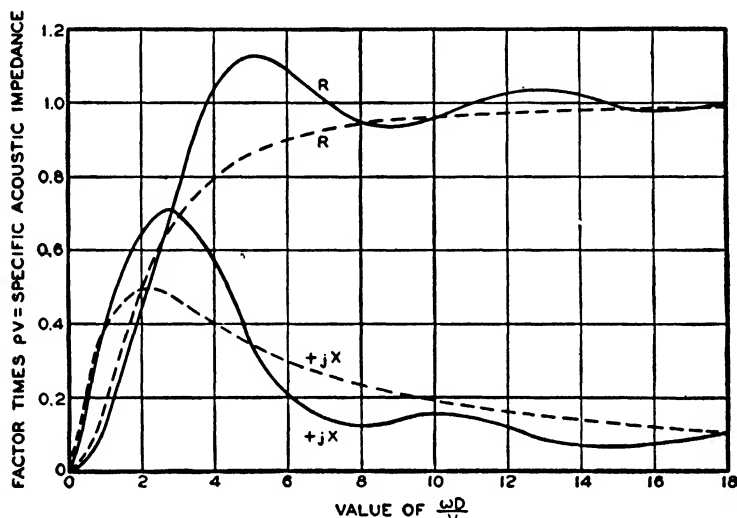


FIG. 4.14—RADIATION IMPEDANCE OF PISTON RADIATOR.

ratio of the average pressure p exerted by the air on the piston to the volume velocity which in this case is $\pi A^2 \xi$. The average pressure can be found by integrating $j\omega\rho\phi$ found from (4.135) over the surface of the piston. This is a rather complicated integration and since it may be found elsewhere⁸ only the result is given here. The impedance per square centimeter is ρv , the specific impedance of air, times the resistance and reactance factors shown in Fig. 4.14. When the diameter of the piston is greater than half a wavelength, the resistance component approaches its final value ρv while the reactance component becomes small. On the other hand, when the piston diameter is considerably less than half a wavelength, the reactance component predominates and adds an effective mass to the piston.

⁸ See "Theory of Vibrating Systems and Sound," I. B. Crandall, Ch. IV, D. Van Nostrand.

The equivalent resistance and reactance for a spherical diaphragm, calculated from equation (4.130), are shown by the dotted lines of Fig. 4.14. The difference is not large but the piston shows the effect of interference between parts of its radiating surfaces while the sphere does not.

4.7. *Highly Directional Receiving and Radiating Devices*

The plane wave piston vibrating in an infinite wall produces a strongly directive effect as shown in Fig. 4.13. It is difficult to produce such a motion, however, for a large area with any direct radiating device. A horn appears to be the nearest practical approach to obtaining such a source. However, with a horn, the wave shape actually emerging from the end is not plane but more nearly spherical in shape, and the directivity predicted by Fig. 4.13 is not realized.

For obtaining directive wave motion in optics, the device most used is the parabolic reflector and such devices have also been used in acoustics. Due to the fact that the reflector is not as large a number of wavelengths in the acoustic as in the optical case, the directivity obtained is not nearly as high. Nevertheless a parabolic reflector with a pressure microphone was one of the first directional receiving devices and remains one of the most directive so far obtained. The directivity of such a device has never been completely calculated but measurements indicate that it is less than half as directive as the plane wave piston shown in Fig. 4.13. The parabolic microphone has also the disadvantage that the energy it picks up varies markedly with frequency being about 25 *db* higher at 5000 cycles than it is at 100 cycles. This follows from the fact that a reflector or other focusing device will concentrate most of the sound evenly over a sphere whose diameter is half a wavelength. A microphone with a face 2 inches in diameter will not pick up the maximum amount until the frequency is 3400 cycles or greater. Hence at low frequencies, the percentage of the energy picked up is considerably less than this and the response falls off.

Another directive device which eliminates this difficulty is the tubular directional microphone recently described.^{9, 10} This device consists of a number of small tubes whose lengths vary by equal increments from a small length to the longest tube. These are wrapped in the form of a circular bundle and all connected to a common face plate which is coupled through a small air chamber to the face of a pressure microphone.

If a plane wave of sound approaches the microphone in the direction of the length, sound is generated in each of the small tubes by the incident wave and is transmitted down each of the tubes to the termination. As long as the wave is in the direction of the unit, then since the velocity of propagation inside and outside is the same, all of the waves picked up by the separate tubes will come to the common air chamber in phase and their energies will add. This will happen for all frequencies. Since the energy in each tube depends on the initial pressure at the input and in a plane wave this is independent of the frequency, the amount of energy picked up will not depend on the frequency and hence the response of the unit for normal incidence does not vary with frequency as does the parabolic reflector microphone. If a wave approaches the microphone at an angle to the length of the device, the various waves picked up by the separate tubes will not all arrive in phase, phase cancellation will take place, and the response of the microphone will be considerably less. In this operation the tubular directional microphone is very similar to the Beverage directional radio antenna.¹¹

In calculating the directivity we make the assumption that all the volume velocities entering the common air chamber will add and that no reflection need be considered. This will be valid if the receiving chamber had the same cross-sectional area as the tube and continued for a long length. Actually, however, the chamber is terminated in the impedance of the microphone which will usually be much higher than the air impedance, with

⁹ "A Tubular Directional Microphone," W. P. Mason and R. N. Marshall, *J. Acoustical Soc. Am.*, Jan. 1939, pp. 206-215.

¹⁰ H. F. Olson, *Jour. Inst. Rad. Eng.*, Vol. 27, No. 7, p. 438, 1939.

¹¹ "The Wave Antenna," H. H. Beverage, C. W. Rice, and E. W. Kellogg, *Trans. A.I.E.E.*, Vol. 42, p. 215, 1923.

the result that a total reflection of the wave occurs. This results in doubling the pressure applied to the microphone but might cause difficulty if the waves reflected into the combination of tubes came back again into the chamber with the wrong phases and amplitudes. It has been shown, however,¹² that the impedance of such a combination of tubes is a resistance from the frequency of resonance of the longest tube up to the frequency of resonance associated with the length difference between adjacent tubes—i.e., over the operating range of the device. Hence the reflected wave enters the series of pipes and does not return to affect the directivity of the device. Actually waves from the separate parts do return but they are of such a magnitude and phase as to cancel out over the operating frequency range of the device.

To calculate the directivity of the device, we assume that all of the openings occur along a single line, and calculate the sum of the volume velocities in the common chamber. Consider a plane wave incident at an angle θ with respect to the axis of the tubes, which generates at a given instant a pressure dp_0 at the mouth of the longest tube. Neglecting the attenuation in the tube, the pressure at the mouth of the tube will be

$$dp_0 e^{-\frac{j\omega l}{v}} \quad (4.145)$$

and the volume velocity will be

$$V_0 = \frac{dp_0 S}{\rho v} e^{-\frac{j\omega l}{v}} \quad (4.146)$$

where S is the cross-sectional area of each tube, since we are assuming that the tube is terminated in its image impedance. The pressure generated at the beginning of the next tube is

$$dp_0 e^{-\frac{j\omega l_s \cos \theta}{v}} \quad (4.147)$$

where ds is the increment of length from the longest tube to the next longest tube. This follows since $ds \cos \theta$ is the distance the

¹² "Propagation Characteristics of Sound Tubes and Acoustic Filters," W. P. Mason, Phys. Rev., Vol. 31, No. 2, p. 283, 1928.

plane wave will have to travel between the end of the longest tube and the end of the next longest tube. This wave will travel down a length $l - ds$ and contribute its volume velocity to the common chamber. This will be

$$V_1 = \frac{dp_0 S}{\rho v} e^{-\frac{j\omega ds \cos \theta}{v}} e^{-\frac{j\omega(l-ds)}{v}} = \frac{dp_0 S}{\rho v} e^{-\frac{j\omega(l-(1-\cos \theta)ds)}{v}}. \quad (4.148)$$

The other tubes can be treated in the same manner, the only difference being that ds is multiplied by integers from 2 to $(n-1)$ where n is the number of tubes. Hence the sum total of the volume velocities entering the common chamber is

$$V_0 = \Sigma V_n = \frac{dp_0 S}{\rho v} e^{-\frac{j\omega l}{v}} \left[1 + e^{\frac{j\omega ds(1-\cos \theta)}{v}} + e^{\frac{j\omega 2ds(1-\cos \theta)}{v}} + \dots + e^{\frac{j\omega(n-1)ds(1-\cos \theta)}{v}} \right]. \quad (4.149)$$

This series is a geometrical progression which has the sum

$$V_\theta = \frac{dp_0 S}{\rho v} e^{-\frac{j\omega l}{v}} \left[\frac{1 - e^{\frac{j\omega nds(1-\cos \theta)}{v}}}{1 - e^{\frac{j\omega ds(1-\cos \theta)}{v}}} \right]. \quad (4.150)$$

For normally incident sound when $\theta = 0$ this becomes

$$V_N = \frac{ndp_0 S}{\rho v} e^{-\frac{j\omega l}{v}}. \quad (4.151)$$

Hence the ratio of the volume velocity at angle θ to that at normal incidence is

$$\begin{aligned} \frac{V_\theta}{V_N} &= \frac{1}{n} \left(\frac{1 - e^{-j2n\beta}}{1 - e^{-j2\beta}} \right) = \frac{1}{n} \frac{e^{-jn\beta}}{e^{-j\beta}} \left(\frac{e^{jn\beta} - e^{-jn\beta}}{e^{j\beta} - e^{-j\beta}} \right) \\ &= \frac{1}{n} e^{-j(n-1)\beta} \left(\frac{\sin n\beta}{\sin \beta} \right) \end{aligned} \quad (4.152)$$

where $\beta = \frac{\omega ds}{2v} (1 - \cos \theta)$. Since the absolute value of the term $e^{-j(n-1)\beta}$ is equal to unity, the value of the directivity ratio is

$$\frac{V_\theta}{V_N} = \frac{1}{n} \left(\frac{\sin n\beta}{\sin \beta} \right). \quad (4.153)$$

A plot of this curve is shown on the full line of Fig. 4.15, the abscissae being

$$\frac{L\omega}{2v} (1 - \cos \theta) \quad (4.154)$$

where L is the difference in length between the shortest and longest tubes. Experiments indicate that this selectivity is obtained in practice.

The simple calculation of the directivity given above does not take account of the attenuation existing in the tubes, nor

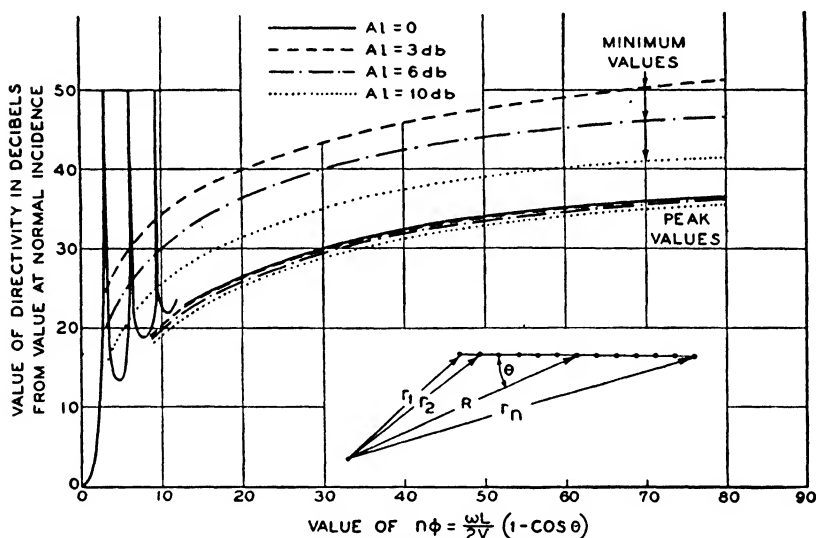


FIG. 4.15—DIRECTIVITY OF TUBULAR DIRECTIONAL MICROPHONE.

does it indicate the effect of placing the source of sound a finite distance from the tubular directional microphone. Both of these effects can be taken account of by considering the case shown in Fig. 4.15. Here we have a point source of sound at a distance R from the center of the microphone, the line from the source to the center making an angle θ with the length of the microphone. From equation (4.134) for a point source, the pressure at the longest tube will be

$$p = \frac{Be^{\frac{j\omega r_1}{v}}}{r_1} \quad (4.155)$$

where B is the strength of the point source dS at r_0 . The attenuation down the longest tube will be Al where A is given as a function of frequency and tube diameter by equation (4.80). Hence the volume velocity due to the longest tube will be

$$V_1 = \frac{BS}{\rho v} \frac{e^{-\frac{j\omega r_1}{v}}}{r_1} e^{-(A + \frac{j\omega}{v})l} \quad (4.156)$$

while the total volume velocity will be

$$V = \frac{BS}{\rho v} e^{-(A + \frac{j\omega}{v})l} \left[\frac{e^{-\frac{j\omega r_1}{v}}}{r_1} + \frac{e^{-[A ds + \frac{j\omega}{v}(r_2 - ds)]}}{r_2} + \dots \right. \\ \left. + \frac{e^{-[\frac{n}{2} A ds + \frac{j\omega}{v}(R - \frac{n}{2} ds)]}}{R} + \dots + \frac{e^{-[n A ds + \frac{j\omega}{v}(r_n - nds)]}}{r_n} \right] \quad (4.157)$$

where r_1 to r_n are the radii from the point source to the openings of the various tubes.

The radii r_i can be expressed as

$$r_1 = \sqrt{\left(R \cos \theta - \frac{n}{2} ds\right)^2 + R^2 \sin^2 \theta} \\ = \sqrt{R^2 - Rnds \cos \theta + \frac{n^2}{4} ds^2} \\ r_n = \sqrt{\left(R \cos \theta + \frac{n}{2} ds\right)^2 + R^2 \sin^2 \theta} \\ = \sqrt{R^2 + Rnds \cos \theta + \frac{n^2}{4} ds^2} \quad (4.158)$$

upon resolving the distances into distances along and perpendicular to the microphone. Now if R is equal to or greater than the length of the microphone the value of $\left(\frac{nds}{2}\right)^2$ will be small compared to R^2 and can be neglected. Then r_1 , r_n can be expressed as

$$r_1 \doteq R \left(1 - \frac{nds \cos \theta}{2R}\right); \quad r_2 \doteq R \left(1 - \frac{(n-1) ds \cos \theta}{2R}\right); \\ r_n \doteq \left(1 + \frac{nds \cos \theta}{2R}\right) \text{ etc.} \quad (4.159)$$

Introducing these values in (4.157) and using the approximation

$$\frac{1}{r_1} \doteq \frac{1}{R \left(1 - \frac{nds \cos \theta}{2R} \right)} \doteq \frac{1 + \frac{nds}{2R} \cos \theta}{R} \doteq \frac{e^{\frac{n ds}{2R} \cos \theta}}{R} \quad (4.160)$$

equation (4.157) can be written as

$$V_\theta = \frac{BS}{\rho v} e^{-\left[A l + \frac{nds}{2} \frac{\cos \theta}{R} + j \frac{\omega}{v} \left(l - \frac{n}{2} ds \right) \right]} \\ \times [1 + e^{-(\alpha + j\beta)ds} + e^{-2(\alpha + j\beta)ds} + \dots + e^{-(n-1)(\alpha + j\beta)ds}] \quad (4.161)$$

where

$$\alpha = \left(A + \frac{\cos \theta}{R} \right); \quad \beta = \frac{\omega}{v} (1 - \cos \theta).$$

This is again a geometrical series which has the sum

$$V_\theta = \frac{BS}{\rho v} e^{-\left[\left(A l + \frac{nds}{2} \frac{\cos \theta}{R} \right) + j \frac{\omega}{v} \left(l - \frac{n}{2} ds \right) \right]} \left[\frac{1 - e^{-n(\alpha + j\beta)ds}}{1 - e^{-(\alpha + j\beta)ds}} \right]. \quad (4.162)$$

If we take the ratio of V_θ to the normal value, and take the real part, the resulting expression becomes

$$\frac{V_\theta}{V_N} = \frac{1}{n} \left| \frac{\sinh \frac{n}{2} ds (\alpha + j\beta)}{\sinh \frac{ds}{2} (\alpha + j\beta)} \right| = \frac{1}{n} \sqrt{\frac{\sinh^2 \frac{\alpha L}{2} + \sin^2 \frac{\beta L}{2}}{\sinh^2 \frac{\alpha ds}{2} + \sin^2 \frac{\beta ds}{2}}} \quad (4.163)$$

where L is the distance between the shortest and longest tubes.

If α is zero this reduces to equation (4.153) obtained previously. Fig. 4.15 shows a plot of equation (4.163) for various values of $\frac{\alpha L}{2}$ for a tubular directional microphone having 50 tubes. As can be seen the principal effect of dissipation and a near approach of the source to the microphone is to raise the secondary minima, without affecting the secondary maxima appreciably, which will not affect the directivity of the micro-

phone appreciably. This holds until $\alpha L = 10 \text{ db}$, when the directivity becomes noticeably impaired. Hence this effect definitely limits the size of the tubes which can be used in the device if we wish to cover high frequency ranges.

This device has also been used as a directional radiator by using a loudspeaker unit in place of the microphone. The output is a uniform function of frequency since the impedance looking into the tube combination is nearly a pure resistance. The output will not be constant with frequency, however, since at the low frequency end the radiation resistance of the ends of the tube is very small, as can be seen from Fig. 4.14, and most of the energy is lost in producing heat inside the tubes. At the high frequency end the radiation resistance becomes higher and a large portion of the input energy is radiated by the tubes. This device has been used extensively in producing a plane wave concentrated field for testing directional microphones and other devices in rooms which are not completely free from reflections.

CHAPTER V

VIBRATION OF MEMBRANES AND PLATES

STRETCHED diaphragms have been used to some extent in vibrating systems, particularly in condenser microphones. Thin plates are also used more extensively in such apparatus as telephone receivers, microphones, loudspeakers, etc. They differ from the mechanical system considered in Chapter III in that they are a two-dimensional system. However, for symmetrical modes or other definite modes all of the properties of the motion can be specified by a single dimension and hence progress can be made by considering their equivalent circuits.

A stretched diaphragm has a potential energy of bending which is determined by the tension of the diaphragm. A thin plate on the other hand has a potential energy of bending which is determined by the elastic constants of the material of the plate. Experiment shows that unless diaphragms are stretched very tightly deviations occur from the theoretical results due to the inherent stiffness of the material of the diaphragm. For this reason it is desirable to take account of this stiffness. In the present chapter the equations for both cases are considered. By letting the natural stiffness of the plate be small compared to the tension, the equations of a stretched diaphragm are obtained. On the other hand when the tension is small, the equations for a thin plate vibrating in flexure are obtained.

5.1. *Variational Equation of Motion for a Thin Stretched Plate*

The potential energy of bending for a thin plate vibrating in flexure depends on two radii of curvature R_1 and R_2 rather than a single radius as does the bar bent in flexure. It is shown in standard works ¹ that the potential energy of bending is given by

¹ "Theory of Sound," Rayleigh, Vol. 1, Ch. X, Macmillan.

$$PE = \frac{Y_0 l_t^3}{24(1 - \sigma^2)} \left(\frac{1}{R_1^2} + \frac{1}{R_2^2} + \frac{2\sigma}{R_1 R_2} \right) \quad (5.1)$$

where Y_0 is the value of Young's modulus, σ the value of Poisson's ratio or the ratio of the lateral contraction to the longitudinal expansion of the material, and l_t the thickness of the plate. This energy is calculated by calculating the energy of stretching part of the plate and compressing the other part about the center line of the plate which is assumed not to change length. This compares to the expression

$$\frac{Y_0 l_t^3}{24} \left(\frac{1}{R_1^2} \right) \quad (5.2)$$

for a bar bent in flexure which has only one radius of curvature.

If in addition we have a tension which stretches the plate as a whole another term has to be added to the potential energy. In calculating this addition to the potential energy the assumption is made that the tension T is so high that the change in tension due to displacing the membrane will be small compared to T . Under these assumptions the increase in potential energy is found by multiplying the tension by the increase in area. If w is the displacement normal to the plane of the diaphragm, the altered area is given by

$$\iint \sqrt{1 + \left(\frac{\partial w}{\partial x} \right)^2 + \left(\frac{\partial w}{\partial y} \right)^2} dS \quad (5.3)$$

where dS is an element of area. Hence the potential energy PE is

$$\begin{aligned} PE &= T \iint \left(\sqrt{1 + \left(\frac{\partial w}{\partial x} \right)^2 + \left(\frac{\partial w}{\partial y} \right)^2} - 1 \right) dS \\ &= \frac{1}{2} T \iint \left(\left(\frac{\partial w}{\partial x} \right)^2 + \left(\frac{\partial w}{\partial y} \right)^2 \right) dS = \frac{1}{2} T \iint (\nabla w)^2 dS \end{aligned} \quad (5.4)$$

where ∇w is the gradient of w .

If w is the displacement perpendicular to the plane of the plate at the point where rectangular co-ordinates are x and y ,

it has been shown from geometrical consideration that

$$\frac{1}{R_1} + \frac{1}{R_2} = \frac{\partial^2 w}{\partial x^2} + \frac{\partial^2 w}{\partial y^2} = \nabla^2 w;$$

$$\frac{1}{R_1 R_2} = \frac{\partial^2 w \partial^2 w}{\partial x^2 \partial y^2} - \left(\frac{\partial^2 w}{\partial x \partial y} \right)^2. \quad (5.5)$$

Hence the complete expression for the potential energy of a thin stretched plate is

$$\text{PE} = \iint \left[\frac{(Y_0 + T)l_i^3}{24(1 - \sigma^2)} \left[(\nabla^2 w)^2 - 2(1 - \sigma) \left(\frac{\partial^2 w \partial^2 w}{\partial x^2 \partial y^2} - \left(\frac{\partial^2 w}{\partial x \partial y} \right)^2 \right) \right] + \frac{T}{2} (\nabla w)^2 \right] dS. \quad (5.6)$$

The added term T to the Young's modulus occurs because the added tension increases the effective modulus as shown by Rayleigh² in connection with stretched bars.

For a complicated system of this type the equation of motion is usually found by employing the variation equation which states that the increase of the potential energy is due to the impressed forces acting through the displacements δw . If p is the transverse pressure on the diaphragm (which may be the resultant of pressure on the two sides of the diaphragm) and ρ is the density of the material, the variation equation of motion is

$$\delta \text{PE} - \iint p \delta w dS + \iint \rho l_i \frac{\partial^2 w}{\partial t^2} \delta w dS = 0. \quad (5.7)$$

This equation states that the increase in potential energy due to a displacement δw is equal to the pressure minus the mass times acceleration multiplied by the displacement δw and integrated over the surface of the plate.

By employing Green's theorem, Rayleigh³ has shown that the variation of the first term of PE can be expressed in terms of the variation in δw and $\frac{d\delta w}{dn}$ by

² "Theory of Sound," Rayleigh, Vol. 1, p. 296, Macmillan.

³ "Theory of Sound," Rayleigh, Vol. 1, Ch. X, Macmillan.

$$\begin{aligned} \delta PE_1 = & \frac{(Y_0 + T)l_t^3}{12(1 - \sigma^2)} \left[\iint \nabla^4 w \delta w dS \right. \\ & - \int \delta w dl \left[\frac{\partial}{\partial n} \nabla^2 w - (1 - \sigma) \frac{\partial}{\partial l} \left(\frac{\partial^2 w}{\partial n \partial l} \right) \right] \\ & \left. + \int \frac{\partial \delta w}{\partial n} dl \left[\frac{\partial^2 w}{\partial n^2} + \sigma \left(\frac{1}{R} \frac{\partial w}{\partial n} + \frac{\partial^2 w}{\partial l^2} \right) \right] \right] \quad (5.8) \end{aligned}$$

where

$$\nabla^4 = \left(\frac{\partial^2}{\partial x^2} + \frac{\partial^2}{\partial y^2} \right) \left(\frac{\partial^2 w}{\partial x^2} + \frac{\partial^2 w}{\partial y^2} \right), \quad (5.9)$$

dS is an element of area, dl is an element of length along the boundary, dn is an element of length normal to the edge, dl is an element of length along the tangent to the edge at the point under consideration and R is the radius of curvature of the edge of the diaphragm at the point under consideration. Simpler expressions for the last two terms are given later for square and circular boundaries.

In a similar manner the variation of the second term in (5.6) has been shown to be

$$\delta PE_2 = T \left[- \iint \nabla^2 w \delta w dS + \int \frac{\partial w}{\partial n} \delta w dl \right]. \quad (5.10)$$

Hence the equation to be satisfied for every point of the surface is

$$\frac{(Y_0 + T)l_t^3}{12(1 - \sigma^2)} \nabla^4 w - T \nabla^2 w - p + l_t \rho \frac{\partial^2 w}{\partial t^2} = 0. \quad (5.11)$$

For every point on the boundary provided that no energy is taken out or put in, the equation to be satisfied is that

$$\begin{aligned} & - \frac{(Y_0 + T)l_t^3}{12(1 - \sigma^2)} \left[\frac{\partial^2 w}{\partial n^2} + \sigma \left(\frac{1}{R} \frac{\partial w}{\partial n} + \frac{\partial^2 w}{\partial l^2} \right) \right] \frac{\partial \delta w}{\partial n} \\ & + \delta w \left[\frac{(Y_0 + T)l_t^3}{12(1 - \sigma^2)} \left[\frac{\partial}{\partial n} \nabla^2 w - (1 - \sigma) \frac{\partial}{\partial l} \left(\frac{\partial^2 w}{\partial n \partial l} \right) \right] \right. \\ & \left. + T \frac{\partial w}{\partial n} \right] = 0. \quad (5.12) \end{aligned}$$

To obtain the significance of equation (5.12) consider the contributions to the potential energy of forces acting at the boundary. If a uniform force F acts on the edge and moves it a distance w , energy to the amount of Fw is added to the potential energy. Similarly if a couple of moment M acts at the boundary and bends the edge through an angle ϵ , an amount of energy $M\epsilon$ is added to the potential energy. Since the displacements are assumed small ϵ is given by $-\frac{\partial w}{\partial n}$. Hence the contribution to the potential energy at the boundary due to the constant force and moment is

$$Fw - M \frac{\partial w}{\partial n}.$$

If the expression is varied we have

$$F\delta w - M \frac{\partial(\delta w)}{\partial n}. \quad (5.13)$$

Hence comparing this with (5.12)

$$F = \frac{(Y_0 + T)l_t^3}{12(1 - \sigma^2)} \left[\frac{\partial}{\partial n} \nabla^2 w - (1 - \sigma) \frac{\partial}{\partial l} \left(\frac{\partial^2 w}{\partial n \partial l} \right) \right] + T \frac{\partial w}{\partial n} \quad (5.14)$$

$$M = \frac{(Y_0 + T)l_t^3}{12(1 - \sigma^2)} \left[\frac{\partial^2 w}{\partial n^2} + \sigma \left(\frac{1}{R} \frac{\partial w}{\partial n} + \frac{\partial^2 w}{\partial l^2} \right) \right]. \quad (5.15)$$

Two cases of interest usually occur, the rectangular-shaped diaphragm and the circular diaphragm. For the rectangular one, Rayleigh has shown that the conditions are

Edge parallel to y

$$F = \frac{(Y_0 + T)l_t^3}{12(1 - \sigma^2)} \left[\frac{\partial}{\partial x} \left[\frac{\partial^2 w}{\partial x^2} + (2 - \sigma) \frac{\partial^2 w}{\partial y^2} \right] \right] + T \frac{\partial w}{\partial x} \quad (5.16)$$

$$M = \frac{(Y_0 + T)l_t^3}{12(1 - \sigma^2)} \left[\frac{\partial^2 w}{\partial x^2} + \sigma \frac{\partial^2 w}{\partial y^2} \right].$$

For edges parallel to x the same expression holds with x and y interchanged. For a circular diaphragm the values are

$$\begin{aligned}
 F &= \frac{(Y_0 + T)l_t^3}{12(1 - \sigma^2)} \left[\frac{\partial}{\partial r} \left(\frac{\partial^2 w}{\partial r^2} + \frac{1}{r} \frac{\partial w}{\partial r} \right) \right. \\
 &\quad \left. + \frac{\partial^2}{\partial \theta^2} \left(\frac{2 - \sigma}{a^2} \frac{\partial w}{\partial r} - \frac{(3 - \sigma)w}{a^3} \right) \right] + T \frac{\partial w}{\partial r} \quad (5.17) \\
 M &= \frac{(Y_0 + T)l_t^3}{12(1 - \sigma^2)} \left[\frac{\partial^2 w}{\partial r^2} + \sigma \left(\frac{1}{a} \frac{\partial w}{\partial r} + \frac{1}{a^2} \frac{\partial^2 w}{\partial \theta^2} \right) \right]
 \end{aligned}$$

where r and θ are the radius and angular co-ordinate of a polar co-ordinate system and a is the radius of the diaphragm. After the differentiations are performed, r is made equal to a .

To obtain the equations for a stretched membrane we let $l_t \rightarrow 0$, while the equations for an unstretched thin plate are determined by letting $T = 0$.

5.2. *Solution for the Displacement of a Stretched Circular Diaphragm*

One of the simplest cases that can be considered is the case of a very thin stretched diaphragm actuated by a constant pressure over the surface. Most diaphragms of this sort are circular and since a symmetrical condition has been assumed no variation will occur when θ , the polar angle, is varied. Under these conditions, the equation of motion (5.11) becomes

$$T \left(\frac{d^2 w}{dr^2} + \frac{1}{r} \frac{dw}{dr} \right) + \omega^2 \rho l_t w + p = 0 \quad (5.18)$$

when we employ the symbolic time variation. A solution for this equation is

$$w = AJ_0(kr) + BK_0(kr) - \frac{p}{\omega^2 \rho l_t} \quad (5.19)$$

where

$$k = \omega \sqrt{\frac{\rho_s}{T}} = \frac{\omega}{v}, \quad (5.20)$$

ρ_s being equal to ρl_t or equal to the surface density and $v = \sqrt{T/\rho_s}$ is the velocity of propagation of a wave on the stretched

diaphragm. In equation (5.19) J_0 is the Bessel's function of zero order of the first kind and K_0 the function of the second kind. Since K_0 goes to infinity when $r = 0$, we can set $B = 0$.

The usual condition assumed to exist at the edge of the diaphragm is that the edge is supported and hence $w = 0$ when $r = a$ the radius of the diaphragm. This gives the constant A as

$$A = \frac{p}{\omega^2 \rho_s J_0 \left(\frac{\omega}{v} a \right)}. \quad (5.21)$$

The displacement of the diaphragm then is given by

$$w = \frac{p}{\omega^2 \rho_s} \left[\frac{J_0 \left(\frac{\omega}{v} r \right)}{J_0 \left(\frac{\omega}{v} a \right)} - 1 \right]. \quad (5.22)$$

A practical case in which this solution is of some interest is that shown in Fig. 5.1 which shows a diaphragm used as an obstruction in a sound-conducting tube. If the diameter of the tube is less than 1.22 times the wavelength, the pressure p of equation (5.22) can be considered as the difference of two plane waves acting on the two sides of the diaphragm. As a result the diaphragm becomes a series impedance. To find out what acoustic impedance the diaphragm introduces, we have to evaluate the volume velocity through the device, or we have to integrate the velocity given by (5.22) over the surface. This gives

$$\begin{aligned} V &= 2\pi \int_0^a \dot{w} r dr = j2\pi\omega \int_0^a r w dr \\ &= \frac{j2\pi p}{\omega \rho_s} \int_0^a \left[\frac{J_0 \left(\frac{\omega}{v} r \right)}{J_0 \left(\frac{\omega}{v} a \right)} - 1 \right] r dr. \end{aligned} \quad (5.23)$$

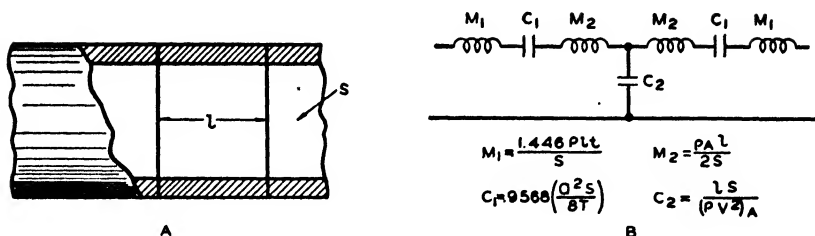


FIG. 5.1—STRETCHED DIAPHRAGM USED IN AN ACOUSTIC BAND-PASS FILTER.

Employing the well-known integral

$$\int r J_0(kr) dr = \frac{r J_1(kr)}{k} \quad (5.24)$$

this integral becomes

$$V = \frac{j2\pi p}{\omega \rho_s} \left[\frac{a J_1\left(\frac{\omega}{v} a\right)}{\frac{\omega}{v} J_0\left(\frac{\omega}{v} a\right)} - \frac{a^2}{2} \right]. \quad (5.25)$$

The series impedance of the diaphragm will then be

$$Z_D = \frac{p}{V} = \frac{-j\omega \rho_s}{S \left[\frac{2 J_1\left(\frac{\omega}{v} a\right)}{\frac{\omega}{v} a J_0\left(\frac{\omega}{v} a\right)} - 1 \right]} = \frac{-j \frac{\omega^2 \rho_s a}{S v} J_0\left(\frac{\omega}{v} a\right)}{2 J_1\left(\frac{\omega}{v} a\right) - \frac{\omega}{v} a J_0\left(\frac{\omega}{v} a\right)} \quad (5.26)$$

where S is the area of the diaphragm. Two cases are of interest, one when the diaphragm is operating below its resonant frequency, so that it acts as a compliance over the frequency range of interest, and the other when the diaphragm is used at its first resonant frequency which comes when $J_0\left(\frac{\omega}{v} a\right) = 0$. The first case can be evaluated by expanding the expression for J_1 and J_0 in series form. There results for significant powers of ω ,

$$Z_D = \frac{-j8T}{\omega \pi a^4} \left[1 - \frac{\omega^2 a^2}{6v^2} + \dots \right]. \quad (5.27)$$

Hence to this order of approximation a diaphragm represents a series compliance C_1 and series inductance M_1 having the values

$$C_1 = \frac{\pi a^4}{8T}; \quad M_1 = \frac{4\rho_s}{3\pi a^2} = \frac{(\frac{4}{3}\rho_s)}{S}. \quad (5.28)$$

A slightly different result is obtained if the impedance of the diaphragm is measured at the first resonant frequency which occurs when

$$J_0\left(\frac{\omega_R a}{v}\right) = 0 \quad \text{or} \quad \frac{\omega_R a}{v} = 2.4048. \quad (5.29)$$

The result can be obtained by finding the impedance Z_D for small variations $\Delta\omega$ in frequency from the value ω_R . Expanding

$J_0\left(\frac{\omega}{v}a\right)$ by MacLaurin's theorem we have

$$\begin{aligned} J_0\left(\frac{\omega_R + \Delta\omega}{v}a\right) &= J_0\left(\frac{\omega_R a}{v}\right) + \frac{\partial}{\partial\omega}\left(J_0\left(\frac{\omega a}{v}\right)\right)\Delta\omega_{\omega=\omega_R} \\ &\quad + \frac{1}{2!}\frac{\partial^2}{\partial\omega^2}\left(J_0\left(\frac{\omega}{v}a\right)\right)\Delta\omega^2 + \dots \end{aligned} \quad (5.30)$$

Hence to first powers of $\Delta\omega$, equation (5.26) becomes

$$Z_D = j \frac{\omega_R^2 a^2 \rho_s \Delta\omega}{2v^2 S}. \quad (5.31)$$

If we compare this with the impedance of an inductance and compliance near resonance given by equation (3.35) we find

$$C_1 = \frac{4\pi a^4}{\left(\frac{\omega_R a}{v}\right)^4 T} = \frac{4\pi a^4}{(2.4048)^4 T} = 0.9568 \left(\frac{\pi a^4}{8T}\right) \quad (5.32)$$

$$M_1 = \frac{1}{\omega_R^2 C_1} = \frac{(2.4048)^2}{4} \frac{\rho_s}{S} = 1.446 \frac{\rho_s}{S}.$$

At the first resonant frequency the effective compliance is 0.9568 times the static compliance, and the effective inductance is 1.446 times the static inductance of the moving part of the diaphragm.

One use to which such a stretched diaphragm can be put is in obtaining a band-pass acoustic filter. If we put a diaphragm across a main conducting tube whose diameter is less than 1.22 times the shortest wavelength of interest, as shown in Fig. 5.1A, the equivalent circuit of a section of this type is shown in Fig. 5.1B. This is obtained by using the T network representation of a tube and combining the effective inertance of the air with the effective inertance of the diaphragm. The resulting band-pass filter is one of the type shown on Table I, number 9, pages 52, 53, and all of the design constants can be obtained from the formulae given there.

One of the principal uses of stretched diaphragms is in the condenser transmitter. The diaphragm is backed up by a thin layer of air for damping purposes. As shown by Crandall ⁴ the effect of this is to reduce the compliance and add resistance to the constants of the diaphragm given above. This raises the resonant frequency and reduces the resonant response that would usually be present.

5.3. *Vibrations of Thin Plates—Telephone Receivers*

A similar problem of interest is one in which a thin plate takes the place of the stretched diaphragm of Fig. 5.1. This solution is not only of interest in acoustic and hydraulic filters but also in the theory of the telephone receiver.

From equation (5.11) the equation of motion satisfied by every point of a thin plate is

$$\frac{Y_0 l_t^3}{12(1 - \sigma)^2} \nabla^4 w - p + l_t \rho \frac{\partial^2 w}{\partial t^2} = 0. \quad (5.33)$$

We assume here simple harmonic motion and a symmetrical motion about the circle. Hence equation (5.33) takes the form

$$\frac{Y_0 l_t^3}{12(1 - \sigma^2)} \nabla^4 w - \omega^2 l_t \rho w - p = 0. \quad (5.34)$$

⁴ "Theory of Vibrating Systems and Sound," Crandall, Ch. I, D. Van Nostrand.

Setting

$$\frac{\frac{\omega^2 l_t \rho}{Y_0 l_t^3}}{12(1 - \sigma^2)} = \frac{12\omega^2 \rho(1 - \sigma^2)}{Y_0 l_t^2} = k^4 \quad (5.35)$$

the equation can be written

$$\left(\frac{d^2}{dr^2} + \frac{1}{r} \frac{d}{dr} + k^2\right) \left(\frac{d^2}{dr^2} + \frac{1}{r} \frac{d}{dr} - k^2\right) w = \frac{12p(1 - \sigma^2)}{Y_0 l_t^3}. \quad (5.36)$$

The solution of this equation will be the sum of the solutions of the two separate factors in w . Since the Bessel's functions of the second kind are inadmissible for this case on account of their infinite values at $r = 0$, a solution of this equation is

$$w = AJ_0(kr) + BJ_0(jkr) - \frac{p}{\omega^2 \rho l_t} \quad (5.37)$$

where

$$J_0(jkr) = I_0(kr) = 1 + \frac{1}{4} k^2 r^2 + \frac{1}{64} k^4 r^4 + \dots \quad (5.38)$$

is the Bessel's function of zero order with imaginary argument.

To obtain the constants A and B , we assume first that the plate is rigidly clamped, i.e., $w = \frac{dw}{dr} = 0$ when $r = a$. Inserting these conditions, the constants A and B are determined by solving the equations

$$\begin{aligned} w = 0 &= AJ_0(ka) + BI_0(ka) - \frac{p}{\omega^2 \rho l_t} \\ \frac{dw}{dr} = 0 &= k[-AJ_1(ka) + BI_1(ka)] \end{aligned} \quad (5.39)$$

where

$$I_1(kr) = -jJ_1(jka) = \frac{kr}{2} + \frac{k^3 r^3}{16} + \frac{k^5 r^5}{384} + \dots$$

Solving these equations, the value of the displacement w at any point becomes

$$w = \frac{p}{\omega^2 \rho l_t} \left[\frac{I_1(ka)J_0(kr) + J_1(ka)I_0(kr)}{I_1(ka)J_0(ka) + J_1(ka)I_0(ka)} - 1 \right]. \quad (5.40)$$

Integrating over the surface to find the volume velocity as in section 5.2, one finds that the volume velocity is

$$V = j\omega 2\pi \int_0^a r w dr = \frac{j\pi p a^2}{\omega \rho l_t} \left[\frac{1}{\frac{ka}{4} \left[\frac{J_0(ka)}{J_1(ka)} + \frac{I_0(ka)}{I_1(ka)} \right]} - 1 \right].$$

Hence the impedance of the plate is

$$Z_p = \frac{p}{V} = + \frac{j\omega \rho l_t}{S} \left[\frac{\frac{ka}{4} \left[\frac{J_0(ka)}{J_1(ka)} + \frac{I_0(ka)}{I_1(ka)} \right]}{\frac{ka}{4} \left[\frac{J_0(ka)}{J_1(ka)} + \frac{I_0(ka)}{I_1(ka)} \right] - 1} \right] \quad (5.41)$$

where S is the area of the plate.

The low-frequency values of the equivalent network can be obtained by expanding this expression in series form. Since

$$\begin{aligned} J_0(ka) &= 1 - \frac{k^2 a^2}{4} + \frac{k^4 a^4}{64} - \frac{k^6 a^6}{2304} + \frac{k^8 a^8}{147,456} + \dots \\ I_0(ka) &= 1 + \frac{k^2 a^2}{4} + \frac{k^4 a^4}{64} + \frac{k^6 a^6}{2304} + \frac{k^8 a^8}{147,456} + \dots \quad (5.42) \\ J_1(ka) &= \frac{ka}{2} - \frac{k^3 a^3}{16} + \frac{k^5 a^5}{384} - \frac{k^7 a^7}{18,432} + \frac{k^9 a^9}{1,474,560} + \dots \\ I_1(ka) &= \frac{ka}{2} + \frac{k^3 a^3}{16} + \frac{k^5 a^5}{384} + \frac{k^7 a^7}{18,432} + \frac{k^9 a^9}{1,474,560} + \dots \end{aligned}$$

it is easily shown that the impedance Z_p at low frequencies becomes

$$\frac{-j16l_t^3 Y_0}{\omega a^4 S(1 - \sigma^2)} \left[1 - \frac{9\omega^2 \rho(1 - \sigma)a^4}{80Y_0 l_t^2} + \dots \right]. \quad (5.43)$$

This will be the impedance of a compliance C in series with an acoustic inertance M having the values

$$C = \frac{a^4 S(1 - \sigma^2)}{16l_t^3 Y_0}; \quad M = \frac{9\rho l_t}{5S}. \quad (5.44)$$

The value of Z_p for large values of (ka) is shown plotted in Fig. 5.2. This is plotted in the form

$$Z_p = \frac{j l_t^2}{a^2 S} \sqrt{\frac{Y_0 \rho}{12(1 - \sigma^2)}} \left[\frac{\frac{k^3 a^3}{4} \left(\frac{J_0(ka)}{J_1(ka)} + \frac{I_0(ka)}{I_1(ka)} \right)}{\frac{ka}{4} \left(\frac{J_0(ka)}{J_1(ka)} + \frac{I_0(ka)}{I_1(ka)} \right) - 1} \right] \quad (5.45)$$

which is obtained from (5.41) by eliminating ω . This curve shows that the resonant frequencies occur at nearly even multiples of ka . Since k is proportional to the square root of the

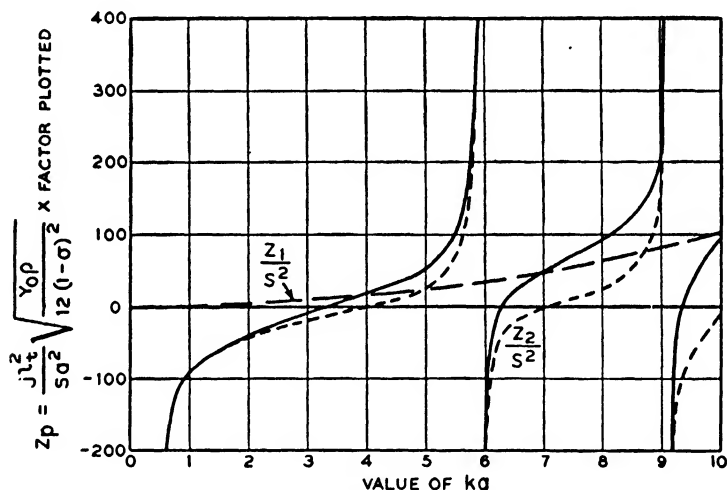


FIG. 5.2—DIAPHRAGM IMPEDANCE PLOTTED AS A FUNCTION OF ka .

frequency it follows that the resonant frequencies are nearly in the ratios of the squares of the harmonic order. It will be noted that the region of negative reactance becomes much smaller for the higher order harmonics and over most of the frequency range the reactance can be represented by a simple acoustic inertance which has the value in acoustic impedance units of

$$M_A = \frac{l_t \rho}{S}. \quad (5.46)$$

This is shown in the dashed line of Fig. 5.2.

In mechanical impedance units this becomes

$$Z_M = \frac{F}{\xi} = \frac{pS}{\frac{V}{S}} = Z_A S^2. \quad (5.47)$$

Hence in mechanical impedance units the mass is

$$M = \frac{l_t \rho}{S} S^2 = \rho l_t S \quad (5.48)$$

which is the static mass of the plate.

This solution is of some interest in filters of the type shown in Fig. 5.1. It is also of interest in such apparatus as telephone receivers in which a thin plate is energized by a magnet

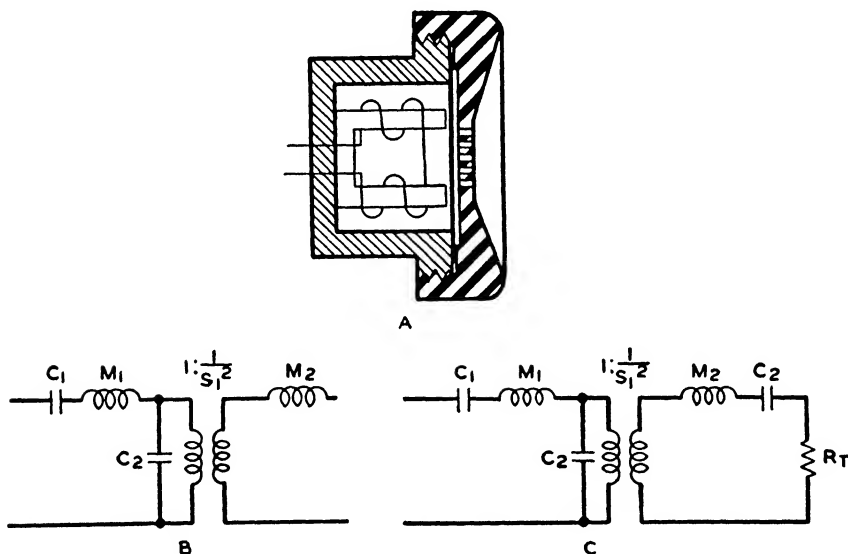


FIG. 5.3—USE OF CLAMPED PLATE IN TELEPHONE RECEIVER.

and made to drive the air in the cap of the receiver as shown in Fig. 5.3A. If we assume that the force is more or less uniformly applied over the surface of the plate, the equivalent circuit for the diaphragm and ear cap air chamber is as shown in Fig. 5.3B. The series resonant circuit M_1, C_1 represent the

compliance and mass of the diaphragm which in mechanical impedance units will be

$$C_1 = \frac{a^2(1 - \sigma^2)}{16\pi l_i^3 Y_0} ; \quad M_1 = \frac{9(\rho l_i S_1)}{5} \quad (5.49)$$

where S_1 is the area of the diaphragm and air chamber. These are obtained from equations (5.44) by multiplying by S_1^2 as indicated by equation (5.47). At the end of this series resonant circuit we have a compliance representing the compliance of the air chamber. From equation (4.85) this will be in mechanical impedance units,

$$C_2 = \frac{tS_1}{\rho v^2} \times \frac{1}{S_1^2} = \frac{t}{\rho v^2 S_1} \quad (5.50)$$

where t is the thickness and S_1 the area of the air chamber.

At this point since a change of area occurs between the air chamber and the holes in the cap it is advantageous to change from the mechanical impedance system, which is advantageous for mechanical structures, to the acoustical impedance system. This can be done by inserting a transformer of impedance ratio 1 to $\frac{1}{S_1^2}$ as shown in Fig. 5.3B. This follows from the fact that in mechanical impedance units the current into the transformer will be ξ_1 , the average particle velocity over the surface of the air chamber. The current out of the transformer will be

$$S_1 \xi = V \quad (5.51)$$

which is the volume velocity. Next we add the series inductance due to the acoustic inertance of the holes which is, according to equation (4.99),

$$M_2 = \frac{\rho(l_h + 2r)}{S_h N} \quad (5.52)$$

where l_h is the length of the holes in the ear cap, r their radius and $S_h N$ the total area of the holes.

If a telephone receiver is used in the open air a good result is not obtained, for the radiation resistance of the holes in the

diaphragm is much too small to absorb much of the energy. When, however, the receiver is placed on the ear, a much better result is obtained since the impedance looking into the ear can be represented as a series compliance and resistance as shown by Fig. 5.3C. By using the right number and sizes of holes, the acoustic inertance of the holes can be made to resonate the compliance of the ear at the same frequency as the diaphragm resonance and a band-pass filter of the type shown on Table I, number 9, pages 52, 53, is obtained.

At this point a difficulty with using a thin clamped diaphragm becomes obvious. The filter of Table I, number 9, has its lower cutoff frequency at the resonant frequency of the diaphragm. This should be made low in order to obtain a good response at low frequencies. The curves of Fig. 5.2 show, however, that the diaphragm becomes anti-resonant at a frequency of 3.2 times the resonant frequency. A large attenuation of sound will occur at this frequency and hence it is not possible to reproduce a frequency range of more than 3 to 1 with a clamped diaphragm of uniform section.



FIG. 5.4—CURVED SHELL DIAPHRAGM.

One method often employed to get around this difficulty is to make the diaphragm in the form of a bent disk as shown in Fig. 5.4. This is connected to the clamping ring by a thin material which has a large compliance. Then on account of the large stiffness of the curved plate it will not anti-resonate until a high frequency and the combination will act much more nearly like the lumped mass and compliance of Fig. 5.3B. The result is that the lower cutoff can be made much lower without running into anti-resonant frequencies or breaking up of the diaphragm. By using such diaphragms high quality receivers have been constructed. The method of taking account of the driving elements is discussed in Chapter VI. When this is done a complete electromechanical filter can be obtained which works from an electrical circuit to the ear impedance.

5.4. *Energy Transmitted to Supports—Soundproof Walls*

We have so far assumed that all of the energy of the vibrating plate is transmitted to the surrounding air and none of it to the supports which hold the plate. This is a good assumption as long as the plate is quite thin, but it fails for larger plates. Hence, although the mathematical difficulties become greater, it appears desirable to investigate the conditions for which it is possible to put most of the energy into the medium and little in the supports.

This problem can be solved by employing the expressions for the force and moment per unit length of support given by equation (5.17). For the symmetrical circular case we have the equations:

Total force

$$F = \frac{2\pi a Y_0 l_i^3}{12(1 - \sigma^2)} \left[\frac{d}{dr} \left(\frac{d^2 w}{dr^2} + \frac{1}{r} \frac{dw}{dr} \right) \right]_{r=a}. \quad (5.53)$$

Total moment

$$M = \frac{2\pi a Y_0 l_i^3}{12(1 - \sigma^2)} \left[\frac{d^2 w}{dr^2} + \frac{\sigma}{a} \frac{dw}{dr} \right].$$

Introducing the solution for w from (5.37), these quantities on the edge of the plate become

$$M = 2\pi\omega a l_i^2 \sqrt{\frac{Y_0}{12(1 - \sigma^2)}} \left[-A \left[J_0(ka) - (1 - \sigma) \frac{J_1(ka)}{ka} \right] + B \left[I_0(ka) - (1 - \sigma) \frac{I_1(ka)}{ka} \right] \right] \quad (5.54)$$

$$F = 2\pi\omega a l_i^2 \sqrt{\frac{Y_0 \rho}{12(1 - \sigma^2)}} [AkJ_1(ka) + BkI_1(ka)].$$

In order to obtain the most general boundary conditions, two impedances are introduced. The first impedance, a force impedance, Z_I , is defined as the ratio of the total force F to the

velocity at the boundary where the plate touches the supports, or

$$Z_t = \frac{F}{\dot{w}} = \frac{1}{j\omega} \frac{F}{w}. \quad (5.55)$$

The other impedance is a moment impedance Z_θ which is defined as the ratio of the total moment to the angular velocity of the edge, so that

$$Z_\theta = \frac{M}{\dot{\theta}} = - \frac{M}{j\omega \left(\frac{dw}{dr} \right)} \quad (5.56)$$

since $-\frac{dw}{dr}$ gives the tangent of the angular displacement of the edge and, since this is small, the tangent of the angle equals the angle of the edge. Thus we have the two equations

$$Z_\theta = \frac{\left\{ 2\pi\omega a l_t^2 \sqrt{\frac{Y_0\rho}{12(1-\sigma^2)}} \left[+A \left[J_0(ka) - (1-\sigma) \frac{J_1(ka)}{ka} \right] - B \left[I_0(ka) - (1-\sigma) \frac{I_1(ka)}{ka} \right] \right] \right\}}{j\omega k [-AJ_1(ka) + BI_1(ka)]}$$

$$Z_t = \frac{2\pi\omega a l_t^2 \sqrt{\frac{Y_0\rho}{12(1-\sigma^2)}} [AkJ_1(ka) + BkI_1(ka)]}{j\omega \left[AJ_0(ka) + BI_0(ka) - \frac{p}{\rho l_t \omega^2} \right]}. \quad (5.57)$$

These two equations give relations between A and B and hence these can be evaluated with the result

$$A = \frac{\frac{p}{\omega^2 \rho l_t} \left[I_0(ka) - \left(1 - \sigma - jZ_\theta \left(\frac{6\omega(1-\sigma^2)}{\pi Y_0 l_t^3} \right) \right) \frac{I_1(ka)}{ka} \right]}{D}$$

$$B = \frac{\frac{p}{\omega^2 \rho l_t} \left[J_0(ka) - \left(1 - \sigma - jZ_\theta \left(\frac{6\omega(1-\sigma^2)}{\pi Y_0 l_t^3} \right) \right) \frac{J_1(ka)}{ka} \right]}{D} \quad (5.58)$$

where

$$\begin{aligned}
 D = & 2J_0(ka)I_0(ka) \\
 & - \left(1 - \sigma - \frac{jZ_\theta 6\omega(1 - \sigma^2)}{\pi Y_0 l_t^3}\right) \left(\frac{J_0(ka)I_1(ka) + I_0(ka)J_1(ka)}{ka}\right) \\
 & + \frac{j2\pi a k l_t^3 \sqrt{\frac{Y_0 \rho}{12(1 - \sigma^2)}}}{Z_l} \left[J_1(ka)I_0(ka) + I_1(ka)J_0(ka) \right. \\
 & \left. - 2 \left(1 - \sigma - \frac{jZ_\theta 6\omega(1 - \sigma^2)}{\pi Y_0 l_t^3}\right) \frac{J_1(ka)I_1(ka)}{ka} \right].
 \end{aligned}$$

If Z_θ and Z_l become very large

$$\begin{aligned}
 A &= \frac{\frac{p}{\omega^2 \rho l_t} I_1(ka)}{J_0(ka)I_1(ka) + I_0(ka)J_1(ka)}; \\
 B &= \frac{\frac{p}{\omega^2 \rho l_t} J_1(ka)}{J_0(ka)I_1(ka) + I_0(ka)J_1(ka)} \quad (5.59)
 \end{aligned}$$

and the solution given before for a clamped plate results.

If Z_θ is a small compliance

$$Z_\theta = \frac{-j}{\omega C_\theta} \quad (5.60)$$

and this is much smaller than the compliance at the edge of the plate,

$$C_p = \frac{6(1 - \sigma^2)}{\pi Y_0 l_t^3} \quad (5.61)$$

as will usually be the case for a stiff clamp, these values simplify to

$$\begin{aligned}
 A &= \frac{\frac{p}{\omega^2 \rho l_t} I_1(ka)}{J_0(ka)I_1(ka) + I_0(ka)J_1(ka) + \frac{j4\omega l_t \rho S}{Z_l} \frac{J_1(ka)I_1(ka)}{ka}} \\
 B &= \frac{\frac{p}{\omega^2 \rho l_t} J_1(ka)}{J_0(ka)I_1(ka) + I_0(ka)J_1(ka) + \frac{j4\omega l_t \rho S}{Z_l} \frac{J_1(ka)I_1(ka)}{ka}} \quad (5.62)
 \end{aligned}$$

where S is the area of the plate, πa^2 .

The force on the support will then be by (5.54)

$$F = \frac{pS}{\frac{ka}{4} \left[\frac{J_0(ka)}{J_1(ka)} + \frac{I_0(ka)}{I_1(ka)} \right] + \frac{j\omega\rho l_t S}{Z_l}} \quad (5.63)$$

At zero frequency if Z_l is finite so that the pressure has something to push against, this gives

$$F = pS \quad (5.64)$$

which shows that the total force of the pressure is opposed by the force of the support.

The shape of the plate and the displacement at every point for a finite support are also of interest. Inserting the values of A and B from (5.62) in equation (5.39) we have

$$w = \frac{p}{\omega^2 \rho l_t} \left[\left(\frac{I_1(ka)J_0(kr) + J_1(ka)I_0(kr)}{J_0(ka)I_1(ka) + I_0(ka)J_1(ka)} + \frac{j4\omega\rho l_t S}{Z_l} \frac{J_1(ka)I_1(ka)}{ka} \right) - 1 \right] \quad (5.65)$$

At low frequencies the shape does not differ from the clamped diaphragm unless the supports have a mass impedance. From (5.65) we can also determine the volume velocity of the medium contained in the circular supports. This is

$$V = j\omega 2\pi \int_0^a r w dr = \frac{jpS}{\omega\rho l_t} \left[\frac{1}{\frac{ka}{4} \left[\frac{J_0(ka)}{J_1(ka)} + \frac{I_0(ka)}{I_1(ka)} \right] + \frac{j\omega\rho l_t S}{Z_l}} - 1 \right] \quad (5.66)$$

Equations (5.63) and (5.66) give us sufficient information to determine an equivalent circuit for the diaphragm which takes account of the transmission in the medium inside the supports and in the supports themselves. This representation is shown in Fig. 5.5. Here we have a source of pressure p_1 , representing the pressure on one side of the diaphragm opposed by another source p_2 representing the pressure on the other side. These go to a transformer of ratio 1 to S^2 , which transforms the

resulting pressure difference into force. This is followed by a series impedance Z_1 , a shunt impedance Z_2 and the terminating impedance Z_l of the support.

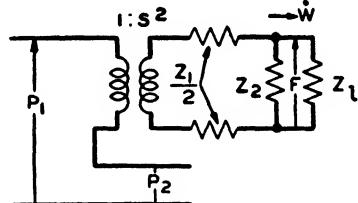


FIG. 5.5—EQUIVALENT CIRCUIT FOR A THIN PLATE AND SUPPORT.

From this figure it is readily shown that the force F across the support impedance Z_l is equal to

$$F = \frac{pS}{\frac{Z_1 + Z_2}{Z_2} + \frac{Z_1}{Z_l}} \quad (5.67)$$

Comparing this with equation (5.63) the two agree provided

$$Z_1 = j\omega\rho l_t S = j\omega M_1$$

$$Z_2 = \frac{j\omega M_1}{\left[\frac{ka}{4} \left(\frac{J_0(ka)}{J_1(ka)} + \frac{I_0(ka)}{I_1(ka)} \right) \right] - 1} \quad (5.68)$$

where M_1 is the total mass of the diaphragm. This equivalence also satisfies equation (5.66) for the volume velocity in the medium enclosed by the circular support. From Fig. 5.5 this should be

$$V = \frac{(p_1 - p_2)}{\left(Z_1 + \frac{Z_2 Z_l}{Z_2 + Z_l} \right)} \quad (5.69)$$

Inserting the values from (5.68) we find that this agrees with (5.66).

Equivalent circuits of this type are useful in considering double soundproof windows and walls for cutting down sound and vibration transmission from one place to another. As an example let us consider the double soundproof window constructed as shown in Fig. 5.6A. Although such windows are usually made in rectangular shape rather than circular, the equivalent circuit of Fig. 5.6 will show qualitatively the action of the device. The window is shown constructed of two frames which hold the glass rigidly. These two frames are connected together by a layer of rubber or other elastic material. The

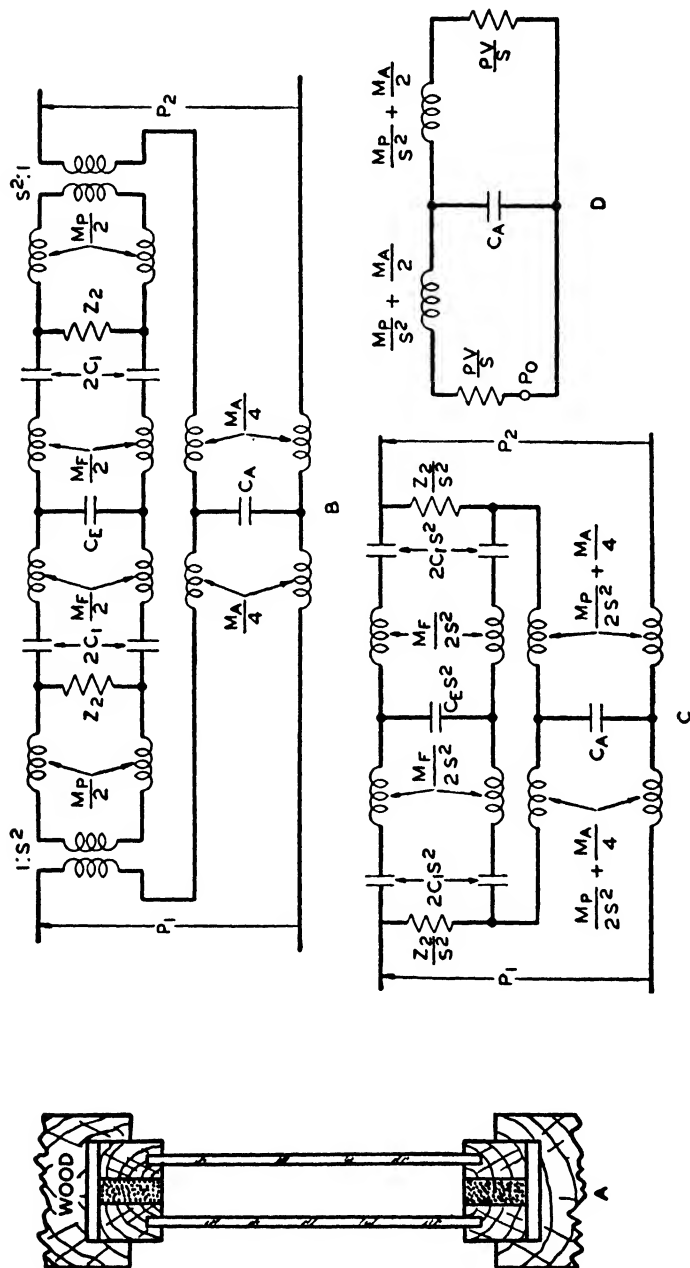


FIG. 5.6—CONSTRUCTION OF DOUBLE SOUNDPROOF WINDOW

equivalent circuit for this combination including the supports is shown in Fig. 5.6B. In this representation M_p is the static mass of the plate, C_1 the series compliance which represents the compliance of the attachment of the first frame to the wall or the second frame to its wall, M_F the mass of each frame, C_E the compliance of the central layer connecting the two frames, M_A the acoustic inertance of the air between the two panes (i.e., $\left(\frac{\rho_A l}{S}\right)$ where l is the separation of the panes), and C_A is the compliance of the air between the panes which in acoustic impedance units is

$$C_A = \frac{Sl}{\rho v^2}. \quad (5.70)$$

The impedance Z_2 is shown in acoustic impedance units by the dotted line of Fig. 5.2. In general this impedance is quite low except near the anti-resonant frequencies of the diaphragm. The representation of Fig. 5.6B can be simplified somewhat by eliminating the transformer 1 to S_1^2 which can be done by expressing all the elements of the support in acoustic impedance units which are the mechanical impedances divided by S_1^2 . Also the position of the plate masses can be changed so that they are in series with the air inertances M_A since no current change is involved thereby. The resulting representation is shown in Fig. 5.6C. Although this is a rather complicated circuit, the resulting attenuation can be obtained approximately by inspection. Z_2/S^2 is usually quite small over most of the frequency range as shown by Fig. 5.2 and hence it short-circuits the path through the supports. Then the resulting attenuation over a good share of the frequency range is due to the low-pass filter shown in Fig. 5.6D. If we calculate the loss due to inserting this between the impedances $\left(\frac{\rho v}{S}\right)_A$, the radiation impedance of air on either side, we find

$$\frac{p'}{p} = \frac{1}{1 - \frac{\omega^2(\rho l_i)_P l}{(\rho v^2)_A} + j\omega \frac{(\rho l_i)_P}{(\rho v)_A} \left[1 - \frac{\omega^2(\rho l_i)_P l}{2(\rho v^2)_A} \right]}. \quad (5.71)$$

At high frequencies this will give a large attenuation and one which increases 18 db per octave. However at the anti-resonant frequencies of the diaphragm this large attenuation is not obtained since then the impedance Z_2 is large and most of the energy goes into the supports. For this reason it is desirable to design the supports as a filter section which is done by using the mass of the supports and the compliance of the joining members to make a filter section. If the attenuation of this filter section is large at the anti-resonant frequencies of the diaphragm, a large attenuation can be obtained at all frequencies by using this double construction. Such a device is much more effective than a single wall having the same weight.

In the general case when Z_0 is finite two modes of motion can be set up in the support, the longitudinal mode discussed above, and a flexural mode in which the central line of the support does not change length. The construction shown in Fig. 5.6 will act as a filter for this mode of motion also. Due to the complexity of the equations, the general case is not considered farther.

5.5. *Diaphragm with Tension and Stiffness*

As mentioned in the introduction stretched diaphragms used in practice differ from the theoretical diaphragm considered in section (5.2) due to the inherent plate stiffness of all materials. It is the purpose of this section to consider the modifications in the equivalent circuit of a stretched diaphragm caused by the inherent stiffness.

The equation of motion satisfied by every point on the surface is by equation (5.11) for a circular diaphragm,

$$\frac{(Y_0 + T)l_t^3}{12(1 - \sigma^2)} \nabla^4 w - T \nabla^2 w - p - \omega^2 \rho l_t w = 0. \quad (5.72)$$

For the case of a diaphragm, Bessel's functions of the second kind are not permissible since the displacement of the center is finite. A solution of (5.72) then is

$$w = AJ_0(k_1 r) + BJ_0(k_2' r) - \frac{p}{\omega^2 \rho l_t} \quad (5.73)$$

where k_1 and k_2' satisfy the equation

$$\frac{(Y_0 + T)l_t^2}{12\rho(1 - \sigma^2)} k^4 + \frac{T}{\rho l_t} k^2 - \omega^2 = 0. \quad (5.74)$$

If we let

$$\frac{(Y_0 + T)l_t^2}{12\rho(1 - \sigma^2)} = c; \quad \frac{T}{\rho l_t} = d \quad (5.75)$$

the two solutions are

$$k_1 = \sqrt{\frac{\sqrt{d^2 + 4c\omega^2} - d}{2c}}; \quad k_2' = j \sqrt{\frac{\sqrt{d^2 + 4c\omega^2} + d}{2c}}. \quad (5.76)$$

Hence the solution for the displacement at any point is

$$w = AJ_0 \left(r \sqrt{\frac{\sqrt{d^2 + 4c\omega^2} - d}{2c}} \right) + BI_0 \left(r \sqrt{\frac{\sqrt{d^2 + 4c\omega^2} + d}{2c}} \right) - \frac{p}{\omega^2 \rho l_t}. \quad (5.77)$$

We determine the constants A and B by the condition for a clamped diaphragm

$$w = \frac{dw}{dr} = 0 \text{ when } r = a. \quad (5.78)$$

These conditions result in the displacement

$$w = \frac{p}{\omega^2 \rho l_t} \left[\frac{k_2 I_1(k_2 a) J_0(k_1 r) + k_1 J_1(k_1 a) I_0(k_2 r)}{J_0(k_1 a) k_2 I_1(k_2 a) + k_1 J_1(k_1 a) I_0(k_2 a)} - 1 \right] \quad (5.79)$$

where k_2 is taken as

$$k_2 = \sqrt{\frac{\sqrt{d^2 + 4c\omega^2} + d}{2c}} = -jk_2'. \quad (5.80)$$

To determine the impedance of such an element, we have first to calculate the volume velocity V . Integrating, this is

$$\begin{aligned}
 V &= j\omega 2\pi \int_0^a r w dr \\
 &= \frac{j p S}{\omega \rho l_t} \left[\frac{\frac{2}{a} \left(\frac{k_2}{k_1} + \frac{k_1}{k_2} \right) I_1(k_2 a) J_1(k_1 a)}{J_0(k_1 a) k_2 I_1(k_2 a) + k_1 J_1(k_1 a) I_0(k_2 a)} - 1 \right]. \quad (5.81)
 \end{aligned}$$

The impedance of the device, being p/V is

$$Z_p = \frac{p}{V} = \frac{j\omega \rho l_t}{S} \left[\frac{\left[k_2 \frac{J_0(k_1 a)}{J_1(k_1 a)} + \frac{k_1 I_0(k_2 a)}{I_1(k_2 a)} \right] \frac{k_1 k_2 a}{2(k_1^2 + k_2^2)}}{\left[k_2 \frac{J_0(k_1 a)}{J_1(k_1 a)} + k_1 \frac{I_0(k_2 a)}{I_1(k_2 a)} \right] \frac{k_1 k_2 a}{2(k_1^2 + k_2^2)} - 1} \right]. \quad (5.82)$$

If either c or d disappear this expression reduces respectively to the equations already derived for a stretched diaphragm or a thin plate.

If ω is treated as a small quantity, the expression for the displacement w reduces to

$$w = \frac{p}{T} \left[\frac{\left\{ \sqrt{\frac{(Y_0 + T) l_t^3}{12 T (1 - \sigma^2)}} a \left[I_0 \left(\sqrt{\frac{12 T (1 - \sigma^2)}{(Y_0 + T) l_t^3}} r \right) - I_0 \left(\sqrt{\frac{12 T (1 - \sigma^2)}{(Y_0 + T) l_t^3}} a \right) \right] \right\}}{2 I_1 \left(\sqrt{\frac{12 T (1 - \sigma^2)}{(Y_0 + T) l_t^3}} a \right)} + \frac{a^2 - r^2}{4} \right]. \quad (5.83)$$

In case $T \rightarrow 0$ the static deflection becomes

$$w = \frac{12 p (1 - \sigma^2)}{Y_0 l_t^3} \left[\frac{r^4 + a^4}{64} - \frac{a^2 r^2}{32} \right]. \quad (5.84)$$

In case $l_t \rightarrow 0$, or the natural stiffness is small compared to the tension T the displacement is

$$w = \frac{p}{T} \left(\frac{a^2 - r^2}{4} \right). \quad (5.85)$$

To determine the low frequency stiffness of the diaphragm the volume displacement can be calculated from (5.83) to be

$$D_v = 2\pi \int_0^a r w dr = \frac{pS}{T} \left[\frac{(Y_0 + T)l_t^3}{12T(1 - \sigma^2)} - a \sqrt{\frac{(Y_0 + T)l_t^3}{12T(1 - \sigma^2)}} \frac{I_0 \left(\sqrt{\frac{12T(1 - \sigma^2)}{(Y_0 + T)l_t^3}} a \right)}{2I_1 \left(\sqrt{\frac{12T(1 - \sigma^2)}{(Y_0 + T)l_t^3}} a \right)} + \frac{a^2}{8} \right] = pC. \quad (5.86)$$

The same result can be obtained by expanding (5.82) in power of ω and taking the first term. The inertance term varies from 4/3 to 9/4 times the factor $\rho l_t/S$ depending on the ratio of d/c .

CHAPTER VI

ELECTROMECHANICAL CONVERTING SYSTEMS

MECHANICAL and acoustical vibrations are usually produced from electrical sources of power by means of electromechanical converting elements. The most common types of driving systems in use are the electromagnetic, the electrostatic, the piezoelectric and the magnetostrictive systems. In the electromagnetic system the mechanical force is obtained through the attraction or repulsion of two electric currents or of an electric current and a permanent magnet. In the electrostatic drive the force is obtained as the result of a repulsion between a fixed polarizing charge and a variable applied charge. Both of these systems result in rather low ratios of force to current or charge but they can be associated with large compliances and low masses in the driven mechanical system so that they are largely used in generating acoustic waves in air.

In a magnetostrictive driving system use is made of a property present for most magnetic materials that if a rod or tube of the material is brought into a magnetic field parallel to its length, the length is changed by a small amount, usually under 25 parts in a million, although under resonance conditions this change in length can be made considerably larger. The change in length may be either positive or negative depending on the nature of the material, depending on its heat and magnetization treatment, and on the temperature. For low flux densities the change in length is approximately proportional to the square of the flux density so that a polarizing field or magnet has to be used. Although the change in length is small the force associated with this expansion is the full elastic force of the bar so that large ratios of force to applied current result. The associated compliance is very small and the masses large so that the mechanical impedance of the resulting system tends to be large.

Such driving systems are very useful in driving liquids, solids, or other high impedance systems but are not suitable for efficiently setting up sound waves in air.

An analogous effect in electrostatics is the electrostrictive effect. In this effect a change of length of a material occurs proportional to the square of the applied potential gradient. This effect is prominent for certain types of rubber and glasses. Although its application has been suggested as an acoustic rectifier when used without biasing voltage or as a linear driving system when used with an electrostatic biasing voltage such driving systems are not extensively applied and will not be considered farther here. For certain types of crystals, however, and for certain other oriented materials there is a change of length with applied charge which is directly proportional to the applied charge, and reverses sign when the sign of the charge changes. This effect is known as the piezoelectric effect. Piezoelectric crystals have received rather wide application as the driving elements of mechanical systems. In a similar manner to the magnetostrictive bar, the ratio of force to applied charge is large for a piezoelectric crystal in longitudinal vibration and the mechanical impedance is also high. Such crystals have been used to set up supersonic vibrations in liquids, solids, and other high impedance systems. For the lower mechanical impedance of devices which set up sound waves in air, bimorph type crystals have been devised and extensively used. They are constructed by glueing together two oppositely poled longitudinal crystals. One expands and the other contracts so that a considerably larger flexural motion is obtained than would be obtained with a longitudinal crystal alone. As shown by section 6.4, the mechanical impedance of such crystals is considerably lower than that for longitudinally vibrating crystals, and bimorph units of Rochelle salt have been widely used in microphones, head phones, phonograph pickups, high-frequency loudspeakers, galvanometers and for many other devices.

It is the purpose of this chapter to describe briefly such systems and to derive the equations pertaining to them. Electro-mechanical equivalent circuits have also been developed for all

these types of systems. With these equivalent circuits it is possible to obtain a complete electromechanical network which describes the action of the electrical system, the mechanical system, and the electromechanical converting elements. This circuit usually takes the form of well-known filter circuits and by employing the known formulae for electrical wave filters, the best design can be obtained for systems converting electrical into acoustical or mechanical energy or vice versa.

6.1. *Electromagnetic Types*

Several electromagnetic type converters are shown schematically in Fig. 6.1. The first is a moving coil type in which the mechanical forces are developed by the interaction of the currents in the coil with the polarizing field. The force in dynes due to the interaction of the current in the voice coil and the polarizing field is

$$F = - Bli \quad (6.1)$$

where B is the flux density of the polarizing field in the coil expressed in gauss, l is the length of the conductor in centimeters, and i is the current in abamperes which are 10 times as large as the usual unit of current, the ampere. The factor Bl , which is the ratio of the force to the applied current, is called the force factor. It is the direct relation between the mechanical and electrical circuits.

In addition we have the inverse relation that the electromotive force generated in the electrical circuit is

$$E = Bl\dot{x} \quad (6.2)$$

where E is the generated electromotive force, expressed in abvolts which are 10^{-8} times the ordinary volt, and \dot{x} is the velocity of the coil in centimeters per second.

If the coil is held from moving the electrical impedance measured at the terminals of the system will be an inductance L of the electrical voice coil. Similarly, if the electrical system is open-circuited so that no current flows, the mechanical impedance measured will consist of a compliance C_M which

restores the coil to its mid-position plus a mass M consisting of the mass of the coil plus the effective mass of the support.

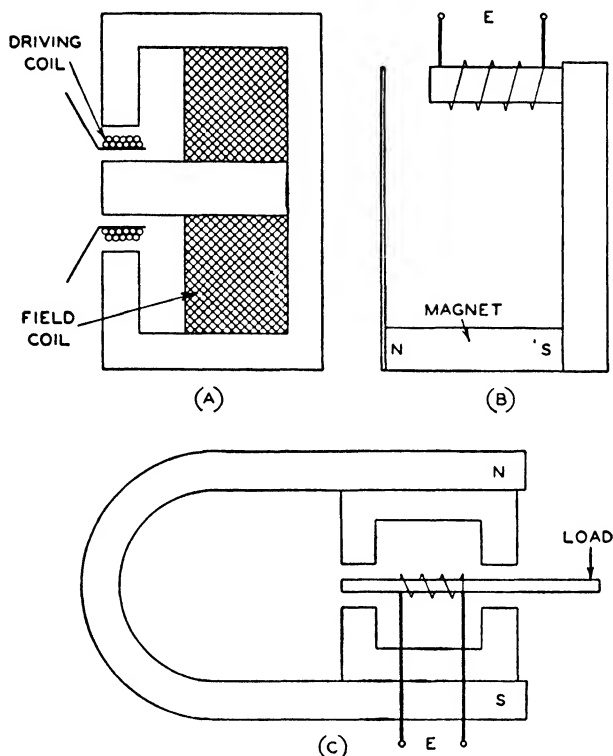


FIG. 6.1—ELECTROMAGNETIC DRIVING SYSTEMS.

If the system which associates force with potential and velocity with current is used, the two equations can be written ¹

$$E = j\omega Li + (Bl \times 10^{-8})\dot{x}$$

$$F = \left(j\omega M - \frac{j}{\omega C_M} \right) \dot{x} - (Bl \times 10^{-1})i. \quad (6.3)$$

For the system free to move $F = 0$ and hence

$$\dot{x} = \frac{(Bl \times 10^{-1})i}{Z_M} \quad (6.4)$$

¹ Equations of this form were first given by R. L. Wegel, Journal A.I.E.E., Vol. XL, No. 10, October 1921.

where Z_M is the mechanical impedance of the system which in this case is $(j\omega M - j/\omega C_M)$. Introducing this in the first equation of (6.3) we have

$$E = i \left[j\omega L + \frac{(Bl)^2 \times 10^{-9}}{Z_M} \right] = iZ_E. \quad (6.5)$$

Hence the impedance on the electrical side will be the electrical impedance plus the inverse of the mechanical impedance times the factor $(Bl)^2 \times 10^{-9}$.

If on the other hand we use the second analogy between electrical and mechanical quantities which relates the force with the current, and the velocity with the electromotive force a simplification is effected. For this case the equations (6.3) become

$$E = j\omega Li + (Bl \times 10^{-8})\dot{x} \quad (6.6)$$

$$F = \frac{\dot{x}}{Z_M} - (Bl \times 10^{-1})i$$

where

$$Z_M = \frac{1}{j\omega M - \frac{j}{\omega C_M}} = \frac{j\omega C_M}{1 - \omega^2 M C_M},$$

that is, the mechanical impedance for this system is the inverse of that for the first system of analogies. For this case the measured electrical impedance then becomes

$$Z_E = j\omega L + (Bl)^2 \times 10^{-9} Z_M. \quad (6.7)$$

If we express E and i in terms of abvolts and abamperes, i.e., units in the cgs electromagnetic system, equations (6.6) become

$$E_A = j\omega(L \times 10^9)i_A + Bl\dot{x} \quad (6.8)$$

$$F = \frac{\dot{x}}{Z_M} - Bl i_A$$

when L is expressed in henries. If \dot{x} is taken as the analogue of voltage, F of current, a simple equivalent circuit for this case is shown in Fig. 6.2. This circuit consists of an inductance rep-

representing the inductance ($L \times 10^9$) in the electromagnetic cgs system, a perfect transformer of impedance ratio

$$\varphi^2 = \frac{1}{B^2 l^2} \quad (6.9)$$

and the mechanical elements of the system. Since any further extension of the mechanical network will have an impedance

$$Z'_M = -\frac{\dot{x}}{F} \quad (6.10)$$

such elements can be added to the representation of Fig. 6.2, and the whole can be designed as one transmission network. Several examples are discussed in the next chapter.

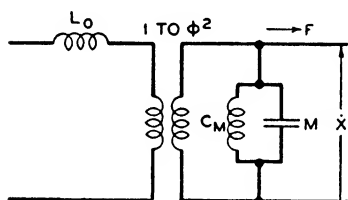


FIG. 6.2—EQUIVALENT CIRCUIT FOR ELECTROMAGNETIC DRIVING SYSTEM.

It is worth while to point out that having derived the first relation

$$\frac{E - j\omega L i_A}{\dot{x}} = B l \quad (6.8A)$$

the second relation

$$\frac{F - \frac{\dot{x}}{Z_M}}{i_A} = -B l \quad (6.8B)$$

follows from the reciprocity theorem proved in section (2.2). From equations (2.23) and (2.24) we have the relation

$$\frac{E_1 - i_1 Z_{sc1}}{E_3} = -\frac{\Delta_{13}}{\Delta_{11} + \Delta_{1133} Z_T} = -\left(\frac{i_3 - E_3 / Z_{oc2}}{i_1} \right). \quad (2.24)$$

Hence if we identify \dot{x} with E_3 the output voltage, F with i_3 the output current, then (6.8B) follows from (6.8A). Z_{sc1} is the impedance at the beginning of the network, when the mechanical side is short-circuited. From Fig. 6.2 it is obvious that this is the impedance of the electrical coil L . The open-circuit impedance looking back from the mechanical side will be the mechanical impedance Z_M and hence (6.8) is the exact analogue of (2.24).

The other types of magnetic drives shown in Fig. 6.1 have equations of the same type as (6.6) to represent their reactions.

For example, the force equations for the reed type are given as follows. The flux in maxwells due to the permanent magnet is given by

$$\Phi_1 = \frac{M}{R_1} \quad (6.11)$$

where M is the magnetomotive force in gilberts and R_1 is the reluctance of the permanent field magnetic circuit in oersteds. Superposed on this we have a sinusoidal flux due to the voice winding equal to

$$\Phi_2 = \frac{4\pi N i_0 \sin \omega t}{R_2} \quad (6.12)$$

where N is the number of turns of the coil, i_0 the maximum current in the coil in abamperes and R_2 the reluctance of the alternating magnetic circuit in oersteds. The force on the armature is

$$\begin{aligned} F &= \frac{(\Phi_1 + \Phi_2)^2}{8\pi\mathcal{A}} \\ &= \frac{1}{8\pi\mathcal{A}} \left[\frac{M^2}{R_1^2} + \frac{8\pi M N i_0 \sin \omega t}{R_1 R_2} + \frac{16\pi^2 N^2 i_0^2 \sin^2 \omega t}{R_2^2} \right] \end{aligned} \quad (6.13)$$

where \mathcal{A} is the effective area of the pole in square centimeters. Since

$$\sin^2 \omega t = \frac{1}{2}(1 - \cos 2\omega t) \quad (6.14)$$

the last term represents a constant force and a harmonic distorting term of twice the frequency of the impressed current. By making the constant flux Φ_1 large compared to the alternating flux this term can be made small. Neglecting all terms except the sinusoidal term we have

$$F = \frac{M N i}{R_1 R_2 \mathcal{A}} = \frac{\Phi_1 N i}{R_2 \mathcal{A}}. \quad (6.15)$$

To determine the back emf in abvolts generated in this structure we can consider that the principal part of the reluctance resides in the air gap so that

$$\Phi_1 = \frac{M \mathcal{A}}{g} \quad (6.16)$$

where x is the spacing between the armature and the pole in centimeters. If this spacing is varied with time the rate of change of flux with time is

$$\frac{d\Phi}{dt} = - \frac{MA \frac{dx}{dt}}{x^2} \doteq - \frac{MA\dot{x}}{a^2} \quad (6.17)$$

where a is the average air gap. The electromotive force in abvolts generated in the coil is

$$E = N \frac{d\Phi}{dt} = - \frac{NMA\dot{x}}{a^2} = - \frac{N\Phi_1\dot{x}}{a}. \quad (6.18)$$

Since we have assumed that the reluctance R_2 is equal to a/A , the complete expressions for the system are

$$\begin{aligned} E_A &= j\omega(L \times 10^9)i_A - \frac{N\Phi_1}{a} \dot{x} \\ F &= \frac{\dot{x}}{Z_M} + \frac{N\Phi_1}{a} i_A \end{aligned} \quad (6.19)$$

where E_A and i_A are the potentials and currents expressed in abvolts and abamperes. These equations are also representable by the network of Fig. 6.2, with the polarity of the transformer reversed—which does not affect the network design—and with the ratio φ equal to

$$\varphi = \frac{a}{N\Phi_1}. \quad (6.20)$$

The reciprocity relation of equations (2.23) and (2.24) can be used here to show that a more general relationship than (6.19) can be derived. Starting with the more general relationship

$$\frac{F - \frac{\dot{x}}{Z_M}}{i_A} = \frac{\Phi_1 N}{R_2 A} = - \left(\frac{E_A - j\omega L \times 10^9 i_A}{\dot{x}} \right) \quad (6.19)'$$

we can write the second half of (6.19)' by virtue of the reciprocity law.

The balanced type armature can be analyzed in a similar manner. The armature is located so that it is in equilibrium with the steady forces and the alternating current winding is wound around the armature. An analysis shows that the force and voltage are equal to twice the factors given in (6.15) and (6.18) so that the transformer ratio will be

$$\varphi = \frac{a_1}{2N\Phi_1} \quad (6.21)$$

When the armature is displaced by the current, means must be provided for returning the armature to the equilibrium position. Since an unbalance in the position of the armature tends to be increased by the magnetic field, the effect of this field is represented by a negative compliance which must be overcome by a positive compliance in the mechanical system. This is a decided advantage for it allows some of the mechanical compliance to be neutralized and allows a wider band of frequencies to be transmitted by the structure. This type of driving system is extensively used for loudspeakers, galvanometers and many other devices.

6.2. *Electrostatic Driving Systems*

Electrostatic driving systems, in which the force results from a repulsion of charges, are also used to some extent in electromechanical systems. The most prominent instrument of this type is the condenser transmitter.² A typical electrostatic system is shown in Fig. 6.3A. The force in dynes between the plates is

$$F = \frac{E^2 S}{8\pi x^2} \quad (6.22)$$

where E is the potential between the plates expressed in cgs electrostatic units, i.e., 1 (cgs) unit equals 300 volts, x the separation between the plates and S the effective area. If we have a polarizing voltage E_0 and an applied sinusoidal voltage $E = E \sin \omega t$, the force between the plates becomes

$$F = \frac{S}{8\pi x^2} \left[E_0^2 + 2EE_0 \sin \omega t + \frac{E^2}{2} (1 - \cos 2\omega t) \right] \quad (6.23)$$

² E. C. Wentz, Phys. Rev., Vol. XIX, p. 498, 1922.

The sinusoidal driving term will be the second term so that we can write

$$F = \frac{EE_0S}{4\pi x^2}. \quad (6.24)$$

In addition, we have a reaction to the force due to the mechanical impedance of the plate. For this case it is advantageous to

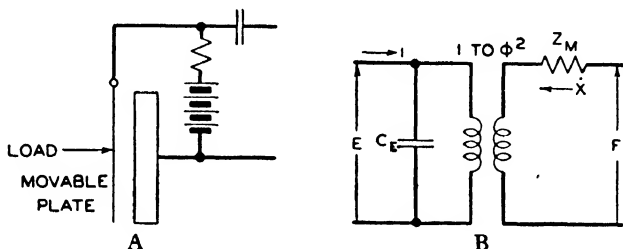


FIG. 6.3—ELECTROSTATIC DRIVING SYSTEM AND EQUIVALENT CIRCUIT.

define the mechanical impedance in the usual manner, namely, as the ratio of force to velocity. The complete equation for the force then becomes

$$F = \frac{SEE_0}{4\pi x^2} + \dot{x}Z_M \quad (6.25)$$

where Z_M is the mechanical impedance of the mechanical part of the system.

When the plate is moved a current is generated in the apparatus which can be calculated as follows. The charge on the condenser in cgs electrostatic units of charge—the coulomb is 3×10^9 electrostatic units of charge—is

$$Q = C_E E_0 \quad (6.26)$$

where C_E is the capacitance in electrostatic units which is equal to

$$C_E = \frac{S}{4\pi x}. \quad (6.27)$$

The current generated by the movement of the plate will be

$$i = \frac{dQ}{dt} = -\frac{E_0 S}{4\pi x^2} \frac{dx}{dt} = -\frac{E_0 S \dot{x}}{4\pi x^2}. \quad (6.28)$$

The complete equation for the current including the electrical circuit is

$$i = -\frac{E_0 S \dot{x}}{4\pi x^2} + \frac{E}{Z_E} \quad (6.29)$$

where Z_E in this case is the capacitive impedance $\frac{-j}{\omega C_E}$.

Equation (6.29) could also be obtained from (6.25) by using the reciprocity relationship given in equation (2.25). Equations (6.25) and (6.29) are the equations of the equivalent network shown in Fig. 6.3B where the transforming ratio φ is

$$\varphi = \frac{SE_0}{4\pi x^2} \quad (6.30)$$

By making this transformation ratio large, the mechanical impedance appearing on the electrical side can be made lower and more important than the shunting electrical impedance C_E . This circuit can be used in the design of electromechanical systems driven by electrostatic means.

6.3. Longitudinal Piezoelectric Driving Systems

The direct piezoelectric effect was discovered by the brothers Curie³ in 1880. They measured it first for quartz crystals. By putting a weight on an X - or Curie-cut crystal they found that a charge appeared on the surface the magnitude of which was proportional to the applied weight. The inverse piezoelectric effect was predicted in 1881 by Lippman⁴ on the basis of the principle of conservation of charge and was verified in the same year by the brothers Curie. In this effect a crystal expands when a voltage is applied to it.

The piezoelectric effects were applied practically by the Curies in measuring voltages and forces. For this purpose they

³ Développement par pression de l'électricité polaire dans les cristaux hemiedres a faces inclinées, Curie, J. and P., C. R. Acad. Su. Paris 91, 294 (1880).

⁴ Principe de la conservation de l'électricité, G. Lippman, Annales de Physique et de chimie, 5th Series, 1881, 24, 145.

constructed a bimorph-type crystal from two oppositely poled *X*-cut quartz crystals. The voltage was measured by observing the deflection of such a crystal with a microscope, while forces were measured by observing the amount of charge generated when the crystal was deformed by a force.

Outside of this use, which was rather minor, the piezoelectric effect remained a scientific curiosity until some time during the great war of 1914–1918. During the war Prof. Langevin in Paris was requested by the French government to devise some way for detecting submarines. After trying several devices he finally found that piezoelectric quartz plates could be used for this purpose. His device ⁵ consisted essentially of a mosaic of quartz glued between steel plates. This device has the property that when a voltage is applied, the crystal will expand and send out a longitudinal wave. Similarly, if a wave strikes it, it will set the quartz in vibration and generate a voltage which can be detected by vacuum tube devices. Langevin did not get his device perfected until after the war so that it was not used at that time to detect submarines. It has, however, been used extensively as a sonic depth finder. In this use a pulse is generated which is recorded directly on a moving recorder and is also sent out into the ocean. It strikes the bottom and is reflected back causing another mark to appear on the record. Knowing the difference in time and the velocity of sound in sea water, the distance to the bottom can be measured.

In 1917 A. M. Nicolson at Bell Telephone Laboratories was experimenting with Rochelle salt, another piezoelectric material having a much larger piezoelectric effect than quartz. He constructed and demonstrated ⁶ loudspeakers, microphones, and phonograph pick-ups, using Rochelle salt. He was also the first one to control an oscillator by means of a crystal—in this case Rochelle salt—and he has the primary crystal oscillator patent.⁷

⁵ Sound Transmitters for Underwater Signalling, P. Langevin, British Patent, No. 145, 691 (1921).

⁶ "The Piezo-Electric Effect in the Composite Rochelle Salt Crystal," A. M. Nicolson, Proc. Amer. Inst. Elec. Engrs., **38**, 1315 (1919).

⁷ U. S. Patent 2,212,845 filed April 10, 1918, issued August 27, 1940.

Following Langevin and Nicolson, Cady at Wesleyan University in 1922⁸ showed that quartz crystals could be used to control oscillators and that much more stable oscillators could be obtained in this fashion. These have been applied to controlling the frequency of broadcasting stations and radio transmitters in general. Quartz crystal oscillators, using some one of the low temperature coefficient quartz crystals,⁹ produce the most stable oscillators and the best time-keeping systems that can be obtained. A later use of crystals in producing very selective filters is discussed in Chapter VIII.

Piezoelectric crystals of materials, such as Rochelle salt and quartz, have been used rather extensively in such devices as loudspeakers, telephone receivers, phonograph pick-ups, supersonic generators, and many other devices. Several types of units are in general use. For low or voice frequencies, a combination of two oppositely poled units, called a bimorph, are usually used due to the fact that it is possible to get a larger displacement by using them. Two types are in general use: the twister type and the bender type. At the higher supersonic frequencies longitudinally vibrating crystals are usually employed, while at frequencies over 500 kilocycles longitudinal vibrations along the thinnest dimension of the crystal are usually employed.

The type of quartz crystal most often used as a transducer in longitudinal length and thickness vibrations is the so-called *X*- or Curie-cut crystal. This is cut out of the natural quartz crystal as shown in Fig. 6.4. The axis along the length of the natural crystal is called the *Z* or optic axis. An axis through two opposite prism edges is the *X* or electrical axis while the third axis which is perpendicular to two of the major faces is called the *Y* or mechanical axis. An *X*-cut crystal as shown by the figure is one in which the major surface of the crystal is perpendicular to the *X* axis. When an electric field is applied

⁸ "The Piezo-Electric Resonator," W. G. Cady, Proc. Inst. Radio Engrs. 19, 363 (1922).

⁹ A description of a number of low temperature coefficient quartz crystals is given in a paper "Low Temperature Coefficient Quartz Crystals," W. P. Mason, B.S.T.J., Vol. XIX, p. 74, January 1940.

to the major surfaces of the crystal through plated or contiguous electrodes, the crystal will expand along the Y or mechanical axis and contract along the X axis. The first type of deformation can be used to set up longitudinal vibrations along the Y axis. These have been used in driving bars and other mechanical systems in the frequency region from 50 kilocycles to several

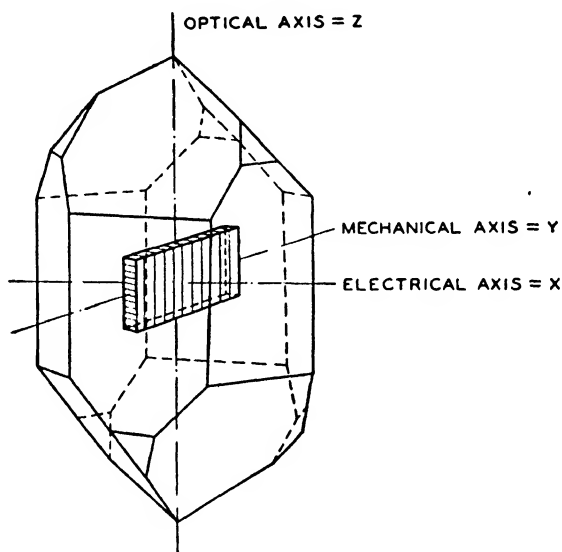


FIG. 6.4—NATURAL QUARTZ CRYSTAL AND X-CUT PLATE.

hundred kilocycles. The second type of deformation sets up a longitudinal vibration along the thickness dimension. Since this dimension can be made considerably smaller than any other dimension, frequencies in the region from 500 kilocycles to 80 megacycles have been obtained with crystals of this type. Such crystals are largely used in setting up supersonic vibrations in liquids and solids.

Rochelle salt is a double tartrate of potassium and sodium ($\text{NaKC}_4\text{H}_4\text{O}^6 \cdot 4\text{H}_2\text{O}$) and belongs to the ortho rhombic sphe-noidal class. The usual form of the crystal is the half crystal shown in Fig. 6.5A which shows the directions of the X , Y and Z axes. The cut usually used is the X -cut, from the bottom of the crystal in which the major faces are perpendicular to the

X axis. A potential applied to electrodes on the major faces causes the crystal to suffer a shearing deformation. As shown by Fig. 6.5B this causes one set of corners to extend outside the original square while the other set is inside the square. To

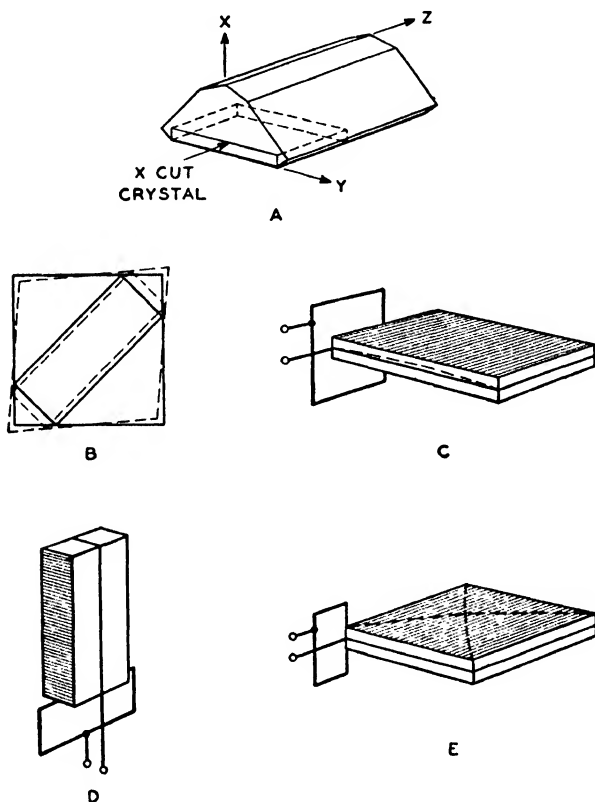


FIG. 6.5—LONGITUDINAL AND BIMORPH ROCHELLE SALT CRYSTALS.

obtain a longitudinal vibration one cuts a crystal at 45° from the Y and Z crystallographic axes as shown in Fig. 6.5B.

To get large deformations at low frequencies two opposing units called bimorph units are widely used. Of these there are three types. The bender type as shown by Fig. 6.5C is made by taking two longitudinal $45^\circ X$ units and orienting them so that the applied field causes one of the crystals to expand and the other to contract. The result is that the whole unit bends

in the manner of a bimetallic thermostat, and if one end is clamped considerable motion is produced on the other end. A twister bimorph is formed by taking two narrow pieces with the length along either the Y or Z axes as shown by Fig. 6.5D and orienting them so that a couple is produced which twists the crystal around its long axis. Such a twisting bimorph can be used to rotate the direction of a mirror and deflect a light beam. The third type of unit is the plate bimorph type in which X -cut plates are oriented so that the shearing strains in the two plates are opposite in sign. As shown by Fig. 6.5E, the resulting distortion is a saddle-shaped displacement. If three of the corners are clamped the fourth one will experience considerable motion and can be used to drive mechanical systems.

Crystals cut perpendicular to the Y axis are also used to some extent to produce longitudinal vibrations. A Y -cut plate will vibrate in shear as does an X -cut plate. By cutting crystals at 45° from the X and Z axes longitudinal vibrations can be obtained. Although the 45° Y -cut crystal does not have as large a motion as the 45° X -cut Rochelle salt crystal, its constants do not change much with temperature and for many purposes it is preferable.

The type of equivalent circuit which can be used to represent a piezoelectric coupling can be determined by solving the case of the longitudinally vibrating driver which is one of the most useful types of elements. To obtain the equations of motion we have to make use of the piezoelectric relations for a crystal. These were originally given by Voigt for a single longitudinal mode of motion in the form

$$\begin{aligned} -y_y &= Y_y/Y_0 + d_{12}E_x \\ -P_x &= \kappa E_x + d_{12}Y_y \end{aligned} \quad (6.31)$$

where Y_y is the longitudinal stress per unit area, E_x the potential gradient (potential divided by thickness), P_x the polarization of the crystal, i.e., the charge per unit area developed on the crystal by virtue of the internal motions of the charges in

the material itself, and y_v the longitudinal strain in the crystal along the Y axis, which is equal to

$$y_v = \frac{\partial \xi}{\partial y}$$

where ξ is the displacement of any point of the crystal along the Y axis. Y_0 is the value of Young's modulus along the length of the crystal, and κ_1 is the susceptibility of the crystal. This is related to the dielectric constant of the crystal by

$$K = 1 + 4\pi\kappa.$$

Experiments with Rochelle salt,¹⁰ however, have shown that this method of expressing the piezoelectric relationships is not advantageous for it results in elastic, dielectric, and piezoelectric constants which vary widely with temperature, plating conditions, and conditions of strain. On the other hand, if we express the piezoelectric relationships in terms of the charge, the elastic and piezoelectric constants are entirely normal and vary little with temperature, plating conditions, etc., while the dielectric constant has a temperature relation entirely consistent with the co-operative phenomena known to exist in the crystal. There are three possible charges which might be used in the piezoelectric relationship, the charge on the surface, the displacement, and the polarization. Of these the polarization which represents the charge due to the molecules of the crystal itself undoubtedly is the most theoretically correct quantity to use. Unfortunately, however, it leads to considerably more complicated relationships. Since the charge per unit area on the surface, or the displacement divided by 4π , is equal to

$$Q = \left(\frac{\text{Displacement}}{4\pi} \right) = \left(\frac{E_x}{4\pi} + P_x \right)$$

and since on account of the high dielectric constant of Rochelle salt the polarization accounts for 99 per cent of the total charge,

¹⁰ Phys. Rev. **55**, 775 (1939), W. P. Mason.

Phys. Rev. **57**, 829 (1940), H. Mueller.

Phys. Rev. **58**, 744 (1940), W. P. Mason.

we express the relationships in terms of Q . This gives results which agree with the polarization theory within the experimental error of measurement, and considerably simpler equations.¹¹ On this basis the piezoelectric relations are

$$\begin{aligned} -Y_y &= y_y Y_0 + DQ \\ E_x &= \frac{4\pi Q}{K} + Dy_y. \end{aligned} \quad (6.32)$$

The constant D varies with the type and orientation of the crystal. For a 45° X -cut Rochelle salt crystal, which is ordinarily used in electromechanical coupling elements, the values of the constants¹² are

$$Y_0 = 3.16 \times 10^{11}; \quad D = 9.70 \times 10^4 \quad (6.33)$$

while K the longitudinally clamped dielectric constant varies considerably with temperature. The measured values are shown in Fig. 6.6. These values are correct when the electrical units are cgs electrostatic units and the stresses are expressed in dynes per square centimeter.

For an X -cut quartz crystal¹³ which has been used extensively in supersonic work the constants are

$$Y_0 = 7.85 \times 10^{11}; \quad D = 14.3 \times 10^4; \quad K = 4.58, \quad k = 0.099. \quad (6.34)$$

Another crystal which has a larger electromechanical coupling than quartz and a dielectric constant which does not vary appreciably with temperature is a 45° Y -cut Rochelle salt crystal. Although it has a smaller piezoelectric effect than a 45° X -cut Rochelle salt crystal, its constants do not vary with temperature. For this crystal the constants are

$$Y_0 = 1.08 \times 10^{11}; \quad D = 11.2 \times 10^4; \quad K = 10.0, \quad k = 0.305. \quad (6.35)$$

¹¹ The derivation of equations (6.32) from the fundamental piezoelectric relations is discussed in Appendix C.

¹² The derivation of the constants for 45° X -cut and 45° Y -cut Rochelle salt crystals is given in Appendix C, pp. 325 and 326.

¹³ The derivation of the constants of X -cut quartz crystals is given in Appendix C, p. 328.

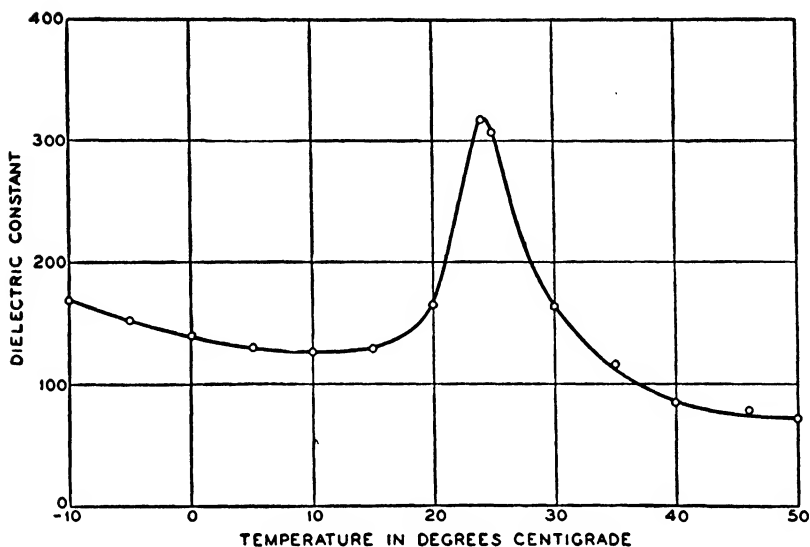


FIG. 6.6—LONGITUDINALLY CLAMPED DIELECTRIC CONSTANT OF 45° X-CUT ROCHELLE SALT CRYSTAL.

In addition to the piezoelectric equations (6.32) we have from Newton's laws of motion

$$\rho l_w l_t dy \frac{\partial^2 \xi}{\partial t^2} = (F_{y_0} - F_{(y_0+dy)}) = -l_w l_t \frac{\partial Y_y}{\partial y} dy \quad (6.36)$$

where F_{y_0} is the force on the section of width l_w and thickness l_t , in the y direction at $y = y_0$, and F_{y_0+dy} the force exerted on the section at $y = y_0 + dy$. Introducing (6.32) into (6.36) we have

$$\rho \frac{\partial^2 \xi}{\partial t^2} = Y_0 \frac{\partial y_y}{\partial y} + D \frac{\partial Q}{\partial y} = Y_0 \frac{\partial^2 \xi}{\partial y^2} + D \frac{\partial Q}{\partial y}. \quad (6.37)$$

Now if the crystal has an electrically conducting plating along its surface, there is no potential difference along it and consequently E_x is independent of y . Hence from the last of equations (6.32) and (6.37) we have

$$\rho \frac{\partial^2 \xi}{\partial t^2} = \frac{\partial^2 \xi}{\partial y^2} Y_0 \left[1 - \frac{D^2 K}{4\pi Y_0} \right] = \frac{\partial^2 \xi}{\partial y^2} Y_0 (1 - k^2) \quad (6.38)$$

where k the electromechanical coupling is defined by

$$k = D \sqrt{\frac{K}{4\pi Y_0}}. \quad (6.39)$$

Equation (6.38) shows that the effective value of the Young's modulus for a fully plated crystal is lower than the modulus Y_0 for a bare crystal by the factor $(1 - k^2)$.

The process of solving equation (6.38) is similar to that for an electric line discussed in Chapter II, so that we will give only the final results expressed in terms of the velocity $\frac{\partial \xi}{\partial t}$, the current $\frac{\partial Q}{\partial t}$, the force F , and potential E .

$$F + \frac{DKl_w E}{4\pi} = \left[F_1 + \frac{DKl_w E}{4\pi} \right] \cos \frac{\omega y}{v'} - j\xi_1 Z_0' \sin \frac{\omega y}{v'}$$

$$\xi = \xi_1 \cos \frac{\omega y}{v'} - j \frac{\left(F_1 + \frac{DKl_w E}{4\pi} \right)}{Z_0'} \sin \frac{\omega y}{v'} \quad (6.40)$$

where

$$Z_0' = l_w l_t \sqrt{\rho Y_0 (1 - k^2)}; \quad v' = \sqrt{\frac{(1 - k^2) Y_0}{\rho}}.$$

Integrating the last of equations (6.32) with respect to y , and expressing the result in terms of the current i and potential E we have

$$i = E \left(j\omega \frac{Kl_w l_y}{4\pi l_t} \right) - \frac{DKl_w}{4\pi} (\xi_2 - \xi_1) \quad (6.41)$$

where ξ_2 and ξ_1 are the velocities on the two ends of the crystal. $\frac{Kl_w l_y}{4\pi l_t}$ is the capacitance C_0 of the longitudinally clamped crystal expressed in cgs electrostatic units. Equations (6.40) and (6.41) can be used to determine the coupling under any terminating conditions.

An equivalent network which will have the same equations as (6.40) and (6.41) is shown in Fig. 6.7. This equivalent

circuit is valid for all frequency ranges, and emphasizes the fact that the crystal can drive from both ends. Usually, however, the crystal is either clamped on one end (clamped drive) or free

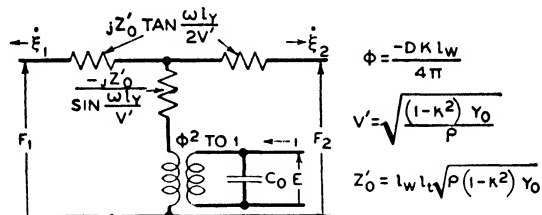


FIG. 6.7—ELECTROMECHANICAL EQUIVALENT CIRCUIT FOR PIEZOELECTRIC CRYSTAL.

on one end (inertia drive). The appropriate exact network can be obtained by open-circuiting the first end or short-circuiting it. Crystals of this type are usually used near their resonant frequencies to drive other electromechanical systems and for this case the generalized mechanical impedances can be somewhat

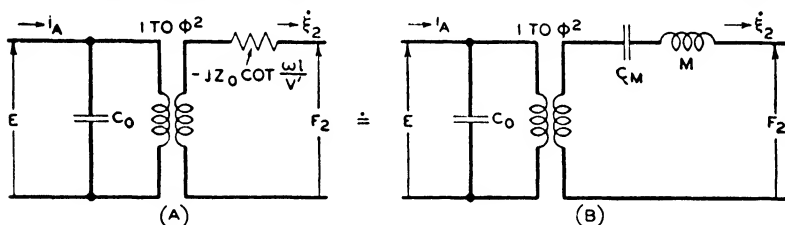


FIG. 6.8—ELECTROMECHANICAL EQUIVALENT CIRCUIT FOR CRYSTAL CLAMPED ON ONE END.

simplified. For example, for the clamped crystal, the resulting exact network is shown in Fig. 6.8A. The single impedance results from combining the two

$$\begin{aligned}
 -\frac{jZ_0'}{\sin \frac{\omega l_y}{v'}} + jZ_0' \tan \frac{\omega l_y}{2v'} &= -\frac{jZ_0'}{\sin \frac{\omega l_y}{v'}} \\
 + jZ_0' \frac{\left(1 - \cos \frac{\omega l_y}{v'}\right)}{\sin \frac{\omega l_y}{v'}} &= -jZ_0' \cot \frac{\omega l_y}{v'}. \quad (6.42)
 \end{aligned}$$

A plot of the negative cotangent function is shown in Fig. 6.9. As a driving element, the device is of use near the resonant frequency which occurs when $\frac{\omega l_y}{v'} = \pi/2$. A lumped mechanical

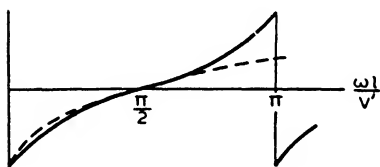


FIG. 6.9—APPROXIMATION OF COTANGENT FUNCTION BY IMPEDANCE OF A COIL AND CONDENSER.

circuit which has nearly the same impedance near the resonant frequency is a series coil and condenser which has the reactance shown by the dotted line. To make the zero of both impedances coincide the coil

must resonate the condenser at the frequency for which the cotangent function goes to zero. In order to make the slopes of the two functions coincide, we have

$$\begin{aligned} -jZ_0' \cot\left(\frac{\omega l_y}{v'}\right) &= -jZ_0' \cot\left(\frac{(\omega_R + \Delta\omega)l_y}{v'}\right) \\ &= -jZ_0' \cot\left[\frac{\pi}{2}\left(1 + \frac{\Delta\omega}{\omega_R}\right)\right] \doteq jZ_0' \left(\frac{\pi}{2} \frac{\Delta\omega}{\omega_R}\right) \quad (6.43) \end{aligned}$$

where ω_R is the resonant frequency. Similarly, the impedance of the coil and condenser near resonance is

$$Z = \frac{j^2 \Delta\omega}{\omega_R^2 C_M} \quad (6.44)$$

Equating these two we find

$$C_M = \frac{4}{\pi \omega_R Z_0'} = \frac{8l_y}{\pi^2 v' Z_0'} = \frac{8l_y}{\pi^2 l_w l_t Y_0 (1 - k^2)} \quad (6.45)$$

upon inserting the values of Z_0' and v' and noting that $\omega_R l_y / v' = \pi/2$. This is equal to $\frac{8}{\pi^2}$ times the static compliance of the plated crystal. The mass required to resonate is

$$M = \frac{1}{\omega_R^2 C_M} = \frac{Z_0' l_y}{2v'} = \frac{l_w l_t l_y \rho}{2} \quad (6.46)$$

or equal to half the static mass of the crystal. This representation is shown in Fig. 6.8B. Comparing this with Fig. 6.3B we

see that a piezoelectric drive can be represented by the same type of network as an electrostatic drive except that the transformer ratio is fixed by the constants of the crystal and cannot

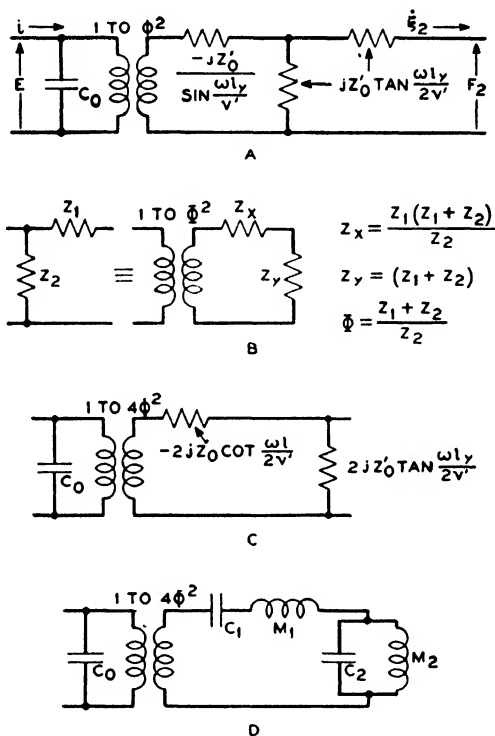


FIG. 6.10—EQUIVALENT CIRCUIT FOR A CRYSTAL FREE ON ONE END AND DRIVING A LOAD ON THE OTHER (INERTIA DRIVE).

be varied. In order to get as high a ratio with an electrostatic drive, however, the static voltage E_0 would have to be prohibitively high.

The other case of interest, the inertia drive, can be worked out in a similar fashion. This is obtained from Fig. 6.7 by setting the force F_1 equal to zero since the crystal exerts no force on its free end. This is equivalent to short-circuiting the first branch. The resulting network is shown in Fig. 6.10A. One of these impedances can be eliminated by employing the relation

shown in Fig. 6.10B, due originally to E. L. Norton,¹⁴ which relates a perfect transformer and L network to the reversed L network form. Applying this equivalence to 6.10A,

$$\Phi = 2; \quad Z_x = 2jZ_0' \tan \frac{\omega l_y}{2v'}; \quad Z_y = 2jZ_0' \tan \frac{\omega l_y}{2v'}. \quad (6.47)$$

It is better to incorporate all the transforming action in one place which can be done by taking the impedance $-jZ_0'/\sin \frac{\omega l_y}{v'}$ through the transformer of impedance ratio 4 to 1. We then have two series impedances which can be combined into a single impedance

$$\begin{aligned} & \frac{-j4Z_0'}{\sin \frac{\omega l_y}{v'}} + 2jZ_0' \tan \frac{\omega l_y}{2v'} \\ &= -jZ_0' \left(\frac{4}{\sin \frac{\omega l_y}{v'}} - \frac{2 \left(1 - \cos \frac{\omega l_y}{v'} \right)}{\sin \frac{\omega l_y}{v'}} \right) = -j2Z_0' \cot \frac{\omega l_y}{2v'}. \end{aligned} \quad (6.48)$$

The resulting exact network is shown in Fig. 6.10C.

Near the resonant frequency of the crystal which occurs when

$$\frac{\omega_R l_y}{2v'} = \frac{\pi}{2} \quad \text{or} \quad f_R = \frac{v'}{2l_y} \quad (6.49)$$

the distributed impedances can be replaced by the lumped constants shown in Fig. 6.10D. The series resonant circuit is derived by expanding

$$\begin{aligned} -2jZ_0' \cot \frac{\omega l_y}{2v'} &= -j2Z_0' \cot \frac{(\omega_R + \Delta\omega)l_y}{2v'} \\ &= -2jZ_0' \cot \left(\frac{\pi}{2} \left(1 + \frac{\Delta\omega}{\omega_R} \right) \right) \doteq -2jZ_0' \left(\frac{\pi}{2} \frac{\Delta\omega}{\omega_R} \right). \end{aligned} \quad (6.50)$$

¹⁴ See U. S. Patent 1,681,554, August 21, 1928; also "Transmission Networks and Wave Filters," T. E. Shea, p. 320, D. Van Nostrand.

Comparing this with the impedance of a series resonant circuit given by (6.44) we have

$$C_1 = \frac{2}{\pi Z_0' \omega_R} = \frac{2l_y}{\pi^2 Z_0' v'} = \frac{2l_y}{\pi^2 l_w l_t Y_0 (1 - k^2)} = \frac{C_M}{4}; \quad (6.51)$$

$$M_1 = \frac{1}{\omega_R^2 C_1} = \frac{\rho l_w l_y l_t}{2} = M$$

where C_M and M have the same values as in (6.45) and (6.46).

The shunt lumped constants can be derived by expanding

$$j2Z_0' \tan \frac{\omega l_y}{2v'} = j2Z_0' \tan \frac{(\omega_A + \Delta\omega)l_y}{2v'}$$

$$= j2Z_0' \tan \left(\frac{\pi}{2} \left(1 + \frac{\Delta\omega}{\omega_A} \right) \right) = -j \frac{4}{\pi} \frac{Z_0' \omega_A}{\Delta\omega}. \quad (6.52)$$

This will be an infinite reactance when $\Delta\omega$ is zero, a positive reactance when $\omega < \omega_R$ and a negative reactance when $\omega > \omega_R$. It will therefore have the same type of reactance as a parallel coil and condenser. From equation (2.138), near anti-resonance this will be

$$Z = -\frac{j\omega_A^2 L}{2\Delta\omega}.$$

Hence, comparing the two equations, the network representing the shunt branch is

$$L_2 = \frac{8}{\pi} \frac{Z_0'}{\omega_A} = \frac{8}{\pi^2} l_w l_t l_y \rho = \frac{16}{\pi^2} M; \quad C_2 = \frac{1}{\omega_A^2 L_2} = \frac{\pi^2}{64} C_M \quad (6.53)$$

where M and C_M have the same values as in equations (6.45) and (6.46).

6.4. *Bimorph Piezoelectric Crystals*

The bender and twister bimorph types of units shown in Fig. 6.5 can be represented by the same types of circuits, as Figs. 6.8 and 6.10 for the clamped and inertia drives, with somewhat different constants.

The constants of a bender type crystal are easily calculated from the piezoelectric relationships (6.32) and the equations for a bar in flexure given in section 3.3. Let us consider two piezoelectric crystals with a central plate glued to both crystals and with the crystals bent as shown in Fig. 6.11. The two outside electrodes are connected together and the crystals are cut so that one expands under the applied field and the other

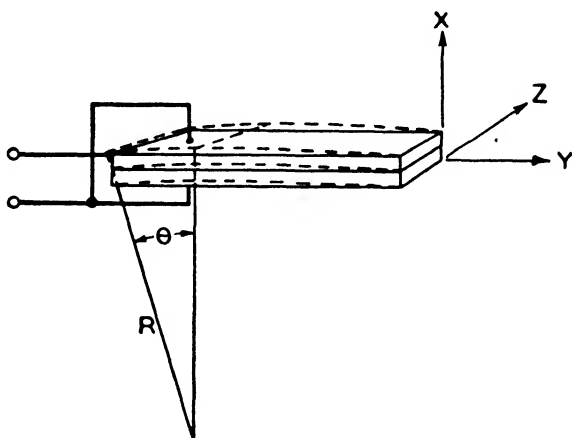


FIG. 6.11—FLEXURE BIMORPH CRYSTAL UNIT.

one contracts. In obtaining the relationship it is assumed that the adherence of the glue is great enough to prevent the two crystals from slipping over each other. The piezoelectric relationships holding for every filament through the crystal are

$$-Y_v = y_v Y_0 + DQ; \quad E_x = \frac{4\pi Q}{K} + Dy_v. \quad (6.54)$$

This follows since the charge Q is equal to the displacement charge which is

$$Q = \frac{E_x}{4\pi} + P_x \quad (6.55)$$

where P_x is the polarization of the filament. This is constant throughout the thickness of the crystal and hence (6.54) holds for a filament of the crystal section.

In order to obtain the equations for a flexure mode we have to obtain the moment and force for the bimorph crystal. As shown in Fig. 6.11 we can consider a unit length of the crystal at the center line bent into the form of a circle. If the radius of curvature of the crystal is R , the angle θ subtended by the unit length is

$$\theta = \frac{1}{R}. \quad (6.56)$$

Now above the central line the crystal expands while below the central line it contracts. The expansion at any point x , positive values being measured from the center line and away from the center of curvature, will be

$$dy = \frac{x}{R} = y_v \text{ since } \frac{dy}{l} = \frac{dy}{1} = y_v. \quad (6.57)$$

This takes care of the filaments nearer the center of curvature since x will be negative and dy also negative indicating a compression. To obtain the moment of the crystal we take the integral

$$\begin{aligned} M &= -l_w \int_{-\frac{l_t}{2}}^{+\frac{l_t}{2}} Y_v x dx = \frac{Y_0 l_w}{R} \int_{-\frac{l_t}{2}}^{+\frac{l_t}{2}} x^2 dx + DQ l_w \int_{-\frac{l_t}{2}}^{+\frac{l_t}{2}} x dx \\ &= \frac{Y_0}{R} (l_w) \frac{l_t^2}{12} + DQ \frac{l_w l_t^2}{4}. \end{aligned} \quad (6.58)$$

$(l_w) l_t^2 / 12$ is the moment of inertia of the section, so that

$$M = \frac{Y_0 I}{R} + \frac{DQ S l_t}{4} \quad (6.59)$$

where S is the cross-sectional area $l_l l_w$. The second equation of (6.54) when integrated with respect to x from 0 to $l_t/2$ yields

$$E_x \frac{l_t}{2} = \frac{4\pi Q l_t}{2K} + \frac{D l_t^2}{8R} \quad \text{or} \quad E_x = \frac{4\pi Q}{K} + \frac{D l_t}{4R}. \quad (6.60)$$

In obtaining both of these equations we make use of the fact that the sign of D changes in going from one crystal to the other of the bimorph unit.

Now for small bending the inverse of the radius of curvature is the second derivative of the displacement x by the length y or

$$\frac{1}{R} = \frac{\partial^2 x}{\partial y^2}. \quad (6.61)$$

Introducing this value, the two piezoelectric relations for a flexure bimorph crystal become

$$M = Y_0 I \frac{\partial^2 x}{\partial y^2} + \frac{D l_t S Q}{4}; \quad E_x = \frac{4\pi Q}{K} + \frac{D l_t}{4} \frac{\partial^2 x}{\partial y^2}. \quad (6.62)$$

Solving for Q from the last of these and eliminating Q from the first we have

$$\begin{aligned} M &= \frac{\partial^2 x}{\partial y^2} I Y_0 \left(1 - \frac{3}{4} \frac{D^2 K}{4\pi Y_0} \right) + \frac{D l_t S K}{16\pi} E_x \\ &= \frac{\partial^2 x}{\partial y^2} I Y_0 \left(1 - \frac{3}{4} k^2 \right) + \frac{D S K E}{8\pi} \end{aligned} \quad (6.63)$$

since $E_x \frac{l_t}{2}$ is the potential E across the crystals. We see that the square of the effective coupling for a flexure crystal is $\frac{3}{4}$ of that for a longitudinally vibrating crystal. This results in a smaller variation of frequency with temperature than for a longitudinal crystal.

The potential E does not vary with the length y of a plated crystal and hence $\frac{\partial E}{\partial y} = 0$. Differentiating (6.63) with respect to y we have

$$\frac{\partial M}{\partial y} = F = \frac{\partial^3 x}{\partial y^3} I Y_0 \left(1 - \frac{3}{4} k^2 \right) \quad (6.64)$$

where F is the lateral force.

Introducing this expression for F in (3.9) the equation of motion becomes

$$\kappa^2 Y_0 \left(1 - \frac{3}{4} k^2 \right) \frac{\partial^4 x}{\partial y^4} = -\rho \frac{\partial^2 x}{\partial t^2} \quad \text{or} \quad \frac{d^4 x}{dy^4} = n^4 y \quad (6.65)$$

where

$$n^4 = \frac{\omega^2 \rho}{\kappa^2 Y_0 (1 - \frac{3}{4} k^2)}$$

for simple harmonic motion, where κ is the radius of gyration $l_t/\sqrt{12}$ for the section. The case of interest is the case where one end is clamped and the other end used to drive a mechanical system. The method of solving the equation is the same as that given in section (3.3) while the four conditions for determining the constants are

$$x = 0 \quad \text{and} \quad \frac{dx}{dy} = 0 \quad \text{when} \quad y = 0 \quad (6.66)$$

and at the moving end the conditions are that the external moment is zero and the external force is given by (6.64). These result in the conditions

$$\begin{aligned} \left. \frac{d^2 x}{dy^2} \right|_{y=l} &= - \frac{3DKE}{2\pi l_t^2 Y_0 (1 - \frac{3}{4}k^2)}; \\ F &= \frac{Y_0 S l_t^2}{12} \left(1 - \frac{3}{4}k^2 \right) \left. \frac{d^3 x}{dy^3} \right|_{y=l}. \end{aligned} \quad (6.67)$$

Using these conditions to determine the constants A, B, C, D of the solution of the form given in (3.12) we have the four constants

$$\begin{aligned} -C = A &= \frac{-F}{S\omega\sqrt{\omega\rho\kappa}\sqrt{Y_0\rho(1-\frac{3}{4}k^2)}} \left(\frac{\sinh nl + \sin nl}{2(1 + \cosh nl \cos nl)} \right) \\ &\quad - \frac{\sqrt{3}DKE}{4\pi\omega l_t \sqrt{\rho Y_0(1-\frac{3}{4}k^2)}} \left(\frac{\cosh nl + \cos nl}{2(1 + \cosh nl \cos nl)} \right) \\ -D = B &= \frac{F}{S\omega\sqrt{\omega\rho\kappa}\sqrt{Y_0\rho(1-\frac{3}{4}k^2)}} \left(\frac{\cosh nl + \cos nl}{2(1 + \cosh nl \cos nl)} \right) \\ &\quad + \frac{\sqrt{3}DKE}{4\pi\omega l_t \sqrt{\rho Y_0(1-\frac{3}{4}k^2)}} \left(\frac{\sinh nl - \sin nl}{2(1 + \cosh nl \cos nl)} \right). \end{aligned} \quad (6.68)$$

Inserting these values we have for the velocity on the end of the unit

$$\begin{aligned} \dot{x} &= \frac{-jF}{S\omega\sqrt{\omega\rho\kappa}\sqrt{Y_0\rho(1-\frac{3}{4}k^2)}} \left(\frac{\cosh nl \sin nl - \sinh nl \cos nl}{1 + \cosh nl \cos nl} \right) \\ &\quad - \frac{j\sqrt{3}DKE}{4\pi l_t \sqrt{\rho Y_0(1-\frac{3}{4}k^2)}} \left(\frac{\sinh nl \sin nl}{1 + \cosh nl \cos nl} \right). \end{aligned} \quad (6.69)$$

For low frequencies the displacement takes the simple form

$$x = -\frac{4Fl^3}{l_w l_t^3 Y_0 (1 - \frac{3}{4}k^2)} - \left(\frac{DKE}{4\pi}\right) \frac{3l^2}{l_t^2} \times \frac{1}{Y_0 (1 - \frac{3}{4}k^2)}. \quad (6.70)$$

For a longitudinal mode we find from (6.32) that the displacement of a crystal of length l , width l_w , and thickness l_t , will be

$$x = -\frac{Fl}{l_w l_t Y_0 (1 - k^2)} - \left(\frac{DKE}{4\pi}\right) \frac{l}{l_t Y_0 (1 - k^2)}. \quad (6.71)$$

Hence, by constructing a bimorph unit of two longitudinal crystals having a total thickness of l_t , the displacement for no external force is increased in the ratio $3l/l_t$. This is accomplished, however, at the expense of the force that can be applied by the unit. For no displacement the relative forces applied by the bimorph flexure and the longitudinal crystal are $(\frac{3}{4}l_t/l)$. A considerable lowering of the natural frequency of response also occurs.

To obtain the complete representation for a flexure crystal we need one more equation relating the current to the applied voltage and displacement. This can be obtained by integrating the last of equations (6.62) with respect to y when we have inserted the value of d^2x/dy^2 obtained from the constants of equation (6.68). Performing this integration we find

$$\begin{aligned} \frac{E_x l_t}{2} l_w = \frac{4\pi l_t}{2K} Q_0 - \left[\frac{\sqrt{3}DF}{4\omega \sqrt{\rho Y_0 (1 - \frac{3}{4}k^2)}} \left(\frac{\sinh nl \sin nl}{1 + \cosh nl \cos nl} \right) \right. \\ \left. + \frac{3}{4} \left(\frac{D^2 K}{4\pi Y_0} \right) \left(\frac{l_w l E [\sinh nl \cos nl + \cosh nl \sin nl]}{(1 - \frac{3}{4}k^2) nl (1 + \cosh nl \cos nl)} \right) \right]. \end{aligned} \quad (6.72)$$

Here Q_0 is the charge on one of the bimorphs which is half the total charge. Also $\frac{E_x l_t}{2}$ is the potential applied across either plate. Introducing the current i which is $2j\omega Q_0$, this expression can be written

$$E \left(1 + \frac{\frac{3}{4}k^2}{1 - \frac{3}{4}k^2} \right) \left(\frac{(\sinh nl \cos nl + \cosh nl \sin nl)}{nl(1 + \cosh nl \cos nl)} \right) \\ = \frac{-ji}{\omega C_0} - \frac{\sqrt{3}DF}{4\omega l_l \sqrt{\rho Y_0(1 - \frac{3}{4}k^2)}} \left(\frac{\sinh nl \sin nl}{1 + \cosh nl \cos nl} \right) \quad (6.73)$$

since $\frac{4Kl_w l}{4\pi l_t} = C_0$ is the total static capacitance of the crystal.

Equations (6.69) and (6.73) can be represented up to the first resonance by the network of Fig. 6.8 provided

$$C_0 = \frac{Kl_w l}{\pi l_t}; \quad \varphi = \frac{3}{4} \left(\frac{DK}{4\pi} \right) \frac{l_l l_w}{l}; \quad C_M = \frac{4l^3}{l_t^3 l_w Y_0 (1 - \frac{3}{4}k^2)}; \\ M = \frac{\rho l l_l l_w}{4} \quad (6.74)$$

are expressed in cgs electrostatic units.

The constants of the twister type are not easily calculated on account of the complexity of the motion but can be evaluated from static measurements of the force and displacement of the driving point of the crystal as a function of the applied voltage.

6.5. Magnetostrictive Driving System

Another type of magnetic driving system which has been used quite extensively at ultrasonic frequencies is the magnetostrictive driving system. In a magnetostrictive material a change in length occurs when a rod or tube of the material is brought into a magnetic field parallel to the length.

The magnetostrictive effect was discovered by Joule¹⁵ in 1847 but did not receive much practical application until the present century. Probably the most extensive use of magnetostrictive material has been made by Pierce^{16, 17} and his

¹⁵ "On the Effects of Magnetism upon the Dimensions of Iron and Steel Bars," J. P. Joule, Phil. Mag. (III), 30, 76 (1847).

¹⁶ "Magnetostriction Oscillators, An Application of Magnetostriction to the Control of Frequency of Audio and Radio Electric Oscillations, To the Production of Sound, and To the Measurement of the Elastic Constants of Metals," G. W. Pierce, Proc. Amer. Acad. of Arts and Sciences 63, 1 (1928).

¹⁷ "Magnetostriction Oscillators," Proc. Inst. Radio Engrs. 17, 42 (1929).

students^{18, 19} who have investigated the use of magnetostrictive bars in the control of oscillators and time standards, the production of supersonic vibrations in gases, liquids, and solids, and in narrow band filters for use in sound analyzers.

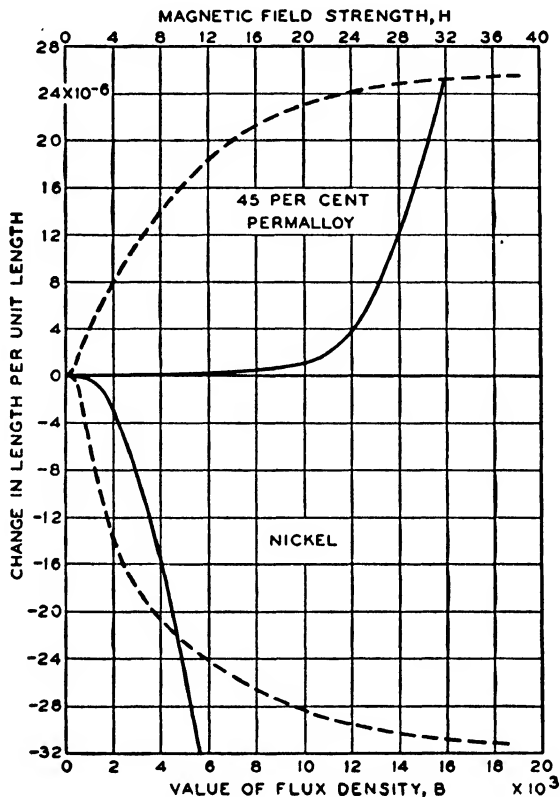


FIG. 6.12—MAGNETOSTRICTIVE EFFECT IN NICKEL AND 45 PER CENT PERMALLOY.

The principal magnetostrictive materials that have been used in producing sound waves are nickel, nickel iron alloys, alloys of chromium, nickel, and iron such as commercial nichrome, monel metal—an alloy of nickel and copper with small percentages of iron, silicon, manganese and carbon,—

¹⁸ "A Dynamic Study of Magnetostriction," K. C. Black, Proc. Amer. Acad. 63, 49 (1928).

¹⁹ H. H. Hall, Proc. Inst. Radio Engrs. 21, 1328 (1933).

and alloys of cobalt and iron. Of these materials nickel and 45 per cent permalloy (45 per cent nickel, 55 per cent iron) have been most extensively used. The full lines of Fig. 6.12 show measurements of the change in length divided by length as a function of the magnetic flux density B in gauss for nickel and 45 per cent permalloy.²⁰ Nickel has a decrease in length while 45 per cent permalloy has a large increase in length. It will be noted that for small flux densities the change in length is nearly proportional to the square of the flux density. The dotted lines of the figure show the strain plotted as a function of field

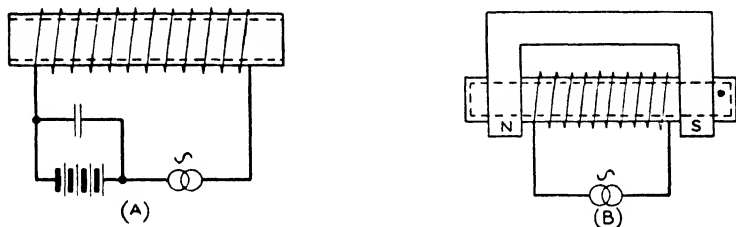


FIG. 6.13—MAGNETOSTRICTIVE BARS.

strength H . On this basis the relative change in length for the two materials is not much different on account of the much larger permeability of the permalloy.

If a nickel rod is brought into an alternating magnetic field it is shortened periodically by magnetization. Since the shortening is independent of the direction of the field it is easy to see that a frequency of twice the applied electric field will be obtained. In order to make the vibration follow the applied electric field it is necessary to put on a polarizing field either by using a superposed constant current as shown in Fig. 6.13A or by using a permanent magnet as shown in Fig. 6.13B.

The change in length will be small unless the frequency of the applied current approaches the natural resonant frequency of the bar, in which case the amplitude of the ends of the bar may be $10^{-4}l$ where l is the length of the bar. The highest frequencies obtainable with a fundamental bar with some degree of

²⁰ "Magnetostriction in Permalloy," L. W. McKeehan and P. P. Cioffi, Phys. Rev., Vol. 28, No. 1, p. 146, July 1926.

power are in the order of 60 kilocycles. Frequencies below this are readily obtained down to 5 or 10 kilocycles.

~~If a solid piece of material is used there will be considerable electrical loss due to eddy currents set up in the material.~~ To get around this difficulty magnetostrictive vibrators are usually constructed in the form of thin tubes or finely laminated wires glued together to form a solid piece.

Such a magnetostrictive bar can be set in oscillation by placing two coils of wire around the bar in close proximity but not touching the bar and connecting the two coils in the plate and grid of an oscillator tube. The bar may also be driven directly by an oscillating current through the two driving coils. In order to avoid mechanical dissipation the bar is usually clamped between knife edges at its center which is a node of the motion.

The equations of motion for such a bar can be obtained by using the magnetostrictive relation between the change of length and the flux density shown experimentally by Fig. 6.12. For small flux densities the change in length is approximately proportional to the square of the flux density or

$$\frac{dl}{l} = aB^2 \quad (6.75)$$

although (aB) is usually taken as the magnetostrictive constant λ . The stress-strain equation for a well-laminated magnetostrictive rod becomes

$$-Y_v = Y_0 \left[\frac{\partial \xi}{\partial y} - aB^2 \right] \quad \text{or} \quad -F = Y_0 S \left[\frac{\partial \xi}{\partial y} - aB^2 \right] \quad (6.76)$$

where S is the cross-sectional area of the rod.

A magnetostrictive element, as shown in Fig. 6.13, has a permanent magnetic field Φ_0 , due to a steady applied voltage or to a permanent magnet with an alternating flux superposed. The total flux generated by a current, expressed in abamperes through the coil, will be

$$\Phi = BS = \frac{4\pi Ni}{R} + \Phi_0 \quad (6.77)$$

where R is the reluctance for the complete magnetic path. Inserting this in (6.76) and separating out the alternating portion of the total flux we have

$$\begin{aligned} -F &= Y_0 S \frac{\partial \xi}{\partial y} - Y_0 \left(\frac{a \Phi_0}{S} \right) \frac{8\pi N i_A}{R} = Y_0 S \frac{\partial \xi}{\partial y} - \left(Y_0 \lambda \frac{8\pi N}{R} \right) i_A \\ &= Y_0 S \frac{\partial \xi}{\partial y} - D i_A \end{aligned} \quad (6.78)$$

since $\frac{a \Phi_0}{S} = a B_0 = \lambda$ for the average value of B_0 for the element. If there is no leakage flux along the rod we have $\frac{\partial B}{\partial y} = 0$, and consequently

$$-\frac{\partial F}{\partial y} = Y_0 S \frac{\partial^2 \xi}{\partial y^2}. \quad (6.79)$$

Combining this with the Newtonian equation

$$\rho S \frac{\partial^2 \xi}{\partial t^2} dy = -\frac{\partial F}{\partial y} dy \quad (6.80)$$

we have

$$\frac{\partial^2 \xi}{\partial t^2} = v^2 \frac{\partial^2 \xi}{\partial y^2} \text{ where } v = \sqrt{\frac{Y_0}{\rho}}. \quad (6.81)$$

The solution of this with the constants determined in terms of the initial displacements and strains is

$$\xi = \xi_1 \cos \frac{\omega l_y}{v} + \left(\frac{\partial \xi}{\partial y} \right)_1 \frac{v}{\omega} \sin \frac{\omega}{v} l_y. \quad (6.82)$$

Introducing the value of $\frac{\partial \xi}{\partial y}$ from (6.78) and expressing in terms of the velocities, we have two equations

$$\xi = \xi_1 \cos \frac{\omega l_y}{v} - j \frac{[F_1 - D i_A]}{S \sqrt{\rho Y_0}} \sin \frac{\omega l_y}{v} \quad (6.83)$$

$$(F - D i_A) = (F_1 - D i_A) \cos \frac{\omega l_y}{v} - j \xi_1 S \sqrt{\rho Y_0} \sin \frac{\omega l_y}{v}.$$

These equations give all the mechanical constants in terms of the applied current i_A , i.e., the direct relation. In order to obtain the complete representation we have to obtain the inverse equation which relates the voltage generated in the coil to the strain in the bar. This is difficult to do since it requires relating the change in the steady flux to the strain. By employing the reciprocity theorem of Chapter II, however, this relation for the complete bar can be obtained.

Since we are dealing with expressions for both ends of the bar we need an extended form of the reciprocity theorem to cover this case. We consider a case in which there may be a large number of meshes in the network but we wish to investigate the reciprocity relationships existing between the currents and voltages in three of the meshes. Since the equations given above do not consider any terminating conditions, we can write equations (2.12) and (2.13) for the three meshes of interest in the form

$$\begin{aligned} i_1 &= \frac{E_1\Delta_{11} + E_2\Delta_{12} + E_3\Delta_{13}}{\Delta} \\ i_2 &= \frac{E_1\Delta_{12} + E_2\Delta_{22} + E_3\Delta_{23}}{\Delta} \\ i_3 &= \frac{E_1\Delta_{13} + E_2\Delta_{23} + E_3\Delta_{33}}{\Delta} \end{aligned} \quad (6.84)$$

Now due to the symmetry existing between the electrical input and the force and velocity conditions at the two ends of the bar we can simplify the above by letting

$$\Delta_{12} = \Delta_{13}; \quad \Delta_{22} = \Delta_{33}. \quad (6.85)$$

Then equations (6.84) reduce to

$$\begin{aligned} i_1 &= \frac{E_1\Delta_{11} + (E_2 + E_3)\Delta_{12}}{\Delta} \\ \Delta i_2 &= E_1\Delta_{12} + E_2\Delta_{22} + E_3\Delta_{23} \\ \Delta i_3 &= E_1\Delta_{12} + E_2\Delta_{23} + E_3\Delta_{22} \end{aligned} \quad (6.86)$$

The first of these can be written

$$\frac{E_1 - i_1 \frac{\Delta}{\Delta_{11}}}{E_2 + E_3} = - \frac{\Delta_{12}}{\Delta_{11}} \quad (6.87)$$

which is one of the relations sought. The other relation can be obtained by adding the last two equations of (6.86) and eliminating E_1 by the first equation. There results

$$\begin{aligned} \frac{(i_2 + i_3) - (E_2 + E_3) \left[\frac{(\Delta_{22} + \Delta_{23})\Delta_{11} - 2\Delta_{12}^2}{\Delta\Delta_{11}} \right]}{2i_1} \\ = \frac{\Delta_{12}}{\Delta_{11}} = - \left(\frac{E_1 - i_1 \frac{\Delta}{\Delta_{11}}}{E_2 + E_3} \right) \end{aligned} \quad (6.88)$$

which is the reciprocity relation sought.

To apply this to the magnetostrictive rod case we have to solve equations (6.83) so that ξ_1 is expressed in terms of ξ and $(F - Di_A)$. This can be done by multiplying the first equation by $\cos \frac{\omega l_y}{v}$, the second by $j \sin \frac{\omega l_y}{v} / S \sqrt{\rho Y_0}$ and adding. The resulting equation is

$$\xi_1 = \xi \cos \frac{\omega l_y}{v} + j \frac{(F - Di_A)}{S \sqrt{\rho Y_0}} \sin \frac{\omega l_y}{v}. \quad (6.89)$$

Subtracting (6.89) from the first equation of (6.83) and transposing we have

$$\frac{(F_1 + F_2) - j(\xi_2 - \xi_1)S \sqrt{\rho Y_0} \cot \frac{\omega l_y}{2v}}{2i_A} = D. \quad (6.90)$$

Associating the forces with the currents i_2 and i_3 and the velocities ξ_1 with E_2 and ξ_2 with $-E_3$, equation (6.90) has the same form as the first equality of (6.88). From (6.88) then follows the relation

$$E_1 - i_A(R + j\omega L) = D(\xi_2 - \xi_1). \quad (6.91)$$

The expression $\Delta/\Delta_{11} = Z_{sc1}$, the short-circuited impedance looking into the electrical side of the network. If ξ_1 and ξ_2 are set equal to zero so the bar cannot move at its first resonant frequency, the short-circuited impedance will be the coil resistance and reactance. Hence, by employing the reciprocity theorem the question of how the steady flux varies with strain is

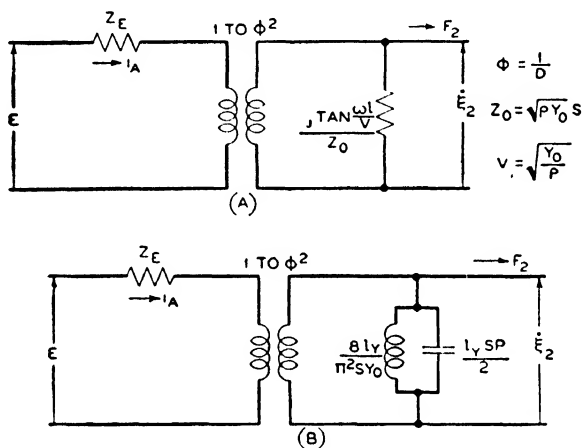


FIG. 6.14—EQUIVALENT ELECTROMECHANICAL CIRCUIT FOR A MAGNETOSTRICTIVE BAR CLAMPED ON ONE END.

answered. Equations (6.83) and (6.90) give the equations of a magnetostrictive bar for any terminating conditions.

If the first end is clamped and the other end used to drive a load the equations are obtained by setting $\xi_1 = 0$ in (6.83) and (6.91) from which we obtain

$$\xi_2 = \frac{j[D i_A - F_2] \tan \frac{\omega l_Y}{v}}{Z_0} \quad (6.92)$$

$$E - D \xi_2 = i_A [R + j\omega L].$$

In obtaining the equivalent network it is advantageous to associate the velocity with voltage, and force with current as in the electromagnetic coupling. For this case the exact electromechanical representation is shown in Fig. 6.14A. The net-

work approximation holding near the resonant frequency is shown in Fig. 6.14B. In this representation the inductance is $8/\pi^2$ times the static compliance of the rod, while the shunt capacitance is half the static mass of the rod. In case one end is

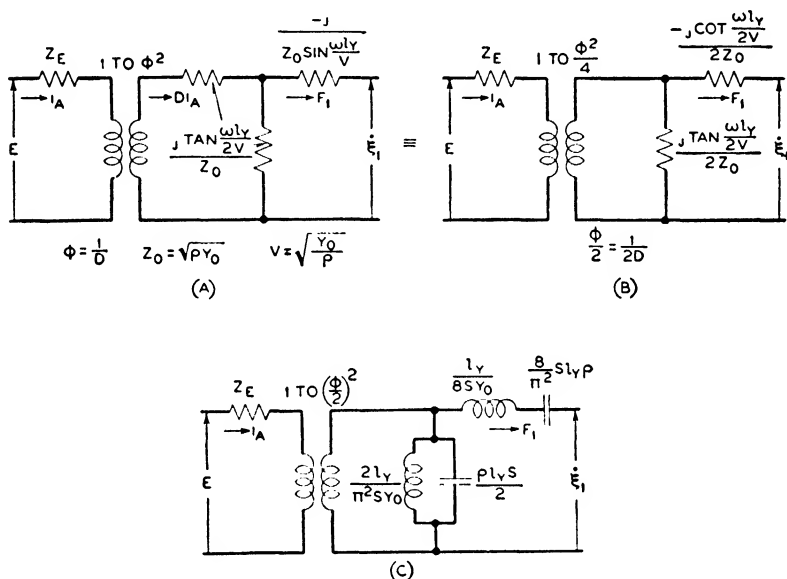


FIG. 6.15—EQUIVALENT ELECTROMECHANICAL CIRCUIT FOR A MAGNETOSTRICTIVE BAR FREE ON ONE END (INERTIA DRIVE).

free and the other end used to drive a load (inertia drive), the equations reduce to

$$\xi_1 = j \frac{(F_1 - D i_A) \left(1 - \cos \frac{\omega l}{v}\right)}{Z_0 \sin \frac{\omega l}{v}} - \frac{j F_1}{Z_0 \sin \frac{\omega l}{v}} \quad (6.93)$$

$$E = i_A \left[Z_E + j \frac{D^2 \tan \frac{\omega l}{2v}}{Z_0} \right] - \frac{j D [F_1 - D i_A] \tan \frac{\omega l}{2v}}{Z_0}.$$

These equations are the same as those for the equivalent network of Fig. 6.15A. One of these impedances can be elimi-

nated by employing the familiar network representation shown in Fig. 6.16, with the resulting network shown in Fig. 6.15B.

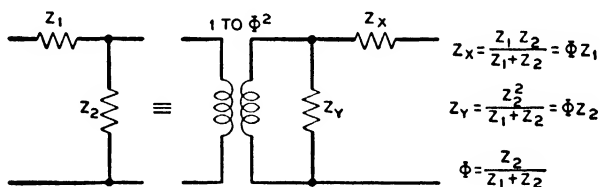


FIG. 6.16—NETWORK EQUIVALENCE.

Near the resonant frequency of the rod which occurs when

$\frac{\omega l_v}{2v} = \pi/2$, the lumped constant representation shown in Fig.

6.15C is valid. Using these equivalent networks, structures incorporating magnetostrictive elements can be designed.

CHAPTER VII

DESIGN OF ELECTROMECHANICAL SYSTEMS

7.1. *Introduction*

HAVING obtained the networks of electromechanical driving systems and the mechanical and electrical systems coupled thereto it is possible to work out designs for complete units employing such elements. Although the number of devices employing such units is large, only two specific designs will be considered in this chapter since the methods employed can easily be extended to any other structures.

The two devices chosen are a horn type loudspeaker driven by a moving coil diaphragm and a crystal-driven supersonic radiator. In both of these systems one of the prime requirements is to transmit as much electrical power as possible into mechanical radiation over as wide a frequency range as possible. This inherently requires a device designed as a filter since the filter is the system which will transmit all the power it receives to its termination over as wide a frequency range as is consistent with the elements composing it. When considerations of efficiency are not so important, as in the microphone, for example, the resulting mechanical structure is not always designed as a filter. For a microphone, power amplification at low power level is easily and cheaply obtained, and in this case the most important requirement is to obtain a uniform response over as wide a frequency range as possible with as small an instrument as can be conveniently designed. In such devices acoustical resistances and compensating elements are often introduced to provide uniformity of response of the microphone in picking up sound from a field. Such devices more nearly resemble equalizers than filters, and the process of designing them is similar to that for obtaining an equalizer to match a given attenuation characteristic.

7.2. Moving Coil Loudspeaker

The moving coil loudspeaker considered here is shown in Fig. 7.1. It consists of a moving coil mounted on a curved diaphragm which is held in position by a flexible support having

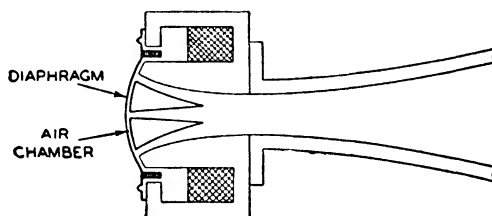


FIG. 7.1—MOVING COIL LOUDSPEAKER WITH HORN.

a high value of compliance. The diaphragm drives the air in the air chamber which communicates its vibration to the horn. Although some radiation occurs from the back of the diaphragm, its effect can be neglected with respect to the energy communicated to the horn since the horn impedance puts a much higher load on the diaphragm. The diaphragm is made curved so that its stiffness is increased. This results in a piston motion for the diaphragm up to high frequencies.

The equivalent circuit for the driving unit, including the diaphragm compliance and support, is the same as that shown in Fig. 6.2. To this we must add a series inductance representing the compliance of the air chamber, and a terminating resistance which is the inverse of $\rho v/S_2$ in acoustical impedance units

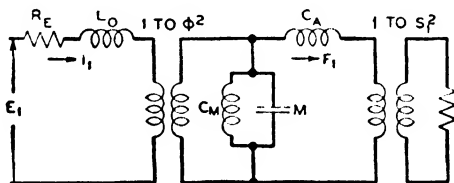


FIG. 7.2—EQUIVALENT CIRCUIT FOR MOVING COIL LOUDSPEAKER.

where S_2 is the area of the horn opening into the air chamber, as shown in Fig. 7.2. This assumes that the frequency is somewhat above the theoretical cut-off of the horn so that its characteristic impedance approaches ρv per square centimeter.

We have expressed all the mechanical elements in mechanical impedance units which for the inverse system used for electromagnetic coupling are the ratio of the velocity \dot{x} to the force F . On the other hand, the horn theory worked out in pages 120 to 125 was expressed in terms of acoustical impedance which in the direct system is ratio of pressure to volume velocity or in the inverse system is the ratio of volume velocity to pressure. To transfer from one system to the other, when the elements are expressed in the inverse system, requires a transformer having an impedance ratio of 1 to S_1^2 where S_1 is the area of the air chamber in this case. This follows from the equations

$$p = \frac{F}{S_1}; \quad V = \dot{x}S_1. \quad (7.1)$$

Since in the inverse system a velocity is the analogue of a voltage, this requires a transformer of impedance ratio 1 to S_1^2 . Equation (4.84) for a diaphragm chamber

$$V_2 = V_1 - jp_1 \omega \frac{(S_1 l_t)}{\rho v^2}; \quad p_2 = p_1$$

becomes

$$V_2 = \dot{x}_1 S_1 - jF_1 \frac{\omega l_t}{\rho v^2} = S_1 \left(\dot{x}_1 - jF_1 \frac{\omega l_t}{S_1 \rho v^2} \right); \quad p_2 = \frac{F_1}{S_1}. \quad (7.2)$$

In the inverse system where a velocity is the analogue of a voltage and a force or pressure the analogue of a current, these relations are satisfied by the network of Fig. 7.3. That is, we should have a transformer of impedance ratio 1 to S_1^2 to transform force to pressure and an inductance ($l_t/S_1 \rho v^2$) representing the compliance of the air chamber. The first transformer changes the impedance of the horn so that the resistive termination impedance is equal to

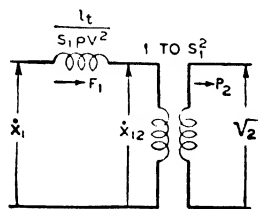


FIG. 7.3—EQUIVALENT CIRCUIT OF AN AIR CHAMBER.

$$\frac{\dot{x}_1}{F_1} = \left(\frac{S_2}{\rho v S_1^2} \right). \quad (7.3)$$

The complete circuit to analyze is then the one shown in Fig. 7.4 which represents all the elements of the network as seen from the electrical side.

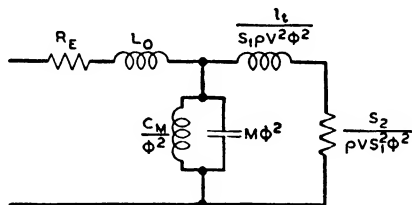


FIG. 7.4—EQUIVALENT CIRCUIT OF LOUDSPEAKER MEASURED FROM ELECTRICAL TERMINALS.

This is a band-pass filter of the type shown in Table I, Filter 12, pages 52, 53, which has the design constants

$$L_0 = (l_1 / S_1 \rho v^2 \phi^2) = \frac{Z_0}{2\pi f_B}; \quad \frac{C_M}{\phi^2} = L_2 = \frac{(f_B^2 - f_A^2)Z_0}{4\pi f_A^2 f_B};$$

$$\phi^2 M = C_2 = \frac{f_B}{\pi(f_B^2 - f_A^2)Z_0}. \quad (7.4)$$

From these equations we see that the lower limit of radiation is determined by the resonant frequency of the diaphragm mass and compliance since

$$MC_M = \frac{1}{4\pi^2 f_A^2}. \quad (7.5)$$

The upper limit is determined by the ratio

$$\left(\frac{C_M}{\phi^2 L_0} \right) = \frac{f_B^2 - f_A^2}{2f_A^2} \quad \text{or} \quad \frac{f_B^2}{f_A^2} = \left(1 + \frac{2C_M}{\phi^2 L_0} \right). \quad (7.6)$$

This can be made large by making the compliance C_M large or the value of ϕ^2 small. From equation (6.9) we have $\phi^2 = 1/B^2 l^2$ expressed in cgs units. This shows that ϕ^2 is inversely as the square of the flux density and the square of the number of turns. Since L_0 will be proportional to the square of the number of turns no advantage in frequency range will be obtained by increasing the number of turns, although the impedance of the loudspeaker will be increased in proportion to the square of the

number of turns of the voice coil. The only way to increase the band width is to increase the product of the compliance C_m and the square of the flux density. The electrical impedance that the loudspeaker works from should be equal to

$$Z_0 = 2\pi f_B L_0 \quad (7.7)$$

and the thickness of the air gap chamber should be adjusted so that

$$\frac{l_t}{S_1 \rho v^2 \varphi^2} = L_0. \quad (7.8)$$

Here again the adjustment is independent of the number of turns on the coil.

The amount of electrical energy transformed into useful acoustic energy can be obtained easily from Fig. 7.4. Calling R_T the motional electrical resistance $S_2/\rho v S_1^2 \varphi^2$, the best electrical impedance for the amplifier will be $R_E + R_T$. All of the energy from such an amplifier will be expended in the damped coil resistance R_E and the mechanical load impedance R_T . That expended in R_T is useful acoustic energy while that expended in R_E is wasted electrical energy. Hence the efficiency of the device is

$$Eff. \% = \frac{R_T}{R_E + R_T} \times 100 \quad (7.9)$$

since this represents the per cent of the electrical energy converted into useful acoustic energy. This is often better than 50 per cent in well-designed loudspeakers.

The frequency range of most loudspeakers is limited by the fact that in order to obtain reasonable ruggedness, the compliance C_M cannot be made too large and the flux densities available in practice cannot be made too large. As a result, the frequency range radiated by one device may not be large enough to meet the requirements. It has become usual to use two or more separate units, one for radiating the low frequency end and the other for radiating the high frequencies. One such unit is described by Wente and Thuras.¹ In order to get the elec-

¹ Journal A.I.E.E., Vol. 53, No. 1, p. 17, 1934.

trical energies into the respective units for their operating frequency ranges, sections of low- and high-pass filters have been inserted, as shown in Fig. 7.5. Over the low frequency unit's pass band the high-pass filter has a low image impedance, as

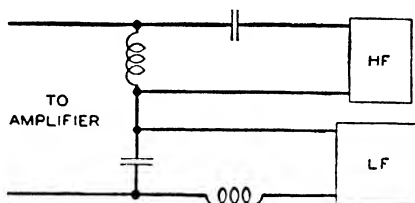


FIG. 7.5—CIRCUIT FOR CONNECTING LOW AND HIGH FREQUENCY LOUDSPEAKERS TO AMPLIFIER.

shown by Filter 4, Table I, while over the high frequency region the low-pass filter has a low impedance, as shown in Filter 1. In this way no loss of electrical energy occurs. In order to minimize phase distortion the effective acoustic path for both instruments should be the same. This may be accomplished by employing a short folded horn for the low frequency unit and setting the high frequency unit toward the back of the low frequency unit.

7.3. *Use of a Crystal as a Supersonic Radiator*

The other example considered is the use of a quartz crystal radiating into a liquid medium. This arrangement has been used extensively in supersonic work for transferring electrical into mechanical vibration. The arrangement considered here is the one shown in Fig. 7.6. The crystal is fastened to the wall of the tank by sealing wax or soldered onto a metal plate deposited on the crystal. One electrode covers the surface of the crystal and makes contact with the outside metallic tank, while the second electrode is plated on the outside surface with a small gap between the plating and the tank for electrical insulation.

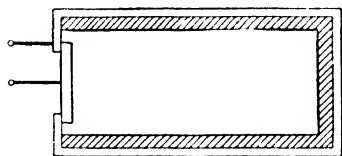


FIG. 7.6—CRYSTAL DRIVEN LIQUID BATH.

The crystal will only radiate over the area of the inside electrode, and this area can be taken as the effective area of the crystal.

The crystal thickness for maximum effectiveness is half a wavelength. The free side works against the very low impedance of the air and hence little energy is lost on this side, while on the driving side the impedance of the liquid is high and practically all the electrical energy is delivered in the form of mechanical energy to the water. The equivalent circuit applicable

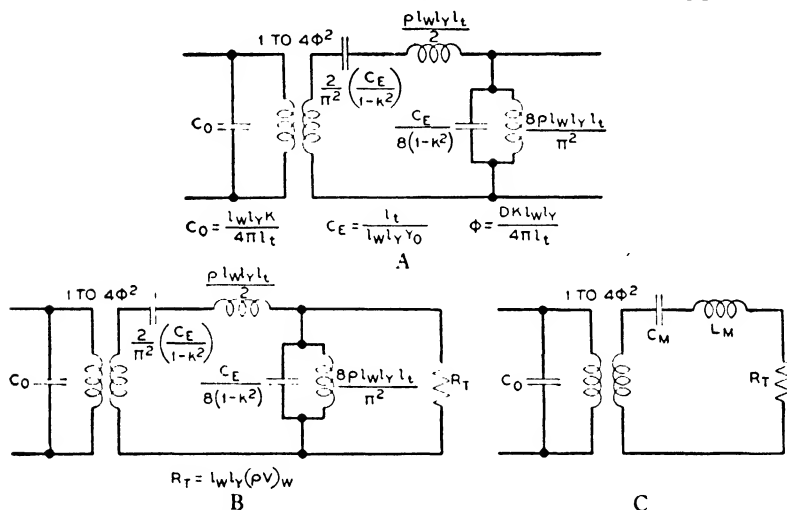


FIG. 7.7—EQUIVALENT CIRCUIT FOR CRYSTAL DRIVING A LIQUID.

to this case is the one shown in Fig. 6.10, modified by replacing l_y by l_t since the thickness is now the direction of vibration. If X -cut quartz vibrating along the X or the thickness axis is used, as is usually the case, the constants of the network are

$$Y_0 = 8.43 \times 10^{11}; \quad \rho = 2.65; \quad D = 14.3 \times 10^4;$$

$$K = 4.55; \quad v' = 5.64 \times 10^5; \quad k = 0.096. \quad (7.10)$$

With these constants the network of Fig. 6.10D become those shown in Fig. 7.7A. If the large dimensions of the radiator are larger than a wavelength, as is usually the case, the impedance of the liquid will be ρv mechanical ohms per square centimeter of the effective radiator surface where ρ is the density of the medium, and v the velocity of propagation. For

water $\rho = 1.0$, and $v = 1.5 \times 10^5$ cm per second so that the impedance on the radiator is

$$Z = 1.5 \times 10^5 S \text{ ohms} \quad (7.11)$$

where S is the effective area of the radiator. Inserting this radiation resistance in the termination the complete equivalent relationship for the radiator is shown in Fig. 7.7B. The impedance of the shunting anti-resonant circuit becomes

$$Z_S = \frac{j\omega \left[\frac{8}{\pi} (\rho v)_q l_w l_y \right]}{1 - \frac{\omega^2}{\omega_R^2}}. \quad (7.12)$$

Since the value of ρv for quartz is about 1.5×10^6 ohms, the value of the shunting impedance is always 20 times as large as the terminating impedance from 50 per cent below the resonant frequency to 50 per cent above, and hence it can be neglected. The resulting circuit to be analyzed is that in Fig. 7.7C.

The output radiation resistance R_T is

$$R_T = (\rho v)_w l_w l_y = 1.5 \times 10^5 l_w l_y. \quad (7.11)$$

When this is taken through the electromechanical transformer this will appear as an electrical resistance

$$R_S = \frac{(\rho v)_w l_w l_y}{(2\phi)^2} = \frac{1.5 \times 10^5 l_w l_y}{4D^2 K^2 l_w^2 l_y^2} = \frac{l_t^2}{l_w l_y} \left(\frac{5.91 \times 10^6}{D^2 K^2} \right). \quad (7.13)$$

To get this resistance into ohms we have to multiply by 9×10^{11} . Also it is more convenient to express the resistance in terms of the resonant frequency of the crystal rather than the thickness l_t , which can be done by the equation

$$l_t = \frac{v'}{2f_R} = \frac{2.82 \times 10^5}{f_R} \quad (7.14)$$

for this cut of quartz. With this substitution

$$R_S = \frac{9.69 \times 10^{17}}{l_w l_y f_R^2} \text{ ohms.} \quad (7.15)$$

This resistance will be shunted by the reactance of the condenser C_0 which will be considerably lower than the resistance R_s . This reactance will be

$$X_C = \frac{1}{2\pi f_R C_0} = \frac{9 \times 10^{11}}{2\pi f_R \frac{l_w l_y \times 4.55}{4\pi l_t}} = \frac{1.12 \times 10^{17}}{l_w l_y f_R^2}. \quad (7.16)$$

Hence the radiation resistance of the crystal is 8.65 times as large as the reactance of the crystal, and if the crystal alone is connected to an amplifier it is impossible to get all of the electrical energy into acoustic energy.

The greatest efficiency of conversion for the crystal alone will be obtained when the output impedance of the amplifier

is equal to the input impedance of the crystal at resonance, which in this case will be nearly the reactance of the crystal. To obtain the efficiency of conversion we have to compare the energy reaching the radiation resistance R_s with what would reach it if the amplifier and radiation resistance were connected by means of a perfect transformer. As shown by equation (2.34) if R_A is the output resistance of the amplifier, the current through the perfect transformer would be

$$i_T = \frac{E}{2\sqrt{R_A R_S}}. \quad (7.17)$$

If we take the absolute value of the ratio between the current through the network of Fig. 7.8 to the current i_T we find

$$\left| \frac{i_N}{i_T} \right| = \frac{2\sqrt{R_A R_S}}{\left\{ \sqrt{\left[R_A + R_S + \frac{R_A C_0}{C_1} \left(1 - \frac{\omega^2}{\omega_R^2} \right) \right]^2} + \left[R_A R_S \omega C_0 - \frac{1}{\omega C_1} \left(1 - \frac{\omega^2}{\omega_R^2} \right) \right]^2 \right\}}. \quad (7.18)$$

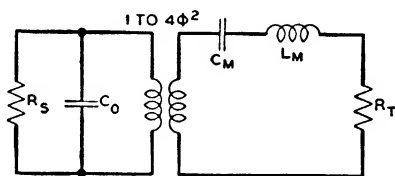


FIG. 7.8—CIRCUIT FOR CALCULATING RESPONSE.

The best value of $R_A = \frac{1}{\omega_R C_0}$, and $C_0/C_1 = r = 134$ the ratio of capacitances of the crystal. Also the ratio of R_A to R_S is

$$\frac{R_A}{R_S} = \frac{1.12}{9.69} = 0.116. \quad (7.19)$$

Inserting these numerical values equation (7.18) becomes

$$\left| \frac{i_Y}{i_T} \right| = \frac{2 \sqrt{0.116}}{\sqrt{\left[1.116 + 15.8 \left(1 - \frac{\omega^2}{\omega_R^2} \right) \right]^2 + \left[\frac{\omega_R}{\omega} - 15.8 \left(1 - \frac{\omega^2}{\omega_R^2} \right) \right]^2}}. \quad (7.20)$$

A plot of this equation is shown by the solid line of Fig. 7.9. The loss at the resonant point is 7.0 db and the efficiency of

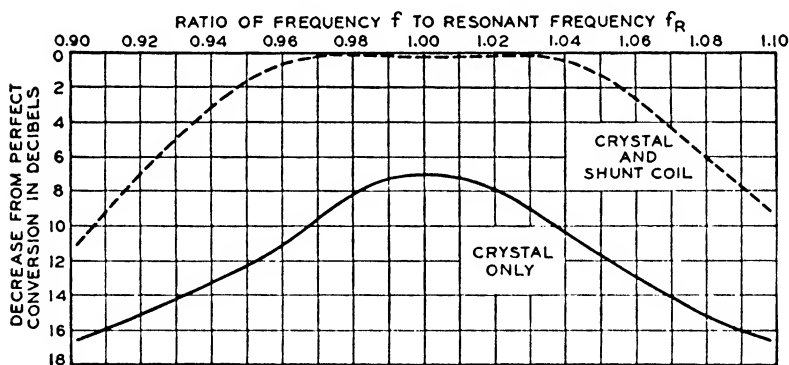


FIG. 7.9—RESPONSE OF CRYSTAL WITH AND WITHOUT SHUNT COIL.

conversion from electrical to mechanical energy is only 20 per cent. The response is slightly dissymmetrical on account of the reactance cancelation above the resonant frequency. The response drops off rapidly around the highest point and has dropped about 6 db, 5 per cent in frequency away from the maximum point. The breadth of the transmission region is controlled principally by the factor

$$\left(\frac{C_0}{C_1} \right) \left(\frac{R_A}{R_S} \right) = 15.8. \quad (7.21)$$

To widen this region requires decreasing the ratio of capacitances C_0/C_1 or increasing the electromechanical coupling. Certain cuts of Rochelle salt have a high coupling and these can be used when it is desirable to radiate wider frequency ranges.

By using a coil to neutralize the static capacitance of the crystal, the region of high efficiency can be extended over a wider frequency range, and the absolute efficiency of conversion can be made considerably higher. This can be done by using either a series coil or a shunt coil. The series coil gives a low impedance circuit while the shunt coil gives a high impedance circuit. If we use a shunt coil the equivalent circuit for

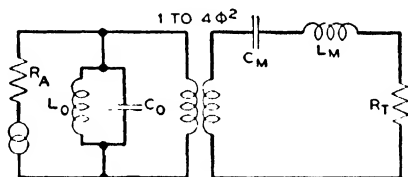


FIG. 7.10—ADDITION OF ELECTRICAL COIL TO IMPROVE RESPONSE.

the combination is as shown in Fig. 7.10 which is a half-section of the filter shown in Table I, Filter 11, provided we put the perfect transformer on the mechanical end of the network. From this table the design equations for the network are

$$L_0 = 2L_2 = \frac{(f_B - f_A)Z_{I_0}}{2\pi f_A f_B}; \quad C_0 = \frac{C_2}{2} = \frac{1}{2\pi(f_B - f_A)Z_{I_0}} \quad (7.22)$$

$$4\phi^2 C_M = 2C_1 = \frac{f_B - f_A}{2\pi f_A f_B Z_{I_0}}; \quad \frac{L_M}{4\phi^2} = \frac{L_1}{2} = \frac{Z_{I_0}}{2\pi(f_B - f_A)}.$$

Taking the ratio of C_0 to $4\phi^2 C_M$, which will be the ratio of capacitances of the crystal considered as an electrical network, and inserting their values in terms of the constants of the crystal we have

$$\frac{C_0}{4\phi^2 C_M} = \frac{\pi^2}{8} \left(\frac{1 - k^2}{k^2} \right) = r = \frac{f_A f_B}{(f_B - f_A)^2}. \quad (7.23)$$

Hence in this case the band width is determined by the coupling existing in the crystal. The image impedances and the mean frequency of the band are given by the relations

$$L_M C_M = \frac{\rho l_t^2}{\pi^2 Y_0 (1 - k^2)} = \frac{l_t^2}{\pi^2 v^2} = \frac{1}{4\pi^2 f_A f_B}; \text{ or}$$

$$f_R = \sqrt{f_A f_B} = \frac{v}{2l_t} \quad (7.24)$$

and

$$Z_{I_0} = \frac{\sqrt{\frac{\pi^2}{8} \left(\frac{1 - k^2}{k^2} \right)}}{\omega_R C_0} = \frac{\sqrt{r}}{\omega_R C_0} = \frac{1}{2\pi (f_B - f_A) C_0}. \quad (7.25)$$

Hence the thickness of the crystal should be made a half wavelength at the mean frequency f_R and the output impedance Z_A of the transmitting amplifier should be equal to the impedance Z_{I_0} given by (7.25). If C_0 is expressed in farads this impedance will be in ohms. The mechanical impedance on the radiating side that this filter should be connected to will be

$$Z_{I_0}(2\varphi)^2 = \sqrt{2} \left(\frac{k}{\sqrt{1 - k^2}} \right) (\rho v)_q l_w l_t = Z_{IM} \quad (7.26)$$

upon inserting the values of C_0 and φ . The constants of quartz given above result in a mechanical image impedance equal to 2.04×10^5 mechanical ohms per square centimeter which is slightly higher than the mechanical impedance of water. If, however, we terminate the filter correctly on the amplifier end the resulting distortion is small.

The resulting efficiency of transferring from electrical to mechanical energy can be calculated by solving the network of Fig. 7.10, using a terminating impedance R_A equal to the image impedance of the filter given by (7.25). Comparing this with the current through a perfect transformer into the terminating impedance

$$R_s = \frac{2.69 \times 10^{17}}{l_w l_v f_R^2} \text{ ohms}$$

we have the relation

$$\left| \frac{i_N}{i_T} \right| = \frac{2 \sqrt{R_A R_S}}{\sqrt{\left[R_A + R_S - \frac{R_A}{\omega^2 L_0 C_1} \left(1 - \frac{\omega^2}{\omega_R^2} \right) \right]^2 + \frac{1}{\omega^2} \left[\left(\frac{R_A R_S}{L_0} + \frac{1}{C_1} \right) \left(1 - \frac{\omega^2}{\omega_R^2} \right) \right]^2}}. \quad (7.27)$$

Inserting the values of these constants given by equations (7.22), (7.23) and (7.25) we have

$$\left| \frac{i_N}{i_T} \right| = \frac{\frac{2 \sqrt{Z_{I_0} R_S}}{(Z_{I_0} + R_S)}}{\sqrt{\left[1 - \left(\frac{Z_{I_0}}{Z_{I_0} + R_S} \right) \frac{\pi^2}{8} \left(\frac{1 - k^2}{k^2} \right) \left(\frac{\omega_R}{\omega} - \frac{\omega}{\omega_R} \right)^2 \right]^2 + \frac{\pi^2}{8} \left(\frac{1 - k^2}{k^2} \right) \left[\frac{\omega_R}{\omega} - \frac{\omega}{\omega_R} \right]^2}}}. \quad (7.28)$$

Inserting the numerical values for this case

$$R_S = \frac{1.5}{2.04} Z_{I_0} = 0.735 Z_{I_0} \quad \text{and} \quad \frac{\pi^2}{8} \left(\frac{1 - k^2}{k^2} \right) = r = 134$$

this becomes

$$\left| \frac{i_N}{i_T} \right| = \frac{0.99}{\sqrt{\left[1 - 77.1 \left(\frac{\omega_R}{\omega} - \frac{\omega}{\omega_R} \right)^2 \right]^2 + 134 \left[\frac{\omega_R}{\omega} - \frac{\omega}{\omega_R} \right]^2}}. \quad (7.29)$$

A plot of this equation is shown by the dotted line of Fig. 7.9. The result of using the extra coil is to make the radiator a filter circuit. The device becomes a much more efficient radiator, transferring at least 70 per cent of the electrical energy into acoustic energy over a 10 per cent frequency band centered around the resonant frequency of the crystal. Outside the pass band of the filter, the amount radiated falls off more rapidly than for the crystal alone.

If it is desired to radiate over a wider range of frequencies, it is necessary to have a higher coupling factor or else to place several crystals of different frequencies in parallel. If they are designed as filter circuits this can be accomplished without appreciable loss of power over a wide frequency range.

7.4. *Methods for Measuring Elastic Constants and Internal Dissipation in Vibrating Bars*

Another similar use of a piezoelectric crystal is in the measurement of the elastic constants and the internal dissipation of longitudinally and torsionally vibrating bars. This method, which was due originally to Balamuth² and Quimby, consists in gluing a nearly half wavelength bar of the material to be measured to a plated quartz crystal. The mechanical impedance of the glue joining the crystal to the bar will be in the nature of a shunt compliance, since its stretching depends on the difference in velocity of the crystal and the bar. Since the stiffness of glues is usually low compared to the stiffness of bar materials it is necessary to have the length of the bar close to a half wavelength at the crystal frequency, or otherwise the measurement will measure the stiffness of the glue rather than the constants of the bar.

The impedance of a bar an integral number of half wavelengths long, will be quite low. This can be shown by employing the equations for a line with dissipation given in section (2.8) which are analogous to those for a bar vibrating longitudinally or torsionally. The internal dissipation in a bar can be represented by either a series resistance or a shunt leakance depending on whether the dissipation is occasioned by the rate of change of stress—i.e., is of a viscous nature—or by the stress itself. In general, it appears that most of the dissipation depends on a hysteresis cycle associated with the stretching and hence appears as a shunt leakance. The inductance of the line per unit length is the analogue of the mass per unit length of the bar, while the capacitance is the analogue of the com-

² Phys. Rev., **45**, 715 (1934).

pliance per unit length. For a long thin bar this compliance will be ³

$$C = \frac{1}{l_w l_t Y_0} = \frac{1}{l_w l_t \frac{\mu(3\lambda + 2\mu)}{\lambda + \mu}} \quad (7.30)$$

where Y_0 is Young's modulus and λ and μ are the fundamental elastic constants for an isotropic solid. On the other hand, when the width and thickness of the bar are half a wavelength or greater the compliance will be less. In terms of the fundamental constants of elasticity λ and μ , the compliance for this case will be

$$C = \frac{1}{l_w l_t (\lambda + 2\mu)}. \quad (7.31)$$

For a torsionally vibrating bar the inductance per unit length will be the analogue of the moment of inertia per unit length which is the density ρ times the cross-sectional area S times the square of the radius of gyration. The capacitance, on the other hand, is the analogue of the moment of compliance which is the inverse of the shear modulus μ times the cross-sectional area S times the square of the radius of gyration or

$$C = \frac{1}{S k^2 \mu}. \quad (7.32)$$

Near an integral half wavelength frequency which occurs when

$$Bx = \omega \sqrt{LC} x = n\pi \quad n = 1, 2, 3 \dots \dots \dots (7.33)$$

the equation (2.124) for a dissipative line becomes

$$\begin{aligned} \cosh \theta x &= \cosh (A + jB)x \\ &= \cosh Ax \cos Bx + j \sinh Ax \sin Bx \\ \sinh \theta x &= \sinh (A + jB)x \\ &= \sinh Ax \cos Bx + j \cosh Ax \sin Bx. \end{aligned} \quad (7.34)$$

³ The derivation of the elastic constants of equations (7.30) and (7.31) is given in Appendix C, p. 314.

In all cases Ax is a small quantity so that its squares can be neglected. Also

$$Bx = (\omega_R + \Delta\omega) \sqrt{LC} x = (n\pi + \Delta\omega) \sqrt{LC} x = n\pi \left(1 + \frac{\Delta\omega}{\omega_R} \right) \quad (7.35)$$

where ω_R is the frequency at the half wavelength point. Hence

$$\begin{aligned} \cosh \theta x &= (-1)^n (1 + jAx n\pi (\Delta\omega/\omega_R)) \\ \sinh \theta x &= (-1)^n (Ax + jn\pi (\Delta\omega/\omega_R)). \end{aligned} \quad (7.36)$$

Assuming that most of the dissipation comes from the stretching cycle the expression for Z_0 , the image impedance in (2.124), becomes

$$Z_0 = \sqrt{\frac{M}{C}} \left[1 + \frac{j}{2} \left(\frac{Ax}{n\pi} \right) \right] \quad (7.37)$$

where M is the mass per unit length and C the compliance. Hence, near an integral half wavelength point, equation (2.122) can be written

$$\begin{aligned} \xi &= (-1)^n \left[\xi_0 \left(1 + jAx n\pi (\Delta\omega/\omega_R) \right) - \frac{F_0 (Ax + jn\pi (\Delta\omega/\omega_R))}{\sqrt{\frac{M}{C}} \left(1 + \frac{j}{2} \frac{Ax}{n\pi} \right)} \right] \\ F &= (-1)^n \left[F_0 (1 + jAx n\pi (\Delta\omega/\omega_R)) \right. \end{aligned} \quad (7.38)$$

$$\left. - \xi_0 \sqrt{\frac{M}{C}} \left(1 + \frac{j}{2} \frac{Ax}{n\pi} \right) (Ax + jn\pi (\Delta\omega/\omega_R)) \right]$$

where F and ξ are the force and particle velocity at any point in the bar. When the bar is measured, it is free to move on the end not attached to the crystal so that $F = 0$. The impedance attached to the crystal end will then be

$$\begin{aligned} Z_M = \frac{F_0}{\xi_0} &= \frac{\sqrt{\frac{M}{C}} \left(1 + \frac{j}{2} \frac{Ax}{n\pi} \right) (Ax + jn\pi \frac{\Delta\omega}{\omega_R})}{1 + jAx n\pi (\Delta\omega/\omega_R)} \\ &= \sqrt{\frac{M}{C}} \left(Ax + \frac{jn\pi \Delta\omega}{\omega_R} \right) \end{aligned} \quad (7.39)$$

dropping squares and higher powers of small quantities. This impedance is similar to that for a mass, compliance, and resistance in series which resonate at f_R . Comparing equation (3.35) for such a combination with (7.39) we have

$$M_M = \frac{Mx}{2}; \quad C_M = \frac{2(Cx)}{n^2\pi^2}; \quad R_M = \sqrt{\frac{M}{C}} (Ax). \quad (7.40)$$

Hence the effective mass for a longitudinal vibration is half the static mass, while the compliance is the total static compliance (Cx) times $2/n^2\pi^2$. We define the Q of such a bar as the ratio of the reactance of one of these elements to the resistance R_M at the half wavelength frequency, or

$$Q = \frac{\omega_R M_M}{R_M} = \frac{\frac{Mx}{2} \left(\frac{n\pi}{\sqrt{MCx}} \right)}{\sqrt{\frac{M}{C}} Ax} = \frac{1}{2} \frac{n\pi}{Ax} = \frac{1}{2} \frac{n\pi}{A_0} = \frac{1}{2} \frac{B_0}{A_0} \quad (7.41)$$

where A_0 is the total attenuation in the bar. Hence the ratio Q is half the phase shift constant B_0 divided by the attenuation constant A_0 .

If such a bar is driven by a crystal free on one end, the electrical impedance measured can be determined by attaching the elements M_M , C_M and R_M in series to the mechanical end of Fig. 6.10. The anti-resonant circuit on the end of Fig. 6.10 will have a very high impedance compared to the terminating impedance and can be neglected. Hence we can combine the mass M_M of equation (7.40) with the mass M_C of the crystal, the compliance C_M with the compliance C_C of the crystal and the resistance R_M with the crystal resistance R_C .

The process of measuring the constants of a longitudinal bar is first to measure the resonance f_R , the anti-resonance f_A , and the resistance at resonance R for the crystal alone. Then the bar is cemented on and the new resonance f_R' , the anti-resonance f_A' , and the resistance at resonance R' of the combination is obtained. From these measurements M_M , C_M , and

R_M can be obtained. The first measurement of the crystal alone gives

$$\frac{8l_y\varphi^2}{\pi^2l_wl_tY_0(1-k^2)} = C_0\left(\frac{f_A^2}{f_R^2} - 1\right); \quad (7.42)$$

$$\frac{R_C}{4\varphi^2} = R; \quad \frac{\rho l_w l_y l_t}{8\varphi^2} = \frac{1}{4\pi^2 C_0(f_A'^2 - f_R'^2)}.$$

The second measurement gives the combination values

$$4\varphi^2 \left(\frac{\frac{2l_y C_M}{\pi^2 l_w l_t Y_0 (1-k^2)}}{C_M + \frac{2l_y}{\pi^2 l_w l_t Y_0 (1-k^2)}} \right) = C_0 \left(\frac{f_A'^2}{f_R'^2} - 1 \right); \quad (7.43)$$

$$\frac{R_M + R_C}{4\varphi^2} = R'; \quad \frac{\left(\frac{\rho l_w l_y l_t}{2} + M_M \right)}{4\varphi^2} = \frac{1}{4\pi^2 C_0 (f_A'^2 - f_R'^2)}.$$

Solving for the values of the constants desired we have

$$C_M = \frac{\frac{2l_y}{\pi^2 l_w l_t Y_0 (1-k^2)}}{\frac{(f_A'^2 - f_R'^2)f_R'^2}{f_R'^2(f_A'^2 - f_R'^2)} - 1}; \quad (7.44)$$

$$R_M = (R' - R)4\varphi^2 = \frac{(R' - R)}{R} R_C;$$

$$M_M = \frac{\rho l_w l_y l_t}{2} \left(\frac{f_A'^2 - f_R'^2}{f_A'^2 - f_R'^2} - 1 \right).$$

Since the stiffness and effective mass of the crystal can be determined easily from the density and frequency of resonance, this determines C_M and M_M completely. The value of R_M is not determined unless φ^2 or R_C are known. If we know the static capacitance of the crystal C_0 , however, the value of Q can be determined. This is given by

$$Q = \frac{\omega_R' M_M}{R_M} = \frac{1}{2\pi f_R' C_0 (R' - R)} \left[\frac{f_R'^2}{f_A'^2 - f_R'^2} - \frac{f_R'^2}{f_A'^2 - f_R'^2} \right] \quad (7.45)$$

upon substituting in the relations given above.

Another method of determining the constants is to adjust the length of the bar until the frequency f_R' of the combination rod is equal to f_R the resonance of the crystal alone. Then the bar is just a half wavelength and hence

$$\omega_R l \sqrt{\frac{Y_0}{\rho}} = \pi. \quad (7.46)$$

Then measuring the density ρ of the rod both Y_0 and ρ can be determined. The internal dissipation can be determined from (7.45).

To determine the constants of a torsionally vibrating rod, a torsionally vibrating crystal ⁴ can be used and the same results hold except that the moment of compliance and the moment of inertia have to be substituted for the compliance and mass per unit length of the crystal.

Table VII shows a list of materials measured in this way.⁵ The first column gives the material, the second the measured density, the third the velocity of wave propagation in the material (which is determined by the value of Young's modulus since long thin bars were used), the fourth column gives the product of ρv which is the specific impedance of the material, the fifth column gives the Q of the material as defined previously, while the sixth column gives the temperature coefficient of the material.

The temperature coefficient of the bar can be obtained by measuring the temperature coefficient of the crystal alone and the temperature coefficient of the combination crystal and bar. The formula for the coefficient can be derived from the formula for the frequency of the bar

$$f_B = f_R \sqrt{\frac{1 - \frac{r}{r'}}{\left(\frac{f_R}{f_R'}\right)^2 - \frac{r}{r'}}} \quad (7.47)$$

⁴ "Quartz Resonators and Oscillators," P. Vigoureux, p. 91.

⁵ These materials were measured by Messrs. H. J. McSkimin and R. A. Sykes.

where r is the ratio of capacitances of the crystal alone and r' that measured for the crystal and bar. In terms of the resonant and anti-resonant frequencies these are given by

$$r = \frac{f_R^2}{f_A^2 - f_R^2}; \quad r' = \frac{f_R'^2}{f_A'^2 - f_R'^2} \quad (7.48)$$

Equation (7.47) follows from (7.44) and (7.42).

If, now, the temperature varies, f_R and f_R' will vary while r and r' will remain relatively constant. Hence differentiating (7.47) with respect to the temperature and dividing through by f_B , we have

$$T_{f_B} = \frac{T_{f_R}}{\left(1 - \frac{r' f_R^2}{r f_R'^2}\right)} + \frac{T_{f_R'}}{1 - \frac{r f_R^2}{r' f_R'^2}} \quad (7.49)$$

where T_{f_B} is the temperature coefficient of the bar defined by

$$T_{f_B} = \frac{df_B}{dT}/f_B$$

and

$$T_{f_R} = \frac{df_R}{dT}/f_R; \quad T_{f_R'} = \frac{df_R'}{dt}/f_R' \quad (7.50)$$

are respectively the temperature coefficient of the crystal alone and of the composite crystal and bar.

Table VII, page 245, gives the measured values for a number of solid materials.

This system of measuring the elastic properties of materials works well as long as the Q of the material is 500 or above. In attempting to measure some plastic materials it was found that the damping was so great that resonant and anti-resonant frequencies could not be located. In order to get around that difficulty another system has been devised. This system consists of two identical crystals used to drive and pick up the vibration from a bar of the material to be investigated which is an even multiple of a half wavelength long. The circuit used is shown in Fig. 7.11A, and the end resistances R_T are made quite low, i.e., under 100 ohms. The procedure is to adjust the

TABLE VII
PROPERTIES OF MATERIALS

Material	Density ρ	Velocity v in cms per sec.	Impedance ρv	Q	T_{fB} in parts per million per °C.
Aluminum....	2.68	5.13×10^5	13.8×10^5	10,000	-215
Magnesium...	1.705	5.10	8.7	5,700	-194
Tungsten Carbide Steel...	8.52	4.72	41.0	8,180	-10.5
Molybdenum Steel.....	8.39	4.70	39.5	4,700	-16.0
Fused Quartz Rod.....	2.20	5.11	11.3	5,000	+ 5.0
702 Pyrex....	2.32	5.35	12.4	1,200	+25.0
Window Glass...	2.42	5.44	13.5	910	-58
Lead Glass....	2.48	5.13	12.8	1,910	+41.0
Micalex.....	3.34	5.35	17.9	2,890	-74.0
Ceramics.....	2.47 to 3.38	4.55 to 6.78	11.5 to 18.4	700 to 5,000	-45 to -215

length of the bar until the current maximum comes at the resonant frequency of the crystals, then to switch over to the variable resistance R and adjust this until the current in the output is the same. From the measured constants of the crystals and the value of this resistance the internal dissipation can be obtained.

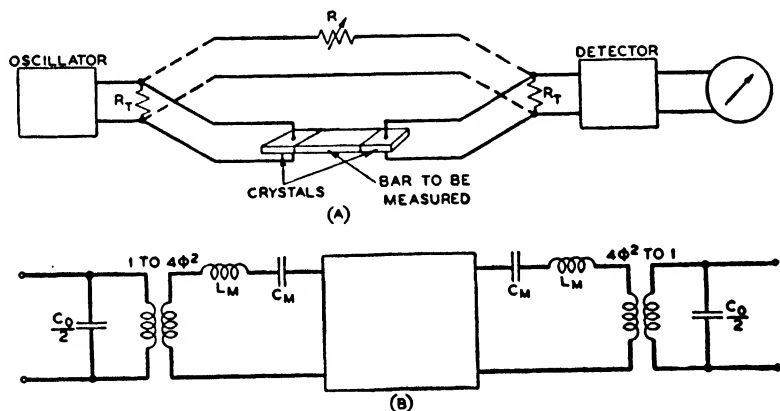


FIG. 7.11—METHOD FOR MEASURING PROPAGATION CHARACTERISTICS OF BARS HAVING LOW Q 's.

The equivalent electromechanical circuit for this combination is the one shown in Fig. 7.11B, with the box representing a transmission line of image impedance Z_0 and transfer constant θ . Since we are going to use it at the half wavelength point, the approximate equations for a line given by (7.38) can be used and $\Delta\omega$ can be set equal to zero. The resulting equation for the output voltage and current in terms of the input voltage becomes

$$i_0 \left(\frac{Z_0 A_0}{4\varphi^2} \right) + E_0 \left(1 + \frac{j\omega C_0 Z_0 A_0}{4\varphi^2} \right) = E_I \quad (7.51)$$

where $Z_0 = (\rho v)_B l_w l_t =$ mechanical image impedance of the bar, C_0 the static capacitance of either crystal and A_0 the total attenuation in the bar. If we terminate the combination in a resistance which is low compared to the static impedance of the crystal, this can be written

$$i_0 = E_I \left(\frac{4\varphi^2}{Z_0 A_0} \right) \quad (7.52)$$

where E_I will be the input voltage across the small resistance R_T , and i_0 the output current with the small output resistance R_T . If now we switch over and adjust the resistance R till the same output current is obtained we have

$$R = \frac{Z_0 A_0}{4\varphi^2} \quad \text{or} \quad A_0 = \frac{4\varphi^2 R}{Z_0}. \quad (7.53)$$

The half wavelength dimensions can be obtained by matching the resonance points of the bar for various lengths to the resonant frequency of the crystals. From this measurement and the density of the bar, the appropriate elastic constant can be determined. From this Z_0 can be calculated. Knowing the type of crystal cut φ^2 can be evaluated, and hence all of the constants of the bar can be determined. Since φ^2 and Z_0 are usually expressed in cgs electrostatic units, the ohmic resistance R has to be divided by 9×10^{11} .

As an example of the use of this method, Fig. 7.12 shows velocity and attenuation measurements of three plastic mate-

rials. The widths and thicknesses of the plastic bars used to determine the properties were in every case greater than a half wavelength so that the elastic constant is $(\lambda + 2\mu)$. It will be noted that the attenuation constant shows frequencies of higher

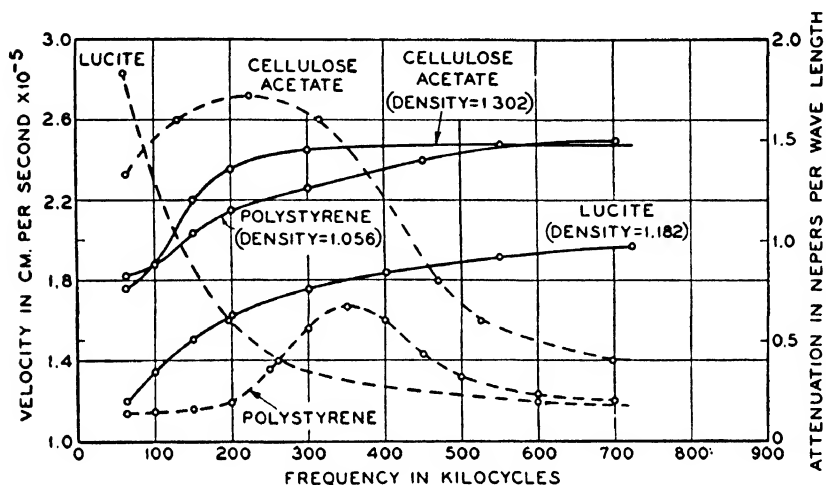


FIG. 7.12—VELOCITY AND ATTENUATION OF PLASTIC MATERIALS. SOLID LINES REPRESENT VELOCITY, DOTTED LINES ATTENUATION.

attenuation and around these frequencies the velocity increases rapidly. If interpreted according to the explanation for a similar phenomena in gases, this would indicate that some molecules or combination of molecules in the material were in a resonant condition at the frequency of highest loss.

CHAPTER VIII

APPLICATION OF ELECTROMECHANICAL IMPEDANCE ELEMENTS IN ELECTRICAL WAVE FILTERS

8.1. *Introduction*

ALTHOUGH electrical elements were used entirely in the first wave filters, in recent years large numbers of filters have been constructed in which some or all of their electrical elements are replaced by electromechanical elements such as piezoelectric crystals, magnetostrictive bars, and mechanically vibrating elements. An example of a mechanical filter has already been considered in Chapter III.

However the largest use of such elements has been in the piezoelectric crystal filter. On account of the very low amount of internal dissipation associated with the motion of piezoelectric crystals—in particular quartz—it is possible to make very narrow band filters and filters in which the insertion loss increases very rapidly with frequency. Such filters have received a wide variety of uses. Very narrow band filters have been used in carrier systems as pilot channel filters for separating out the pilot or control frequency from the other frequencies present, in radio systems for separating the carrier frequency from the side-band frequencies, and in heterodyne sound analyzing devices for analyzing the frequencies present in industrial noises, speech, and music. Wider band filters employing coils as well as crystals have provided very selective devices which are able to separate one band of speech frequencies from another band different by only a small frequency percentage from the desired band. This property makes it possible to space channels close together, with only a small frequency separation up to a high frequency, and such filters have had a wide use in the high

frequency carrier systems^{1, 2} and in the coaxial system which transmits more than 480 conversations over one pair of conductors. In radio systems such filters have been used extensively in separating one sideband from the other in single sideband systems.

It is the purpose of this chapter to provide an introduction to the use of electromechanical elements in electrical wave filters.

8.2. *Equivalent Circuits for Piezoelectric Crystals with Normal and Divided Electrodes*

In the frequency range from 50 kilocycles to 500 kilocycles filters employing crystals will ordinarily use longitudinally vibrating crystals. Above this frequency, high frequency shear crystals, similar to the *AT* and *BT* type are commonly employed. Whenever longitudinal crystals can be employed they are usually preferable because they satisfy the condition that a single resonance free from secondary resonances is more easily obtained when the dimension along the direction of vibration is large compared to the other dimensions.

The equivalent circuit of a crystal free on one end and driving a load on the other is shown in Fig. 6.10. In a filter circuit it is the electrical impedance of a crystal, free to vibrate on both ends, that is of interest. To obtain this we have only to terminate the mechanical end of Fig. 6.10 in a short circuit and bring the mechanical elements through the electromechanical transformer with the result shown in Fig. 8.1 which represents the equivalent electrical circuit of a crystal near its reso-

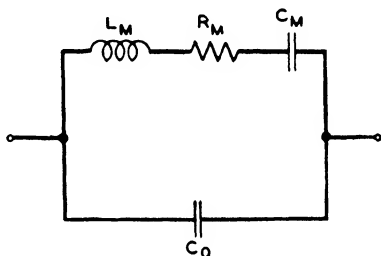


FIG. 8.1—EQUIVALENT ELECTRICAL CIRCUIT OF PIEZOELECTRIC CRYSTAL.

¹ "The Evolution of the Crystal Wave Filter," O. E. Buckley, *Journal of Applied Physics*, October 1936.

² "Crystal Channel Filters for the Cable Carrier System," C. E. Lane, *B.S.T.J.*, January 1938, pp. 125, 137.

nant frequency. The crystal ordinarily used in filter work is the -18.5° X -cut quartz crystal³ which can be made to have a single resonance over a wide range of frequencies. This crystal has the fundamental constants

$$K = 4.55; D = 13.05 \times 10^4; Y_0 = 6.84 \times 10^{11}; \rho = 2.65. \quad (8.1)$$

Introducing these values in the expressions for the element values given by equations (6.45), (6.46) and Fig. 6.10, the constants of a -18.5° X -cut quartz crystal are

$$\begin{aligned} C_0 &= \frac{4.55 \times 1.11 \times 10^{-12} l_w l_y}{4\pi l_t} \text{ Farads} \\ &= \frac{0.402 \times l_w l_y \times 10^{-12}}{l_t} \text{ Farads} \\ C_1 &= 2.924 \times 10^{-15} \frac{l_w l_y}{l_t} \text{ Farads} \\ L_1 &= 139 \frac{l_v l_t}{l_w} \text{ Henries.} \end{aligned} \quad (8.2)$$

In addition to these reactance elements there is a resistance element R_1 shown which represents the mounting resistance, the internal dissipation in the crystal and the radiation loss from the ends of the crystal. In addition there may be some diffusion waves set up by the motion along the sides of the crystal as discussed in section (4.3) but the effect of these can be neglected compared to the radiation losses. In a well-mounted longitudinally vibrating crystal the principal source of loss is in the radiation resistance of the surrounding atmosphere. If the smallest dimension is greater than half a wavelength the effect of this radiation resistance is easily calculated by terminating each mechanical end in a mechanical resistance $R_M = (\rho v)_A l_w l_t$ where

$$(\rho v)_A = 43 \text{ ohms per square centimeter.} \quad (8.3)$$

³ "Electrical Wave Filters Employing Quartz Crystals as Elements," W. P. Mason, B.S.T.J., July 1934.

To determine the effect, we have to start with the exact network representation of Fig. 6.7 and terminate both mechanical ends in R_M . The two end arms will be in parallel and can be combined with the impedance $-jZ_0/\sin \frac{\omega l_y}{v}$ to give the mechanical arm

$$\left(\frac{-jZ_0}{2} \tan \frac{\omega l_y}{2v'} - \frac{jZ_0}{\sin \frac{\omega l_y}{v'}} \right) + \frac{R_M}{2} = \frac{-jZ_0}{2} \cot \frac{\omega l_y}{2v} + \frac{R_M}{2}. \quad (8.4)$$

Near the resonant frequency of the crystal this reduces to a compliance C_M , a mass $M/4$ and a resistance $R_M/2$ where C_M and M have the values shown in equations (6.45) and (6.46). Defining the mechanical Q of the crystal as the ratio of the reactance of one of the elements at resonance to the resistance, we have

$$Q_M = \frac{\omega_R(\rho)l_u l_y l_t}{8 \times \frac{(\rho v)_A l_u l_t}{2}} = \frac{\pi (\rho v')_q}{4 (\rho v)_A} \quad (8.5)$$

upon substituting the relation for a resonant crystal

$$\frac{\omega_R l_y}{v'} = \pi. \quad (8.6)$$

Since the same ratio holds on taking the mechanical elements through the electromechanical transformer, the electrical Q will be equal to the mechanical Q . For example for a -18.5° X-cut crystal the limiting Q will be

$$Q = \frac{\pi}{4} \left(\frac{2.65 \times 5.08 \times 10^5}{43} \right) = 24,500. \quad (8.7)$$

For narrow band or very selective filters it is often desirable to have a value of Q higher than this. This can be obtained by putting the crystal in an evacuated container. Crystals in an evacuated container and clamped at their nodal points can easily be made to have Q 's as high as 300,000. By etching the

surface to remove any surface cracks and suspending the crystal in a vacuum Van Dyke ⁴ has obtained Q 's as high as 6,000,000. It appears therefore that most of the resistances measured in a crystal are due to mounting and radiating sources rather than to the internal dissipation in the crystal.

When the thickness of the crystal is less than half a wavelength the radiation resistance will be less than $(\rho v)_A$ per square centimeter and the atmosphere will also introduce a reactive component, as can be seen qualitatively from Fig. 4.14. The effect of this reactive component, which is always a positive reactance, is to lower the frequency of the crystal. Since the reactive component is always less than about 70 per cent of the resistive component, the maximum frequency change caused by this effect will be evaluated by adding this reactance to the reactance of the mass $M/8$. The resonant frequency will then be

$$\begin{aligned}\omega_R' &= \frac{1}{\sqrt{M'C_M}} = \frac{1}{\sqrt{\left(\frac{\rho l_w l_y l_t}{8} + \frac{.7(\rho v)_A l_w l_t}{2\omega_R}\right) C_M}} \\ &= \frac{\omega_R}{\sqrt{1 + \frac{2.8}{\pi} \frac{(\rho v)_A}{(\rho v')_q}}} \doteq \omega_R \left(1 - \frac{1.4}{\pi} \frac{(\rho v)_A}{(\rho v')_q}\right).\end{aligned}\quad (8.8)$$

Hence for the -18.5° X -cut crystal the maximum reduction in frequency due to the surrounding air will be

$$\frac{f_R'}{f_R} = (1 - 14.5 \times 10^{-6}) \quad (8.9)$$

or an increase of 14.5 parts in a million may take place as the crystal is evacuated. This effect usually has to be allowed for when crystals are put in vacuum containers.

In crystal filter work, crystals with two equal sets of plating are often employed. They were first employed in balanced lat-

⁴ "A Determination of Some of the Properties of the Piezo Electric Quartz Resonator," K. S. Van Dyke, Proc. Inst. Radio Engrs., April 1935, Vol. 23, No. 4, p. 386.

tice filters to take the place of the two identical crystals in the series or lattice arms. More recently they have been employed in obtaining unbalanced filters with both narrow and wide bands. To obtain the equivalent network of a crystal with two sets of plates we start with the electromechanical equivalent network of a crystal free to vibrate on both ends which can be

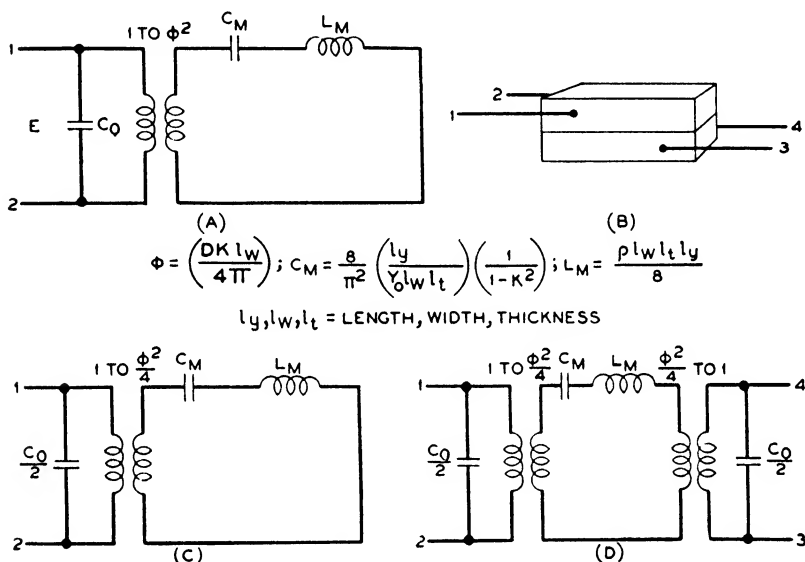


FIG. 8.2—EQUIVALENT CIRCUIT OF CRYSTAL WITH TWO SETS OF PLATES.

obtained from Fig. 6.10 by short-circuiting the mechanical end. This results in Fig. 8.2A with the constants given in the figure. Now we wish to divide the plating of the crystal as shown in Fig. 8.2B with the terminals numbered as shown. As far as the longitudinal vibration is concerned if we use only the set of plates numbered 1, 2, the equivalent circuit of the crystal with the half plating will be as shown in Fig. 8.2C. That is, the mechanical constants will remain unchanged but the impedance transformation ratio ϕ^2 will be changed to $\phi^2/4$ since the force applied to the crystal will be halved by applying only half the plating. The static capacitance C_0 will also be halved due to the reduction in area of the plates. For the two

sets of plates the equivalent circuit is as shown in Fig. 8.2D in which there are two driving circuits coupled through the mechanical elements C_M and L_M . The numbering of the terminals shown has to be resorted to in order that a voltage directed from 2 to 1 will produce the same mechanical velocity as that from 4 to 3. By dividing the plating in this manner another effect also occurs, namely, that the low frequency flexure mode will be driven. This follows from the fact that the plates 1, 2

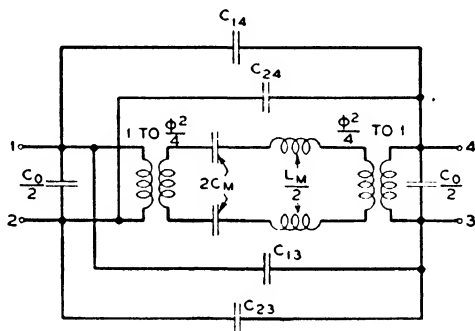


FIG. 8.3—COMPLETE EQUIVALENCE OF CRYSTAL WITH TWO SETS OF PLATES TAKING ACCOUNT OF STRAY CAPACITANCES.

will cause an elongation of the top of the crystal without any corresponding elongation of the bottom half. In general, however, the flexure mode is too low in frequency to interfere with the longitudinal mode and can be neglected. This illustrates the fact, however, that crystals with two sets of plates will excite more modes of motion than fully plated crystals.

As long as we neglect stray capacitances from the terminals the representation of Fig. 8.2D is exact and shows that voltages from 1 to 3 or 2 to 4, for example, will not excite any mechanical motion for there is no path for currents to flow or voltages to be applied. If account is taken of the stray capacitances the exact representation will be as shown in Fig. 8.3. Due to the symmetry of the crystal the capacitances C_{13} and C_{24} will be the same as will also the capacitances C_{14} and C_{23} . The network of Fig. 8.3 is shown in a balanced form since the electrical network is balanced.

There are four ways of connecting a crystal in a balanced network and these four methods are shown in Fig. 8.4. The

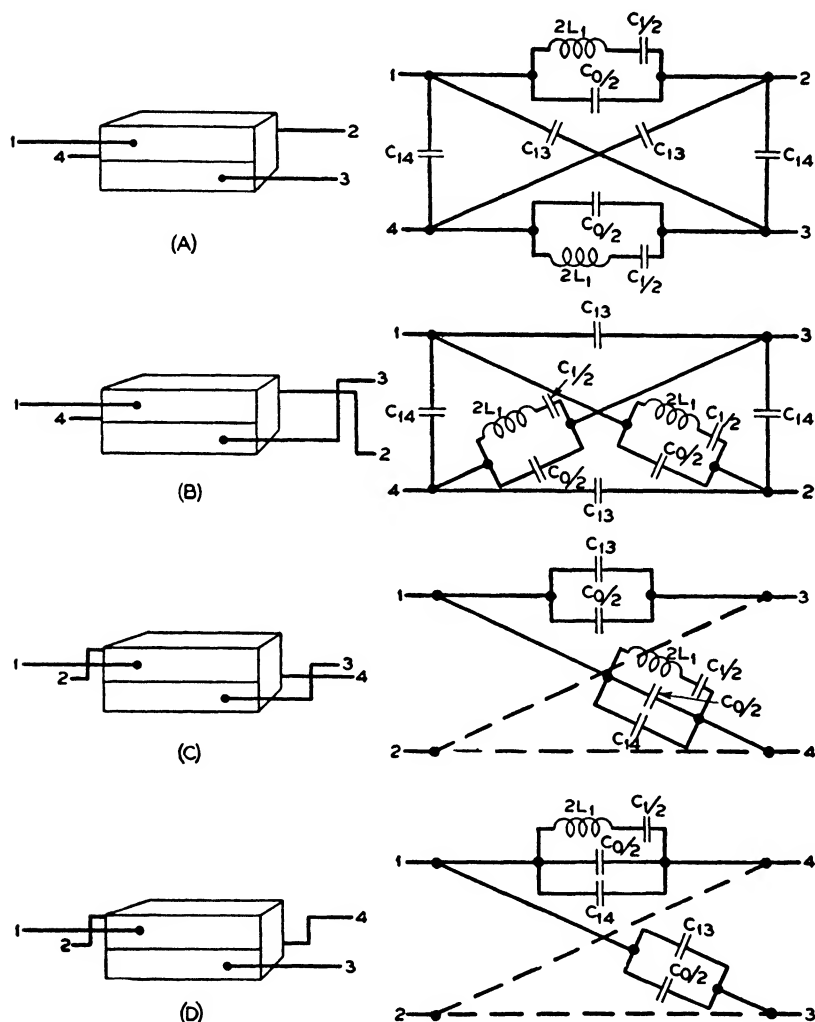


FIG. 8.4—METHODS FOR USING DOUBLE PLATE CRYSTALS IN BALANCED STRUCTURES.

equivalent circuits when used in a lattice network are shown on the right side of the figure. The last equivalence is easily worked out by applying Bartlett's theorem to the network of

Fig. 8.3. The next to the last equivalence is obtained by interchanging the terminals 3 and 4 of Fig. 8.3, and applying the network theorem of Fig. 2.8. The first two equivalences, however, involve a consideration of a perfect transformer.

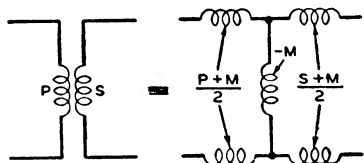


FIG. 8.5—EQUIVALENT H CIRCUIT OF A TRANSFORMER.

A perfect transformer is usually defined as a transformer which neither stores nor dissipates energy. Ideally, it would consist of a primary and secondary, each having an infinite in-

ductance and a mutual inductance equal to the square root of the product of the primary by the secondary. It has been shown⁵ that any transformer can be represented by the H network of Fig. 8.5. Applying this representation to Fig. 8.3, the first equivalence of Fig. 8.4 takes the form shown in Fig. 8.6. To reduce this to its equivalent lattice we employ

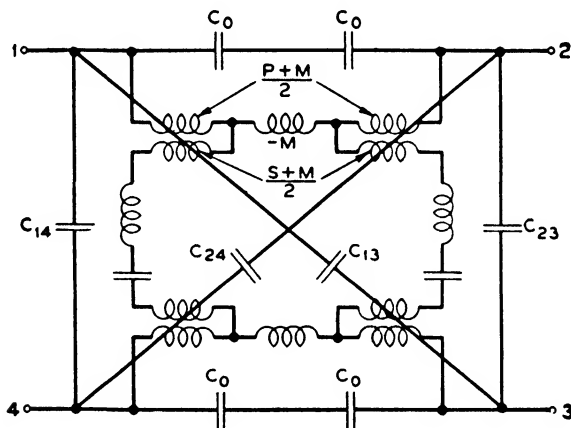


FIG. 8.6—EQUIVALENT CIRCUIT FOR CONNECTION OF FIG. 8.4.

the network theorem given on page 35. The lattice arm will evidently be C_{14} and C_{13} (assuming $C_{13} = C_{24}$ and $C_{14} = C_{23}$) since the rest of the open circuit arm will have the inductance

⁵ "Transmission Circuits for Telephone Communications," K. S. Johnson, p. 281, D. Van Nostrand.

$P + S + 2M$ in series which is an infinite impedance. The series arm reduces to the form shown in Fig. 8.7A. On

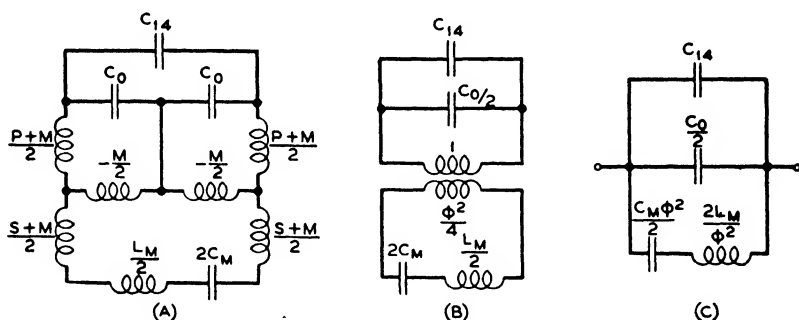


FIG. 8.7—RESULTANT SERIES IMPEDANCE FOR CONNECTION OF FIG. 8.4.

account of the symmetry of the circuit the wire 1, 2 carries no current and can be removed. The transformer then reduces to the perfect transformer of ratio 1 to $\varphi^2/4$ as shown in Fig.

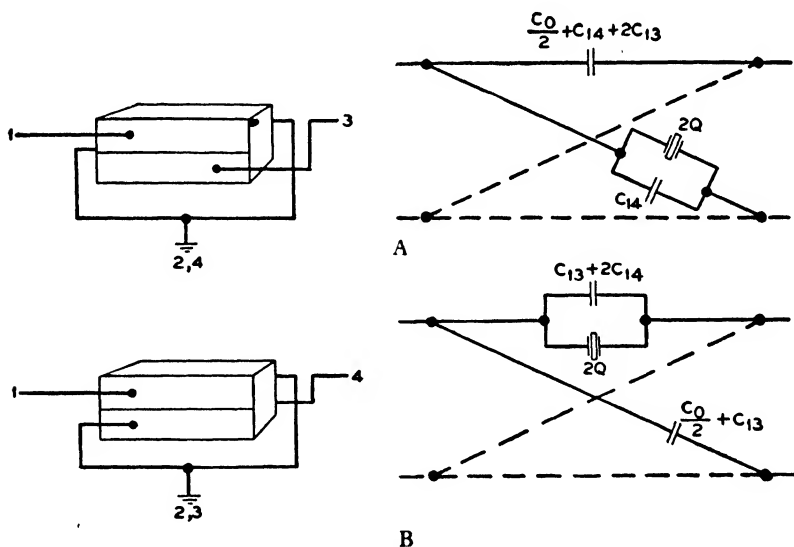


FIG. 8.8—METHODS FOR USING CRYSTAL WITH TWO SETS OF PLATES IN UNBALANCED CIRCUITS.

8.7B, and the impedance of the series arm is that of a crystal of twice the impedance of the fully plated crystal shunted by C_{14}

which proves the first equivalence of 8.4A. The second equivalence is proved in a similar manner.

A split-plating crystal is often used in an unbalanced form. The two possible connections are shown in Fig. 8.8, with their equivalent circuits. These are easily derived from Fig. 8.3 by applying Bartlett's theorem and the theorem of page 35. It will be noted that across the series arm of the equivalent lattice of Fig. 8.8A we have the extra capacitance $2C_{13}$ which is not balanced by anything in the lattice arm. This tends to

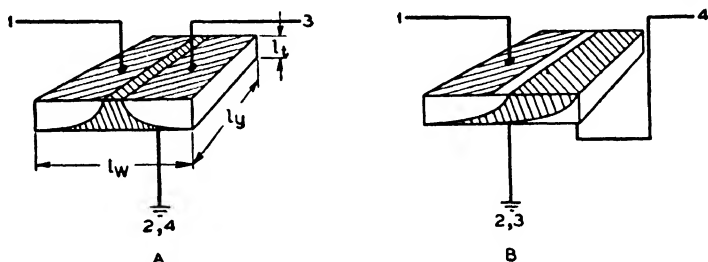


FIG. 8.9—METHODS FOR REDUCING STRAY CAPACITANCES.

limit the type of filter characteristic which can be obtained with such crystals. To keep the capacitance $2C_{13}$ low, shielding strips connected to the ground terminal 2, 4 are sometimes used to separate the plates 1, 3 as shown in Fig. 8.9A. These grounding strips act like a guard ring to reduce the stray capacitance. For the connection of Fig. 8.8B the stray capacitance $2C_{14}$ can be reduced by making the grounded plates 2, 3 slightly larger than 1, 4.

8.3. *Narrow Band Filters Employing Crystals and Condensers*

The values of the constants of the equivalent electrical circuit of the crystal given by equation (8.2) show that there is a definite ratio between the static capacitance C_0 and the motional capacitance of the crystal C_1 which depends on the electromechanical coupling existing in the crystal. For a -18.5° X-cut quartz crystal, this ratio is about 138. As a result of this high ratio, the reactance characteristic of a crystal will have an anti-resonant frequency f_A only 0.36 per cent in

frequency above the resonant frequency of the crystal. It is a consequence of this small separation that filters constructed from crystals alone or from crystals and condensers will of necessity

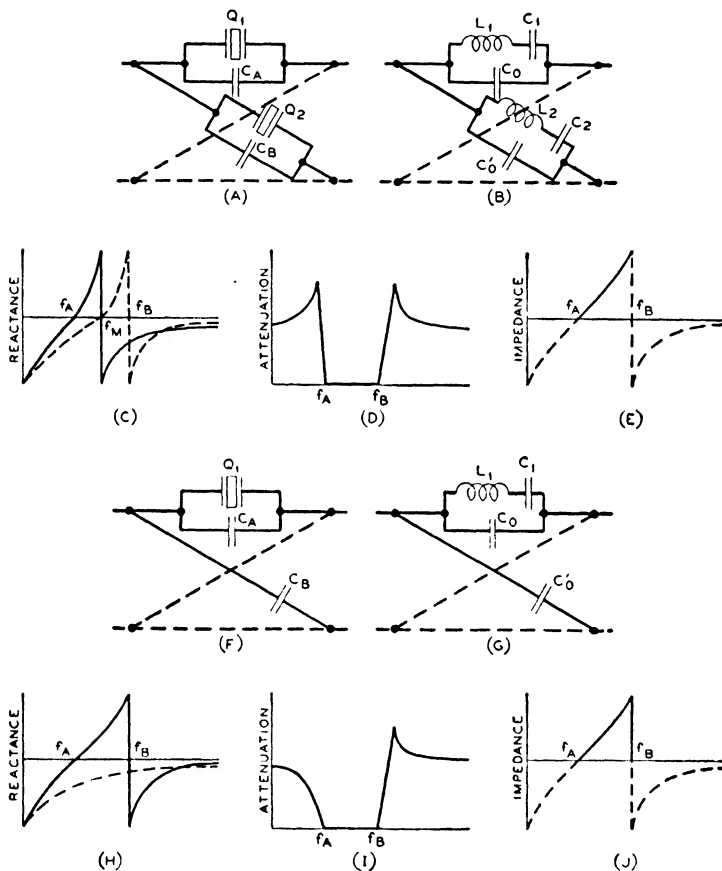


FIG. 8.10—NARROW BAND FILTERS EMPLOYING CRYSTALS AND CONDENSERS.

have pass bands whose widths are a small percentage of the mean frequency.

As pointed out in Chapter II, the most general filter characteristics are obtained by the use of lattice networks. Hence we shall consider first the use of crystals in lattice networks. If we limit ourselves to crystals and condensers, the only two networks are shown in Fig. 8.10. The lattice with the crystal in

each arm will produce the wider band and higher attenuation. In order that a single band shall result it is necessary that the resonance of one arm coincide with the anti-resonance of the other arm for then the reactances of the two arms are of opposite sign from the lowest resonance of one arm to the highest anti-resonance of the other arm. This frequency range will be at a maximum twice the separation between the resonance and anti-resonance of a single crystal or at most 0.72 per cent. This band width can always be made less than this by putting condensers in parallel with the crystals and the band widths can be adjusted in this manner. The attenuation characteristic and image impedance resulting are shown in Fig. 8.10 D and E. It is possible to obtain two attenuation peaks with this section and the attenuation is equal to the sum of the attenuation of two of the simple type sections discussed in Chapter II. If we solve for the element values in terms of the two values of m for the section, the image impedance at the mean frequency of the filter, and the two cutoff frequencies, the values are given by Table VIII.

TABLE VIII
DESIGN FORMULAE FOR NARROW BAND FILTERS

Element	Formula
C_0	$\frac{f_A(m_1 + m_2)}{2\pi Z_0(f_A^2 + m_1 m_2 f_B^2)}$
C_0'	$\frac{f_A^2 + m_1 m_2 f_B^2}{2\pi Z_0 f_A f_B^2 (m_1 + m_2)}$
C_1	$\frac{(m_1 + m_2)(m_1 m_2)(f_B^2 - f_A^2)}{2\pi Z_0 f_A (1 + m_1 m_2)(f_A^2 + f_B^2 m_1 m_2)}$
C_2	$\frac{f_B^2 - f_A^2}{2\pi Z_0 f_A f_B^2 (m_1 + m_2)}$
L_1	$\frac{Z_0(f_A^2 + m_1 m_2 f_B^2)^2}{2\pi f_A f_B^2 (m_1 + m_2) m_1 m_2 (f_B^2 - f_A^2)}$
L_2	$\frac{Z_0 f_B^2 (m_1 + m_2)}{2\pi f_A (f_B^2 - f_A^2)}$

Since in this table

$$m = \sqrt{\frac{1 - f_{\infty}^2/f_B^2}{1 - f_{\infty}^2/f_A^2}}$$

one of the sections can be made to disappear by letting $m = 0$ or ∞ since then the peak will come at the upper or lower cutoff and no attenuation would be added by the section. For $m_2 \rightarrow 0$, $L_1 \rightarrow 0$ and $C_1 \rightarrow 0$, so that the series arm would contain only the condenser C_0 , while if $m_2 \rightarrow \infty$, $C_2 \rightarrow 0$ and $L_2 \rightarrow \infty$, giving only the condenser C_0' in the lattice arm which corresponds to

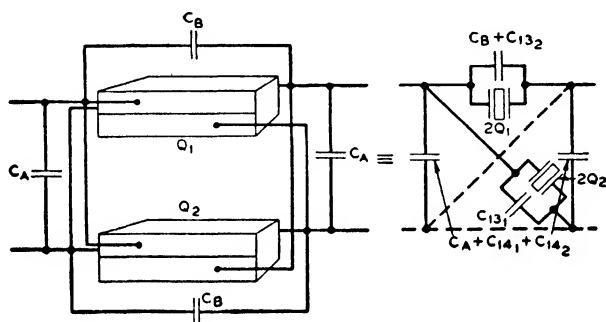


FIG. 8.11—NARROW BAND FILTER EMPLOYING DIVIDED PLATE CRYSTALS.

the second case shown in Fig. 8.10F. The one crystal filter will have only half the band width of the two crystal section and an attenuation corresponding to one of the simple sections discussed in Chapter II.

When a balanced filter can be used, by far the largest number of narrow band crystal filters are constructed by using the balanced lattice filter of Fig. 8.10A. To save crystals, this section is usually constructed from two crystals with two sets of platings connected as shown in Fig. 8.11. As shown by Fig. 8.4 this connection is the equivalent of Fig. 8.10A. The condensers C_A are used to adjust the band widths while the condensers C_B adjust the position of the attenuation peaks. Fig. 8.12 shows a measured characteristic of a five cycle filter constructed from one section of this kind and used in a commercial noise and vibration analyzer.

When an unbalanced filter is desired, several methods can be

employed. For certain values of m and band widths the filter of Fig. 8.10A can be reduced to a T network with equal crystals

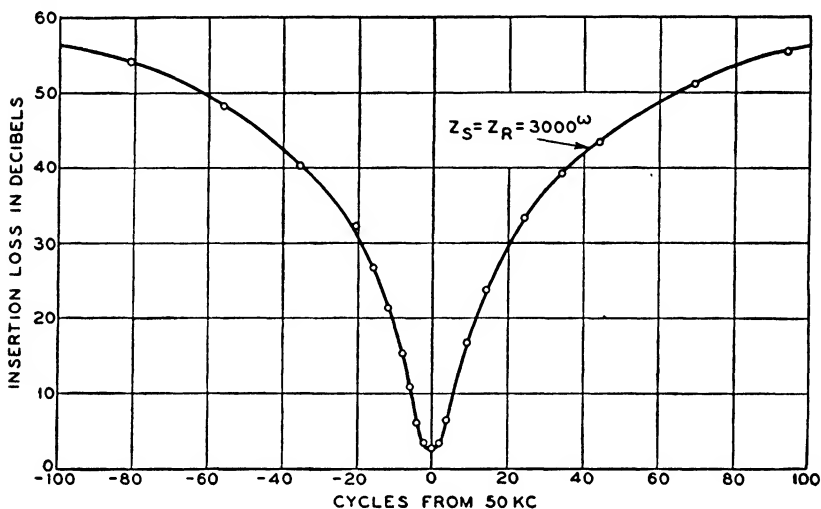


FIG. 8.12—ATTENUATION CHARACTERISTIC OF NARROW BAND FILTER.

in the series arms and a different crystal in the shunt arm having its anti-resonance at the resonance of the series arm. Another method sometimes used is to employ a three-winding transformer with separate crystals—employed for the impedances

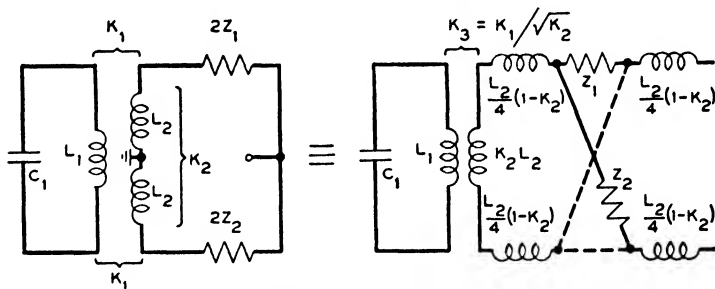


FIG. 8.13—HYBRID COIL TYPE OF FILTER.

Z_1 and Z_2 —in the output as shown in Fig. 8.13. If there is a high coupling in the secondary this can be shown⁶ to be equiva-

⁶ "Resistance Compensated Band Pass Crystal Filters for Unbalanced Circuits," W. P. Mason, B.S.T.J., October 1937, p. 423.

lent to a lattice of the type shown in Fig. 8.10A and a transformer. To obtain this characteristic, however, a close balance of the two output coils has to be maintained. Probably the simplest and most satisfactory method is to use two crystals in parallel, one connected as shown in Fig. 8.8A and the other as in Fig. 8.8B. This combination will give the same attenuation characteristic as the balanced combination of Fig. 8.11 but will be limited to half the band width possible with the circuit of Fig. 8.11.

8.4. *Wide Band Pass Crystal Filters Employing Coils as Well as Crystals and Condensers*

The filters described in section (8.3) are useful for single frequencies or narrow bands of frequencies but cannot be made

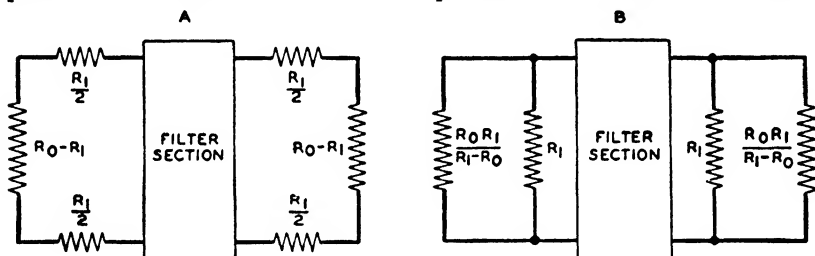


FIG. 8.14—FILTER SECTIONS WITH ALL RESISTANCES ON ENDS OF FILTER.

wide enough to pass voice bands such as are useful in radio and carrier telephony. In order to get wider bands it is necessary to employ coils as well as crystals and condensers. Since the ratio of reactance to resistance of the best coils mounted in a reasonable space does not exceed 400, attention must be given to the effect of dissipation.

In a filter the effect of dissipation is twofold. It may add a constant loss to the insertion loss characteristic of the filter, and it may cause a loss varying with frequency in the transmitting band of the filter. The second effect is much more serious for most systems since an additive loss can be overcome by the use of vacuum tube amplifiers whereas the second effect limits the slope of the insertion loss frequency curve. Hence if the dissipation in the coils needed to widen the band of the filter pro-

duces only an additive loss which is independent of the frequency a satisfactory result is obtained.

If all the dissipation is concentrated on the ends of the filter section, either in series or in parallel as shown in Fig. 8.14, this result will be obtained. This follows from the fact that the

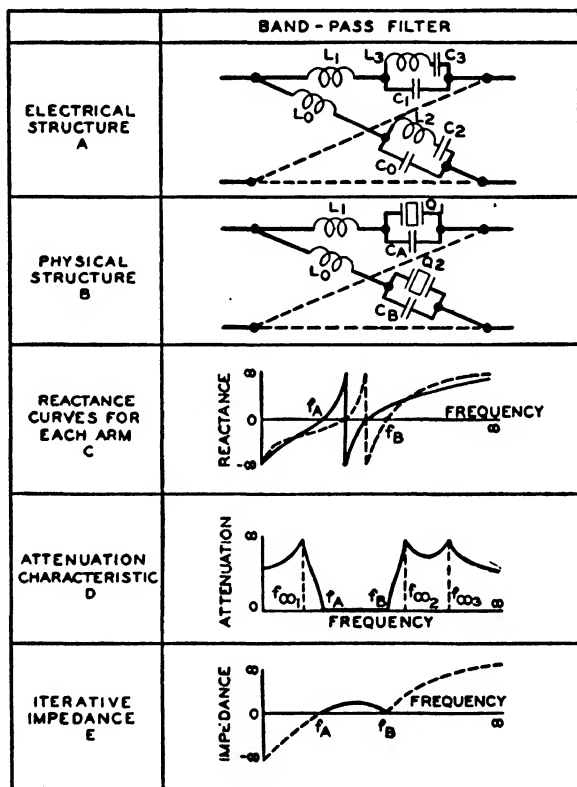


FIG. 8.15—WIDE BAND CRYSTAL FILTER EMPLOYING SERIES COILS.

terminating resistance can be altered to incorporate these resistances in the termination so that we have in effect a resistanceless filter section terminated in its correct impedances. The added resistance then merely causes a constant loss at all frequencies. Between sections the resistances on the ends of the filter can be incorporated with other resistances in such a way as to make a constant resistance attenuator of essentially the same impedance as the filter. For a series coil this can be done

by putting a shunt resistance between sections while for a shunt coil it can be done by putting series resistances between sections.

Suppose that we consider first a lattice network with series coils in each arm as shown in Fig. 8.15B, the remainder of each arm consisting of a crystal in parallel with a condenser. If we place a coil in series with a crystal the sum of the reactances of the two are given by

$$X = j\omega L_1 + \frac{-j}{\omega(C_1 + C_3)} \left(\frac{1 - \omega^2/\omega_R^2}{1 - \omega^2/\omega_A^2} \right)$$

where

$$\omega_R^2 = \frac{1}{L_3 C_3} \quad (8.10)$$

$$\omega_A^2 = \frac{(C_1 + C_3)}{L_3 C_3 C_1} = \omega_R^2 \left[1 + \frac{C_3}{C_1} \right].$$

If we add these reactances and express the numerator as a factor we have

$$X = \frac{-j}{\omega(C_1 + C_3)} \left[\frac{1 - \omega^2(L_1 C_1 + C_3(L_1 + L_3)) + \omega^4 L_1 L_3 C_1 C_3}{1 - \omega^2/\omega_A^2} \right]$$

$$= \frac{-j}{\omega(C_1 + C_3)} \left(\frac{\left(1 - \frac{\omega^2}{\omega_1^2}\right) \left(1 - \frac{\omega^2}{\omega_3^2}\right)}{1 - \omega^2/\omega_2^2} \right) \quad (8.11)$$

where

$$\omega_1^2 = \frac{1}{2} [\omega_A^2 + \omega_\alpha^2 - \sqrt{(\omega_A^2 + \omega_\alpha^2)^2 - 4\omega_\alpha^2 \omega_R^2}]$$

$$= \frac{1}{2} \left[\frac{\left\{ L_1(C_1 + C_3) + L_3 C_3 - \sqrt{(L_1(C_1 + C_3) + L_3 C_3)^2 - 4L_1 L_3 C_1 C_3} \right\}}{L_1 L_3 C_1 C_3} \right]$$

$$\omega_2^2 = \omega_A^2 = \frac{C_1 + C_3}{L_3 C_3 C_1}$$

$$\omega_3^2 = \frac{1}{2} [\omega_A^2 + \omega_\alpha^2 + \sqrt{(\omega_A^2 + \omega_\alpha^2)^2 - 4\omega_\alpha^2 \omega_R^2}]$$

$$= \frac{1}{2} \left[\frac{\left\{ L_1(C_1 + C_3) + L_3 C_3 + \sqrt{(L_1(C_1 + C_3) + L_3 C_3)^2 - 4L_1 L_3 C_1 C_3} \right\}}{L_1 L_3 C_1 C_3} \right]$$

and $\omega_\alpha^2 = \frac{1}{L_1 C_1}$. Taking the product of $\omega_1 \omega_3$ we find

$$\omega_1 \omega_3 = \omega_\alpha \omega_R. \quad (8.12)$$

If we wish to make the resonances symmetrical about the anti-resonance frequency of the crystal it is necessary to let L_1 resonant C_1 at f_A the anti-resonant frequency of the crystal. Under this condition

$$f_{1,3}^2 = f_A^2 \left[1 \mp \sqrt{1 - \frac{\omega_R^2}{\omega_A^2}} \right] = f_A^2 \left[1 \mp \sqrt{\frac{C_3}{C_1}} \right]. \quad (8.13)$$

Hence for the crystal in which the ratio $C_1/C_3 = r = 138$, the two resonances will occur at

$$f_1 = 0.9542f_A; \quad f_3 = 1.0415f_A; \quad f_3/f_1 = 1.0915. \quad (8.14)$$

By putting a coil in series with a crystal we have introduced two resonances in place of one and have separated them by 9.15 per cent.

The filter of Fig. 8.15B has a combination of this sort in each arm. To make a single band-pass filter we have to have the resonances of one arm coincide with the anti-resonances of the other and vice versa as shown in Fig. 8.15C. The ratio between the highest resonance in one arm and the lowest resonance in the other arm will be

$$\frac{f_3}{f_1} = 1.0915 \times 1.0415 = 1.137. \quad (8.15)$$

Since the signs of the reactances of the two arms are opposite throughout the whole region, it is possible to obtain a pass band nearly 14 per cent wide.

This configuration meets the requirements that all the dissipation shall be on the ends of the filter section. If the resistances of the two coils are equal they can be taken out on the ends by the network relation of Fig. 2.9A. If they are not equal they can be made equal by adding a separate resistance to the arm with the lowest equivalent resistance. The attenuation characteristic obtainable is shown in Fig. 8.15D. The reactance of the two arms can be made to coincide three times so that three attenuation peaks will result. The total amount of attenuation is equal to that for three simple sections of the type discussed in Chapter II. The image impedance as shown by Fig. 8.15E is zero at the two edges of the band and be-

comes a large reactance when the frequency is outside the pass band. This impedance characteristic is suitable for paralleling with other filters of the same kind without introducing losses from the parallel circuits.

To determine the eight elements of the filter we have the six quantities, $m_1, m_2, m_3, f_A, f_B, Z_0$ and the two conditions that the lowest resonance of one arm coincides with the anti-resonance of the second arm while the higher resonance of the second arm coincides with the anti-resonance of the first arm. The elements of any one arm are determined in terms of the critical frequencies of the network and the value of the arm at zero frequency by the equations (8.11) so that the element values can be determined when the initial frequencies are specified.

The method for specifying the critical frequencies in terms of the m values of a two-section network was discussed in section (2.6), page 51. To obtain the critical frequencies for networks representing more equivalent sections it is only necessary to obtain the hyperbolic tangent of the sum of a number of sections. The largest number that can be expressed in terms of algebraic functions is five. If we carry out this process for five sections it is easily shown ⁷ that the expression for the propagation constant becomes

$$\begin{aligned} \tanh \frac{(\theta_1 + \theta_2 + \theta_3 + \theta_4 + \theta_5)}{2} \\ = \frac{A + C + E}{1 + B + D} \sqrt{\frac{(1 - \omega^2/\omega_A^2)(1 - \omega^2/\omega_3^2)^2(1 - \omega^2/\omega_5^2)^2}{(1 - \omega^2/\omega_2^2)^2(1 - \omega^2/\omega_4^2)^2(1 - \omega^2/\omega_B^2)}} \end{aligned} \quad (8.16)$$

where

$$A = \sum_{n=1}^5 m_n = m_1 + m_2 + m_3 + m_4 + m_5$$

$$B = \sum_{n=1}^5 \sum_{o=1}^5 m_n m_o = m_1(m_2 + m_3 + m_4 + m_5)$$

$$+ m_2(m_3 + m_4 + m_5) + m_3(m_4 + m_5) + m_4 m_5; \quad n \neq o$$

⁷ "Electrical Wave Filters Employing Crystals with Normal and Divided Electrodes," W. P. Mason and R. A. Sykes, B.S.T.J., April 1940, p. 221.

$$C = \sum_{n=1}^5 \sum_{o=1}^5 \sum_{p=1}^5 m_n m_o m_p; \quad n \neq o; \quad n \neq p; \quad o \neq p$$

$$D = \sum_{n=1}^5 \sum_{o=1}^5 \sum_{p=1}^5 \sum_{q=1}^5 m_n m_o m_p m_q; \quad n \neq o, p, q; \quad o \neq p, q; \quad p \neq q$$

$$E = m_1 m_2 m_3 m_4 m_5.$$

The critical frequencies (i.e., the resonant or anti-resonant frequencies of the network coming between f_A and f_B) are given by

$$f_2^2 = \frac{2f_A^2 f_B^2 (1 + B + D)}{f_A^2 (2 + B - \sqrt{B^2 - 4D}) + f_B^2 (B + 2D + \sqrt{B^2 - 4D})}$$

$$f_4^2 = \frac{2f_A^2 f_B^2 (1 + B + D)}{f_A^2 (2 + B + \sqrt{B^2 - 4D}) + f_B^2 (B + 2D - \sqrt{B^2 - 4D})} \quad (8.17)$$

$$f_3^2 = \frac{2f_A^2 f_B^2 (A + C + E)}{f_A^2 (2A + C - \sqrt{C^2 - 4AE}) + f_B^2 (C + 2E + \sqrt{C^2 - 4AE})}$$

$$f_5^2 = \frac{2f_A^2 f_B^2 (A + C + E)}{f_A^2 (2A + C + \sqrt{C^2 - 4AE}) + f_B^2 (C + 2E - \sqrt{C^2 - 4AE})}.$$

For the filter under consideration which has three equivalent sections, we have only two critical frequencies f_2 and f_3 . We can get these from the above equations by letting $m_4 = m_5 = 0$. Then

$$A = m_1 + m_2 + m_3 \quad C = m_1 m_2 m_3$$

$$B = m_1(m_2 + m_3) + m_2 m_3 \quad D = E = 0. \quad (8.18)$$

The critical frequencies become

$$f_2^2 = \frac{f_A^2 f_B^2 (1 + B)}{f_A^2 + f_B^2 (B)}; \quad f_3^2 = \frac{f_A^2 f_B^2 (A + C)}{A f_A^2 + C f_B^2}; \quad f_4^2 = f_5^2 = f_B^2 \quad (8.19)$$

and the expression for the propagation constant becomes

$$\tanh \frac{(\theta_1 + \theta_2 + \theta_3)}{2} = \frac{(A + C)}{(1 + B)} \sqrt{\frac{(1 - \omega^2/\omega_A^2)(1 - \omega^2/\omega_3^2)^2}{(1 - \omega^2/\omega_2^2)^2(1 - \omega^2/\omega_B^2)}}. \quad (8.20)$$

The impedance of each arm has the form of the expression of (8.11). If we let the series arm have its first resonance at ω_A while the lattice arm has its last resonance at ω_B , the image impedance of the structure becomes

$$Z_I = \sqrt{\frac{-(1 - \omega^2/\omega_A^2)(1 - \omega^2/\omega_B^2)}{\omega^2(C_1 + C_3)(C_0 + C_2)}}. \quad (8.21)$$

At the mean frequency $\sqrt{f_A f_B}$, this becomes

$$Z_{I_0} = \frac{(f_B - f_A)}{2\pi f_A f_B \sqrt{(C_0 + C_2)(C_1 + C_3)}}. \quad (8.22)$$

At zero frequency the ratio of the two arms becomes

$$\frac{Z_1}{Z_2} = \sqrt{\frac{C_0 + C_2}{C_1 + C_3}} = \tanh \frac{(\theta_1 + \theta_2 + \theta_3)_0}{2} = \frac{A + C}{1 + B}. \quad (8.23)$$

Equations (8.22) and (8.23) determine the two capacitances $C_0 + C_2$ and $C_1 + C_3$. The remainder are determined by the

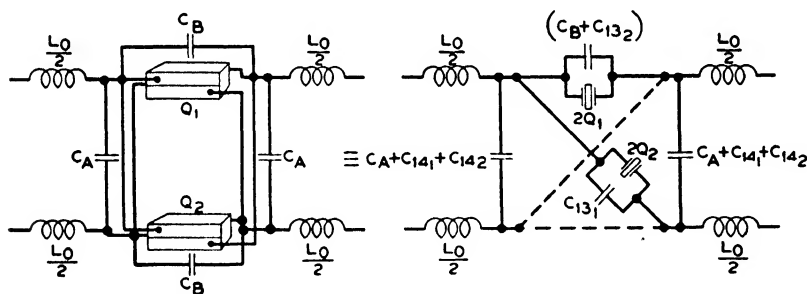


FIG. 8.16—WIDE BAND CRYSTAL FILTER EMPLOYING CRYSTALS WITH TWO SETS OF PLATES.

relations of (8.11) and (8.19). Solving for all the element values we have the design equations given in Table IX.

In case one of the peaks comes at infinity or $m_3 = f_A/f_B$ it is readily shown that L_0 and L_1 are equal. By the network theorem of Fig. 2.9A, these coils can be taken outside of the lattice in series with it. All the common capacitances of the two arms can then be taken outside of the lattice and placed in shunt with it by virtue of Fig. 2.9B. There remain then in

the lattice four crystals, two alike in the series arms and two alike in the lattice arms, and a small capacitance C_B which usually comes across the series arms. By employing crystals with two sets of platings the two identical series and lattice crystals can be replaced by single crystals with two platings thus reducing the required number of crystals by half. In a similar manner the two balanced coils on the ends of the filter can be ob-

TABLE IX
DESIGN FORMULAE FOR WIDE BAND CRYSTAL FILTER

Element	Formula
L_0	$\frac{Z_0 f_B (f_A^2 A + f_B^2 C)}{2\pi f_A (f_B - f_A) (f_A^2 + f_B^2 B)}$
L_1	$\frac{Z_0 f_A (f_A^2 + f_B^2 B)}{2\pi f_B (f_B - f_A) (f_A^2 A + f_B^2 C)}$
L_2	$\frac{Z_0 [f_B^4 (B(A + C) - C) + 2f_A^2 f_B^2 C + f_A^4 A]^2}{2\pi f_A f_B (f_B - f_A)^3 (f_B + f_A)^2 [f_A^2 + B f_B^2] (AB - C)}$
L_3	$\frac{Z_0 [f_B^4 BC + 2f_A^2 f_B^2 + f_A^4]^2 (A(1 + B) - C)}{2\pi f_A f_B (f_B - f_A)^3 (f_B + f_A)^2 (A f_A^2 + C f_B^2) C (AB - C)}$
C_0	$\frac{(f_B - f_A) (f_A^2 + B f_B^2)^2}{2\pi Z_0 f_A f_B [f_B^4 (B(A + C) - C) + 2f_A^2 f_B^2 C + f_A^4 A]}$
C_1	$\frac{(f_B - f_A) (A f_A^2 + C f_B^2)^2}{2\pi Z_0 f_A f_B [f_B^4 BC + 2f_A^2 f_B^2 C + f_A^4 (A(1 + B) - C)]}$
C_2	$\frac{(AB - C) (f_B - f_A)^3 (f_B + f_A)^2}{2\pi Z_0 f_A f_B [f_B^4 (B(A + C) - C) + 2f_A^2 f_B^2 C + f_A^4 A] (A + C)}$
C_3	$\frac{C (AB - C) (f_B - f_A)^3 (f_B + f_A)^2}{2\pi Z_0 f_A f_B [f_B^4 BC + 2f_A^2 f_B^2 C + f_A^4 (A(1 + B) - C)] (1 + B)}$

tained from a single coil with two balanced windings so that the total number of elements per section is 2 coils, 4 condensers and 2 crystals. The usual arrangement is shown in Fig. 8.16. Filters composed of sections of this type have been used very extensively in carrier and radio systems, whenever it is desirable to obtain a rapid rise of attenuation with frequency, or a narrow band width on a percentage basis.

Filters of this type result in a low image impedance which usually runs from 600 ohms to 25 ohms in the frequency range 60 kilocycles to 500 kilocycles. Whenever it is desirable to obtain high impedance filters, which is the case, for example, when

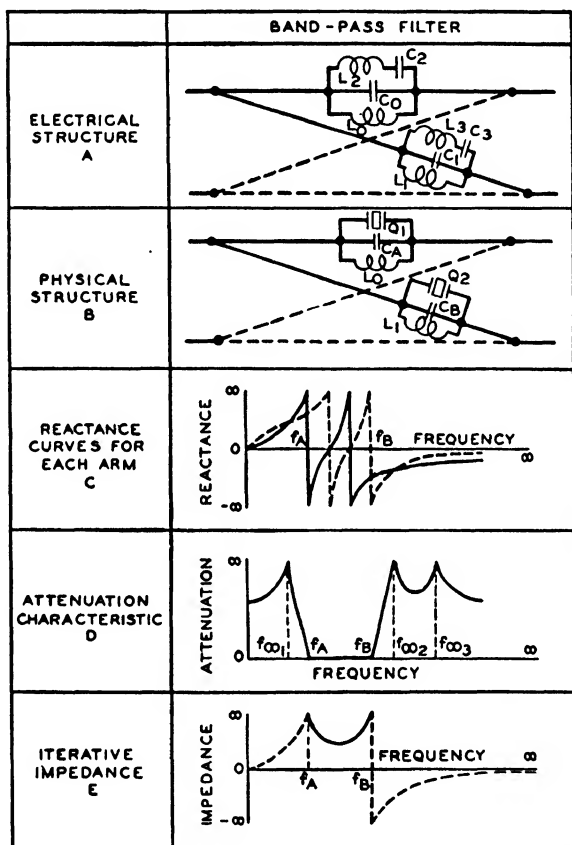


FIG. 8.17—WIDE BAND CRYSTAL FILTER EMPLOYING SHUNT COILS.

such filters are to be used between vacuum tubes, this type of section is not advantageous. For high impedance networks the series coils are replaced by shunt coils. The resulting filter network and its characteristics are shown in Fig. 8.17. The method for evaluating the elements is entirely similar to that for the series case and the resulting element values are given by Table X.

TABLE X

DESIGN FORMULAE FOR CRYSTAL FILTER WITH SHUNT COILS

Element	Formula
L_0	$\frac{Z_0(f_B - f_A)(1 + B)}{2\pi f_A f_B(A + C)}$
L_1	$\frac{Z_0(f_B - f_A)(A + C)}{2\pi f_A f_B(1 + B)}$
L_2	$\frac{Z_0(1 + B)(f_A^2 + Bf_B^2)^2}{2\pi f_A f_B(f_B - f_A)(f_B + f_A)^2(AB - C)}$
L_3	$\frac{Z_0(A + C)(Af_A^2 + Cf_B^2)^2}{2\pi f_A f_B(f_B - f_A)(f_B + f_A)^2C(AB - C)}$
C_0	$\frac{(Af_A^2 + Cf_B^2)f_B}{2\pi Z_0 f_A(f_B - f_A)(f_A^2 + Bf_B^2)}$
C_1	$\frac{f_A(f_A^2 + Bf_B^2)}{2\pi Z_0 f_B(f_B - f_A)(Af_A^2 + Cf_B^2)}$
C_2	$\frac{(f_B - f_A)(f_B + f_A)^2(AB - C)}{2\pi Z_0 f_A f_B(f_A^2 + Bf_B^2)(1 + B)^2}$
C_3	$\frac{(f_B - f_A)(f_B + f_A)^2C(AB - C)}{2\pi Z_0 f_A f_B(A + C)^2(Af_A^2 + Cf_B^2)}$

In this table A , B and C have the significance shown in equation (8.18).

The procedure in designing a crystal filter from the element value equations given in Tables IX and X is as follows. The m values to give the required insertion loss characteristics are first determined. Next the crystal motional capacitances C_2 and C_3 are determined and an image impedance Z_0 selected of such a magnitude that these capacitances can be realized with practically obtainable crystals. This can be determined by using the value of the capacitance C_1 in equation (8.2) for a fully plated crystal or half that value for a split plating crystal. Next the other element values are calculated and the whole filter determined.

In case it is desired to obtain the band-pass filter in an unbalanced form this may be done in several ways.⁸ Probably the simplest and most effective way is to use crystals with two sets of plates with grounded electrodes connected as shown in

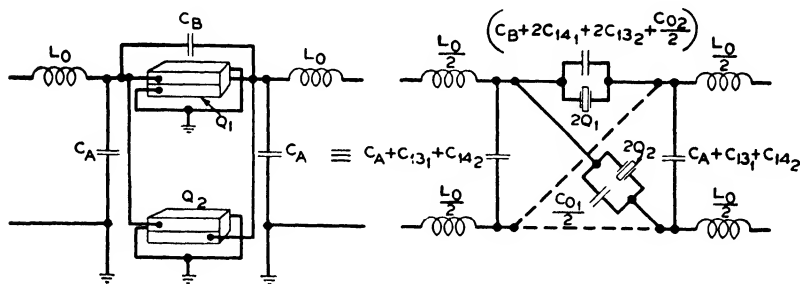


FIG. 8.18—WIDE BAND UNBALANCED CRYSTAL FILTER EMPLOYING CRYSTALS WITH TWO SETS OF PLATES.

Fig. 8.8. By employing the two connections shown in this figure together with coils and condensers, as shown in Fig. 8.18, all of the attenuation characteristics of a balanced lattice filter can be obtained but the band width is limited to 9.5 per cent of the lower cutoff frequency.

Since practically all the loss in crystal filter sections of this kind is caused by the resistances associated with the coils required to widen the bands of the filters, it would be desirable to

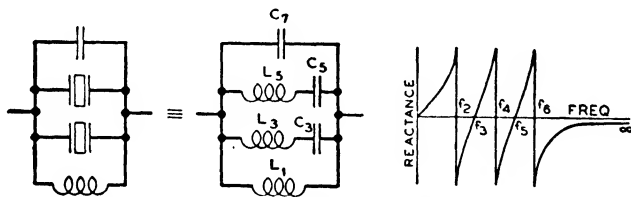


FIG. 8.19—IMPEDANCE OF TWO CRYSTALS IN PARALLEL SHUNTED BY A COIL.

be able to increase the losses due to the crystal portions. This can be accomplished by using more crystals than one in the

⁸ A number of methods are discussed in the paper "Resistance Compensated Band Pass Crystal Filters for Unbalanced Circuits," W. P. Mason, B.S.T.J., October 1937.

series or lattice arms of the filter. The impedance of a coil in parallel with a parallel combination of two crystals and a condenser is shown in Fig. 8.19. We have now three anti-resonant frequencies and two resonant frequencies. The question arises as to whether the band width obtainable with a filter using more than one crystal per arm is different than for a section using one crystal per arm. By employing Foster's theorem,⁹

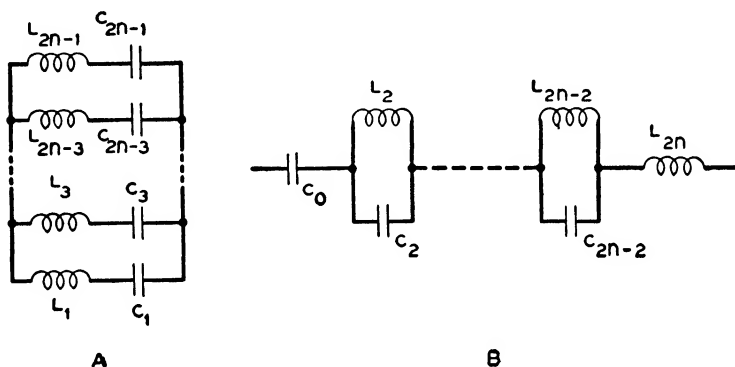


FIG. 8.20—COMBINATION OF IMPEDANCES FOR APPLYING FOSTER'S THEOREM.

relating the element values of a network to the critical frequencies, it can be proved that the same limitations hold.

Foster's theorem deals with impedances in the form of a number of series resonant circuits in parallel as shown in Fig. 8.20A or a number of anti-resonant circuits in series as shown in Fig. 8.20B. In either case the impedance of the network can be written in the form

$$Z = -jH \left[\frac{\left(1 - \frac{\omega^2}{\omega_1^2}\right) \left(1 - \frac{\omega^2}{\omega_3^2}\right) \times \cdots \times \left(1 - \frac{\omega^2}{\omega_{2n-1}^2}\right)}{\omega \left(1 - \frac{\omega^2}{\omega_2^2}\right) \times \cdots \times \left(1 - \frac{\omega^2}{\omega_{2n-2}^2}\right)} \right] \quad (8.24)$$

where $H \geq 0$ and $0 = \omega_0 \leq \omega_1 \leq \cdots \leq \omega_{2n-1} \leq \omega_{2n} = \infty$.

That is, the impedance consists of a series of resonant frequencies ω_1, ω_3 , etc., between which are a series of anti-resonant

⁹ "A Reactance Theorem," R. Foster, B.S.T.J., April 1924, p. 259.

frequencies $\omega_2, \omega_4 \dots$, etc. For the series resonant circuits of Fig. 8.20A, the element values are given by

$$L_i = \frac{1}{C_i \omega_i^2} = \left(\lim_{\omega \rightarrow \omega_i} \right) \left(\frac{j\omega Z}{\omega_i^2 - \omega^2} \right); \quad i = 1, 3, \dots, 2n-1. \quad (8.25)$$

If the last resonant frequency occurs at ∞ or $\omega_{2n-1} = \infty$, one of the coils will drop out. Formula (8.25) contains this as the limiting case and shows that the value of the condenser will be

$$C_{2n-1} = \frac{1}{H} \left(\frac{\omega_1^2 \omega_3^2 \times \dots \times \omega_{2n-3}^2}{\omega_2^2 \omega_4^2 \times \dots \times \omega_{2n-2}^2} \right). \quad (8.26)$$

For the case where the lowest resonance ω_1 coincides with zero frequency, the condenser C_1 disappears and the value of the coil L_1 is

$$L_1 = H. \quad (8.27)$$

The equivalent formula for the anti-resonant circuits in series is

$$C_i = \frac{1}{L_i \omega_i^2} = \left(\lim_{\omega \rightarrow \omega_i} \right) \left(\frac{j\omega}{Z(\omega_i^2 - \omega^2)} \right); \quad i = 0, 2, 4, \dots, 2n. \quad (8.28)$$

These values include the limiting values

$$C_0 = \frac{1}{H}; \quad L_0 = \infty; \quad C_{2n} = 0; \quad L_{2n} = \frac{H(\omega_2^2 \omega_4^2 \times \dots \times \omega_{2n-2}^2)}{(\omega_1^2 \omega_3^2 \times \dots \times \omega_{2n-1}^2)}. \quad (8.29)$$

In applying the formula let us consider first the case of two crystals in parallel to see if the use of more than one crystal in an arm can broaden the band width possible with crystals alone. The equivalent circuit of the two crystals in parallel will be similar to Fig. 8.20A with two series resonant combinations L_1, C_1 and L_3, C_3 in parallel with a capacitance C_5 . From the crystal point of view the limitation is the same as before, namely, that

$$r = C_5 / (C_1 + C_3) = 138 \quad (8.30)$$

or the sum of the static capacitances of the two crystals divided by the sum of the motional capacitances is still equal to 138 for a

—18.5° *X*-cut filter crystal. From (8.25) and (8.26) the values of the three elements are

$$C_1 = \frac{\left(1 - \frac{\omega_1^2}{\omega_2^2}\right)\left(1 - \frac{\omega_1^2}{\omega_4^2}\right)}{H\left(1 - \frac{\omega_1^2}{\omega_3^2}\right)}; \quad C_3 = \frac{\left(\frac{\omega_3^2}{\omega_2^2} - 1\right)\left(1 - \frac{\omega_3^2}{\omega_4^2}\right)}{H\left(\frac{\omega_3^2}{\omega_1^2} - 1\right)};$$

$$C_5 = \frac{\omega_1^2 \omega_3^2}{H \omega_2^2 \omega_4^2}. \quad (8.31)$$

Taking the ratio of $C_5/(C_1 + C_3)$ we have after adding terms

$$\left(\frac{C_5}{C_1 + C_3}\right) = \left(\frac{\omega_2^2 \omega_4^2}{\omega_1^2 \omega_3^2}\right) - 1 = \frac{1}{138} \quad \text{or} \quad \frac{\omega_2}{\omega_1} \times \frac{\omega_4}{\omega_3}$$

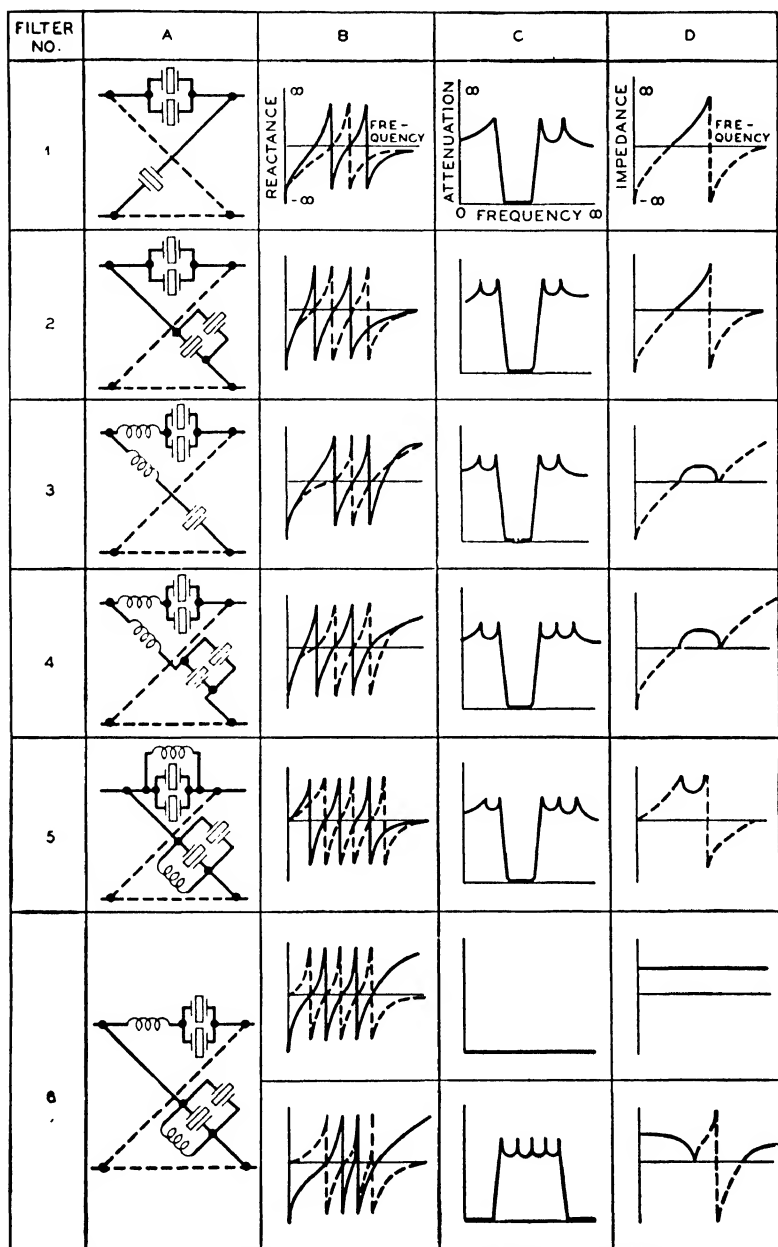
$$= \sqrt{1 + \frac{1}{138}} \doteq 1 + \frac{1}{276}. \quad (8.32)$$

Hence the ratio of the first anti-resonance to the first resonance, times the ratio of the second anti-resonance to the second resonance for two crystals in parallel is the same as the ratio of the anti-resonance to resonance for a single crystal. If we connect two crystals in the lattice arm, the disposition of resonances and anti-resonances for a single band is as shown in Fig. 8.21 for the second filter in the B column. The ratio between the last anti-resonance of the lattice arm to the first resonance of the series arm will then be

$$\frac{f_A}{f_R} = 1 + \frac{1}{138} = 1.00725 \quad (8.33)$$

so that the addition of more crystals will not widen the band.

As shown by the first two filters of Fig. 8.21, the addition of crystals will, however, increase the number of simple sections that can be obtained in one lattice section. The addition of one crystal in the series arm adds the equivalent of one simple type band-pass section as discussed in Chapter II. The addition of another crystal in the lattice arm adds another section so that the second filter of Fig. 8.21 has the equivalent of four simple



NOTE -- IN COLUMN D, DOTTED LINES INDICATE REACTIVE IMPEDANCE
SOLID LINES INDICATE RESISTIVE IMPEDANCE

FIG. 8.21—CRYSTAL FILTERS EMPLOYING MORE THAN ONE CRYSTAL IN AN ARM

sections. The method of designing these more complicated sections is obvious from the above work. First the disposition of the m values is made to obtain the desired attenuation characteristic. Next the critical resonant and anti-resonant frequencies are determined from equation (8.17). From these and the desired characteristic impedance at mid-band all of the element values can be obtained from Foster's theorem.

We next consider the characteristics of several crystals in one arm when a coil is used to widen the band. The simplest case to consider is the case of a coil in parallel with two crystals as shown in Fig. 8.19 since the configuration is covered by Foster's theorem. It can be shown also that the limitations for a series coil are the same. For the combination of coil and crystals in parallel the impedance Z has the form

$$Z = j\omega H \left[\frac{(1 - \omega^2/\omega_3^2)(1 - \omega^2/\omega_5^2)}{(1 - \omega^2/\omega_2^2)(1 - \omega^2/\omega_4^2)(1 - \omega^2/\omega_6^2)} \right]. \quad (8.34)$$

From Foster's theorem the element values for the arm become

$$\begin{aligned} L_1 = H; \quad C_3 &= \frac{\left(\frac{\omega_3^2}{\omega_2^2} - 1\right)\left(1 - \frac{\omega_3^2}{\omega_5^2}\right)\left(1 - \frac{\omega_3^2}{\omega_6^2}\right)}{\omega_3^2 H (1 - \omega_3^2/\omega_5^2)}; \quad L_3 = \frac{1}{\omega_3^2 C_3} \\ C_5 &= \frac{\left(\frac{\omega_5^2}{\omega_2^2} - 1\right)\left(\frac{\omega_5^2}{\omega_4^2} - 1\right)\left(1 - \frac{\omega_5^2}{\omega_6^2}\right)}{\omega_5^2 H \left(\frac{\omega_5^2}{\omega_3^2} - 1\right)}; \quad L_5 = \frac{1}{\omega_5^2 C_5}; \\ C_7 &= \frac{\omega_3^2 \omega_5^2}{H \omega_2^2 \omega_4^2 \omega_6^2}. \end{aligned} \quad (8.35)$$

If we take the ratio $(C_3 + C_5)$ to C_7 and set the ratio equal to $1/138$, the limiting condition is

$$\frac{\left\{ \omega_5^4 (\omega_3^2 - \omega_2^2) (\omega_4^2 - \omega_3^2) (\omega_6^2 - \omega_3^2) + \omega_3^4 (\omega_5^2 - \omega_2^2) (\omega_5^2 - \omega_4^2) (\omega_6^2 - \omega_5^2) \right\}}{\omega_3^4 \omega_5^4 (\omega_5^2 - \omega_3^2)} = \frac{1}{138}. \quad (8.36)$$

While there is no definite limitation on the band widths as there is in an all-crystal filter, nevertheless if we make the separation

between successive resonances and anti-resonances about an equal percentage a band width limitation appears. If we let

$$\frac{\omega_3}{\omega_2} = \frac{\omega_4}{\omega_3} = \frac{\omega_5}{\omega_4} = \frac{\omega_6}{\omega_5} = X \text{ so that } \frac{\omega_6}{\omega_2} = X^4 \quad (8.37)$$

equation (8.36) gives a value of $X = 1.0248$. Since the ratio of the upper cutoff to the lower cutoff for a complete filter of

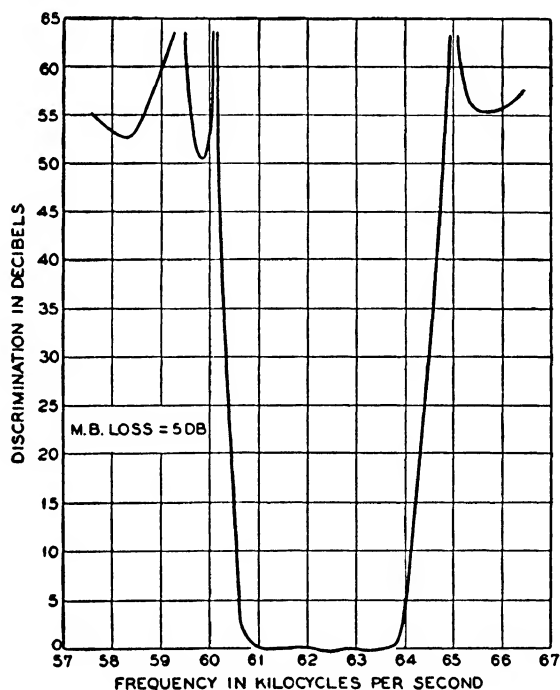


FIG. 8.22—INSERTION LOSS CHARACTERISTIC OF FILTER EMPLOYING TWO CRYSTALS IN EACH ARM.

the type shown in Fig. 8.21 filter 5 will be X^5 , this allows a band width of 1.13 which is about the same as for a single crystal in each arm. The design values of the elements are easily obtained after the m values and hence the critical frequencies are specified and are obtained by using the relations of (8.35).

Fig. 8.21 shows the types of filter sections that can be obtained by using up to two crystals in each arm of the lattice

with or without coils in series or shunt. The attenuation characteristic and the type of image impedance are shown in columns *C* and *D*. The last filter results in either an all-pass filter or a band elimination filter depending on how the critical frequencies are arranged. The method of obtaining the design constants of all these filters is similar to that given above. For the arm having a series inductance, the series inductance is given by equation (8.29) and subtracted from the impedance Z . This leaves an impedance

$$Z' = Z - j\omega L \quad (8.38)$$

from which the constants of the two crystals in parallel can be evaluated by employing (8.25).

Fig. 8.22 shows a measured attenuation characteristic of a filter constructed like filter 4 of Fig. 8.21. The two series crystals were obtained by using two split plating crystals connected in parallel as were also the lattice crystals. The coils were made equal and taken out to the ends of the filter while the common capacitances were brought out to the ends of the lattice. The number of elements to obtain this characteristic was two coils, four crystals, two large condensers, and two small peak-adjusting condensers. With this construction, coils with lower Q 's can be tolerated due to the fact that since only one section is required the total loss due to coil resistance will be considerably reduced.

8.5. Other Types of Crystal Filters

Although band-pass crystal filters have been more extensively used than any other types, crystals have also been employed in high-pass, low-pass, and band-elimination filters. The use of crystals in such filters has been rather completely discussed,¹⁰ and it is the purpose of this section to merely describe the more useful types.

The three types of sections that have been most extensively used are shown in Fig. 8.23. The first column shows the

¹⁰ "Electrical Wave Filters Employing Normal and Divided Crystals," W. P. Mason and R. A. Sykes, B.S.T.J., April, 1940, pp. 221-249.

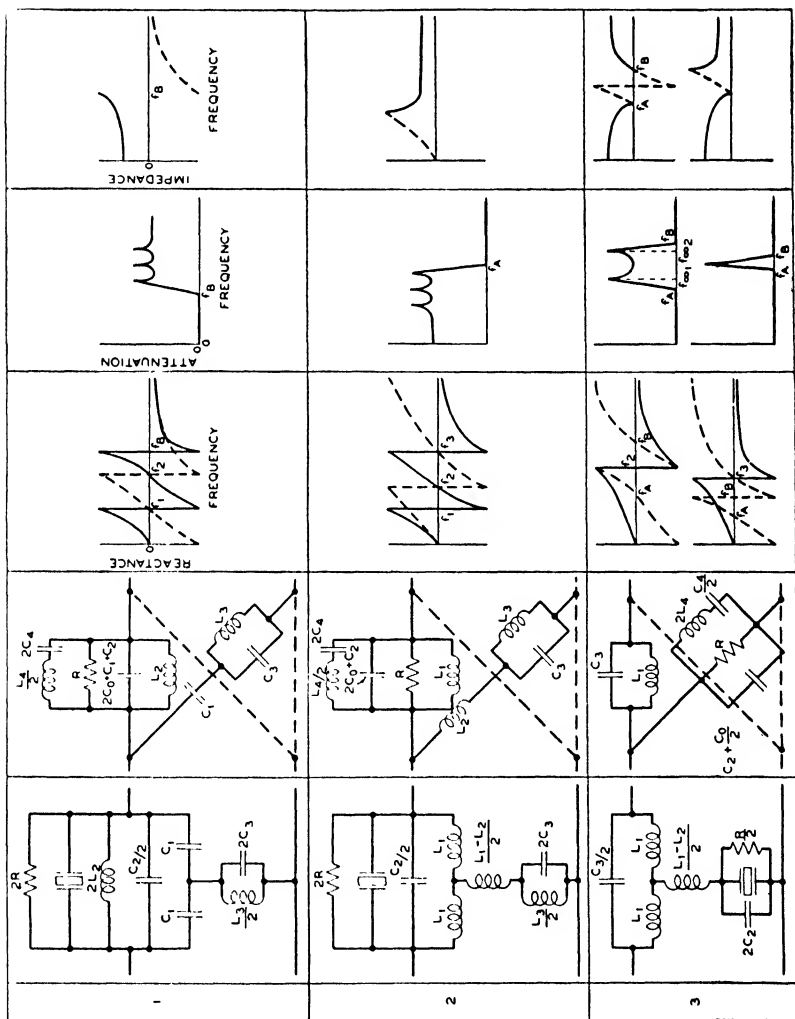


FIG. 8.23—Low-Pass, High-Pass, and Band-Elimination Crystal Filters.

structure of the filters in bridge T form since they are most often used in this configuration. The next column shows the lattice of electrical elements which represents the crystal circuit. The third column shows the reactance-frequency curves for the two arms, the fourth column shows the attenuation characteristic, while the fifth column gives the image impedance-frequency curves. Two forms are shown for the band elimination filter 3. The upper configuration of reactances is used for a relatively wide suppression band whereas the lower configuration is used when a narrow suppression band is desired.

If we wish to have a sharply rising attenuation in the low-pass filter, for example, it is necessary to have the critical frequency f_2 come very close to the cutoff frequency f_B . For this reason the crystal with its high Q is used, for otherwise a large distortion would occur near the cutoff frequency. The separation between f_1 and f_2 is considerably larger and a reasonably small loss distortion can be obtained by employing a high Q coil L_3 in the shunt arm. None of these filters are exactly resistance compensated, i.e., all the coil resistances cannot be brought out to the ends of the filter and combined with the terminating resistance. Over a frequency range near the cutoff, however, resistance compensation can be practically obtained. The impedance of the lattice arm near the cutoff will be controlled by the anti-resonant circuit L_3, C_3 . The coil resistance of L_3 can be considered to be a high resistance in parallel with the anti-resonant circuit. To balance this near the cutoff a high resistance $2R$ parallels the crystal and is adjusted so that the effective shunt resistance of the coil L_2 in parallel with R is equal to the effective shunt resistance of the coil L_3 . If this is done the attenuation peaks near the cutoff will have their full value and the loss distortion near the cutoff becomes small. In this way a reasonably flat attenuation-frequency characteristic is obtained in the pass band, and a sharp attenuation rise above the cutoff is obtained. The same considerations apply to the other two filters also. In this way the added crystals can be made to give a considerably sharper cutoff than could be obtained without them.

The impedances of these filters, as shown by the fifth column, depart considerably from their nominal values near the cutoff frequency. If used alone the reflection loss near the cutoff frequency will cause the characteristic to be very rounded and will limit the rapidity with which the attenuation can be made to increase in a given frequency range. To get around this difficulty electrical half-sections of the m or double m types¹¹ are connected on each end of the crystal low-pass section. As discussed in section (2.5) these sections have an image impedance equal to that for the crystal section on one end and an image impedance on the other end which can be made much flatter up to nearly the cutoff frequency than can the constant K image impedance of the crystal section. In this way the reflection loss can be eliminated and at the same time extra attenuation is added to the low-pass characteristic which reaches its maximum value at a frequency somewhat higher than the cutoff.

TABLE XI
DESIGN FORMULAE FOR WIDE BAND ELIMINATION FILTER

Element	Formula
L_1	$Z_0 \frac{\sqrt{(f_B^2 - f_{\infty_1}^2)(f_{\infty_1}^2 - f_A^2)}}{2\pi f_A f_B f_{\infty_1}}$
L_2	$\frac{Z_0 f_{\infty_1}}{2\pi \sqrt{(f_B^2 - f_{\infty_1}^2)(f_{\infty_1}^2 - f_A^2)}}$
$2L_4$	$\frac{Z_0 f_{\infty_1} [(f_B - f_A)^2 + f_A f_B]^2}{2\pi f_A f_B (f_B - f_A)^2 \sqrt{(f_B^2 - f_{\infty_1}^2)(f_{\infty_1}^2 - f_A^2)}}$
$\left(C_2 + \frac{C_0}{2}\right)$	$\frac{\sqrt{(f_B^2 - f_{\infty_1}^2)(f_{\infty_1}^2 - f_A^2)}}{2\pi Z_0 f_{\infty_1} [(f_B - f_A)^2 + f_A f_B]}$
C_3	$\frac{f_{\infty_1}}{2\pi Z_0 \sqrt{(f_B^2 - f_{\infty_1}^2)(f_{\infty_1}^2 - f_A^2)}}$
$\frac{C_4}{2}$	$\frac{(f_B - f_A)^2 \sqrt{(f_B^2 - f_{\infty_1}^2)(f_{\infty_1}^2 - f_A^2)}}{2\pi Z_0 f_A f_{\infty_1} f_B [(f_B - f_A)^2 + f_A f_B]}$

¹¹ "Extensions to the Theory and Design of Electric Wave Filters," O. J. Zobel, B.S.T.J., April 1931, pp. 284-342.

The element values of the low-and high-pass filters are easily calculated in the usual manner by determining the critical frequencies from the m values of the filters. The element values can then be calculated by employing Foster's theorem. The element values of the two-peak band elimination filters are given in Table XI.

In this table Z_0 is the image impedance at zero frequency, and f_{∞_1} is the first frequency of infinite attenuation. These equations are based on the assumption that the two frequencies of infinite attenuation satisfy the relation,

$$f_{\infty_1} f_{\infty_2} = f_A f_B. \quad (7.38)$$

For the narrow band suppression filter with only one peak the equations are given by Table XII.

TABLE XII
DESIGN FORMULAE FOR NARROW BAND ELIMINATION FILTER

Element	Formula
$L_1 \dots \dots \dots$	$\frac{Z_0 f_B}{2\pi b f_{\infty} f_A}$
$L_2 = L_1 \dots \dots$	$\frac{Z_0 f_B}{2\pi b f_{\infty} f_A}$
$2L_4 \dots \dots \dots$	$\frac{Z_0(f_A^2 + b^2 f_{\infty}^2 - f_B^2)^2 f_B}{2\pi b f_A f_{\infty} (f_B^2 - f_A^2)(b^2 f_{\infty}^2 - f_B^2)}$
$\left(C_2 + \frac{C_0}{2}\right)$	$\frac{b f_A f_{\infty}}{2\pi Z_0 f_B [f_A^2 + b^2 f_{\infty}^2 - f_B^2]}$
$C_3 \dots \dots \dots$	$\frac{f_A}{2\pi Z_0 b f_B f_{\infty}}$
$\frac{C_4}{2} \dots \dots \dots$	$\frac{(f_B^2 - f_A^2)(b^2 f_{\infty}^2 - f_B^2)}{2\pi Z_0 b f_A f_B f_{\infty} [f_A^2 + b^2 f_{\infty}^2 - f_B^2]}$

$$\text{where } b = \frac{1}{2} \sqrt{\left(\frac{f_B^2 + f_{\infty}^2 - 2f_A^2}{f_{\infty}^2 - f_A^2}\right)} + \sqrt{\left(\frac{f_B^2 + f_{\infty}^2 - 2f_A^2}{f_{\infty}^2 - f_A^2}\right)^2 - 4}.$$

In the narrow band filter $L_1 = L_2$ and hence the series coil ($L_2 - L_1$) in series with the crystal disappears.

Filters of this type have been used to suppress a single frequency, such as a carrier frequency, without disturbing the transmission at other frequencies.

8.6 Filters Employing Magnetostrictive Elements

Magnetostrictive elements have an impedance which is the inverse of that for a crystal. Hence one should be able to construct filters employing such elements of a similar nature to the crystal filters discussed above. Such elements by themselves inherently give narrow band filters but such bands can be widened by employing series or shunt condensers with magnetostrictive elements. Due, however, to the large resistance or low value of Q inherent in the driving coil impedance, such elements introduce considerably more loss than do crystals. This is due primarily to the eddy current and hysteresis losses inherent in the magnetostrictive material. By laminating this material, the eddy current losses can be considerably reduced and Q 's as high as 100 have been obtained in the driving coils. With such elements wide band filters with sharp attenuation characteristics have been obtained. Due, however, to the large loss in the band, to the necessity for maintaining a polarizing current or a permanent magnet in each of the elements, and to the non-linearity of the magnetic material which produces harmonic and modulation products of the input currents in the output of the filters, such elements have not been widely used in filters.

Narrow band filters have been constructed¹² by using two windings on a magnetostrictive rod, one as the driving element and the other as the pickup element. The equivalent circuit for a magnetostrictive rod free to vibrate on both ends is given by Fig. 6.15A when the mechanical output end is open-circuited,

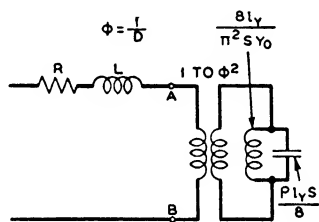


FIG. 8.24—EQUIVALENT CIRCUIT OF MAGNETOSTRICTIVE ROD WITH ONE WINDING.

¹² H. H. Hall, Proc. I.R.E. 21, 1328 (1933).

i.e., $F_1 = 0$. Near the resonant frequency this reduces to the network shown in Fig. 8.24. The representation of a magnetostrictive bar with two windings is complicated by the fact that there is an electromagnetic coupling between the two coils even in the absence of any motion in the bar. An equivalence good for a measurement from any of the four terminals can be obtained by employing the lattice network in Fig. 8.25B to represent a bar with two windings, with the terminals numbered as shown in Fig. 8.25A. In this representation P is the inductance of the coils 1, 2 or 3, 4 since they are assumed equal,

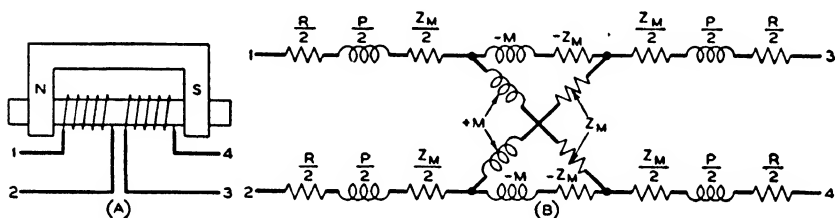


FIG. 8.25—EQUIVALENT CIRCUIT OF MAGNETOSTRICTIVE ROD WITH TWO WINDINGS.

M is the mutual inductance coupling between the two coils, while Z_M is one-fourth of the electrical impedance—as measured from the terminals A, B of Fig. 8.24—generated by the mechanical motion of the magnetostrictive rod. If we connect terminal 2 to 3 and determine the resulting impedance, we find an impedance

$$Z = j2\omega(P + M) + 4Z_M \quad (8.39)$$

that is, we have the inductance of the full coil which will be twice the inductance of each winding plus twice the mutual inductance between them, and the mechanical impedance put in by the vibrating bar. On the other hand, if we connect terminal 2 to 4 the resulting impedance will be

$$Z = 2j\omega(P - M) \quad (8.40)$$

and the resulting inductance will be twice the inductance of either winding minus twice the mutual inductance between them. No mechanical impedance appears since the force produced by one winding will be equal and opposite to that in the

other winding and no fundamental vibration is excited. A second harmonic vibration can be excited in this way but the equivalent network applies to only one mode of motion.

Using this network and the equivalence of page 36, Chapter II, it is readily seen that the equivalent lattice of the filter using the 1, 2 terminals on the input and the 2, 4 as the output will be as shown in Fig. 8.26A. The reactance curves are shown in Fig. 8.26B, the attenuation in Fig. 8.26C, while the

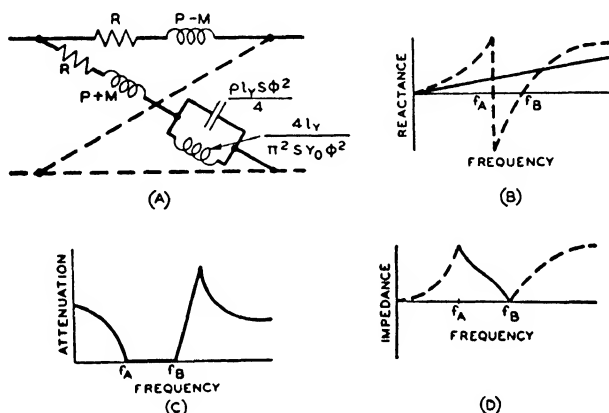


FIG. 8.26—CHARACTERISTICS OF NARROW BAND MAGNETOSTRICTIVE FILTER.

characteristic impedance is shown in Fig. 8.26D. Due to the resistance R associated with each arm (which is high compared to the image impedance at midband), the loss at midband will be high. On the other hand, near the lower cutoff which comes at the mechanical resonant frequency of the bar, the image impedance is high. By terminating the filter in a high resistance, the loss near f_A , due to the resistance of the driving coil, can be made rather small and a narrow frequency range can be passed. It is not possible to obtain a uniform pass band over the theoretical band width of the filter as can be done with a crystal filter.

By employing two magnetostrictive bars with double windings, and the series condensers C_A and C_B , as shown in Fig. 8.27A, wide band magnetostrictive filters can be constructed.¹³

¹³ Such filters are discussed in patent 2,094,044, September 28, 1937.

By employing the network representation of Fig. 8.25B it is easily shown that the equivalent lattice circuit of this combination is that shown in Fig. 8.27B. We have in each series arm the equivalent of the magnetostrictive bar 1, but of half the impedance of the complete winding, in series with the condenser C_A . In the lattice arm, similarly, we have half the impedance of bar number 2 in series with C_B . The reactance curves of the

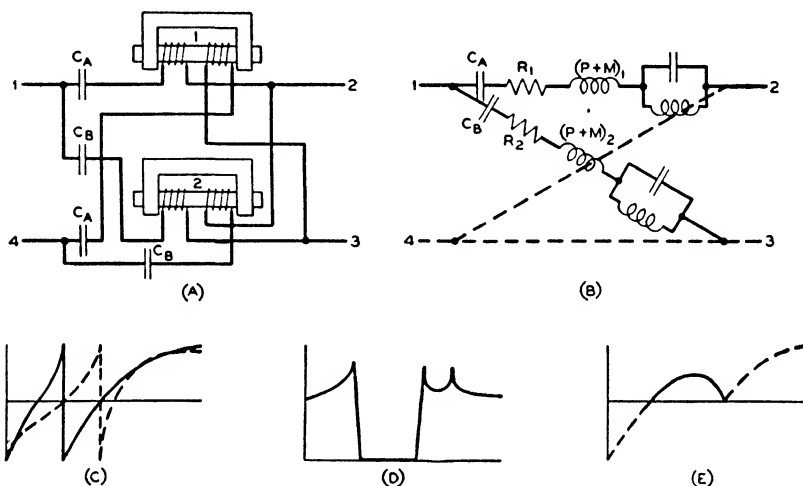


FIG. 8.27—METHOD FOR OBTAINING WIDE BAND MAGNETOSTRICTIVE FILTER. IDEAL CHARACTERISTICS.

two arms are shown in Fig. 8.27C. It is obvious that these curves are similar to the crystal filter curves of Fig. 8.15, and hence a widening of the possible band width can be accomplished by using series condensers. The resulting attenuation characteristic is shown in Fig. 8.27D while the image impedance is shown in Fig. 8.27E. Since the resistances of the magnetostrictive elements are in series they can be brought out to the end and combined with the terminating resistance provided that they are not larger than the terminating resistance. For band widths greater than 3 or 4 per cent and with highly laminated magnetostrictive bars this can be accomplished and selective band-pass filters can be made in this way.

By analogy with the crystal filter types discussed previously, high-pass, low-pass, band-elimination filters, and more complicated band-pass filters are theoretically possible by using magnetostrictive bars and condensers. Such filters, however, have not come into practical use.

APPENDIX A

MOTION AND IMPEDANCE OF A BAR VIBRATING IN FLEXURE, TAKING ACCOUNT OF ROTARY INERTIA

A.1. *Equations of Motion*

THE equations of motion of a bar vibrating in flexure given in Chapter III neglect the effect of rotary inertia, which may be an appreciable factor when the width of the bar becomes comparable with the length. It is the purpose of this appendix to indicate the effect of this added term and to apply the bar equations to practical cases of interest.

The equation of motion of a bar vibrating in flexure, taking account of the rotary inertia term, is given by ¹

$$\rho \frac{\partial^2 y}{\partial t^2} + Y_0 \kappa^2 \frac{\partial^4 y}{\partial x^4} - \rho \kappa^2 \frac{\partial^4 y}{\partial x^2 \partial t^2} = 0 \quad (\text{A.1})$$

where ρ is the density of the bar, Y_0 the value of Young's modulus and κ is the radius of gyration of the section. This differs from (3.10) by the inclusion of the last term, which represents the force reaction of the rotary inertia term. This results from the added kinetic energy of the section rotating about an axis located normal to the central line of the bar.

The added term also affects the equation for the force. When the rotary inertia term is included, the moment and lateral force at any point become ²

$$\begin{aligned} \text{Moment } M &= Y_0 I \frac{\partial^2 y}{\partial x^2} \\ \text{Lateral Force } F &= I \left[Y_0 \frac{\partial^3 y}{\partial x^3} - \rho \frac{\partial^3 y}{\partial x \partial t^2} \right]. \end{aligned} \quad (\text{A.2})$$

¹ "Theory of Sound," Rayleigh, Vol. I, Ch. VIII, p. 258.

² "Theory of Sound," Rayleigh, Vol. I, Ch. VIII, p. 258, noting that multiplier of δy in equation (37) is the force.

Since we are interested only in the solution for steady state conditions, the symbolic time variation is employed and the equations reduce to

$$\frac{d^4 y}{dx^4} + \frac{\omega^2}{v^2} \frac{d^2 y}{dx^2} - n^4 y = 0 \quad (\text{A.3})$$

$$M = Y_0 I \frac{d^2 y}{dx^2}; \quad F = I \left[Y_0 \frac{d^3 y}{dx^3} + \omega^2 \rho \frac{dy}{dx} \right]$$

where $v = \sqrt{Y_0/\rho}$ = longitudinal velocity of sound in a long thin bar, and $n^4 = \frac{\omega^2 \rho}{Y_0 \kappa^2}$.

A solution for (A.3) is obtained as usual by writing the equation

$$y = A \cos \alpha x + B \sin \alpha x + C \cosh \beta x + D \sinh \beta x \quad (\text{A.4})$$

where A, B, C , and D are arbitrary constants. Substituting this in (A.3), we find that it is a solution provided

$$\alpha = \sqrt{\sqrt{\frac{\omega^4}{4v^4} + n^4} + \frac{\omega^2}{2v^2}}; \quad \beta = \sqrt{\sqrt{\frac{\omega^4}{4v^4} + n^4} - \frac{\omega^2}{2v^2}}. \quad (\text{A.5})$$

In case κ^2 is quite small, n^4 becomes much larger than $\frac{\omega^4}{4v^4}$ and the solution approaches $\alpha = \beta = n$ which is the solution obtained in Chapter III when the rotary inertia was neglected.

A.2. Impedance of a Vibrating Reed

As a first example, the correction for rotary inertia has been evaluated for the vibrating reed of the mechanical filter discussed in Chapter III. This reed was clamped at one end, and the impedance or ratio of force to velocity was determined for the other end. The conditions then are

$$y = \frac{dy}{dx} = 0 \text{ when } x = 0$$

$$M = Y_0 I \frac{d^2 y}{dx^2} = 0 \text{ when } x = l \quad (\text{A.6})$$

and the fourth constant is determined by taking the ratio of force to velocity at the point $x = l$.

Introducing the first two conditions of equation (A.6) we have

$$A + C = 0 \quad \text{or} \quad C = -A; \quad B\alpha + D\beta = 0 \quad \text{or} \quad D = -\frac{B\alpha}{\beta}. \quad (\text{A.7})$$

Hence with these conditions

$$y = A(\cos \alpha x - \cosh \beta x) + B(\sin \alpha x - (\alpha/\beta) \sinh \beta x). \quad (\text{A.8})$$

Differentiating this to obtain the moment and setting this equal to zero when $x = l$, the third condition gives

$$B = -A \left[\frac{\alpha^2 \cos \alpha l + \beta^2 \cosh \beta l}{\alpha^2 \sin \alpha l + \alpha \beta \sinh \beta l} \right], \quad (\text{A.9})$$

so that finally

$$y = A \left[\cos \alpha x - \cosh \beta x - \left[\frac{\alpha^2 \cos \alpha l + \beta^2 \cosh \beta l}{\alpha^2 \sin \alpha l + \alpha \beta \sinh \beta l} \right] [\sin \alpha x - (\alpha/\beta) \sinh \beta x] \right]. \quad (\text{A.10})$$

The constant A is eliminated and the impedance at the end of the bar evaluated by taking the ratio

$$Z = \frac{F}{\dot{y}} = \left[\frac{I \left[Y_0 \frac{d^3 y}{dx^3} + \omega^2 \rho \frac{dy}{dx} \right]}{j\omega y} \right]_{x=l} \quad (\text{A.11})$$

when $x = l$. Performing this differentiation and collecting terms we find

$$Z = \frac{-jY_0 I}{\omega} \left(\frac{2\alpha^3 \beta^3}{\alpha^2 + \beta^2} \right) \left[\frac{\left\{ 1 + [(\alpha^4 + \beta^4)/(2\alpha^2 \beta^2)] \cos \alpha l \cosh \beta l + [(\beta^2 - \alpha^2)/2\alpha\beta] \sin \alpha l \sinh \beta l \right\}}{\alpha \cos \alpha l \sinh \beta l - \beta \sin \alpha l \cosh \beta l} \right] \quad (\text{A.12})$$

after making use of the relations

$$Y_0 \alpha^2 - \omega^2 \rho = Y_0 \left[\sqrt{\frac{\omega^4}{4\nu^4} + n^4} + \frac{\omega^2 \rho}{2Y_0} - \frac{\omega^2 \rho}{Y_0} \right] = Y_0 \beta^2 \quad (\text{A.13})$$

$$Y_0 \beta^2 + \omega^2 \rho = Y_0 \left[\sqrt{\frac{\omega^4}{4\nu^4} + n^4} - \frac{\omega^2 \rho}{2Y_0} + \frac{\omega^2 \rho}{Y_0} \right] = Y_0 \alpha^2.$$

If equation (A.12) is expanded in powers of ω , the expression for Z becomes

$$Z = \frac{-j3Y_0 l}{\omega l^3} + j\omega(\rho S l) \left[\frac{.33}{1.40} + \frac{1}{10} \frac{l_t^2}{l^2} \right] \quad (\text{A.14})$$

where l_t is the thickness of the bar and S its area. We see that the low-frequency stiffness is the same as obtained when the rotary inertia is neglected but the low-frequency mass is increased. The effective mass at low frequencies will be the static mass $M = \rho S l$ multiplied by the factor

$$\left(\frac{.33}{1.40} + \frac{1}{10} \frac{l_t^2}{l^2} \right) = \left(0.236 + \frac{l_t^2}{10l^2} \right). \quad (\text{A.15})$$

The resonant frequencies of a bar clamped at one end and driven on the other are given when the numerator of equation (A.12) vanishes or

$$\left(\frac{\alpha^4 + \beta^4}{2\alpha^2\beta^2} \right) \cos \alpha l \cosh \beta l + \frac{\beta^2 - \alpha^2}{2\alpha\beta} \sin \alpha l \sinh \beta l = -1. \quad (\text{A.16})$$

Two limiting cases are of interest. When the rod is long and thin so that $n^4 \gg \frac{\omega^4}{4v^4}$ we have

$$\alpha l = \beta l = nl = \sqrt[4]{\frac{\omega^2 \rho}{Y_0 k^2}} l = m. \quad (\text{A.17})$$

In this case the frequency equation given in Chapter III holds, namely,

$$\cos m \cosh m = -1. \quad (\text{A.18})$$

The first value of m for which this will happen is

$$m = 1.875104 \quad (\text{A.19})$$

so that the frequency of resonance becomes

$$f = \frac{\kappa m^2 \sqrt{Y_0/\rho}}{2\pi l^2} = \frac{l_t m^2 \sqrt{Y_0/\rho}}{2\pi \sqrt{12} l^2} \quad (\text{A.20})$$

for a bar with a rectangular cross section. The other limiting case occurs when the rod is thick compared to its length. For that case

$$\alpha l \doteq \frac{\omega l}{v}; \quad \beta l \rightarrow 0. \quad (\text{A.21})$$

The frequency is then given by

$$\cos \frac{\omega l}{v} = 0 \quad \text{or} \quad f = \frac{v}{4l} \quad (\text{A.22})$$

which is the frequency of a bar in longitudinal vibration clamped on one end and free on the other. Hence as the width is increased the frequency does not increase proportional to l_t but bends over and finally becomes asymptotic to the value given in equation (A.22).

If we introduce the value of m for a rectangular section, we have

$$m = \sqrt[4]{\frac{12\omega^2}{v^2 l_t^2}} l = \sqrt{\frac{\sqrt{12} \omega l}{v R}} \quad (\text{A.23})$$

where R is the ratio of the thickness l_t to the length l . Equation (A.16) can then be written in the simpler form

$$\begin{aligned} & \left[1 + \frac{m^4 R^4}{288} \right] \cos \left[m \sqrt{\sqrt{1 + \frac{m^4 R^4}{(24)^2}} + \frac{m^2 R^2}{24}} \right] \\ & \cosh \left[m \sqrt{\sqrt{1 + \frac{m^4 R^4}{(24)^2}} - \frac{m^2 R^2}{24}} \right] \\ & - \frac{m^2 R^2}{24} \sin \left[m \sqrt{\sqrt{1 + \frac{m^4 R^4}{(24)^2}} + \frac{m^2 R^2}{24}} \right] \\ & \sinh \left[m \sqrt{\sqrt{1 + \frac{m^4 R^4}{(24)^2}} - \frac{m^2 R^2}{24}} \right] = -1. \quad (\text{A.24}) \end{aligned}$$

From this equation the values of m can be calculated for different values of R . Table XIII shows these calculated values for the first mode of motion. The frequency of a bar of given length and thickness in the direction of flexure can then be calculated from these values of m by employing equation (A.20)

TABLE XIII
VALUES OF m FOR CLAMPED-FREE BAR

First Mode			
R	m	R	m
0	1.875	0.4	1.848
0.1	1.873	0.5	1.832
0.2	1.868	0.7	1.795
0.3	1.860	1.0	1.725

A.3. *Natural Frequencies of a Bar Free on Both Ends*

A related problem which has some practical interest in the investigation of crystal modes of motion is the problem of the resonant frequencies of a bar free to vibrate on both ends when account is taken of the rotary inertia term. This problem is discussed in a former paper.³ The result can be obtained from the above discussion by applying the condition

$$M = F = 0 \quad \text{when} \quad x = 0, \quad \text{and} \quad x = l. \quad (\text{A.25})$$

Applying these conditions one finds the frequency equation

$$1 - \cos \alpha l \cosh \beta l + \left(\frac{\alpha^6 - \beta^6}{2\alpha^3\beta^3} \right) \sin \alpha l \sinh \beta l = 0. \quad (\text{A.26})$$

³ "The Motion of a Bar Vibrating in Flexure, including the Effect of Rotary and Lateral Inertia," W. P. Mason, J. Acoustical Soc. Am., Vol. VI, p. 246, April 1935.

Inserting the value of m given in equation (A.23) this takes the form suitable for calculation

$$\begin{aligned}
 0 = & 1 - \cos \left[m \sqrt{\sqrt{1 + \frac{m^4 R^4}{(24)^2} + \frac{m^2 R^2}{24}}} \right] \\
 & \cosh \left[m \sqrt{\sqrt{1 + \frac{m^4 R^4}{(24)^2} - \frac{m^2 R^2}{24}}} \right] \\
 & + \left(\frac{3m^2 R^2}{24} + \frac{4m^6 R^6}{(24)^3} \right) \sin \left[m \sqrt{\sqrt{1 + \frac{m^4 R^4}{(24)^2} + \frac{m^2 R^2}{24}}} \right] \\
 & \sinh \left[m \sqrt{\sqrt{1 + \frac{m^4 R^4}{(24)^2} - \frac{m^2 R^2}{24}}} \right].
 \end{aligned} \tag{A.27}$$

A number of values of m , as a function of the ratio R , are given for the first three modes of motion by Table XIV.

TABLE XIV
VALUES OF m FOR FREE-FREE BAR

First Mode		Second Mode		Third Mode	
R	m	R	m	R	m
0	4.730	0	7.853	0	10.995
0.1	4.682	0.1	7.683	0.1	10.599
0.2	4.549	0.2	7.268	0.2	9.717
0.3	4.367	0.3	6.752	0.3	8.835
0.4	4.161	0.5	5.837	0.4	8.068
0.5	3.952	0.7	5.172	0.5	7.442
0.8	3.411	1.0	4.456	0.7	6.511
1.0	3.132	1.5	3.711	1.0	5.565
1.5	2.641				
2.0	2.310				
3.0	1.893				

APPENDIX B

GENERAL WAVE PROPAGATION TAKING ACCOUNT OF VISCOSITY EFFECTS

IN section (4.3) was considered the effect of viscosity in modifying the propagation of a wave through a tube. The only viscosity term of importance was the drag exerted by a layer of air attached to the wall. In a general wave propagated in a medium, other viscous components enter than this shear component present for a wave in a tube. It is the purpose of this appendix to present the general equations of a gas or liquid, taking account of the effects of viscosity.

B.1. *General Viscous Forces*

As discussed in section (4.3) it follows from the definition of a coefficient of viscosity that the stress exerted by the medium between two parallel planes a distance dy apart, and having a relative velocity $d\xi$ in the x -direction is a tangential stress equal to

$$X_y = -\mu \frac{d\xi}{dy}. \quad (\text{B.1})$$

The negative sign is chosen since the force exerted by the medium is always opposite to that of the speed of the surface with respect to the medium. The designation of the tangential stress as X_y has the significance that the force is exerted in the x -direction on a unit area having its normal in the Y direction. Similarly, a Y_y stress would be one directed along the Y axis for a unit surface having its normal along the Y axis. It is obvious that a stress in any direction for a surface normal to Y can be resolved into three components, one a stress along the X axis X_y , one a stress along the Y axis Y_y , and the third a stress along the Z axis denoted by Z_y .

On the opposite edge we have similar forces X_v , Y_v , Z_v directed in the opposite direction. The two Y_v forces acting alone will exert a longitudinal stress since their direction is normal to the surface upon which they act. The two X_v forces will exert a stress known as a simple shearing stress. In general, on all six faces nine sets of stresses will be exerted, three longitudinal stresses and six shearing stresses. For bodies in equilibrium or in non-rotational motion, however, two of the shear stresses balance. For example, the Y_x shearing stress exerts a couple which tends to rotate the element around the X axis in a counter-clockwise direction, while the X_y shearing stress tends to rotate the element around the X axis in a clockwise direction. If the body is in equilibrium or in non-rotational motion, we must have that

$$X_y = Y_x, \text{ also } X_z = Z_x, Y_z = Z_y. \quad (\text{B.2})$$

Hence, the state of stress of any element in the body can be specified by specifying six stresses, three longitudinal, X_x , Y_y , Z_z , and three shearing stresses, Y_x , Z_x , and X_y .

Equation (B.1) is a special case of motion in which the two opposite surfaces of the element are moving parallel to each other. Let us consider a continuous medium and consider the relative velocities of the medium around the element being considered. Then, if ξ_1 , η_1 , ζ_1 are the velocities of the medium on one face of the element and ξ_2 , η_2 , ζ_2 the velocities on the opposite face, we can write

$$\begin{aligned} \xi_2 &= \xi_1 + \frac{\partial \xi}{\partial x} dx + \frac{\partial \xi}{\partial y} dy + \frac{\partial \xi}{\partial z} dz \\ \eta_2 &= \eta_1 + \frac{\partial \eta}{\partial x} dx + \frac{\partial \eta}{\partial y} dy + \frac{\partial \eta}{\partial z} dz \\ \zeta_2 &= \zeta_1 + \frac{\partial \zeta}{\partial x} dx + \frac{\partial \zeta}{\partial y} dy + \frac{\partial \zeta}{\partial z} dz. \end{aligned} \quad (\text{B.3})$$

Since

$$\xi_2 - \xi_1 = \Delta \xi = \frac{\partial \xi}{\partial x} dx + \frac{\partial \xi}{\partial y} dy + \frac{\partial \xi}{\partial z} dz$$

this equation states that the change in velocity in the X direction in going a distance dx is the gradient of $\dot{\xi}$ with respect to x , etc. We now define the gradient velocities in a similar manner to the strains in an elastic body, namely, as

$$\begin{aligned}\dot{x}_x &= \frac{\partial \dot{\xi}}{\partial x} = \frac{\partial}{\partial t} \left(\frac{\partial \xi}{\partial x} \right); \quad \dot{y}_y = \frac{\partial \dot{\eta}}{\partial y}; \quad \dot{z}_z = \frac{\partial \dot{\zeta}}{\partial z} \\ \dot{y}_z &= \frac{\partial \dot{\zeta}}{\partial y} + \frac{\partial \dot{\eta}}{\partial z}; \quad \dot{z}_x = \frac{\partial \dot{\xi}}{\partial z} + \frac{\partial \dot{\zeta}}{\partial x}; \quad \dot{x}_y = \frac{\partial \dot{\eta}}{\partial x} + \frac{\partial \dot{\xi}}{\partial y}.\end{aligned}\quad (\text{B.4})$$

The first equation states that the gradient of the velocity in the X direction with respect to X is the same as the time rate of change of the elongation strain. The other equations show that all of the relative velocity gradients can be expressed as time rates of change of the six components of strain. In addition to the strains we may have three time rates of change of rotation given by the equations

$$\dot{\omega}_x = \frac{\partial \dot{\zeta}}{\partial y} - \frac{\partial \dot{\eta}}{\partial z}; \quad \dot{\omega}_y = \frac{\partial \dot{\xi}}{\partial z} - \frac{\partial \dot{\zeta}}{\partial x}; \quad \dot{\omega}_z = \frac{\partial \dot{\eta}}{\partial x} - \frac{\partial \dot{\xi}}{\partial y}. \quad (\text{B.5})$$

An analysis of these terms show that they correspond to the time rate of change of the rotation of a body considered as rigid, about one of the axes. In the present section we are interested only in irrotational motions so that for these we can set $\dot{\omega}_x = \dot{\omega}_y = \dot{\omega}_z = 0$. The remaining possible time rates of change of strains are then given in equation (B.4).

For the most unsymmetrical type of a medium the relations between frictional stresses and velocity gradients, assuming that the stresses are proportional to the gradients, can be expressed in the form:

$$\begin{aligned}-X_x &= \mu_{11}\dot{x}_x + \mu_{12}\dot{y}_y + \mu_{13}\dot{z}_z + \mu_{14}\dot{y}_z + \mu_{15}\dot{z}_x + \mu_{16}\dot{x}_y \\ -Y_y &= \mu_{21}\dot{x}_x + \mu_{22}\dot{y}_y + \mu_{23}\dot{z}_z + \mu_{24}\dot{y}_z + \mu_{25}\dot{z}_x + \mu_{26}\dot{x}_y \\ -Z_z &= \mu_{31}\dot{x}_x + \mu_{32}\dot{y}_y + \mu_{33}\dot{z}_z + \mu_{34}\dot{y}_z + \mu_{35}\dot{z}_x + \mu_{36}\dot{x}_y \\ -Y_z &= \mu_{41}\dot{x}_x + \mu_{42}\dot{y}_y + \mu_{43}\dot{z}_z + \mu_{44}\dot{y}_z + \mu_{45}\dot{z}_x + \mu_{46}\dot{x}_y \\ -Z_x &= \mu_{51}\dot{x}_x + \mu_{52}\dot{y}_y + \mu_{53}\dot{z}_z + \mu_{54}\dot{y}_z + \mu_{55}\dot{z}_x + \mu_{56}\dot{x}_y \\ -X_y &= \mu_{61}\dot{x}_x + \mu_{62}\dot{y}_y + \mu_{63}\dot{z}_z + \mu_{64}\dot{y}_z + \mu_{65}\dot{z}_x + \mu_{66}\dot{x}_y.\end{aligned}\quad (\text{B.6})$$

In these equations the μ 's are generalized coefficients of viscosity. μ_{11} , for example, relates the stress in the X direction on the two X faces, to the velocity gradient along the X axis in the absence of any other velocity gradients, etc. It can be shown from the reciprocity theorem or from the law of conservation of energy that

$$\mu_{21} = \mu_{12} \quad \text{and in general} \quad \mu_{ij} = \mu_{ji}$$

so that the 36 possible coefficients are reduced to 21. Furthermore if we have any symmetry in the medium the possible number of independent coefficients becomes less. If we have an isotropic medium so that the expression for the forces in any one direction is the same as in any other direction, the greatest possible number of viscosity coefficients is two and these become ¹ $\mu_{11} = \mu_{22} = \mu_{33} = \lambda + 2\mu$; $\mu_{12} = \mu_{13} = \mu_{23} = \lambda$; $\mu_{44} = \mu_{55} = \mu_{66} = \mu$. All other coefficients are zero. Hence the stress equations reduce to the form:

$$\begin{aligned} -X_x &= \lambda(\dot{x}_x + \dot{y}_y + \dot{z}_z) + 2\mu\dot{x}_x; & -Y_z &= \mu\dot{y}_z \\ -Y_y &= \lambda(\dot{x}_x + \dot{y}_y + \dot{z}_z) + 2\mu\dot{y}_y; & -Z_x &= \mu\dot{z}_x \\ -Z_z &= \lambda(\dot{x}_x + \dot{y}_y + \dot{z}_z) + 2\mu\dot{z}_z; & -X_y &= \mu\dot{x}_y. \end{aligned} \quad (\text{B.7})$$

These equations reduce the possible viscous constants to two for a homogeneous medium, which is as far as they can be reduced by symmetry arguments. As we shall see later these two constants are assumed to be related so that one suffices to express all the relationships.

B.2. Equations of Motion for a Viscous Medium

To equation (B.7) giving the viscous forces on the surface of a small element of the medium, we must add the hydrostatic stresses to obtain the complete stresses. In a gas or liquid which cannot support shear stresses except by viscous motions, the hydrostatic stress will be simply the pressure p . Then equations (B.7) become

¹ This proof is the same as that given for the reduction of elastic constants to two for an isotropic medium and may be found in "Theory of Elasticity," Love, Ch. VI, p. 155.

$$\begin{aligned}
X_x &= p - \lambda(\dot{x}_x + \dot{y}_y + \dot{z}_z) - 2\mu\dot{x}_x; Y_z = -\mu\dot{y}_z \\
Y_y &= p - \lambda(\dot{x}_x + \dot{y}_y + \dot{z}_z) - 2\mu\dot{y}_y; Z_x = -\mu\dot{z}_x \quad (\text{B.8}) \\
Z_z &= p - \lambda(\dot{x}_x + \dot{y}_y + \dot{z}_z) - 2\mu\dot{z}_z; X_y = -\mu\dot{x}_y.
\end{aligned}$$

To obtain the equation of motion of such a viscous medium we consider a small element of volume and calculate all the forces in a given direction on all of the faces. For the X direction the X face at $x = x_0$ has a force ($dy dz X_{x_0}$) in the positive X direction while the opposite face has an opposite force $X_{(x_0+dx)} dy dz$. The resultant force is equal to

$$\begin{aligned}
dy dz (X_{x_0} - X_{(x_0+dx)}) &= dy dz \left[X_{x_0} - \left(X_{x_0} + \frac{\partial X_x}{\partial x} dx \right) \right] \\
&= - \frac{\partial X_x}{\partial x} dx dy dz. \quad (\text{B.9})
\end{aligned}$$

The force in the X direction acting on the Y face is

$$dx dz (X_{y_0} - X_{(y_0+dy)}) = - \frac{\partial X_y}{\partial y} dx dy dz. \quad (\text{B.10})$$

Hence the total resultant in the X direction is

$$- \left(\frac{\partial X_x}{\partial x} + \frac{\partial X_y}{\partial y} + \frac{\partial X_z}{\partial z} \right) dx dy dz. \quad (\text{B.11})$$

This force is opposed by the inertia force

$$\rho \frac{\partial \xi}{\partial t} dx dy dz \quad (\text{B.12})$$

so that the complete equation in the absence of body forces of the gravitational type is

$$- \left(\frac{\partial X_x}{\partial x} + \frac{\partial X_y}{\partial y} + \frac{\partial X_z}{\partial z} \right) - \rho \frac{\partial \xi}{\partial t} = 0.$$

Similarly for the other directions we have

$$\begin{aligned}
- \left(\frac{\partial Y_x}{\partial x} + \frac{\partial Y_y}{\partial y} + \frac{\partial Y_z}{\partial z} \right) - \rho \frac{\partial \eta}{\partial t} &= 0 \\
- \left(\frac{\partial Z_x}{\partial x} + \frac{\partial Z_y}{\partial y} + \frac{\partial Z_z}{\partial z} \right) - \rho \frac{\partial \zeta}{\partial t} &= 0.
\end{aligned} \quad (\text{B.13})$$

Now if we introduce the expression for the stresses given in (B.8), these three equations become

$$\begin{aligned}
 & -\frac{\partial p}{\partial y} + \lambda \frac{\partial}{\partial x} (\dot{x}_x + \dot{y}_y + \dot{z}_z) + 2\mu \frac{\partial \dot{x}_x}{\partial x} \\
 & \quad + \mu \left(\frac{\partial \dot{x}_y}{\partial y} + \frac{\partial \dot{x}_z}{\partial z} \right) - \rho \frac{\partial \xi}{\partial t} = 0 \\
 & -\frac{\partial p}{\partial y} + \lambda \frac{\partial}{\partial y} (\dot{x}_x + \dot{y}_y + \dot{z}_z) + 2\mu \frac{\partial \dot{y}_y}{\partial y} \\
 & \quad + \mu \left(\frac{\partial \dot{x}_y}{\partial x} + \frac{\partial \dot{y}_z}{\partial z} \right) - \rho \frac{\partial \eta}{\partial t} = 0 \\
 & -\frac{\partial p}{\partial z} + \lambda \frac{\partial}{\partial z} (\dot{x}_x + \dot{y}_y + \dot{z}_z) + 2\mu \frac{\partial \dot{z}_z}{\partial z} \\
 & \quad + \mu \left(\frac{\partial \dot{z}_x}{\partial x} + \frac{\partial \dot{z}_y}{\partial y} \right) - \rho \frac{\partial \zeta}{\partial t} = 0.
 \end{aligned} \tag{B.14}$$

It has been suggested by Stokes that a motion of dilation, in which an expansion or contraction occurs uniformly in all directions, will not give rise to viscous forces and will result in the actual pressure being equal to the static pressure corresponding to the actual density. Such a motion will occur if

$$\dot{x}_x = \dot{y}_y = \dot{z}_z = \dot{r}_r = \frac{\partial \dot{r}}{\partial r} \quad \text{and} \quad \dot{x}_y = \dot{z}_x = \dot{y}_z = 0 \tag{B.15}$$

where \dot{r} is the radial velocity of the expansion in the direction r . Adding equations (B.14) under these conditions we have

$$\begin{aligned}
 & -\left(\frac{\partial p}{\partial x} + \frac{\partial p}{\partial y} + \frac{\partial p}{\partial z} \right) + (3\lambda + 2\mu) \left(\frac{\partial \dot{r}}{\partial x} + \frac{\partial \dot{r}}{\partial y} + \frac{\partial \dot{r}}{\partial z} \right) \\
 & \quad - \rho \left(\frac{\partial \xi}{\partial t} + \frac{\partial \eta}{\partial t} + \frac{\partial \zeta}{\partial t} \right) = 0. \tag{B.16}
 \end{aligned}$$

If the expansion is to occur with no frictional forces operative, we must have

$$3\lambda + 2\mu = 0 \quad \text{or} \quad \lambda = -\frac{2\mu}{3}. \tag{B.17}$$

Introducing this value into equations (B.14) the three equations of motions for a viscous medium become

$$\begin{aligned}
 \frac{\partial p}{\partial x} + \frac{2\mu}{3} \frac{\partial}{\partial x} (\dot{x}_x + \dot{y}_y + \dot{z}_z) - 2\mu \frac{\partial \dot{x}_x}{\partial x} \\
 - \mu \left(\frac{\partial \dot{x}_y}{\partial y} + \frac{\partial \dot{x}_z}{\partial z} \right) + \rho \frac{\partial \xi}{\partial t} = 0 \\
 \frac{\partial p}{\partial y} + \frac{2\mu}{3} \frac{\partial}{\partial y} (\dot{x}_x + \dot{y}_y + \dot{z}_z) - 2\mu \frac{\partial \dot{y}_y}{\partial y} \\
 - \mu \left(\frac{\partial \dot{x}_y}{\partial x} + \frac{\partial \dot{y}_z}{\partial z} \right) + \rho \frac{\partial \eta}{\partial t} = 0 \\
 \frac{\partial p}{\partial z} + \frac{2\mu}{3} \frac{\partial}{\partial z} (\dot{x}_x + \dot{y}_y + \dot{z}_z) - 2\mu \frac{\partial \dot{z}_z}{\partial z} \\
 - \mu \left(\frac{\partial \dot{x}_z}{\partial x} + \frac{\partial \dot{y}_z}{\partial y} \right) + \rho \frac{\partial \zeta}{\partial t} = 0.
 \end{aligned} \tag{B.18}$$

B.3. Propagation of a Plane Wave in a Viscous Medium

The attenuation of a plane progressive wave in a medium can easily be calculated from the above equations. If the wave is propagated in the X direction

$\dot{y}_y = \dot{z}_z = \dot{y}_z = \dot{z}_x = \dot{x}_y = 0$ and equation (B.18) becomes

$$\frac{\partial p}{\partial x} - \frac{4\mu}{3} \frac{\partial^2 \xi}{\partial x^2} + \rho \frac{\partial \xi}{\partial t} = 0. \tag{B.19}$$

When the pressure gradient is caused by a compression along the X axis alone, it was shown by equation (4.75) that

$$\frac{\partial p}{\partial x} = -p_0 \gamma \frac{\partial^2 \xi}{\partial x^2}. \tag{B.20}$$

Introducing this equation into (B.19) and using the symbolic time variation, the equation of motion becomes

$$\frac{\omega^2}{v^2} \xi + j \frac{4}{3} \frac{\mu \omega}{v^2} \frac{d^2 \xi}{dx^2} + \frac{d^2 \xi}{dx^2} = 0. \tag{B.21}$$

A solution of this equation in terms of the input pressure and linear velocity becomes

$$\begin{aligned} p &= p_0 \cosh \theta x - \xi_0 Z_0 \sinh \theta x \\ \xi &= \xi_0 \cosh \theta x - \frac{p_0}{Z_0} \sinh \theta x \end{aligned} \quad (\text{B.22})$$

where

$$\begin{aligned} \theta &= \frac{j \frac{\omega}{v}}{\sqrt{1 + j \frac{4}{3} \frac{\mu \omega}{\rho v^2}}} \doteq \frac{2}{3} \frac{\mu \omega^2}{\rho v^3} + j \frac{\omega}{v} = \frac{8 \mu \pi^2 f^2}{3 \rho v^3} + j \frac{2 \pi f}{v} \\ Z_0 &= \rho v \sqrt{1 + j \frac{4}{3} \frac{\mu \omega}{\rho v^2}} \doteq \rho v \left[1 + j \frac{4}{3} \frac{\pi \mu f}{\rho v^2} \right]. \end{aligned} \quad (\text{B.23})$$

These equations indicate that there is an attenuation due to viscosity of

$$A = \frac{8 \mu \pi^2 f^2}{3 \rho v^3} \text{ nepers per centimeter} \quad (\text{B.24})$$

which is proportional to the square of the frequency. In addition, as in the case of transmission in a tube, heat conduction losses add to the value. Kirchoff² has shown that the total attenuation should be

$$A = \frac{2 \pi^2 f^2}{\rho v^3} \left[\frac{4}{3} \mu + \frac{(\gamma - 1) K}{C_p} \right] \quad (\text{B.25})$$

where γ is the ratio of specific heats, K the thermal conductivity and C_p the specific heat at constant pressure. For gases, the last term adds an attenuation comparable with the viscosity but for liquids this term is negligible and adds little attenuation.

Experiment agrees with equation (B.25) as far as the frequency variation of attenuation is concerned but the absolute value of the multiplying constant is somewhat larger. For air the ratio between measured and calculated values is about 2. For liquids at high frequencies the attenuation can be more

² "Über den Einfluss der Wärmeleitung in einem Gase auf die Schallbewegung," Pogg. Ann. 134, 177 (1868).

accurately measured. Table XV gives comparisons between measured and calculated values for several liquids. (Taken from "Ultrasonics," L. Bergmann, John Wiley and Sons.)

TABLE XV
CALCULATED AND MEASURED VALUES OF ATTENUATION

Liquid	$\frac{A \times 10^{+15}}{f^2}$ (Measured)	$\frac{A \times 10^{+15}}{f^2}$ (Calculated)	Ratio
Acetone.....	0.32	0.0696	4.6
Benzol.....	9.19	0.0855	107.0
Chloroform.....	4.75	0.1040	44.5
Ether.....	0.55	0.0901	6.1
Ethyl Acetate.....	0.78	0.1060	7.35
Metaxylol.....	0.74	0.1230	6.0
Methyl Acetate.....	1.09	0.0840	13.0
Toluol.....	0.85	0.0775	11.0
Water.....	0.25	0.0850	2.9

On the other hand, for certain oils for which the coefficient of viscosity μ is very large, it has been shown recently³ that the attenuation agrees quite closely with the theoretical value given by (B.25).

One possible explanation of the discrepancy is that Stokes' assumption is not correct for liquids that have low shear viscosity coefficients μ and that there are two coefficients of viscosity, one for shear μ and the other for compression λ . Equation (B.25) for the attenuation of a sound wave would become:

$$A = \frac{2\pi^2 f^2}{\rho v^3} \left[\lambda + 2\mu + \frac{(\gamma - 1)K}{C_p} \right] \quad (\text{B.26})$$

and if λ were the same sign as μ and comparable, considerably larger attenuations would result. To measure the compressional constant λ , one would have to measure the difference between the applied stress and the static pressure of a dilational

³ "The Absorption of Ultrasonic Waves in Highly Viscous Liquids," J. L. Hunter, J. Acoustical Soc. Am., Vol. 13, No. 1, July 1941.

motion of the substance as a function of the rapidity of application and this would be a difficult matter to accomplish. This explanation would not conflict with the observed agreement between attenuation of sound in a tube and the coefficient of viscosity since only the shear coefficient μ is involved in the flow of air in a pipe.

If one wishes to obtain a network representation of the propagation of a free plane wave, he finds that the resistive element producing dissipation is now in the shunt arm. This follows from equations (4.81) and equations (B.23) of this section. The distributed series element per unit length is

$$Z_1 = Z_0 \theta = j \omega \rho \quad (\text{B.27})$$

while the shunt distributed element per unit length is

$$Z_2 = \frac{Z_0}{\theta} = \lambda + 2\mu - j \frac{\rho v^2}{\omega} \quad (\text{B.28})$$

where the impedances are expressed per unit area.

If the propagation takes place inside a tube, one would have both series and shunt resistances per unit length given by

$$\begin{aligned} Z_1 &= \left[\frac{P}{S} \sqrt{\frac{\mu \omega \rho}{2}} + j \omega \rho \left(1 + \frac{P}{S} \sqrt{\frac{\mu}{2 \omega \rho}} \right) \right] \times \frac{1}{S} \\ Z_2 &= \frac{1}{S} \left[\lambda + 2\mu - j \frac{\rho v^2}{\omega} \right] \end{aligned} \quad (\text{B.29})$$

where P is the perimeter and S the area of the tube.

APPENDIX C

ELASTIC AND PIEZOELECTRIC EQUATIONS FOR CRYSTALS

THE piezoelectric equations for a single mode of motion given in section (6.3) can be derived from the general piezoelectric and elastic equations for an aelotropic medium. Since such equations are useful in understanding the complete operation of a crystal transducer or resonator, it has seemed worth while to set them down and incorporate them in Appendix C. A short account of the elastic relations in an isotropic body is also included.

C.1. *Stress and Strain Relations in an Aelotropic Medium*

It was shown in Appendix B that the stresses on a small element of volume in equilibrium, or in non-rotational motion, can be specified by stating the values of three extensional stresses X_x, Y_y, Z_z , and three shearing stresses Y_z, Z_x , and X_y .

To specify the strains in a body we consider two points P and Q in the medium, which upon straining go to the positions P', Q' . In order to specify the strains, we have to calculate the difference in the length after straining, or have to evaluate $P'Q' - PQ$. Let P be located at the center of co-ordinates and Q have the co-ordinates x, y, z . After the material is stretched, P will have moved to P' having the co-ordinates ξ_1, η_1, ζ_1 , while Q' will have the co-ordinates $x + \xi_2, y + \eta_2, z + \zeta_2$. But the displacements are a continuous function of the co-ordinates x, y , and z so that we have

$$\xi_2 = \xi_1 + \frac{\partial \xi}{\partial x} x + \frac{\partial \xi}{\partial y} y + \frac{\partial \xi}{\partial z} z. \quad (\text{C.1})$$

Similarly

$$\begin{aligned} \eta_2 &= \eta_1 + \frac{\partial \eta}{\partial x} x + \frac{\partial \eta}{\partial y} y + \frac{\partial \eta}{\partial z} z \\ \zeta_2 &= \zeta_1 + \frac{\partial \zeta}{\partial x} x + \frac{\partial \zeta}{\partial y} y + \frac{\partial \zeta}{\partial z} z. \end{aligned} \quad (\text{C.2})$$

Hence subtracting the two lengths, we find that the increases in separation in the three directions are

$$\begin{aligned}\delta_x &= x \frac{\partial \xi}{\partial x} + y \frac{\partial \xi}{\partial y} + z \frac{\partial \xi}{\partial z} \\ \delta_y &= x \frac{\partial \eta}{\partial x} + y \frac{\partial \eta}{\partial y} + z \frac{\partial \eta}{\partial z} \\ \delta_z &= x \frac{\partial \zeta}{\partial x} + y \frac{\partial \zeta}{\partial y} + z \frac{\partial \zeta}{\partial z}.\end{aligned}\tag{C.3}$$

We now define the strain components as

$$\begin{aligned}x_x &= \frac{\partial \xi}{\partial x}; \quad y_y = \frac{\partial \eta}{\partial y}; \quad z_z = \frac{\partial \zeta}{\partial z} \\ y_z &= \frac{\partial \zeta}{\partial y} + \frac{\partial \eta}{\partial z}; \quad z_x = \frac{\partial \xi}{\partial z} + \frac{\partial \zeta}{\partial x}; \quad x_y = \frac{\partial \eta}{\partial x} + \frac{\partial \xi}{\partial y}\end{aligned}\tag{C.4}$$

and the rotation coefficients by the equations

$$\omega_x = \frac{\partial \zeta}{\partial y} - \frac{\partial \eta}{\partial z}; \quad \omega_y = \frac{\partial \xi}{\partial z} - \frac{\partial \zeta}{\partial x}; \quad \omega_z = \frac{\partial \eta}{\partial x} - \frac{\partial \xi}{\partial y}.\tag{C.5}$$

Hence the relative displacements of any two points can be expressed as

$$\begin{aligned}\delta_x &= xx_x + y \frac{(x_y - \omega_z)}{2} + z \frac{(z_x + \omega_y)}{2} \\ \delta_y &= x \frac{(x_y + \omega_z)}{2} + yy_y + z \frac{(y_z - \omega_x)}{2} \\ \delta_z &= x \frac{(z_x - \omega_y)}{2} + y \frac{(y_z + \omega_x)}{2} + zz_z\end{aligned}\tag{C.6}$$

which represents the most general type of displacement that the line PQ can undergo. It can be shown, however, that the ω 's result in a rotation of the line PQ without any change in length. For any body in equilibrium or in non-rotational vibration, the ω 's can be set equal to zero.

For an element suffering an extensional strain x_x alone, the displacement is along x and proportional to the x dimension.

For an element suffering a shearing strain x_y , the displacement along x is proportional to y , while the displacement along y is proportional to the x dimension. A cubic element of volume will be strained into a rhombic form, and the cosine of the resulting angle measures the shearing deformation.

In obtaining the equations of motion of oriented crystals, it is often necessary to know how the strains for one set of axes are related to those for another set of axes rotated with respect to the first set. Suppose that we consider a set of axes X' , Y' , Z' rotated with respect to the original axes. Let the direction cosines of the new axes with respect to the old be given by the relation

$$\begin{array}{cccc}
 & X & Y & Z \\
 X' & l_1 & m_1 & n_1 \\
 Y' & l_2 & m_2 & n_2 \\
 Z' & l_3 & m_3 & n_3.
 \end{array} \tag{C.7}$$

Then by resolving the extension caused by the strains along the different set of axes X' , Y' , Z' , Love ¹ has shown that the strains along the new axes can be expressed in terms of the strains along the old axes by the equations

$$\begin{aligned}
 x'_x &= l_1^2 x_x + m_1^2 y_y + n_1^2 z_z + m_1 n_1 y_z + n_1 l_1 z_x + l_1 m_1 x_y \\
 y'_y &= l_2^2 x_x + m_2^2 y_y + n_2^2 z_z + m_2 n_2 y_z + n_2 l_2 z_x + l_2 m_2 x_y \\
 z'_z &= l_3^2 x_x + m_3^2 y_y + n_3^2 z_z + m_3 n_3 y_z + n_3 l_3 z_x + l_3 m_3 x_y \\
 y'_z &= 2l_2 l_3 x_x + 2m_2 m_3 y_y + 2n_2 n_3 z_z + (m_2 n_3 + m_3 n_2) y_z \\
 &\quad + (n_2 l_3 + n_3 l_2) z_x + (l_2 m_3 + l_3 m_2) x_y \\
 z'_x &= 2l_3 l_1 x_x + 2m_3 m_1 y_y + 2n_3 n_1 z_z + (m_3 n_1 + m_1 n_3) y_z \\
 &\quad + (n_3 l_1 + n_1 l_3) z_x + (l_3 m_1 + l_1 m_3) x_y \\
 x'_y &= 2l_1 l_2 x_x + 2m_1 m_2 y_y + 2n_1 n_2 z_z + (m_1 n_2 + m_2 n_1) y_z \\
 &\quad + (n_1 l_2 + n_2 l_1) z_x + (l_1 m_2 + l_2 m_1) x_y.
 \end{aligned} \tag{C.8}$$

Having specified stresses and strains we next consider the relationship between them. For small displacements it is a

¹ "Theory of Elasticity," Love, Cambridge University Press, p. 42.

consequence of Hooke's law that the stresses are proportional to the strains. For the most unsymmetrical medium, this proportionality can be written in the form:

$$\begin{aligned}
 -X_x &= c_{11}x_x + c_{12}y_y + c_{13}z_z + c_{14}y_z + c_{15}z_x + c_{16}x_y \\
 -Y_y &= c_{21}x_x + c_{22}y_y + c_{23}z_z + c_{24}y_z + c_{25}z_x + c_{26}x_y \\
 -Z_z &= c_{31}x_x + c_{32}y_y + c_{33}z_z + c_{34}y_z + c_{35}z_x + c_{36}x_y \\
 -Y_z &= c_{41}x_x + c_{42}y_y + c_{43}z_z + c_{44}y_z + c_{45}z_x + c_{46}x_y \\
 -Z_x &= c_{51}x_x + c_{52}y_y + c_{53}z_z + c_{54}y_z + c_{55}z_x + c_{56}x_y \\
 -X_y &= c_{61}x_x + c_{62}y_y + c_{63}z_z + c_{64}y_z + c_{65}z_x + c_{66}x_y
 \end{aligned} \tag{C.9}$$

where c_{11} for example is an elastic constant expressing the proportionality between the x_x strain and the X_x stress in the absence of any other strains. The negative sign occurs for the stress since a stress is usually reckoned as positive for a compression and negative for an extension. Due to the reciprocity relationship we find that

$$c_{12} = c_{21} \text{ and in general } c_{ij} = c_{ji}. \tag{C.10}$$

This reduces the number of independent elastic constants for the most unsymmetrical medium to 21.

If we strain the body it has been shown by Love ² that the potential energy stored in the body is

$$PE = -\frac{1}{2}[X_x x_x + Y_y y_y + Z_z z_z + Y_z y_z + Z_x x_x + X_y x_y]. \tag{C.11}$$

Introducing the values of the stresses from equation (C.9) the potential energy becomes

$$\begin{aligned}
 2PE &= c_{11}x_x^2 + 2c_{12}x_x y_y + 2c_{13}x_x z_z + 2c_{14}x_x y_z + 2c_{15}x_x z_x + 2c_{16}x_x x_y \\
 &\quad + c_{22}y_y^2 + 2c_{23}y_y z_z + 2c_{24}y_y y_z + 2c_{25}y_y z_x + 2c_{26}y_y x_y \\
 &\quad + c_{33}z_z^2 + 2c_{34}z_z y_z + 2c_{35}z_z z_x + 2c_{36}z_z x_y \\
 &\quad + c_{44}y_z^2 + 2c_{45}y_z z_x + 2c_{46}y_z x_y \\
 &\quad + c_{55}z_x^2 + 2c_{56}z_x x_y \\
 &\quad + c_{66}x_y^2.
 \end{aligned} \tag{C.12}$$

² "Theory of Elasticity," Love, p. 95.

The relations (C.9) then can be obtained by differentiating the potential energy by the strain according to the relation

$$X_x = - \frac{\partial PE}{\partial x_x}; \quad \dots; \quad X_y = - \frac{\partial PE}{\partial x_y}. \quad (\text{C.13})$$

If there is any symmetry about the aelotropic medium, some of the elastic constants will be zero and some relations will exist between some of the other constants. For example, suppose that we have a digonal axis of symmetry such that conditions are unchanged if we interchange the positive and negative directions of the axis. If this axis were the Z axis we would have

$$\begin{aligned} l_1 &= 1, m_1 = 0, n_1 = 0 \\ l_2 &= 0, m_2 = -1, n_2 = 0 \\ l_3 &= 0, m_3 = 0, n_3 = -1. \end{aligned} \quad (\text{C.14})$$

Then applying these values to equations (C.8) we find

$$\begin{aligned} x_x' &= x_x; \quad y_y' = y_y; \quad z_z' = z_z; \quad y_z' = y_z; \\ x_x' &= -z_x; \quad x_y' = -x_y. \end{aligned} \quad (\text{C.15})$$

The only way the potential energy can remain invariant to this transformation is for

$$c_{15} = c_{16} = c_{25} = c_{26} = c_{35} = c_{36} = c_{45} = c_{46} = 0. \quad (\text{C.16})$$

The two principal cases of interest are quartz and Rochelle salt. Quartz satisfies the condition discussed above for the Z axis and in addition for rotations around the Z axis, the properties repeat themselves every 120° . The first symmetry results in the constants of equation (C.16) being zero. The second symmetry results in

$$\begin{aligned} c_{22} &= c_{11}; \quad c_{23} = c_{13}; \quad c_{24} = -c_{14}; \quad c_{44} = c_{55}; \\ c_{56} &= c_{14}; \quad c_{66} = \frac{c_{11} - c_{12}}{2}; \quad c_{34} = 0. \end{aligned} \quad (\text{C.17})$$

Hence the strain energy function for quartz becomes

$$\begin{aligned} 2PE &= c_{11}(x_x^2 + y_y^2) + 2c_{12}x_x y_y + 2c_{13}(x_x z_z + y_y z_z) \\ &\quad + 2c_{14}(x_x y_z - y_y z_x) + c_{33}z_z^2 + c_{44}(y_z^2 + z_x^2) \\ &\quad + 2c_{14}z_x x_y + \left(\frac{c_{11} - c_{12}}{2} \right) x_y^2. \end{aligned} \quad (\text{C.18})$$

Measurements by Voigt³ have determined the six elastic constants as

$$\begin{aligned} c_{11} &= 8.51 \times 10^{11} \frac{\text{dynes}}{\text{cm}^2}; \quad c_{33} = 10.53 \times 10^{11}; \\ c_{44} &= 5.71 \times 10^{11}; \quad c_{12} = 0.695 \times 10^{11}; \\ c_{13} &= 1.41 \times 10^{11}; \quad c_{14} = 1.68 \times 10^{11}; \\ c_{66} &= \frac{c_{11} - c_{12}}{2} = 3.91 \times 10^{11}. \end{aligned} \quad (\text{C.19})$$

Rochelle salt belongs to the rhombic hemihedral class of crystals and possesses three digonal axes of symmetry which are identical with the three crystallographic axes. By a consideration of the symmetry expressed in equation (C.14) it is evident that this degree of symmetry will result in all the coefficients given in equation (C.20) being equal to zero.

$$\begin{aligned} c_{14} = c_{15} = c_{16} = c_{24} = c_{25} = c_{26} = c_{34} \\ = c_{35} = c_{36} = c_{45} = c_{46} = c_{56} = 0. \end{aligned} \quad (\text{C.20})$$

This leaves nine elastic constants. These were recently measured⁴ by a dynamical method, with the result given by equation (C.21)

$$\begin{aligned} c_{11} &= 4.25 \times 10^{11} \frac{\text{dynes}}{\text{cm}^2}; \quad c_{22} = 5.15 \times 10^{11}; \\ c_{33} &= 6.29 \times 10^{11}; \quad c_{44} = 1.252 \times 10^{11}; \\ c_{55} &= 0.304 \times 10^{11}; \quad c_{66} = 0.996 \times 10^{11}; \\ c_{12} &= 2.96 \times 10^{11}; \quad c_{13} = 3.57 \times 10^{11}; \\ c_{23} &= 3.425 \times 10^{11}. \end{aligned} \quad (\text{C.21})$$

For isotropic bodies, where axes in any direction result in the same expression for the potential energy, only two elastic constants remain. For this case we have

$$\begin{aligned} c_{11} = c_{22} = c_{33} = \lambda + 2\mu; \quad c_{12} = c_{13} = c_{23} = \lambda; \\ c_{44} = c_{55} = c_{66} = \mu. \end{aligned} \quad (\text{C.22})$$

³ "Lehrbuch der Kristallphysik," W. Voigt.

⁴ "A Dynamic Measurement of the Elastic, Electric, and Piezoelectric Constants of Rochelle Salt," W. P. Mason, Phys. Rev., Vol. 55, April 15, 1939.

All other constants are zero. The strain energy function then becomes

$$2PE = \lambda(x_x + y_y + z_z)^2 + 2\mu(x_x^2 + y_y^2 + z_z^2) + \mu(y_z^2 + z_x^2 + x_y^2). \quad (\text{C.23})$$

The stress-strain equations become

$$\begin{aligned} -X_x &= \lambda(x_x + y_y + z_z) + 2\mu x_x; & -Y_z &= \mu y_z \\ -Y_y &= \lambda(x_x + y_y + z_z) + 2\mu y_y; & -Z_x &= \mu z_x \\ -Z_z &= \lambda(x_x + y_y + z_z) + 2\mu z_z; & -X_y &= \mu x_y. \end{aligned} \quad (\text{C.24})$$

If we are stretching a long thin bar along the X axis by an X_x stress, we would have

$$Y_y = Z_z = Y_z = Z_x = X_y = 0. \quad (\text{C.25})$$

Under these conditions the relation between stress and strain is given by Young's modulus Y_0 . Eliminating all strains except x_x by means of the relations of (C.25) we find

$$-X_x = \mu \left(\frac{3\lambda + 2\mu}{\lambda + \mu} \right) x_x, \quad \text{hence} \quad Y_0 = \mu \left(\frac{3\lambda + 2\mu}{\lambda + \mu} \right) \quad (\text{C.26})$$

in agreement with the result given in equation (7.30).

When the width of the medium is considerably larger than a wavelength, the medium does not have time to contract laterally and the condition that $Y_y = Z_z = 0$ is no longer valid. A better approximation is to assume that

$$y_y = z_z = y_z = z_x = x_y = 0. \quad (\text{C.27})$$

For that case the relation between stress and strain becomes

$$-X_x = (\lambda + 2\mu)x_x \quad (\text{C.28})$$

in agreement with equation (7.31).

Another quantity of some interest in elastic theory is Poisson's ratio relating the lateral contraction to the longitudinal expansion for a long thin bar. This is given by (C.24) and (C.25) as

$$-\frac{y_y}{x_x} = \sigma = \frac{\lambda}{2(\lambda + \mu)}. \quad (\text{C.29})$$

C.2. Piezoelectric Relations for an Aelotropic Medium

When the aelotropic medium is piezoelectric, other strains are added when an electrical charge is applied to the surface of the crystal. These added strains produce additional terms in the potential energy equation. It has been shown recently ⁵ that the most advantageous way of expressing these strains is in terms of the polarization of the crystal. For the most general type of medium the potential energy can be expressed ⁵ as

$$\begin{aligned}
 2PE = & c_{11}^* x_x^2 + 2c_{12}^* x_x y_y + 2c_{13}^* x_x z_z + 2c_{14}^* x_x y_z \\
 & + 2c_{15}^* x_x z_x + 2c_{16}^* x_x x_y \\
 & + c_{22}^* y_y^2 + 2c_{23}^* y_y z_z + 2c_{24}^* y_y y_z + 2c_{25}^* y_y z_x + 2c_{26}^* y_y x_y \\
 & + c_{33}^* z_z^2 + 2c_{34}^* z_z y_z + 2c_{35}^* z_z z_x + 2c_{36}^* z_z x_y \\
 & + c_{44}^* y_z^2 + 2c_{45}^* y_z z_x + 2c_{46}^* y_z x_y \\
 & + c_{55}^* z_x^2 + 2c_{56}^* z_x x_y \\
 & + c_{66}^* x_y^2 \quad (C.30) \\
 & + 2f_{11}^* x_x P_x + 2f_{12}^* y_y P_x + 2f_{13}^* z_z P_x + 2f_{14}^* y_z P_x + 2f_{15}^* z_x P_x + 2f_{16}^* x_y P_x \\
 & + 2f_{21}^* x_x P_y + 2f_{22}^* y_y P_y + 2f_{23}^* z_z P_y + 2f_{24}^* y_z P_y + 2f_{25}^* z_x P_y + 2f_{26}^* x_y P_y \\
 & + 2f_{31}^* x_x P_z + 2f_{32}^* y_y P_z + 2f_{33}^* z_z P_z + 2f_{34}^* y_z P_z + 2f_{35}^* z_x P_z + 2f_{36}^* x_y P_z \\
 & + \chi_1 P_x^2 + \chi_2 P_y^2 + \chi_3 P_z^2.
 \end{aligned}$$

In this equation the f_{ij}^* constants are the piezoelectric constants of the material and χ_i are the reciprocals of the electric susceptibilities of the clamped crystal, i.e., free from strain. These are related to the dielectric constants of the crystal by the equation

$$K_i = 1 + 4\pi/\chi_i$$

where K_i is the dielectric constant of the clamped crystal in the i th direction. The c elastic constants are shown starred since they are not measured in the usual manner by determining the distortion for an applied stress in the absence of any metallic

⁵ Phys. Rev. **55**, 775 (1939), W. P. Mason.

Phys. Rev. **57**, 829 (1940), H. Mueller

Phys. Rev. **58**, 744 (1940), W. P. Mason.

conducting surfaces near the crystal. Rather, as shown by equation (C.30), they would have to be measured with the polarizations P_x , P_y , and P_z equal to zero. The usual way of measuring elastic constants of piezoelectric crystals will result in the charge on the surface being zero. Since the charge on the surface is

$$Q_x = \frac{E_x}{4\pi} + P_x, \quad (\text{C.31})$$

to measure the starred constants of equation (C.30) we would have to maintain a charge on the surface equal and opposite to the piezoelectric field $E_x/4\pi$ developed by the distortion of the crystal. Suitable transformations to determine the usually measured elastic constants are discussed later. The difference in any case is very small for all crystals.

Polarizations, being vectors, transform according to the equations

$$\begin{aligned} P_x' &= l_1 P_x + m_1 P_y + n_1 P_z \\ P_y' &= l_2 P_x + m_2 P_y + n_2 P_z \\ P_z' &= l_3 P_x + m_3 P_y + n_3 P_z. \end{aligned} \quad (\text{C.32})$$

A result of the symmetry existing in crystals is that some of the 18 possible piezoelectric constants f_{ij}^* will be zero or related to other constants. For example consider the transformation given in (C.14) in which the properties for the two directions of the Z axis remain unchanged. Then the strains are given by (C.5) and the polarizations become

$$P_x' = P_x; P_y' = -P_y; P_z' = -P_z. \quad (\text{C.33})$$

For the potential energy function to have the same form for both orientations we must have the elastic constants of (C.16) equal to zero and in addition

$$\begin{aligned} f_{15}^* = f_{16}^* = f_{21}^* = f_{22}^* = f_{23}^* = f_{24}^* = f_{31}^* \\ = f_{32}^* = f_{33}^* = f_{34}^* = 0. \end{aligned} \quad (\text{C.34})$$

If we apply the same condition to the X and Y axes, the conditions for Rochelle salt result. For this case all of the piezoelectric constants must be zero except f_{14}^* , f_{25}^* and f_{36}^* .

Hence the potential energy for Rochelle salt can be written in the form

$$\begin{aligned}
 2PE = & c_{11}^* x_x^2 + 2c_{12}^* x_x y_y + 2c_{13}^* x_x z_z + c_{33}^* z_z^2 \\
 & + c_{22}^* y_y^2 + 2c_{23}^* y_y z_z + c_{44}^* y_z^2 + c_{55}^* z_x^2 \\
 & + c_{66}^* x_y^2 + 2f_{14}^* y_z P_x + 2f_{25}^* z_x P_y + 2f_{36}^* x_y P_z \\
 & + \chi_1 P_x^2 + \chi_2 P_y^2 + \chi_3 P_z^2.
 \end{aligned} \quad (C.35)$$

The symmetry of quartz results in

$$f_{12}^* = -f_{11}^*; f_{25}^* = -f_{14}^*; f_{26}^* = -f_{11}^* \text{ and } \chi_1 = \chi_2. \quad (C.36)$$

All other constants are zero.

The potential energy expression then becomes for quartz

$$\begin{aligned}
 2PE = & c_{11}^* (x_x^2 + y_y^2) + 2c_{12}^* x_x y_y + 2c_{13}^* (x_x z_z + y_y z_z) \\
 & + 2c_{14}^* (x_x y_z - y_y z_x) + c_{33}^* z_z^2 + c_{44}^* (y_z^2 + z_x^2) \\
 & + 2c_{14}^* z_x x_y + \left(\frac{c_{11}^* - c_{12}^*}{2} \right) x_y^2 + 2f_{11}^* x_x P_x \\
 & - 2f_{11}^* y_y P_x + 2f_{14}^* y_z P_x - 2f_{14}^* z_x P_y - 2f_{11}^* x_y P_y \\
 & + \chi_1 (P_x^2 + P_y^2) + \chi_3 P_z^2.
 \end{aligned} \quad (C.37)$$

The piezoelectric equations can be derived from these expressions by employing the relations

$$\begin{aligned}
 X_x = -\frac{\partial PE}{\partial x_x}, \dots, X_y = -\frac{\partial PE}{\partial x_y}; \\
 E_x = \frac{\partial PE}{\partial P_x}, \dots, E_z = \frac{\partial PE}{\partial P_z}.
 \end{aligned} \quad (C.38)$$

C.3. Piezoelectric Equations for Rochelle Salt

For Rochelle salt these result in the nine piezoelectric equations

$$\begin{aligned}
 -X_x = & c_{11} x_x + c_{12} y_y + c_{13} z_z; \quad -Y_z = c_{44}^* y_z + f_{14}^* P_x \\
 -Y_y = & c_{12} x_x + c_{22} y_y + c_{23} z_z; \quad -Z_x = c_{55}^* z_x + f_{25}^* P_y \\
 -Z_z = & c_{13} x_x + c_{23} y_y + c_{33} z_z; \quad -X_y = c_{66}^* x_y + f_{36}^* P_z \\
 E_x = & f_{14}^* y_z + \chi_1 P_x; \quad E_y = f_{25}^* z_x + \chi_2 P_y; \\
 E_z = & f_{36}^* x_y + \chi_3 P_z.
 \end{aligned} \quad (C.39)$$

The absence of the stars in the first three equations shows that there is no difference for these constants since no polarizations appear in the equations. To obtain the elastic constant c_{44} ordinarily measured we substitute for P_x

$$P_x = Q_x - \frac{E_x}{4\pi} \quad (\text{C.40})$$

in the equations involving Y_z and E_x . Solving these simultaneously we find that they can be written in the form

$$-Y_z = c_{44}y_z + f_{14}Q_x; \quad E_x = f_{14}y_z + \frac{4\pi}{K_1} Q_x \quad (\text{C.41})$$

where K_1 is the clamped dielectric constant of the crystal along the X axis, provided that

$$c_{44} = c_{44}^* - \frac{f_{14}^{*2}}{4\pi} \frac{(K_1 - 1)}{K_1};$$

$$f_{14} = \frac{f_{14}^*}{1 + \frac{\chi_1}{4\pi}} = \frac{f_{14}^*(K_1 - 1)}{K_1}. \quad (\text{C.42})$$

Since K_1 for Rochelle salt is 100 or greater, f_{14}^* will not differ from f_{14} by more than 1 per cent. f_{14} has an absolute value in cgs units of about 7.8×10^4 . Hence the correction to c_{44}^* to obtain c_{44} is in the order of 4.8×10^8 which is less than 0.4 per cent of c_{44} . Performing the same substitutions for P_y and P_z , the piezoelectric equations for Rochelle salt become

$$\begin{aligned} -X_x &= c_{11}x_x + c_{12}y_y + c_{13}z_z; & -Y_z &= c_{44}y_z + f_{14}Q_x \\ -Y_y &= c_{12}x_x + c_{22}y_y + c_{23}z_z; & -Z_x &= c_{55}z_x + f_{25}Q_y \\ -Z_z &= c_{13}x_x + c_{23}y_y + c_{33}z_z; & -X_y &= c_{66}x_y + f_{36}Q_z \\ E_x &= f_{14}y_z + \frac{4\pi}{K_1} Q_x; & E_y &= f_{25}z_x + \frac{4\pi}{K_2} Q_y; \end{aligned} \quad (\text{C.43})$$

$$E_z = f_{36}x_y + \frac{4\pi}{K_3} Q_z$$

where

$$f_{25} = \frac{f_{25}^*(K_2 - 1)}{K_2}; \quad f_{36} = \frac{f_{36}^*(K_3 - 1)}{K_3};$$

$$c_{55} = c_{55}^* - \frac{f_{25}^{*2}}{4\pi} \left(\frac{K_2 - 1}{K_2} \right); \quad c_{66} = c_{66}^* - \frac{f_{36}^{*2}}{4\pi} \left(\frac{K_3 - 1}{K_3} \right).$$

Measurements⁶ indicate that f_{14} , f_{25} , f_{36} are nearly absolute constants independent of temperature and frequency, and have, in cgs units, the values

$$f_{14} = 7.8 \times 10^4; f_{25} = 6.33 \times 10^4; f_{36} = 4.81 \times 10^4. \quad (\text{C.44})$$

The dielectric constants K_2 and K_3 along the Y and Z axis vary little with temperature and have the values

$$K_2 = 9.8; K_3 = 9.2. \quad (\text{C.45})$$

The dielectric constant K_1 of the clamped crystal along the X axis varies considerably with temperature as shown in Fig. C.1

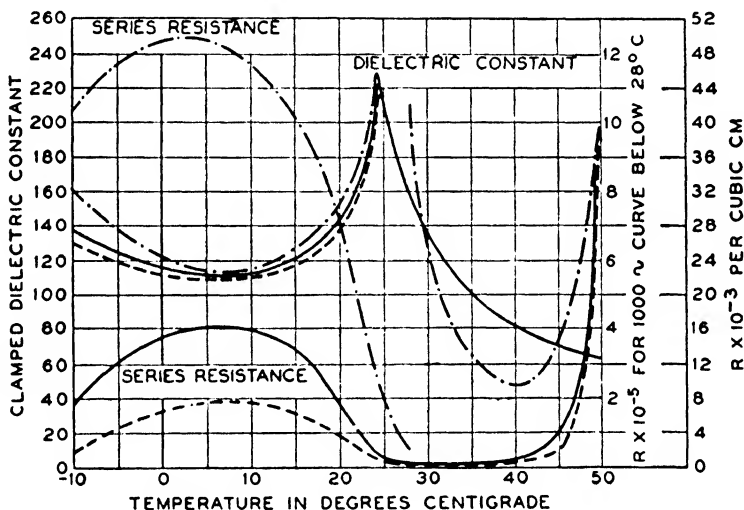


FIG. C.1—MEASUREMENTS OF THE CLAMPED DIELECTRIC CONSTANT AND ASSOCIATED SERIES OHMIC RESISTANCE OF A 45° X -CUT ROCHELLE SALT CRYSTAL FOR THREE FREQUENCY RANGES. SOLID LINES ARE MEASUREMENTS AT 80 KC, DOTTED LINES AT 160 KC, AND DOT-DASH LINES AT 1000 CYCLES.

This constant varies slightly with frequency as shown by the three curves, and has a resistance component as shown by the dotted lines.

By solving the equations of (C.39) for the strain and polarizations in terms of the stresses and potential gradients, the

⁶ "A Dynamical Measurement of the Elastic, Electric, and Piezoelectric Constants of Rochelle Salt," W. P. Mason, *Phys. Rev.* **55**, 775 (1939).

piezoelectric equations can be expressed in the alternate form

$$\begin{aligned}
 -x_x &= s_{11}X_x + s_{12}Y_y + s_{13}Z_z; & -y_z &= s_{44}Y_z + d_{14}E_x \\
 -y_y &= s_{12}X_x + s_{22}Y_y + s_{23}Z_z; & -z_x &= s_{55}Z_x + d_{25}E_y \\
 -z_z &= s_{13}X_x + s_{23}Y_y + s_{33}Z_z; & -x_y &= s_{66}X_y + d_{36}E_z \quad (\text{C.46}) \\
 P_x &= d_{14}Y_z + \kappa_1 E_x; & P_y &= d_{25}Z_x + \kappa_2 E_y; \\
 P_z &= d_{36}X_y + \kappa_3 E_z
 \end{aligned}$$

where

$$s_{11} = \frac{\Delta_{11}}{\Delta}; \quad s_{23} = \frac{\Delta_{23}}{\Delta}; \text{ etc., where } \Delta \text{ is the determinant}$$

$$\Delta = \begin{vmatrix} c_{11} & c_{12} & c_{13} \\ c_{12} & c_{22} & c_{23} \\ c_{13} & c_{23} & c_{33} \end{vmatrix} \quad (\text{C.47})$$

and Δ_{11} is the determinant obtained from this by suppressing the first row and first column. Similarly

$$d_{14} = f_{14}^*/D_x; \quad s_{44} = \chi_1/D_x; \quad \kappa_1 = c_{44}^*/D_x \quad (\text{C.48})$$

where

$$D_x = c_{44}^*\chi_1 - f_{14}^{*2}.$$

The s_{11} , s_{12} , s_{13} , s_{22} , s_{23} , s_{33} constants are the moduli of compliance which can be measured by mechanical means when the crystal is plated or unplated. The compliance s_{44} is the compliance of the crystal when $E_x = 0$ or when the crystal is plated and short-circuited. Similarly d_{14} is the ratio of the strain to the applied field when $Y_z = 0$ or the crystal is free to move, and κ_1 is the susceptibility of the crystal when $Y_z = 0$ or the crystal is free to move. All of these constants vary widely with the temperature, plating conditions, etc. Hence it is more advantageous to use the constants f_{14} , c_{44} , and K_1 , and this has been done in this book.

When Rochelle salt is used to set up longitudinal or flexural vibrations, the cuts used are the 45° X -cut or the 45° Y -cut. The first cut has the normal to its major face along the X axis and its longest dimension 45° from the Y and Z axes. The second cut has the normal to its major face along the Y axis and

its longest dimension 45° from the X and Z axes. Either cut requires a rotated system of axes to specify the constants for longitudinal vibrations. One method for determining the constants of the rotated system is to substitute the values of the strains in the first system in terms of the strains of the second system and form a new expression for the potential energy in terms of the new strains. The piezoelectric equations can then be determined by differentiation. In order to perform this operation we need to have an expression for the first strains in terms of the second. This can be determined by solving equations (C.8) simultaneously with the result given in equation (C.49).

$$\begin{aligned}
 x_x &= l_1^2 x'_x + l_2^2 y'_y + l_3^2 z'_z + l_2 l_3 y'_z + l_3 l_1 z'_x + l_1 l_2 x'_y \\
 y_y &= m_1^2 x'_x + m_2^2 y'_y + m_3^2 z'_z + m_2 m_3 y'_z + m_3 m_1 z'_x \\
 &\quad + m_1 m_2 x'_y \\
 z_z &= n_1^2 x'_x + n_2^2 y'_y + n_3^2 z'_z + n_2 n_3 y'_z + n_3 n_1 z'_x \\
 &\quad + n_1 n_2 x'_y \\
 y_z &= 2m_1 n_1 x'_x + 2m_2 n_2 y'_y + 2m_3 n_3 z'_z + (m_2 n_3 + m_3 n_2) y'_z \\
 &\quad + (m_3 n_1 + m_1 n_3) z'_x + (m_1 n_2 + m_2 n_1) x'_y \quad (\text{C.49}) \\
 z_x &= 2n_1 l_1 x'_x + 2n_2 l_2 y'_y + 2n_3 l_3 z'_z + (n_2 l_3 + n_3 l_2) y'_z \\
 &\quad + (n_3 l_1 + n_1 l_3) z'_x + (n_1 l_2 + n_2 l_1) x'_y \\
 x_y &= 2l_1 m_1 x'_x + 2l_2 m_2 y'_y + 2l_3 m_3 z'_z + (l_2 m_3 + l_3 m_2) y'_z \\
 &\quad + (l_3 m_1 + l_1 m_3) z'_x + (l_1 m_2 + l_2 m_1) x'_y.
 \end{aligned}$$

Similarly in the converse system the polarizations become

$$\begin{aligned}
 P_x &= l_1 P'_x + l_2 P'_y + l_3 P'_z \\
 P_y &= m_1 P'_x + m_2 P'_y + m_3 P'_z \\
 P_z &= n_1 P'_x + n_2 P'_y + n_3 P'_z.
 \end{aligned} \quad (\text{C.50})$$

For the 45° X -cut Rochelle salt crystals the direction cosines of the new system in terms of the crystallographic axis system are

$$\begin{aligned}
 l_1 &= 1; \quad m_1 = 0; \quad n_1 = 0 \\
 l_2 &= 0; \quad m_2 = .707; \quad n_2 = .707 \\
 l_3 &= 0; \quad m_3 = -.707; \quad n_3 = .707.
 \end{aligned} \quad (\text{C.51})$$

With these values the relations between strains and polarizations become

$$\begin{aligned}
 x_x &= x_x'; \quad y_y = \frac{1}{2}(y_y' + z_z' - y_z'); \\
 z_z &= \frac{1}{2}(y_y' + z_z' + y_z'); \quad y_z = (y_y' - z_z') \\
 z_x &= .707(z_x' + x_y'); \quad x_y = .707(-z_x' + x_y'); \quad P_x = P_x'; \\
 P_y &= .707(P_y' - P_z'); \quad P_z = .707(P_y' + P_z').
 \end{aligned} \tag{C.52}$$

Substituting these values in equation (C.35) and collecting terms, the potential energy for the rotated axes is given by the equation

$$\begin{aligned}
 2PE &= c_{11}x_x'^2 + (c_{12} + c_{13})x_x'y_y' + (c_{12} + c_{13})x_x'z_z' \\
 &+ (c_{13} - c_{12})x_x'y_z' + \left(\frac{c_{22} + c_{33} + 2c_{23} + 4c_{44}^*}{4}\right)y_y'^2 \\
 &+ \left(\frac{c_{22} + c_{33} + 2c_{23} - 4c_{44}^*}{2}\right)y_y'z_z' \\
 &+ \left(\frac{c_{33} - c_{22}}{2}\right)y_y'y_z' + \left(\frac{c_{22} + c_{33} + 2c_{23} + 4c_{44}^*}{4}\right)z_z'^2 \\
 &+ \left(\frac{c_{33} - c_{22}}{2}\right)z_z'y_z' + \left(\frac{c_{22} + c_{33} - 2c_{23}}{4}\right)y_z'^2 \\
 &+ \left(\frac{c_{55}^* + c_{66}^*}{2}\right)z_x'^2 + (c_{55}^* - c_{66}^*)z_x'x_y' \\
 &+ \left(\frac{c_{55}^* + c_{66}^*}{2}\right)x_y'^2 + 2f_{14}^*y_y'P_x' - 2f_{14}^*z_z'P_x' \\
 &+ (f_{25}^* - f_{36}^*)z_x'P_y' + (f_{25}^* + f_{36}^*)x_y'P_y' \\
 &+ (f_{25}^* + f_{36}^*)z_x'P_z' + (f_{36}^* - f_{25}^*)x_y'P_z' \\
 &+ \chi_1P_x'^2 + \left(\frac{\chi_2 + \chi_3}{2}\right)P_y'^2 \\
 &+ (\chi_3 - \chi_2)P_y'P_z' + \left(\frac{\chi_2 + \chi_3}{2}\right)P_z'^2.
 \end{aligned} \tag{C.53}$$

From this equation the nine piezoelectric equations can be obtained. For an X -cut crystal the only equations of interest are

$$\begin{aligned}
 -X_{x'} &= \frac{\partial PE}{\partial x_{x'}} = c_{11}x_{x'} + \left(\frac{c_{12} + c_{13}}{2}\right)y_{y'} \\
 &\quad + \left(\frac{c_{12} + c_{13}}{2}\right)z_{z'} + \left(\frac{c_{13} - c_{12}}{2}\right)y_{y'} \\
 -Y_{y'} &= \frac{\partial PE}{\partial y_{y'}} = \left(\frac{c_{12} + c_{13}}{2}\right)x_{x'} \\
 &\quad + \left(\frac{c_{22} + c_{33} + 2c_{23} + 4c_{44}^*}{4}\right)y_{y'} \\
 &\quad + \left(\frac{c_{22} + c_{33} + 2c_{23} - 4c_{44}^*}{4}\right)z_{z'} \\
 &\quad + \left(\frac{c_{33} - c_{22}}{4}\right)y_{z'} + f_{14}^*P_{x'} \\
 -Z_{z'} &= \frac{\partial PE}{\partial z_{z'}} = \left(\frac{c_{12} + c_{13}}{2}\right)x_{x'} \\
 &\quad + \left(\frac{c_{22} + c_{33} + 2c_{23} - 4c_{44}^*}{4}\right)y_{y'} \\
 &\quad + \left(\frac{c_{22} + c_{33} + 2c_{23} + 4c_{44}^*}{4}\right)z_{z'} \\
 &\quad + \left(\frac{c_{33} - c_{22}}{4}\right)y_{z'} - f_{14}^*P_{x'} \\
 -Y_{z'} &= \frac{\partial PE}{\partial y_{z'}} = \left(\frac{c_{13} - c_{12}}{2}\right)x_{x'} + \left(\frac{c_{33} - c_{22}}{4}\right)y_{y'} \\
 &\quad + \left(\frac{c_{33} - c_{22}}{4}\right)z_{z'} + \left(\frac{c_{22} + c_{33} - 2c_{23}}{4}\right)y_{y'} \\
 E_x &= \frac{\partial PE}{\partial P_{x'}} = f_{14}^*(y_{y'} - z_{z'}) + \chi_1 P_{x'}.
 \end{aligned} \tag{C.54}$$

If we make the substitution $P_x = \left(Q_x - \frac{E_x}{4\pi}\right)$, these equations can be written in the form

$$\begin{aligned}
 -X_x' &= c_{11}x_x' + \left(\frac{c_{12} + c_{13}}{2}\right)y_y' + \left(\frac{c_{12} + c_{13}}{2}\right)z_z' \\
 &\quad + \left(\frac{c_{13} - c_{12}}{2}\right)y_s' \\
 -Y_y' &= \left(\frac{c_{12} + c_{13}}{2}\right)x_x' + \left(\frac{c_{22} + c_{33} + 2c_{23} + 4c_{44}}{4}\right)y_y' \\
 &\quad + \left(\frac{c_{22} + c_{33} + 2c_{23} - 4c_{44}}{4}\right)z_z' \\
 &\quad + \left(\frac{c_{33} - c_{22}}{4}\right)y_s' + f_{14}Q_x' \\
 -Z_z' &= \left(\frac{c_{12} + c_{13}}{2}\right)x_x' + \left(\frac{c_{22} + c_{33} + 2c_{23} - 4c_{44}}{4}\right)y_y' \quad (\text{C.55}) \\
 &\quad + \left(\frac{c_{22} + c_{33} + 2c_{23} + 4c_{44}}{4}\right)z_z' \\
 &\quad + \left(\frac{c_{33} - c_{22}}{4}\right)y_s' - f_{14}Q_x' \\
 -Y_s' &= \left(\frac{c_{13} - c_{12}}{2}\right)x_x' + \left(\frac{c_{33} - c_{22}}{4}\right)y_y' \\
 &\quad + \left(\frac{c_{33} - c_{22}}{4}\right)z_z' + \left(\frac{c_{22} + c_{33} - 2c_{23}}{4}\right)y_s' \\
 E_x &= f_{14}(y_y' - z_z') + \frac{4\pi}{K_1} Q_x'.
 \end{aligned}$$

These are the equations holding for a 45° X -cut crystal.

If this crystal is in longitudinal vibration along the Y' axis we can set $X_x' = Z_z' = Y_s' = 0$ provided the width is small

compared to the length. Solving these equations and eliminating x'_z, z'_z, y'_z , we find

$$\begin{aligned}
 -Y'_y &= y'_y \left(\frac{4}{1/c_{44} + s_{22} + s_{33} + 2s_{23}} \right) \\
 &\quad + \frac{f_{14}Q_x}{2c_{44}} \left(\frac{4}{1/c_{44} + s_{22} + s_{33} + 2s_{23}} \right) \\
 E_x &= Q_x \left[\frac{4\pi}{K_1} - \frac{f_{14}^2}{c_{44}} \left(\frac{s_{22} + s_{33} + 2s_{23}}{1/c_{44} + s_{22} + s_{33} + 2s_{23}} \right) \right] \\
 &\quad + \frac{f_{14}y'_y}{2c_{44}} \left[\frac{4}{1/c_{44} + s_{22} + s_{33} + 2s_{23}} \right].
 \end{aligned} \tag{C.56}$$

We designate

$$\frac{4\pi}{K_1} - \frac{f_{14}^2}{c_{44}} \left(\frac{s_{22} + s_{33} + 2s_{23}}{1/c_{44} + s_{22} + s_{33} + 2s_{23}} \right) = \frac{4\pi}{K_{LC}} \tag{C.57}$$

indicating that K_{LC} is the dielectric constant measured when the crystal is longitudinally clamped, i.e., prevented from moving along the length but not along the width or thickness. This quantity is shown plotted for a 45° X -cut crystal by Fig. 6.6. We have also that

$$\frac{4}{1/c_{44} + s_{22} + s_{33} + 2s_{23}} = \frac{1}{s_{22}'} = Y_0 \tag{C.58}$$

the value of Young's modulus along the length of the crystal, as determined by ordinary mechanical measurements. With these substitutions equations (C.56) become

$$\begin{aligned}
 -Y'_y &= Y_0 y'_y + D Q_x \\
 E_x &= \frac{4\pi}{K_{LC}} Q_x + D y'_y
 \end{aligned} \tag{C.59}$$

where $D = \frac{f_{14}Y_0}{2c_{44}}$. This agrees in form with equations (6.32) given in section (6.3). To determine the value of Young's modulus and D we have to know the values of s_{22} , s_{33} , and s_{23} . From

equation (C.47) and the measured values of the c constants given in equation (C.21) the values of the s constants are

$$\begin{aligned} s_{11} &= 5.18 \times 10^{-12} \text{ cm}^2/\text{dyne}; \quad s_{22} = 3.49 \times 10^{-12}; \\ s_{33} &= 3.34 \times 10^{-12}; \quad s_{12} = -1.53 \times 10^{-12}; \\ s_{13} &= -2.11 \times 10^{-12}; \quad s_{23} = -1.03 \times 10^{-12}; \\ \frac{1}{c_{44}} &= 7.98 \times 10^{-12}; \quad \frac{1}{c_{55}} = 32.8 \times 10^{-12}; \\ \frac{1}{c_{66}} &= 10.08 \times 10^{-12}. \end{aligned} \quad (\text{C.60})$$

With these values

$$Y_0 = 3.16 \times 10^{11}; \quad D = 9.7 \times 10^4. \quad (\text{C.61})$$

For the 45° Y-cut crystal, the corresponding values are

$$\begin{aligned} Y_0 &= \frac{4}{s_{11} + s_{33} + 2s_{13} + \frac{1}{c_{55}}} = 1.08 \times 10^{11}; \\ D &= \frac{f_{25} Y_0}{2c_{55}} = 11.2 \times 10^4. \end{aligned} \quad (\text{C.62})$$

The value of the longitudinally clamped dielectric constant is given by

$$\frac{4\pi}{K_2} - \frac{f_{25}^2}{c_{55}} \left[\frac{s_{33} + s_{11} + 2s_{13}}{1/c_{55} + s_{33} + s_{11} + 2s_{13}} \right] = \frac{4\pi}{K_{LC}}. \quad (\text{C.63})$$

With these values the longitudinally clamped constant becomes

$$K_{LC} = 10.0. \quad (\text{C.64})$$

C.4. Piezoelectric Equations for Quartz

For quartz the nine stress-strain and piezoelectric equations can be obtained by differentiating the expression for the potential energy given by (C.37). The resulting equations are

$$\begin{aligned}
-X_x &= c_{11}^* x_x + c_{12}^* y_y + c_{13} z_z + c_{14}^* y_z + f_{11}^* P_x \\
-Y_y &= c_{12}^* x_x + c_{11}^* y_y + c_{13} z_z - c_{14}^* y_z - f_{11}^* P_x \\
-Z_z &= c_{13} x_x + c_{13} y_y + c_{33} z_z \\
-Y_z &= c_{14}^* x_x - c_{14}^* y_y + c_{44}^* y_z + f_{14}^* P_x \\
-Z_x &= c_{44}^* z_z + c_{14}^* x_y - f_{14}^* P_y \\
-X_y &= c_{14}^* z_z + c_{66}^* x_y - f_{11}^* P_y \\
E_x &= f_{11}^* x_x - f_{11}^* y_y + f_{14}^* y_z + \chi_1 P_x \\
E_y &= -f_{14}^* z_z - f_{11}^* x_y + \chi_1 P_y \\
E_z &= \chi_3 P_z.
\end{aligned} \tag{C.65}$$

If we substitute for P_x and P_y

$$P_x = Q_x - \frac{E_x}{4\pi}; \quad P_y = Q_y - \frac{E_y}{4\pi}$$

and solve the above equations simultaneously, we find that the piezoelectric equations can also be written in the form which involves the usually measured elastic constants, as shown in equation (C.66)

$$\begin{aligned}
-X_x &= c_{11} x_x + c_{12} y_y + c_{13} z_z + c_{14} y_z + f_{11} Q_x \\
-Y_y &= c_{12} x_x + c_{11} y_y + c_{13} z_z - c_{14} y_z - f_{11} Q_x \\
-Z_z &= c_{13} x_x + c_{13} y_y + c_{33} z_z \\
-Y_z &= c_{14} x_x - c_{14} y_y + c_{44} y_z + f_{14} Q_x \\
-Z_x &= c_{44} z_z + c_{14} x_y - f_{14} Q_y \\
-X_y &= c_{14} z_z + c_{66} x_y - f_{11} Q_y \\
E_x &= f_{11} x_x - f_{11} y_y + f_{14} y_z + \frac{4\pi}{K_1} Q_x; \\
E_y &= -f_{14} z_z - f_{11} x_y + \frac{4\pi}{K_1} Q_y; \quad E_z = \frac{4\pi}{K_3} Q_z
\end{aligned} \tag{C.66}$$

where

$$\begin{aligned} c_{11} &= c_{11}^* - \frac{f_{11}^{*2}}{4\pi} \left(\frac{K_1 - 1}{K_1} \right); \quad c_{12} = c_{12}^* + \frac{f_{11}^{*2}}{4\pi} \left(\frac{K_1 - 1}{K_1} \right); \\ c_{14} &= c_{14}^* - \frac{f_{11}^* f_{14}^*}{4\pi} \left(\frac{K_1 - 1}{K_1} \right); \quad c_{44} = c_{44}^* - \frac{f_{14}^{*2}}{4\pi} \left(\frac{K_1 - 1}{K_1} \right) \\ c_{66} &= \frac{c_{11} - c_{12}}{2} = c_{66}^* - \frac{f_{11}^{*2}(K_1 - 1)}{4\pi K_1}; \quad f_{11} = f_{11}^* \left(\frac{K_1 - 1}{K_1} \right); \\ f_{14} &= f_{14}^* \left(\frac{K_1 - 1}{K_1} \right). \end{aligned}$$

The dielectric constants K_1 and K_3 have the values

$$K_1 = 4.55; \quad K_3 = 4.70. \quad (\text{C.67})$$

The constants f_{11} and f_{14} , as obtained from Voigt's measurements, have the values

$$f_{11} = -13.15 \times 10^4; \quad f_{14} = -3.4 \times 10^4. \quad (\text{C.68})$$

Most later measurements, however, give somewhat larger values than these. By measuring the separation of resonant and antiresonant frequencies for X -cut crystals and rotated X -cut crystals, the writer obtained the values

$$f_{11} = -13.65 \times 10^4; \quad f_{14} = -3.4 \times 10^4. \quad (\text{C.69})$$

The equations for a longitudinally vibrating crystal, such as discussed in section (6.3), can be obtained from (C.66) by setting $X_z = Z_z = Y_z = 0$. The resulting equations after the elimination of x_z, z_z, y_z become

$$\begin{aligned} -Y_v &= y_v Y_0 + D Q_z \\ E_z &= y_v D + \frac{4\pi}{K_{LC}} \end{aligned} \quad (\text{C.70})$$

where

$$Y_0 = \frac{\Delta}{\Delta_{11}} = \frac{\begin{vmatrix} c_{11} & c_{12} & c_{13} & c_{14} \\ c_{12} & c_{11} & c_{13} & -c_{14} \\ c_{13} & c_{13} & c_{33} & 0 \\ c_{14} & -c_{14} & 0 & c_{44} \end{vmatrix}}{\begin{vmatrix} c_{11} & c_{13} & -c_{14} \\ c_{13} & c_{33} & 0 \\ -c_{14} & 0 & c_{44} \end{vmatrix}} = \frac{1}{s_{11}} = 7.85 \times 10^{11}$$

$$\begin{aligned} D &= - \left[f_{11} - \frac{c_{14}}{c_{44}} f_{14} \right] \left[\frac{\Delta_{11} - \Delta_{12}}{\Delta_{11}} \right] \\ &= - \left[f_{11} - \frac{c_{14}}{c_{44}} f_{14} \right] \left[\frac{s_{11} - s_{12}}{s_{11}} \right] = 14.3 \times 10^4 \end{aligned}$$

$$\frac{4\pi}{K_{LC}} = \frac{4\pi}{K_1} - \frac{\left(f_{11} - \frac{f_{14}c_{14}}{c_{44}} \right)^2}{c_{11} - \frac{c_{13}^2}{c_{33}} - \frac{c_{14}^2}{c_{44}}} = \frac{4\pi}{4.58}$$

which are the values given in equation (6.34).

INDEX OF SUBJECTS

(Numbers refer to pages)

- Analogies
 - Electrical and mechanical, direct system, 80
 - Electrical and mechanical, inverse system, 83
 - Electrical and torsional, 95
- Attenuation units
 - Decibel, 27
 - Neper, 27
- Crystal-driven supersonic radiator
 - Coil coupled, 234
 - Use of filter relations in, 235
 - Multiple unit, 238
 - Description of, 230
 - Efficiency of, 234
 - Equivalent circuit of, 233
 - Radiation resistance of, 232
- Crystal resonator
 - Divided plate, 253
 - Equivalent circuit of balanced, 255
 - Equivalent circuit of unbalanced, 257
 - Effect of radiation resistance on Q of, 251
 - Effect of radiation reactance on frequency of, 252
 - Equivalent circuit of, 249
- Elastic properties of bars
 - Definition of Q of, 241
 - Equivalent circuit representing, 241
 - Single crystal method for measuring, 238
 - Table of, 245
 - Temperature coefficient of, 244
 - Two-crystal method for measuring, 245
- Electromagnetic driving system
 - Balanced armature type of, 193
 - Moving coil type of, 187
 - Equation of motion of, 188
 - Equivalent circuit of, 190
 - Reciprocal properties of, 190
 - Transformation ratio of, 190
- Electromagnetic driving system—*Cont.*
 - Vibrating reed type of, 191
 - Equations of motion of, 192
 - Transformation ratio of, 192
- Electrostatic driving system
 - Equations of motion of, 194
 - Equivalent circuit of, 194
 - Reciprocal properties of, 195
- Equalizer
 - Constant resistance attenuation, 57
- Equation
 - For pressure and volume in an adiabatic medium, 103
 - Of continuity, 104
- Factor
 - Interaction, 26
 - Reflection, 25
 - Transformation, 24
 - Transmission, 25
- Filters, acoustic
 - Band pass, 142
 - Measurement of, 140
 - Table of, 128
 - With circular side branch, 135
 - With distributed constants, 131
- Filter, electric
 - Definition, 28
 - Distributed constant, 58
 - Multiple section band pass, 49
 - Resistance compensated, 56
 - Simple, 36
 - All pass, 45
 - Band pass, 37
 - High pass, 44
 - Low pass, 43
 - Table of, sections, 52
 - Using short sections of line, 68
- Filter, employing crystals
 - Band suppression type of, 283
 - High pass type of, 282
 - Low pass type of, 282

Filter, employing crystals—*Cont.*

Narrow band type of, 258

Description of, 258

Design equations of, 260

Lattice types of, 259

Measured characteristics of, 262

Wide band type of, employing coils,
263

Critical frequencies of, 268

Description of, 263

Design equations for series type of,
270Design equations for parallel type of,
272

Divided plate type of, 272

Effect of dissipation in, 263

Multi crystal type of, 278

Unbalanced type of, 273

Filter, employing magnetostrictive bars

Description of, 285

Equivalent circuit of, 286

Narrow band type of, 287

Wide band type of, 288

Filter, mechanical

Band pass, using vibrating reeds, 86

Natural frequencies of low pass, 98

Torsional vibrating low pass, 97

Foster's theorem, 274**Horns**

Directivity of, 150

Theory of, 120

Transformation due to, 124

Impedance

Definition of, 13

Determinant, 14

Reactance component of, 13

Resistance component of, 13

Use of elements to improve image, 46

Kirchhoff's laws, 13**Losses**

Attenuation, 28

Interaction, 28

Transfer, 28

Transformer, 28

Transmission, 28

Magnetostrictive driving systems

Equations of motion of, 219

Equivalent circuit of, 223

Historical development of, 215

Magnetostrictive driving systems—*Cont.*

Magnetostrictive equations of, 218

Reciprocal properties of, 220

Moving coil loud speaker

Cutoff frequencies of, 228

Description of, 226

Efficiency of, 229

Equivalent circuit of, 226

Multiple unit, 230

Use of filter relations in design of, 228

Networks T and π , 29Bridge T , 29

Lattice, 29

 T and π , for acoustic tube, 119**Network parameters**

Addition of, 51

Definition of image, 20

Relation between A , B , C , D , 15Relation to impedance determinant of
 T , π , bridge, T , and lattice, 30**Piezoelectric driving systems**

Bimorph type of

Equations of motion of, 212

Equivalent circuit of, 215

Piezoelectric equations of, 211

Historical development of, 195

Longitudinal type of

Constants of, 202

Equations of motion of, 204

Equivalent circuit of, 205

Piezoelectric equations of, 202

Derivation of, 308

Quartz type of, 197

Rochelle salt type of, 199

Plane Waves

Conditions for, 110

Equation for, 111

Potential and kinetic energy of, 112

Propagation in a tube of, 106

Radiator

Piston, 146

Directivity pattern of, 148

Impedance reaction on, 149

Point source, 145

Spherical, 143

Impedance reaction on, 144

Solution

For tuned circuit, 12

Steady state, 11

Solution—Cont.

Transient, 11

Soundproof walls

Attenuation due to, 180

Design of, 178

Equivalent circuit of, 179

Stretched membranes

Boundary conditions for, 162

Displacement equation of, 164

Equation of motion for, 161

Equivalent circuit of, 165

Potential energy of, 160

Use of, in acoustic filters, 165

Use of, in condenser transmitter, 166

Stretched thin plate

Displacement of, 182

Equation of motion of, 181

Equivalent circuit of, 184

Impedance of, 182

Theorem

Bartlett's, 32

Compensation, 18

Foster's, 274

Reciprocity, 16

extended, 18

Thevenin's, 15

Thin plates

Boundary conditions for, 162

Displacement solution of, 168

Effect of supports on vibration of, 174

equivalent circuit of, 178

Equation of motion of, 161

Equivalent circuit of, 169

Impedance of, 169

Potential energy of, 160

Use of, in telephone receivers, 171

Time functions

Sinusoidal, 11

Symbolic, 11

Transformers

Narrow band, using quarter wave-length line, 66

Wide band, using short sections of line, 70

Transmission line

Constants of, 59

Equivalent T and π networks of, 62

Propagation characteristics of, 61

Short section of, as transformer, 66

Use of, as tuned circuit, 65

Tubular directional microphone, 151

Directivity of, 154

Effect of tube attenuation on, 156

Use of, for directional radiator, 157

Velocity potential

Definition of, 105

Equation of, for a medium, 106

For a point source, 145

For a piston radiator, 147

Vibration

Bar in flexural, 87

Effect of rotary inertia on, 291

Bar in torsional, 96

Equivalent circuit of bar in flexural, 91

Effect of rotary inertia on, 294

Frequency of bar in flexural, 90

Effect of rotary inertia on, 295

Impedance of bar in flexural, 89

Effect of rotary inertia on, 293

Reducer, with damping, for, 83

Viscosity

Attenuation of sound in a plane wave due to, 298

Attenuation of sound in a tube due to, 118

Definition of, 114

Effect of, on flow of air, 116

